



# Design, Development and Testing of New Experimental Equipment for the Measurement of Multiphase Equilibrium

**José M. S. Fonseca**

Ph.D. Thesis

2010

**CERE - Centre for Energy Resources Engineering**



**DTU Chemical Engineering**

Department of Chemical and Biochemical Engineering

---

Copyright©: José M. S. Fonseca  
2010

Address: Department of Chemical and Biochemical Engineering  
Søltofts Plads, Building 229  
Technical University of Denmark  
DK-2800 Kgs. Lyngby  
Denmark

Telephone: +45 4525 2800  
Fax: +45 4588 2258  
E-mail: [kt@kt.dtu.dk](mailto:kt@kt.dtu.dk)  
Internet: [www.kt.dtu.dk](http://www.kt.dtu.dk)

Print: J&R Frydenberg A/S  
København  
December 2010

ISBN: 978-87-92481-27-6

**“The test of all knowledge is experiment.  
Experiment is the sole judge of scientific ‘truth’.”**

Richard P. Feynman (1918 – 1988),  
Nobel Prize in Physics, 1965

**“No amount of experimentation can ever prove me right;  
a single experiment can prove me wrong.”**

Albert Einstein (1879 – 1955)  
Nobel Prize in Physics, 1921



## **Summary**

The main purpose of this work, focusing on the phase equilibria of complex systems containing thermodynamic gas inhibitors, is to give a modest, although solid contribution in bridging the existing gaps in what experimental data is concerned. This was achieved not just with the measurement of new data, but through the development of new experimental equipment for the study of multi-phase equilibria, by means of different methods. This experimental effort was complemented by the modelling of a number of systems of interest.

In the second part of the work, the attention is driven to the prominent topic of carbon dioxide capture, more specifically to the absorption of carbon dioxide in aqueous solutions of alkaline salts of amino-acids. An experimental study for a number of relevant systems was performed using one of the apparatus developed in the first part of the work.

After a brief introduction to the central themes of this work, presented in Chapter 1, the subsequent chapters are organised as following:

In Chapter 2, the result of a thorough literature survey focusing on the phase equilibria of systems containing gas inhibitors is presented, allowing the acknowledgment of the lack of experimental data verified for particular systems and in specific conditions of temperature and pressure. Furthermore, examples of discrepancy between different sets of data available for the same system are provided.

In Chapter 3, a comprehensive categorisation of the experimental methods available for the measurement of phase equilibria, with emphasis on the methods applicable at high pressures, is presented, together with a description of each of the methods and recent examples of their application taken from the literature. A comparison between the different methods, underlining the advantages and disadvantages inherent to each one of them is also performed.

Chapter 4 deals with the design, assembling and testing of a new experimental apparatus for the measurement of multiphase equilibrium by using an analytical method. Firstly, a general insight on the processes behind the development of new equipment is given, followed by the complete description of the apparatus developed in this work, initially with an overall presentation and subsequently focusing on the most important parts

and components, emphasising the grounds for its design or for its selection. The results obtained in the study of reference systems are also presented, confirming the quality of the equipment and its potential for the attainment of high quality data.

In Chapter 5, a second experimental apparatus is described, developed using a decommissioned equilibrium cell, for use with a synthetic method. As in the previous chapter, a complete description of the apparatus is made, and the results obtained in the study of reference systems presented, confirming the quality of the equipment.

Chapter 6 is dedicated to the application of an associative model, the simplified PC-SAFT equation of state, to a number of relevant systems, in an attempt to verify the applicability of this model to the systems under consideration.

In Chapter 7, the results obtained in the experimental study and in the modelling of a multiphase complex system are presented.

In Chapter 8, a short introduction to the subject of carbon dioxide capture by absorption is provided, preceding the presentation of the experimental results obtained in the study of the solubility of carbon dioxide in a number of different solvents.

Finally, in Chapter 9, some brief conclusions are drawn regarding the accomplishments of the present work, and considerations concerning future work are presented.

## **Resumé**

Dette arbejde fokuserer på fase-ligevægte af komplekse systemer, der indeholder termodynamiske gas-hydrat inhibitor. Det vigtigste formål med arbejdet, er at give et beskedent, men solidt bidrag til eksisterende eksperimentelle data, med henblik på at udfylde huller i den nuværende viden. Dette blev opnået ikke blot med måling af nye data, men også gennem udvikling af nyt eksperimentelt udstyr til undersøgelse af multi-fase-ligevægte, ved forskellige metoder. Det eksperimentelle arbejde blev suppleret med modellering af en række systemer af interesse.

I anden del af arbejdet, er opmærksomheden fokuseret på det stadig voksende emne, nemlig kuldioxid fangst fra røggas, mere specifikt absorptionen af kuldioxid ved hjælp af vandige basiske opløsninger af aminosyrer salte. En eksperimentel undersøgelse af en række relevante systemer blev udført ved hjælp af et af de eksperimentelle udstyr, som blev udviklet i den første del af arbejdet.

Efter en kort introduktion til arbejdes centrale temaer som præsenteres i Kapitel 1, er de næste kapitler organiseret som følgende:

Kapitel 2 præsenterer et grundig litteratur-studie med fokus på de fornævnte emner, herunder uddybes det hvilke eksperimentelle data, som mangler på nuværende tidspunkt for de forskellige systemer ved specifikke temperaturer og tryk. Desuden gives eksempler på uoverensstemmelse mellem forskellige sæt af litteraturdata for det samme system.

I Kapitel 3 gives en omfattende kategorisering af de eksperimentelle metoder til måling af fase-ligevægte, med vægt på metoder, der anvendes ved høje tryk. Samtidig beskrives hver af metoderne og de seneste eksempler fra litteraturen angående deres anvendelse præsenteres. Ydermere sammenlignes metoderne specielt med henblik på fordele og ulemper forbundet med hver enkelt metode.

Kapitel 4 omhandler design konstruktion og testning af et nyt eksperimentelt apparatur til måling af multifase ligevægte ved hjælp af en analytisk metode. Først gives der indsigt i processerne omkring udvikling af nyt udstyr. Herefter gives en fuldstændig beskrivelse af apparaturet, indledningsvis med en samlet præsentation, hvilken efterfølges af en beskrivelse, der fokuserer på de vigtigste dele og komponenter, hermed understreges grundene til det specifikke design og udvælgelsen af de enkelte komponenter. Ydermere

præsenteres opnåede resultater fra studiet af referencesystemer, hvilke bekræfter kvaliteten af udstyret og dets potentiale til at opnå data af høj kvalitet.

I kapitel 5, præsenteres endnu et eksperimentel apparatet, som er udviklet ved hjælp af en gammel ligevægt celle, til anvendelse med en syntetisk metode. Ligesom i det foregående kapitel, gives en komplet beskrivelse af apparatet, og de opnåede resultater fra studiet af referencesystemer præsenteres, hvilke igen bekræfter kvaliteten af udstyret.

Kapitel 6 er dedikeret til anvendelsen af en associativ model, den ”simplified PC-SAFT” på en række relevante systemer, med formålet at verificerer om modellen kan anvendes på de systemer, som undersøges i dette arbejde.

I kapitel 7 præsenteres opnåede resultater fra den eksperimentelle undersøgelse og modellering af en multifase komplekst system.

Kapitel 8 giver først en kort introduktion til emnet kuldioxid fangst med kemisk absorption, efterfulgt af en præsentation af eksperimentelle resultater fra studiet af opløseligheden af kuldioxid i en række forskellige opløsningsmidler.

Endelig, i Kapitel 9 drages konklusioner på det nuværende arbejde, og overvejelser om fremtidigt arbejde præsenteres.

## **Preface**

The present thesis is submitted for partial fulfilment of the requirements for the Ph.D. degree at the Technical University of Denmark. The work was carried out at the Centre for Energy Resources Engineering (CERE), formerly Centre of Phase Equilibria and Separation Processes (IVC-SEP), in the Department of Chemical and Biochemical Engineering Department of the Technical University of Denmark, from January 2006 to April 2010, under the supervision of Associate Professor Nicolas von Solms. The work is included in a broader research project under the title “Gas Hydrates - from Threat to Opportunity”, financially supported by the Danish Technical Research Council.

This challenging work would not have been possible without the valued contribution of a number of persons, to whom I would like to express my gratitude.

I would specially like to thank Nicolas von Solms for the work proposed and for all the support, suggestions and comments given during the length of this work and in the writing of this thesis. I am grateful to Erling Stenby for receiving me in his research group and by offering me the opportunity to work in such a stimulating environment. I am also thankful to all the team of technicians for the support provided during the experimental work, in addition, to Bianca Larsen and Randi Neerup for their help in the gas chromatography tests.

I also would like to express my gratitude to Prof. Ralf Dohrn, from Bayer Technology Services GmbH, for giving me the opportunity to participate in the series of reviews on high-pressure phase equilibria, which allowed me to greatly increase my knowledge on experimental phase equilibrium, exceptionally valuable for the development of this work. My thankfulness goes also to Prof. Luís Belchior Santos from the Faculty of Sciences of the University of Porto, for the inspiration and for instilling in me the enthusiasm for instrumentation and for the design of new experimental equipment.

To Benedicte Mai Lerche, I would like to thank the introduction into the subject of carbon dioxide capture and for the help in translating the summary into Danish.

I wish to thank Nuno Garrido for the constant presence which allowed so many fruitful discussions, for the contagious good humour, as well as for the help provided with

reviewing the thesis. My appreciation goes also to Spencer and to Yiannis, for their valuable advices in the review of the thesis.

To my parents, for all the support throughout the years, which made it possible to reach this stage, and for the permanent encouragement to always pursue my goals, *muito, muito obrigado por tudo!* I also want to thank Maja for all the company and the constant support along this last two years.

A special “thank you” goes to Claudia, for the uplifting company and support during the writing of this thesis. To Yiannis, Andreas, Ferran, Benedicte, Jens, Ricardo, Nuno, Bess, and to all the other friends and colleagues who have shared with me this period of my life, and in one way or another have contributed to the success of this work, I would like to express my gratitude.

Kongens Lyngby, July 2010

A handwritten signature in cursive script, appearing to read "José Manuel S. Fonseca".

José Manuel S. Fonseca

## ***Index of Contents***

Summary	v
Resumé (Dansk)	vii
Preface	ix
Index of Contents	xi
Index of Figures	xv
Index of Tables	xxv
<b>Chapter 1 – Introduction</b>	<b>1</b>
References	7
<b>Chapter 2 – Experimental Data for Systems Related to Hydrate Inhibition – a Review</b>	<b>9</b>
References	16
<b>Chapter 3 – Experimental Methods for the Measurement of Phase Equilibria</b>	<b>21</b>
3.1. Analytical methods	23
3.1.1. Analytical isothermal methods	27
3.1.2. Analytical isobaric-isothermal methods	32
Continuous-flow methods	32
Semi-flow methods	34
Chromatographic methods	36
3.1.3. Analytical isobaric methods	37
3.1.4. Analytical spectroscopic methods	38
3.1.5. Analytical gravimetric methods	39
3.1.6. Other analytical methods	41
3.2. Synthetic methods	43
3.2.1. Visual synthetic methods	46
3.2.2. Non-Visual synthetic methods	48
3.2.3. Synthetic isothermal methods	52
3.2.4. Synthetic isobaric methods	54
3.2.5. Other synthetic methods	55
References	56

<b>Chapter 4 – New Experimental Set-up, Analytical Method</b>	<b>71</b>
4.1. Development of a new experimental apparatus – preliminary steps	72
4.2. New experimental set-up, analytical method	74
4.2.1. Description of the apparatus	76
The cell	80
Thermostatisation of the cell	83
Temperature and pressure measurements	85
The sampling system	87
The analytical method	90
Valve configuration	91
Additional systems	93
4.2.2. Experimental procedure	94
4.3. Testing of the new apparatus	96
4.3.1. Preliminary tests	96
4.3.2. Measurement of reference systems	99
Binary system methanol + ethane	100
Carbon dioxide	106
Ethane	111
4.4. Gas chromatography	117
4.4.1. Development of the chromatographic method	117
4.4.2. Calibration of the gas chromatograph	122
4.5. Analytical measurements on reference systems	124
4.5.1. Calibration for water and methane	124
4.5.2. Analytical results for the system methane + water	135
4.6. Conclusions	141
References	142
<b>Chapter 5 – Re-commission of an Existing Equilibrium Cell,</b>	
<b>Synthetic Method</b>	<b>147</b>
5.1. Limitations of the existing apparatus	147
5.2. Re-commissioning the apparatus – a first approach	151
5.3. Re-commissioning the apparatus – final configuration	153
5.3.1. Description of the apparatus	153
The cell	155

Thermostatisation of the cell	157
Temperature and pressure measurements	158
Valve configuration	159
Additional systems	160
5.4. Testing the re-commissioned cell	161
5.4.1. Measurements with the intermediate configuration	161
5.4.2. Preliminary tests	164
5.4.3. Measurement of reference systems	166
Ethane	166
Carbon dioxide	167
5.4.4. Validation of experimental methods	169
Formation of gas hydrates	170
Solubility of a gas in a non-volatile condensed phase	172
Binary system water + methane	174
5.5. Conclusions	179
References	179

## **Chapter 6 – Modelling of Phase Equilibrium in Hydrate Inhibitor Systems**

<b>Using Simplified PC-SAFT</b>	<b>185</b>
6.1. Introduction	186
6.1.1. The SAFT equation of state	187
6.1.2. The PC-SAFT equation of state	189
6.1.3. The simplified PC-SAFT equation of state	194
6.2. Results	195
6.2.1. Binary system methane + <i>n</i> -hexane	196
6.2.2. Binary system <i>n</i> -hexane + water	198
6.2.3. Binary system <i>n</i> -octane + water	200
6.2.4. Binary system <i>n</i> -hexane + methanol	201
6.2.5. Binary system methanol + water	202
6.3. Conclusions	204
References	205

<b>Chapter 7 – Experimental Study and Modelling of the Quaternary System</b>	
<b>Methane + <i>n</i>-hexane + Methanol + Water</b>	<b>209</b>
7.1. Experimental results	209
7.2. Modelling	213
7.2.1. Binary system methane + water	213
7.2.2. Binary system methane + methanol	222
7.2.2. Quaternary system methane + <i>n</i> -hexane + methanol + water	223
References	227
<b>Chapter 8 – Solubility of Carbon Dioxide in Aqueous Solutions of</b>	
<b>Amino-acid Salts</b>	<b>229</b>
8.1. Sorption of carbon dioxide in amine-based aqueous solutions	230
8.2. Experimental results	236
8.2.1. Solubility of carbon dioxide in water	236
8.2.2. Solubility of carbon dioxide in aqueous solutions of 2-aminoethanol	239
8.2.3. Solubility of carbon dioxide in aqueous solutions of amino-acid salts	242
L-Proline	242
References	245
<b>Chapter 9 – Conclusions and Future Work</b>	<b>251</b>
9.1. Conclusions	251
9.2. Future work	253
References	257
<b>Appendix 1 – Tables and List of References for Experimental Data for</b>	
<b>Systems Related to Hydrate Inhibition</b>	<b>259</b>
References	278
<b>Appendix 2 – List of Individual Experimental Data Points Obtained in the</b>	
<b>Analytical Measurements</b>	<b>293</b>

## ***Index of Figures***

<b>Figure 3.1</b>	Categorisation of the experimental methods available for the measurement of high-pressure phase equilibrium.	23
<b>Figure 3.2</b>	Picture of an electromagnetic ROLSI™ sampler-injector, showing the actuator and the capillary through which sampling is made.	25
<b>Figure 3.3</b>	Schematic diagram showing the three fundamental steps in the application of analytical isothermal methods.	28
<b>Figure 3.4</b>	Schematic drawing of the apparatus used by Tsivintzelis et al.	30
<b>Figure 3.5</b>	Schematic representation of the experimental procedure adopted by Nikitin et al. in the study of sorption of carbon dioxide in polystyrene.	31
<b>Figure 3.6</b>	Schematic diagram showing a typical design of a continuous-flow method, evincing the three fundamental steps of the method.	33
<b>Figure 3.7</b>	Schematic diagram showing a typical design of a semi-flow method, emphasising the fundamental steps of the method.	35
<b>Figure 3.8</b>	Schematic representation of the analytical gravimetric apparatus employed by von Solms et al.	40
<b>Figure 3.9</b>	Schematic representation of a magnetic suspension balance.	41
<b>Figure 3.10</b>	Schematic diagram of a generic diamond anvil cell, as presented by Cohen-Adad.	46
<b>Figure 3.11</b>	Schematic diagram of the apparatus used by Kodama et al.	48
<b>Figure 3.12</b>	Typical result obtained in the determination of hydrate formation conditions using the change in the $(dp/dT)$ slope method.	49
<b>Figure 3.13</b>	Schematic representation of the experimental apparatus employed by Manara et al.	51
<b>Figure 4.1</b>	General aspect of the new developed experimental set-up for the measurement of multi-phase equilibria, showing the cell inside the temperature chamber and the GC unit.	77
<b>Figure 4.2</b>	Schematic representation of the new experimental set-up for the measurement of multi-phase equilibria.	77

<b>Figure 4.3</b>	Image of the equilibrium cell mounted on a structure specially designed and constructed for this application, inside the temperature chamber.	79
<b>Figure 4.4</b>	Three-dimensional computer generated images of the high pressure cell.	80
<b>Figure 4.5</b>	Mupu seals.	83
<b>Figure 4.6</b>	Electromagnetic ROLSI™ sampler.	87
<b>Figure 4.7</b>	Control panel for the ROLSI™ samplers, with the timer, the temperature controllers, and additional switches to chose from which valve to use at a given time.	89
<b>Figure 4.8</b>	Schematic drawing of the connection of the ROLSI™ samplers with the gas chromatograph.	89
<b>Figure 4.9</b>	Schematic representation of the valve configuration showing the existence of one single connection to the equilibrium cell.	92
<b>Figure 4.10</b>	Print screen of the program READ30 showing the deviation of the pressure readings as a function of the temperature of the electronics of the pressure transmitter.	98
<b>Figure 4.11</b>	Influence of small oscillations of the temperature of the cell in the pressure values, evidence of a good thermal contact between the cell and the platinum resistance thermometers.	99
<b>Figure 4.12</b>	Results obtained in the study of the three-phase (vapour-liquid-liquid) coexisting line for the binary system methanol + ethane, and comparison with values found in the literature.	101
<b>Figure 4.13</b>	Deviations from the experimental points to the values given by Equation 4.1, for the results obtained in this work and the values found in literature, in the study of the three-phase coexisting line for the binary system methanol + ethane.	102
<b>Figure 4.14</b>	Deviations from the experimental points to the values given by Equation 4.2, for the results obtained in this work and the values found in literature, in the study of the three-phase coexisting line for the binary system methanol + ethane.	103

<b>Figure 4.15</b>	Deviations from the experimental points to the values given by Equation 4.3, for the results obtained in this work and the values found in literature, in the study of the three-phase coexisting line for the binary system methanol + ethane.	104
<b>Figure 4.16</b>	Chromatogram of the analysis of one sample withdrawn from the methanol rich phase during the study of the three-phase coexisting line for the binary system methanol + ethane.	105
<b>Figure 4.17</b>	Image of the sapphire window in the equilibrium cell during the study of the three-phase coexisting line for the binary system methanol + ethane, where the three phases are visible.	106
<b>Figure 4.18</b>	Results obtained in the study of the vapour-liquid equilibrium line for pure carbon dioxide.	108
<b>Figure 4.19</b>	Relative and absolute deviations from the data points obtained in this work for the vapour-liquid equilibrium line for pure carbon dioxide, to the reference values recommended by the DIPPR database.	109
<b>Figure 4.20</b>	Relative and absolute deviations from the second set of data points obtained in this work in the study of the vapour-liquid equilibrium line for pure carbon dioxide, to the reference values recommended by the DIPPR database.	110
<b>Figure 4.21</b>	Results obtained in the study of the vapour-liquid equilibrium line for pure ethane.	113
<b>Figure 4.22</b>	Relative and absolute deviations from the results obtained in this work for the vapour-liquid equilibrium line for pure ethane, to the reference values recommended by the DIPPR database.	114
<b>Figure 4.23</b>	Similarity between the absolute deviations verified for the results obtained for the vapour liquid equilibrium line for carbon dioxide and ethane, relatively to reference values.	114
<b>Figure 4.24</b>	Similarity between the relative deviations verified for the results obtained for the vapour liquid equilibrium line for carbon dioxide and ethane, relatively to reference values.	115

<b>Figure 4.25</b>	Combined analysis of the relative deviations of the results obtained for the vapour liquid equilibrium line for carbon dioxide and ethane relatively to reference values, and proposed equations for correction of the raw experimental values.	116
<b>Figure 4.26</b>	Chromatogram (TCD) of the analysis of a mixture of water, <i>n</i> -pentane and ethylene glycol, and respective temperature program.	119
<b>Figure 4.27</b>	Chromatogram (FID and TCD) of the analysis of a mixture of solution of methane, <i>n</i> -pentane, <i>n</i> -hexane, water and MEG in methanol.	120
<b>Figure 4.28</b>	Chromatogram (FID and TCD) of the analysis of a mixture of solution of <i>n</i> -pentane, <i>n</i> -hexane, methanol and water in ethanol.	121
<b>Figure 4.29</b>	Areas of the chromatographic peaks yielded by the TCD as a function of the number of moles of water injected, relatively to the GC calibration of water using an automatic injector	125
<b>Figure 4.30</b>	Percentage of the water peak area from the total areas yielded by the TCD (water + solvent), as a function of the number of moles of water injected, relatively to the GC calibration of water using an automatic injector.	126
<b>Figure 4.31</b>	Chromatogram (FID and TCD) obtained during the calibration for water, using solutions of this compound in ethanol.	127
<b>Figure 4.32</b>	Areas of the chromatographic peaks yielded by the TCD as a function of the number of moles of water injected, relatively to the GC calibration of water through manual injection.	128
<b>Figure 4.33</b>	Average areas of the chromatographic peaks yielded by the TCD as a function of the number of moles of water injected, relatively to the GC calibration of water through manual injection.	128
<b>Figure 4.34</b>	Comparison between the non-corrected calibration curve, and the curves obtained applying the two described correction methods.	132
<b>Figure 4.35</b>	Areas of the chromatographic peaks yielded by the TCD as a function of the number of moles of methane injected, during the GC calibration of this gas.	134

<b>Figure 4.36</b>	Areas of the chromatographic peaks yielded by the FID as a function of the number of moles of methane injected, relatively to the GC calibration of this gas.	134
<b>Figure 4.37</b>	Individual data points obtained for the liquid phase in the analytical study of the system methane + water, and comparison with values found in the literature.	138
<b>Figure 4.38</b>	Results (average values) obtained for the liquid phase in the analytical study of the system methane + water, and comparison with values found in the literature.	139
<b>Figure 4.39</b>	Individual data points obtained for the gas phase in the analytical study of the system methane + water, and comparison with values found in the literature.	140
<b>Figure 5.1</b>	Picture of the old experimental set-up as it was by 2003.	148
<b>Figure 5.2</b>	Schematic representation of the new experimental set-up for the measurement of phase equilibria.	154
<b>Figure 5.3</b>	Lid of the cell.	156
<b>Figure 5.4</b>	Image of the high-pressure equilibrium cell together a gas cylinder and other parts, inside the temperature chamber.	157
<b>Figure 5.5</b>	Schematic representation of the valve configuration and positioning of the pressure sensor on the top of the equilibrium cell.	159
<b>Figure 5.6</b>	Output of the pressure sensor at atmospheric pressure, as a function of its temperature of operation.	162
<b>Figure 5.7</b>	Deviations from the experimental results obtained in this work and from the literature values to Equation 4.3, in the study of the three-phase coexisting line for the binary system methanol + ethane.	163
<b>Figure 5.8</b>	Reflexion in the pressure values of small oscillations in the temperature of the cell, showing a good thermal contact between the cell and the platinum resistance thermometers.	165
<b>Figure 5.9</b>	Results obtained in the study of the vapour-liquid equilibrium line for carbon dioxide.	168

<b>Figure 5.10</b>	Relative and absolute deviations from the results obtained in this work for the vapour-liquid equilibrium line for carbon dioxide, to the reference values recommended by the DIPPR database.	169
<b>Figure 5.11</b>	Pressure and temperature profiles registered during the cooling process for the promotion of methane hydrates in the system methane + water.	171
<b>Figure 5.12</b>	Results obtained during the calibration of the scale in the window of the equilibrium cell.	173
<b>Figure 5.13</b>	Results obtained in the first series of measurements of the solubility of methane in pure water, at 298 K, and comparison with values found in literature.	176
<b>Figure 5.14</b>	Results obtained in the second series of measurements of the solubility of methane in pure water, at 283 K and 298 K, and comparison with values found in literature.	177
<b>Figure 6.1</b>	Schematic representation of the physical basis of PC-SAFT.	190
<b>Figure 6.2</b>	Results obtained in the modelling of the binary system methane + <i>n</i> -hexane, at isothermal conditions, between 248 K and 411 K, using simplified PC-SAFT correlations with $k_{ij} = 0.01$ , and comparison with experimental data found in literature.	197
<b>Figure 6.3</b>	Results obtained in the modelling of the binary system methane + <i>n</i> -hexane, at isothermal conditions, between 248 K and 411 K, using simplified PC-SAFT correlations with $k_{ij} = 0.01$ , and comparison with experimental data found in the literature. Detail for higher values of the methane mole fraction.	197
<b>Figure 6.4</b>	Results obtained in the modelling of the LLE for the binary system <i>n</i> -hexane + water with simplified PC-SAFT, using a $k_{ij} = 0.00$ and different sets of parameters for water, and comparison with experimental data found in literature.	198

- Figure 6.5** Results obtained in the modelling of the LLE for the binary system *n*-hexane + water with simplified PC-SAFT, using  $k_{ij} = 0.00$  and  $k_{ij} = 0.055$ , and comparison with experimental data found in literature. 199
- Figure 6.6** Results obtained in the modelling of the VLLE for the binary system *n*-octane + water with simplified PC-SAFT, using a  $k_{ij} = 0.035$ , and comparison with experimental data found in literature. 200
- Figure 6.7** Results obtained in the modelling of the VLE at 0.101 MPa, and the LLE at 85 MPa for the binary system *n*-hexane + methanol, considering a  $k_{ij} = 0.03$ , and comparison with experimental values from literature. 201
- Figure 6.8** Results obtained in the correlation of isobaric VLE for the system methanol + water, at a pressure of 0.101 MPa, using simplified PC-SAFT and a  $k_{ij} = -0.04$ , and comparison with experimental literature data. 203
- Figure 6.9** Simplified PC-SAFT correlation of the isothermal VLE behaviour of the system methanol + water, at 298.15 K, 323.15 K, 338.15 K, 373.15 K, 423.15 K, 473.15 K and 523.15 K, using  $k_{ij} = -0.04$ , and comparison with experimental data. 204
- Figure 7.1** Example of a chromatogram relative to a sample withdrawn from the organic phase of the system methane + *n*-hexane + methanol + water, showing the peaks corresponding to the four constituents of the system. 212
- Figure 7.2** Modelling of the binary system methane + water, at 283 K, using sPC-SAFT correlations with different values of  $k_{ij}$ , and comparison with experimental data obtained in this work by the synthetic method and literature data for the liquid phase. 214
- Figure 7.3** Modelling of the binary system methane + water, at 283 K, using sPC-SAFT correlations with different values of  $k_{ij}$ , and comparison with literature data for the gas phase. 215

- Figure 7.4** Modelling of the binary system methane + water, at 298 K, using sPC-SAFT correlations with different values of  $k_{ij}$ , and comparison with experimental data obtained in this work by the analytical and the synthetic method and data found in literature for the liquid phase. 216
- Figure 7.5** Modelling of the binary system methane + water, at 298 K, using sPC-SAFT correlations with different values of  $k_{ij}$ , and comparison with experimental data obtained in this work by the analytical method and data found in literature for the gas phase. 216
- Figure 7.6** Modelling of the binary system methane + water, at 303 K, using sPC-SAFT correlations with different values of  $k_{ij}$ , and comparison with experimental data obtained in this work by the analytical method and data found in literature for the liquid phase. 217
- Figure 7.7** Modelling of the binary system methane + water, at 303 K, using sPC-SAFT correlations with different values of  $k_{ij}$ , and comparison with experimental data obtained in this work by the analytical method and data found in literature for the gas phase. 218
- Figure 7.8** Modelling of the binary system methane + water, at 323 K, using sPC-SAFT correlations with different values of  $k_{ij}$ , and comparison with experimental data found in literature for the liquid phase. 218
- Figure 7.9** Modelling of the binary system methane + water, at 323 K, using sPC-SAFT correlations with different values of  $k_{ij}$ , and comparison with experimental data found in literature for the gas phase. 219
- Figure 7.10** Modelling of the binary system methane + water, at 373 K, using simplified PC-SAFT correlations with different values of  $k_{ij}$ , and comparison with experimental data found in literature for the liquid phase. 220
- Figure 7.11** Modelling of the binary system methane + water, at 373 K, using simplified PC-SAFT correlations with different values of  $k_{ij}$ , and comparison with experimental data found in literature for the gas phase. 220

<b>Figure 7.12</b>	Values of $k_{ij}$ found in the modelling of the binary system methane + water, at five different temperatures between 283 K and 373 K, showing the dependence of the $k_{ij}$ values with temperature	221
<b>Figure 7.13</b>	Results obtained in the modelling of the binary system methane + methanol, at 298 K, using sPC-SAFT correlations with different values of $k_{ij}$ , and comparison with experimental data found in literature.	222
<b>Figure 8.1</b>	Flow-sheet of the amine absorption process of carbon dioxide, from the flue-gas of fossil-fuelled power plants.	232
<b>Figure 8.2</b>	Equilibrium curve relative to a solution with a concentration of $6 \text{ mol.dm}^{-3}$ of an undisclosed amino-acid salt, at a temperature of 313 K (40 °C),	234
<b>Figure 8.3</b>	Results obtained in the measurements of the solubility of carbon dioxide in pure water, at temperatures around 298 K, and comparison with values from literature.	239
<b>Figure 8.4</b>	Results obtained in the measurements of the sorption of carbon dioxide in an aqueous solution of 2-ethanolamine 30 wt%, at temperatures around 298 K, and comparison with experimental values from literature and with the extended UNIQUAC model.	240
<b>Figure 8.5</b>	Results obtained in the measurements of the sorption of carbon dioxide in an aqueous solution of 2-ethanolamine 30 wt%, at temperatures around 298 K, corrected for a possible degradation of 5% of 2-ethanolamine, and comparison with experimental values from literature and with the extended UNIQUAC model.	241
<b>Figure 8.6</b>	Results obtained in the in the measurements of the sorption of carbon dioxide in an aqueous solution of L-proline 7.0 molal, at 300 K and 353 K, and comparison with values from literature	244

- Figure 9.1** Schematic representation of a hypothetical equilibrium cell of small dimensions, to be built from the spare material available from this work. 255
- Figure 9.2** Schematic representation of a hypothetical inexpensive LLE cell, based in the design of the cell used by Folas et al. in the Statoil Research Centre in Trondheim, Norway. 256

## ***Index of Tables***

<b>Table 4.1</b>	Results obtained during the study of the three-phase coexisting line for the binary system methanol + ethane, using the new cell.	100
<b>Table 4.2</b>	Experimental results obtained in the study of the vapour-liquid equilibrium line for pure carbon dioxide.	107
<b>Table 4.3</b>	Experimental results obtained in the study of the vapour-liquid equilibrium line for ethane.	112
<b>Table 4.4</b>	List of the different chromatographic capillary columns tested in the present work and their main characteristics: length, internal diameter, film thickness and temperature of applicability.	118
<b>Table 4.5</b>	List of the most important parameters of the generic chromatographic method developed for the analysis of the mixtures of interest for this work.	120
<b>Table 4.6</b>	Approximate retention times observed for the compounds involved in these analyses presented in Figure 4.27 and 4.28, according with the chromatographic method developed.	121
<b>Table 4.7</b>	Determined values for the parameters <i>A</i> and <i>B</i> , and for the concentration of water in the solvent, <i>C</i> , relative to Equation 4.9, in the calibration for water.	131
<b>Table 4.8</b>	Average areas of the chromatographic peaks obtained in the calibration of the GC for water, and number of moles injected.	132
<b>Table 4.9</b>	Results obtained in the analytical study of the system methane + water.	137
<b>Table 5.1</b>	Results obtained during the study of the three-phase coexisting line for the binary system methanol + ethane, using the re-commissioned cell.	162
<b>Table 5.2</b>	Experimental results obtained in the study of the vapour-liquid equilibrium line for carbon dioxide, using the re-commissioned cell.	167

<b>Table 5.3</b>	Results obtained in the first series of measurements of the solubility of methane in pure water, at 298 K.	175
<b>Table 5.4</b>	Results obtained in the second series of measurements of the solubility of methane in pure water, at 298 K and at 283 K.	177
<b>Table 6.1</b>	Synthesis of the modifications implemented in the sPC-SAFT EoS relatively to the original PC-SAFT EoS.	195
<b>Table 6.2</b>	Summary of the sets of PC-SAFT pure component parameters used in the present work.	196
<b>Table 7.1</b>	Approximate global composition of the quaternary mixture methane + <i>n</i> -hexane + methanol + water studied in this work, given in molar fraction of the components.	210
<b>Table 7.2</b>	Results obtained in the study of the quaternary mixture methane + <i>n</i> -hexane + methanol + water, at 298.42 K and 9.8 MPa.	211
<b>Table 7.3</b>	Results obtained in the study of the quaternary mixture methane + <i>n</i> -hexane + methanol + water, at 298.31 K and 7.3 MPa.	211
<b>Table 7.4</b>	Summary of the sets of PC-SAFT pure component parameters used in the calculations presented in the current chapter, included in the SPECS software.	213
<b>Table 7.5</b>	Values of $k_{ij}$ found in the modelling of the binary system methane + water, at five different temperatures between 283 K and 373 K.	221
<b>Table 7.6</b>	Values of $k_{ij}$ found in the modelling of the six binary systems binary systems formed with the constituents of the quaternary system methane + <i>n</i> -hexane + methanol + water.	223
<b>Table 7.7</b>	Results obtained in a multiphase flash calculation using sPC-SAFT, for the mixture methane + <i>n</i> -hexane + methanol + water, at 298.42 K and 9.8 MPa, and comparison with experimental values.	224

<b>Table 7.8</b>	Influence of $k_{ij}$ values for the binary system methane + <i>n</i> -hexane in the multiphase flash calculation for the mixture methane + <i>n</i> -hexane + methanol + water, at 298.42 K and 9.8 MPa.	225
<b>Table 7.9</b>	Results obtained in a multiphase flash calculation using sPC-SAFT, for the mixture methane + <i>n</i> -hexane + methanol + water, at 298.31 K and 7.3 MPa, and comparison with experimental values.	226
<b>Table 8.1</b>	List of references found in a literature search for the binary system carbon dioxide + water.	237
<b>Table 8.2</b>	Results obtained in the in the measurements of the solubility of carbon dioxide in pure water, at temperatures around 298 K.	238
<b>Table 8.3</b>	Results obtained in the in the measurements of the sorption of carbon dioxide in an aqueous solution of 2-ethanolamine 30 wt%, at temperatures around 298 K.	240
<b>Table 8.4</b>	Results obtained in the in the measurements of the sorption of carbon dioxide in an aqueous solution of L-proline 7.0 molal, at temperatures of 300 K and 353 K	243
<b>Table A1.1</b>	List of references for systems containing mixtures of methane and other hydrocarbons.	260
<b>Table A1.2</b>	List of references for systems containing mixtures of ethane and other hydrocarbons.	261
<b>Table A1.3</b>	List of references for binary systems containing methane and water.	262
<b>Table A1.4</b>	List of references for binary systems containing ethane and water.	264
<b>Table A1.5</b>	List of references for binary systems containing propane and water.	265
<b>Table A1.6</b>	List of references for binary systems containing <i>n</i> -butane and water.	266

<b>Table A1.7</b>	List of references for binary systems containing <i>n</i> -pentane and water.	267
<b>Table A1.8</b>	List of references for binary systems containing <i>n</i> -hexane and water.	267
<b>Table A1.9</b>	List of references for binary systems containing <i>n</i> -heptane and water.	268
<b>Table A1.10</b>	List of references for binary systems containing <i>n</i> -octane and water.	268
<b>Table A1.11</b>	List of references for binary systems containing <i>n</i> -nonane and water.	269
<b>Table A1.12</b>	List of references for binary systems containing <i>n</i> -decane and water.	269
<b>Table A1.13</b>	List of references for multi-component systems of hydrocarbons and water.	269
<b>Table A1.14</b>	List of references for systems containing methanol and hydrocarbons.	270
<b>Table A1.15</b>	List of references for systems containing MEG and hydrocarbons.	272
<b>Table A1.16</b>	List of references for systems containing DEG, TEG or TeEG and hydrocarbons.	273
<b>Table A1.17</b>	List of references for systems containing methanol and water.	274
<b>Table A1.18</b>	List of references for systems containing MEG, DEG, TEG or TeEG and water.	275
<b>Table A1.19</b>	List of references for systems containing water, methanol and hydrocarbons.	275
<b>Table A1.20</b>	List of references for systems containing water, MEG, DEG, TEG or TeEG as hydrate inhibitor and hydrocarbons.	276
<b>Table A1.21</b>	List of references for systems containing methane, water and salts.	277
<b>Table A1.22</b>	List of references for other relevant systems	277

<b>Table A2.1</b>	List of individual data points obtained for the water mole fraction in the gas phase, in the analytical study of the system methane + water.	293
<b>Table A2.2</b>	List of individual data points obtained for the methane mole fraction in the aqueous phase, in the analytical study of the system methane + water.	295
<b>Table A2.3</b>	List of individual data points obtained in the analytical study of the system methane + <i>n</i> -hexane + methanol + water, at 298 K and 9.8 MPa.	297
<b>Table A2.4</b>	List of individual data points obtained in the analytical study of the system methane + <i>n</i> -hexane + methanol + water, at 298 K and 7.3 MPa.	297







# **Chapter 1**

## **Introduction**

---

Vast quantities of so-called "production chemicals" are used by the natural gas industry, in order to facilitate production from reservoirs and transport in pipelines. Examples of such chemicals are hydrate inhibitors, such as methanol or glycols, which are injected to the natural gas well stream, in order to prevent the formation of gas hydrates during transportation and further processing.

Hydrates, or clathrates, are crystalline solid compounds formed when water assumes a cage-like structure around smaller guest molecules such as the ones present in natural gas, and their discovery is usually credited to Sir Humphrey Davy, in 1810 [1]. Hydrates remained a mere chemical curiosity until the mid-1930s, when it was discovered that pipelines and processing equipment used in the natural gas industry were becoming plugged with what appeared to be ice, at temperatures above the formation temperature of ice. It was Hammerschmidt [2] who demonstrated that this "ice" was in fact gas hydrates. The relevance of the problem is increasing with the exploration of arctic fields and the tendency towards longer offshore pipelines, placed on the seabed. The blocking of a pipeline due to the formation of hydrates translates into high economic losses, not only due to the need to remediate the situation, but also due to the consequent disruption in the production.

Compounds like methanol or ethylene glycol are good thermodynamic inhibitors, lowering the temperature of hydrate formation for a given pressure. But due to the occurrence of problems with the formation of hydrates under conditions in which problem-free operation would be expected, especially in places of peaks of flow such as choke valves, the tendency in the use of hydrate inhibitors has gone in the direction of

applying considerable safety margins, with an excess of inhibitors being regularly used in the processes, with economical and environmental consequences.

With the trend towards long distance multiphase flow pipelines, a considerable amount of money is spent on these chemicals. In the case of offshore production, these inhibitors are transported through pipelines to the well. In the Statoil Hammerfest LNG (liquefied natural gas) plant in Norway, for example, ethylene glycol (MEG) is transferred in its own pipeline from land and injected offshore into the well stream at the choke [3,4]. A mixture of gas, condensate, water and ethylene glycol (MEG) arrives onshore after a 143 km long pipeline, with a diameter of 680 mm, with all the components distributed through all the phases. At the process plant, at the island of Melkøya, the phases are separated for further processing. The gas undergoes further treatment, in which triethylene glycol (TEG) is used to promote the dehydration of the gas, since the presence of water could lead to the plugging of pipelines and process equipment and contributes to corrosion problems. TEG is also used in the drying of the recovered carbon dioxide, before this can be liquefied and piped back to the Snøvit field for injection in a different formation, for storage. MEG is treated in order to remove solid particles, salt and most of the water, before it can be recycled back to the field with about 10% of water, through a dedicated pipeline. For the optimization of all these treatment processes, the precise knowledge of the phase equilibria involving these compounds is critical, even in the cases of very low concentrations. It is essential to evaluate the amount of glycol lost in the gas phase and in the condensate and to determine the solubility of aromatics in the glycol rich phase, due to possible emissions during the regeneration process of the glycol. It is also desirable to have a better understanding of the hydrate formation conditions for such complex systems, allowing a reduction in the safety margins.

In order to provide an idea of the amount of money spent on hydrate inhibitors, Sloan [5] cites the example of the Canyon Express project, a joint development in the Gulf of Mexico with a combined tieback gas production of 500 million standard cubic feet per day and 1000 barrels per day of water. The costs involved in the use of methanol as hydrate inhibitor are approximately 18 million USD per year, taking into account a saving of 4 to 5 million USD per year supported by the recovery and recycling of the methanol. A reduction of 5% in the amounts of methanol used would lead to additional savings close to 1 million USD per year.

Different methods and software can be used to obtain more or less accurate predictions of the conditions for hydrate formation, even for some complex systems, but the results are still poor for high pressure systems (above 30 MPa), systems with high concentrations of acid gas or for estimating the partition of the inhibitor between the aqueous and the organic phases [5]. In the prediction of phase equilibrium, there is still much room for improvement in the different methods, especially concerning the characterisation of complex systems such as the aforementioned example of the Statoil Hammerfest LNG plant. In some cases, only precise and accurate experimental data from “real-life” systems can provide the necessary basis, not only to optimize the different processes, but also to reduce safety margins, leading to a reduction in the amounts of inhibitors used. Using only the amount of inhibitor that is strictly necessary for risk-free operation has inherent economic and environmental advantages.

The need for high-quality experimental phase equilibria data is true for the chemical industry in general. Examples include pharmaceutical processes, the food industry, chemical separation processes, refrigeration, reservoir simulation, gas processing, applications involving supercritical fluids or chromatography, and new fields such as ionic liquids, carbon dioxide sequestration and storage or “green solvents”. All these areas deal with processes whose optimisation is dependent on phase equilibria data. The importance of reliable and precise experimental phase equilibrium data is recognised by the scientific community as well as by industry. Richon [6] has documented statements by several prominent scientists and engineers, unanimously of the opinion that more high quality data is necessary.

Despite the fact that computational methods for prediction of phase equilibria have made considerable progress lasting recent years, the experimental measurement of phase equilibrium remains an indispensable source of data, especially where theoretical methods fail, for example for high pressures, or in complex systems. The continuous developments in science and industry require data for new types of compounds, or simply for new temperature and pressure ranges. The oil and gas industry is a good example of this. As oil prices increase, new locations become profitable for drilling, often meaning new product compositions and/or new climatic conditions. In especially sensitive areas, environmental regulations may impose limitations on emissions, requiring higher efficiency separation

processes, or may even prohibit the use of some of the common production chemicals, which have then to be replaced with new and more environmentally friendly compounds.

Even for simpler systems, which have been studied at various times over the years by different researchers, the data is sometimes scarce in particular ranges of pressure and temperature. In other cases, the abundance of data reveals considerable discrepancies in the results obtained by different research groups, as recently demonstrated for example by Folas et al. [7], who gathered several published values concerning the solubility of methane in water.

Computational models, molecular simulations and correlation methods can however be used in order to reduce the number of experimental data points to be measured. Ultimately, a combination of both experimental measurements and computational methods is desirable, but experimental data will always have a decisive role in the validation of theoretical methods and in the adjustment of parameters in correlations [8].

Despite the overwhelming importance of experimental data, reliable and precise measurements can be difficult to achieve and are often expensive and relatively slow, representing a serious investment, not only concerning the acquisition of equipment or the development of custom-made experimental set-ups, but also regarding human resources. However, the costs for a company of using imprecise data can be much higher, and may have serious consequences where safety is concerned. Also, young researchers are sometimes influenced by the idea that performing calculations or simulations in an office is more comfortable than tedious hours spent in the lab, and that theoretical work will bring them more recognition and possibly publishable results at a faster rate. This may be the cause of the worrying lack of experimentalists, lamented in some of the cited statements in the article by Richon [6].

Another serious problem is the existence of experimental data of dubious quality. Either because the lack of experimental data prompts researchers with little or no experimental experience to go into the laboratory in order to produce data which they can use to back-up their models, or because of a lack of understanding of the sensitivity of some experimental aspects, there exist in the literature several works in which a simple analysis of the apparatus used or of the experimental procedure, reveals the existence of important sources of errors. These are either neglected or not quantified, as noticed in the

preparation of two recent works which involved the analysis of approximately 1500 articles containing experimental high-pressure phase equilibrium data, published between 2000 and 2008 [9,10].

In some cases, it is verified that the real accuracy of published experimental data is much lower than the accuracy claimed by the authors for the apparatus used. Often, this can be explained by the fact that less experienced staff has overlooked sources of errors in the experimental procedure. Quality measurements are not easy to perform and many mistakes can be made. In many cases, the quality of the staff performing and supervising the experiment has a higher impact on the results than details of the equipment, as recently demonstrated in an example provided in Fonseca et al. [10]. Experience is very important, since experimental difficulties and mistakes are rarely published, though they are an essential part of the know-how for measuring high-quality data. This knowledge can be developed and maintained within the research group, but only if a certain level of ongoing experimental activity exists. A survey of the European Federation of Chemical Engineering on industrial needs for thermodynamics and transport properties [11] showed that there is a clear need for qualified laboratories with experienced staff to provide experimental measurements.

The present work, included in a broader research project under the title “Gas Hydrates - from Threat to Opportunity”, financially supported by the Danish Technical Research Council, sets out to provide a modest yet solid contribution to bridging the abovementioned gaps in experimental data, not only by measuring new data, but by developing new experimental equipment for the study of phase equilibria through the use of different methods.

The work was particularly challenging as it involved developing custom-made set-ups in an area in which the laboratory has little or no experimental experience. The development of new apparatus comprises invariably a number of time consuming steps, such as designing, procuring parts, machining, building and testing the equipment, some of them depending on the work of third parties. In the present work, some of these steps took much longer than anticipated, with the consequence that it was only possible to generate data in the latter part of the project. A considerable amount of time was equally spent on setting-up, calibrating and on acquiring the necessary expertise in gas chromatography methods, since these are not routinely used in the laboratory at present.

Parallel to this, a simplified version of the PC-SAFT equation of state, proposed by von Solms et al. [12] and already applied to a number of complex systems [13,14], was used in the modelling of mixtures containing hydrocarbons, water and thermodynamic hydrate inhibitors. Such systems, containing associating compounds, are challenging from a theoretical point of view since the components form hydrogen bonds and often exhibit an unusual thermodynamic behaviour.

An additional part of the work focused on the topic of carbon dioxide capture, through the experimental study of the sorption of this gas in amine and amino-acid salts solutions. The removal of carbon dioxide and other acidic gases has been an important operation in several industries for a long time. In the production of natural gas for example, carbon dioxide is often present in the production gas mixtures, as in the case of the Snøvit field already mentioned, and the extraction of this gas is one of the first steps of the gas processing at the Statoil LNG plant, in the island of Melkøya, close to Hammerfest [3]. Removing this gas is essential, as its presence would contribute to the occurrence of corrosion in pipes and other equipment, due to its acidic nature. Furthermore, the presence of carbon dioxide in the final product would decrease the heating value of the natural gas.

Over the last decades, the removal of CO<sub>2</sub> from flue gas streams became potentially advantageous from an economic point of view, due to its applications in enhanced oil recovery, its applications in supercritical processes and in many other industrial applications such as the carbonation of brine, as an inert gas in welding, food and beverage carbonation, dry ice, urea production and soda ash industry [15,16]. More recently, the problem of climate change has led to concerns about the emission of greenhouse gases. Although having a global warming potential lower than that of methane and other hydrocarbons, carbon dioxide is estimated to account for 60% of the enhanced greenhouse effect due to the volume of emissions [17], a fact that has placed this gas in the centre of many environmental policies, leading consequently to a substantial intensification of the research around carbon dioxide capture and sequestration, with attempts to improve the existing technologies and the development of innovative ones.

Several technologies are available for the separation and capture of carbon dioxide, from absorption techniques to adsorption, membrane separation, cryogenic separation or biological capture [15,18]. Capture by absorption is currently one of the most common technologies, and it is regarded by some authors as the most viable solution, at least for the

near future, when compared with other methods [19]. Nevertheless, further developments and optimisations are still necessary, in order to reduce the cost associated with the process [20]. One of the possible improvements is related to the use of new solvents, and several options have recently been considered. Currently the most common sorbents used are aqueous solutions of alkanolamines, mainly monoethanolamine (MEA), which presents several advantages over other alkanolamines, but which also presents some disadvantages, as recently pointed out by Ma'mun et al. [17], therefore opening possibilities for improvements.

The search for new solvents has included, amongst others, aqueous solutions of different amines, newly developed compounds such as ionic liquids and solutions of amino-acid salts. It is on this last option that this work focused, as a contribution to a project currently going on in our research group, also involving two members of the energy industry.

Due to the innovative aspects of their application, both the use of ionic liquids and aqueous solutions of amino-acid salts as sorbents, again constitute good examples of areas for which new and accurate experimental data is essential, in order to supply the basis for an eventual subsequent establishment of theoretical predictive methods.

## **References**

- [1] H. Davy, *Philos Trans R Soc London* 101 (1811) 1-35.
- [2] E. G. Hammerschmidt, *Ind. Eng. Chem.* 26 (1934) 851-855.
- [3] *The Long road to LNG*, Statoil ASA, 2005.
- [4] E. Berger, W. Förg, R. S. Heiersted, P. Paurola, *The Snøhvit Project*, in: *Linde Technology - Reports on Science and Technology*, Linde AG, 2003, 12-23.
- [5] E. D. Sloan, *Fluid Phase Equilib.* 228-229 (2005) 67-74.
- [6] D. Richon, *Pure Appl. Chem.* 81 (2009) 1769-1782.

- [7] G. K. Folas, E. W. Froyna, J. Lovland, G. M. Kontogeorgis, E. Solbraa, *Fluid Phase Equilib.* 252 (2007) 162-174.
- [8] R. Dohrn, *Berechnung von Phasengleichgewichten*, Vieweg-Verlag, Wiesbaden, 1994.
- [9] R. Dohrn, S. Peper, J. M. S. Fonseca, *Fluid Phase Equilib.* 288 (2010) 1-54.
- [10] J. M. S. Fonseca, S. Peper, R. Dohrn, *Fluid Phase Equilib.*, *In press*
- [11] E. Hendriks, G. Kontogeorgis, R. Dohrn, J.-C. de Hemptinne, I. G. Economou, L. Fele Žilnik, V. Vesovic, *Ind. Eng. Chem. Res.* (2010).
- [12] N. von Solms, M. L. Michelsen, G. M. Kontogeorgis, *Ind. Eng. Chem. Res.* 42 (2003) 1098-1105.
- [13] N. von Solms, J. Kristensen, *Int. J. Refrig.* 33 (2010) 19-25.
- [14] N. Muro-Sune, G. M. Kontogeorgis, N. von Solms, M. L. Michelsen, *Ind. Eng. Chem. Res.* 47 (2008) 5660-5668.
- [15] A. B. Rao, E. S. Rubin, *Environ. Sci. Technol.* 36 (2002) 4467-4475.
- [16] T. Suda, M. Iijima, H. Tanaka, S. Mitsuoka, T. Iwaki, *Environ. Prog.* 16 (1997) 200-207.
- [17] S. Ma'mun, H. F. Svendsen, K. A. Hoff, O. Juliussen, *Energy Convers. Manage.* 48 (2007) 251-258.
- [18] B. Freeman and R. Rhudy, *Assessment of Post-Combustion Capture Technology Developments*, EPRI, Electric Power Research Institute, Inc., 2007.
- [19] A. Meisen, X. S. Shuai, *Energy Convers. Manage.* 38 (1997) S37-S42.
- [20] I. Kim, H. F. Svendsen, *Ind. Eng. Chem. Res.* 46 (2007) 5803-5809.

# **Chapter 2**

## **Experimental Data for Systems Related to Hydrate Inhibition – a Review**

---

Phase equilibrium is a very broad subject, of great importance in many industrial and scientific areas. It is, therefore, not surprising to find that large collections of experimental data on phase equilibrium have been gathered over the years, some more general, and some focusing on specific areas or on special types of compounds. The DECHEMA Chemistry Data Series for example, from DECHEMA e.V., Germany, is a collection of 15 volumes, each dedicated to a specific type of data, such as vapour-liquid equilibrium (VLE), liquid-liquid equilibrium (LLE), solid-liquid equilibrium (SLE), critical data, electrolytes, polymers, etc. Another renowned collection of data is the IUPAC Solubility Data Series, a set of 88 volumes published since 1979, with the data appearing also in the Journal of Physical Chemistry and Reference Data since volume 66, published in 1998. 18 of these volumes are also integrated in an IUPAC-NIST Solubility Database, available online.

Set aside these large databases, it is also possible to find a great number of books and reviews in the literature, published over the years by several authors. Hála et al. [1] presented in 1967 an extensive list of systems for which experimental VLE data at moderate pressures had been published up to May of 1965 inclusive. The total number of references found by the authors in the literature was 2656, with an even higher number of systems considered. Hála et al. [1] also mentioned several other existing reviews and books which can be used as a source of data. Books frequently constitute good indirect sources of

references for experimental works. On the subject of gas hydrates, for example, several books can be mentioned, such as the work of Sloan [2], the book of Carroll [3], or the book by Maurer [4], among others. However, nowadays, it is often more practical to search for data online, in scientific journals, which allow access to more recent data, and often to the direct sources of experimental data.

Countless reviews on phase equilibrium can be found in the literature, and being such an extensive topic, most of the reviews available are restricted to certain pressure ranges [1], or to certain pressure ranges and specific periods of time [5-9], or more commonly, limited to a specific topic, for instance, the solubility of particular compounds on supercritical carbon dioxide, such as the review of Bartle et al. [10] focusing on solids and liquids of low volatility, the works of Güçlü-Üstündag and Temelli [11-13] on the solubility of lipids, the work published by Higashi and co-workers [14] focusing on high-boiling compounds, or the work by Lucien and Foster [15] on solid mixtures. Esperança et al. [16] recently presented a review on the volatility of aprotic ionic liquids for the period 2003-2008. Among other recent reviews, the publications of Keskin et al. [17] on the phase behaviour of ionic liquids with supercritical fluids, of Marsh et al. [18,19] focusing the critical properties of elements and compounds, and of Sawamura [20] on the solubility of inorganic and organic compounds in liquids at high pressures can also be mentioned. Loveday and Nelmes recently presented a review on gas hydrates for pressures above 0.5 GPa [21]. Additional reviews published over the last years can also be mentioned, some more general [22,23], others of a more restricted objective, focusing on the phase equilibria of long chain *n*-alkanes in supercritical ethane [24], on phase equilibria in systems with esterification reactions [25] or on the extraction of metal ions using supercritical carbon dioxide [26]. Other reviews focus on the phase equilibria measurements of one particular system or substance, such as the case of the one by Diamond and Akenfiev [27] and the review by Spycher et al [28], both for the binary system carbon dioxide + water, or the work of Loerting [29] for phase transitions in ice.

Also for the literature survey presented in this work, it was necessary to impose some restrictions, in order to unequivocally define its boundaries. This chapter will focus on the phase equilibrium in systems containing exclusively light hydrocarbons, more precisely *n*-alkanes with a number of carbon atoms up to 10, water and hydrate inhibitors such as methanol and ethylene glycols, ranging from monoethylene glycol (MEG) to tetraethylene

glycol (TeEG). Some works referring to the phase equilibria in systems containing water with salts are also mentioned.

Since it is virtually impossible to collect all the existing references for this specific area, it should be understood that the aim of this literature review is to gather a significant amount of data sets for the types of systems under consideration, representative enough to provide a clear overview of the existing data and its gaps, as well as to compare and, whenever possible, evaluate the quality of the available data sets. Furthermore, it is a clear objective of this work to mention the publications where the original raw data can be found, avoiding reviews, and works presenting only fitted equations or other smoothed data. Only by accessing the original sources of data, has the reader the possibility to make his own evaluation on the quality and precision of the data, with information on the scattering of individual points, on the experimental method used, and on the apparatus employed in the measurements, avoiding the simple indiscriminate use of “numbers” which in some cases are already the product of extrapolations or correlations.

In addition, this literature search focuses only on data published in widely available international journals. For almost every particular area of interest it is possible to find a considerable amount of data in smaller and very specific publications, such as the GPA (Gas Processors Association) reports in natural gas production. Besides the limited availability of this type of publications, much of the data is frequently published in the major international journals as well, although in some cases with some delay.

The search for relevant works started with a systematic search for articles published over the last 6 years in the most relevant journals in the thermodynamics and phase equilibria areas, and continued with an analysis of the references cited in those articles. Some of the general phase equilibria reviews previously mentioned [5-9], were also used in the search for relevant articles. Additionally, around 30 recent articles focusing on the modelling of phase equilibrium by means of equations of state and a few works based on molecular simulation were also used in this literature search, as these sometimes constitute excellent sources of references for articles containing experimental data.

In an internal report presented by the author [30], a total of 442 experimental references were provided, referring to experimental data on systems of interest, related to the gas hydrate inhibition. The report was the result of a literature search focusing on the

aforementioned compounds, but also comprises other references found during the survey, referring to systems containing other components, also of relevance for this area of work. Therefore, references to hydrate containing systems, systems containing the so-called “BTEX” compounds (benzene, toluene, ethylbenzene, and xylenes), systems including electrolytes, and other hydrocarbons were also mentioned. The report also includes references to literature sources of limited availability, such as GPA reports, industrial reports, PhD thesis, etc.

To the works mentioned in this internal report, a significant number of additional references were subsequently added, making up for a total of almost 700 references. In order to simplify the consultation of this amount of gathered information, a database was developed, using commonly available software, Microsoft Office Excel<sup>TM</sup>, allowing the user to select a series of parameters, such as the number and the nature of the components of interest, so as to easily obtain a selection of experimental references for the desired system(s), from the bulk of more than 650 references.

This database was used to generate the tables presented in Appendix 1, which contain references to a number of experimental studies, presenting for each case the composition of the system, the temperature and pressure ranges of the study, as well as the reference to the respective work. These 22 tables are structured in terms of the types of systems they refer to. Thus, Table A1.1 and Table A1.2 present a series of references for systems containing respectively, mixtures of methane and of ethane with other light hydrocarbons. Tables A1.3 to A1.13 refer to mixtures of hydrocarbons and water, while tables A1.14 to A1.16 deal with mixtures of the mentioned thermodynamic hydrate inhibitors with hydrocarbons. Tables A.17 and A.18 refer to mixtures of inhibitors with water, Tables A1.19 and A1.20 contain information regarding mixtures of hydrocarbons, water and hydrate inhibitors. Table A1.21 presents a series of references to systems consisting of hydrocarbons, water and salts, and finally, Table A1.22 comprises information on a small number of additional systems, not included in the previous tables.

In total, more than 250 references are given in these tables, for articles containing experimental results for systems containing exclusively light *n*-alkanes, water and hydrate inhibitors. The articles cited often also contain data for other systems not mentioned in the tables, as they are not of relevance for the present work. For the same reason, many articles included in the database referring to systems containing hydrates were also not presented

in the tables, even when the data is not directly related to the hydrate phase itself, such as the case of studies on the solubility of gas in the aqueous liquid phase, in equilibrium with gas hydrates.

Aside from the systematic citation of the experimental works, given in the tables, it is worth mentioning a number of particular works. A notable example, although not focusing exclusively on the systems considered of interest for this work, is the series of experimental works on high pressure phase equilibria published by the late Erwin Brunner, over a period of several years [31-40].

The simpler systems considered in this work consist of mixtures of hydrocarbons. Uribe-Vargas and Trejo [41] presented a review on systems consisting mostly of methane and several different heavier hydrocarbons. The authors present an extended list of references for the solubility of methane and of mixtures of gaseous hydrocarbons in liquid hydrocarbons.

Also relatively simpler type of systems considered in this work are the mixtures containing water and hydrocarbons. Several articles can be found in the literature, mainly for the systems methane + water and ethane + water, simple systems of great interest for the natural gas industry, which also constitute good test systems for the evaluation of thermodynamic models. From an experimental point of view however, these are challenging systems, due the very low solubility of the gas in water, and even lower amounts of water in the gas phase, especially for high pressure systems.

The first study of the solubility of methane in water was performed by Bunsen, in the year of 1855 [42], in a work which included the measurement of the solubility of various gases in water under atmospheric pressure, using a synthetic method (see Chapter 3 for the categorization of experimental methods). The same method was also used by Winkler in 1901 [43]. Data for high pressure solubility of pure methane in water were first reported by Frohlich et al. in 1931 [44]. These and several other sources of data for the solubility of this gas in water are mentioned by Lekvam and Bishnoi [45], who presented a small review for this binary system, in conjunction with new data relative to pressures up to 10 MPa at different temperatures. In a work containing new data for the solubility of natural gas components in water with and without hydrate inhibitor, Wang et al. [46] also presented a small review on the solubility of methane in water, emphasising the lack of consistency

between the different data sets existing in the literature, justified by the author as being mainly due to the difficulties in quantifying such low solubility values.

Even lower solubilities are found for water in the gaseous hydrocarbon phase, especially when high pressures are considered. Mohammadi et al. [47] recently presented a work on the experimental measurement of the water content in methane and ethane. In this work, the authors included a review on the experimental methods commonly used in the determination of the low water content or water dew point in gases. Parallel to this, a review on the water content in major constituents of natural gas is also presented. Folas et al. [48] also focused on the water content of high pressure gases, particularly nitrogen, methane and natural gas. In this work, the authors presented a table containing the concentrations of water in methane and in nitrogen at high pressures, obtained by different authors and different methods, underlining the observable discrepancy between the different values. In the case of water in methane, for instance, the value obtained by Chapoy et al. [49] for a temperature of 283 K and a pressure around 6 MPa, is about one half of the values found by the authors, which are in agreement with other sets of data found in the literature [50,51]. Concerning the values for the binary system nitrogen and water, the disparity between the different values found in the literature for the same experimental conditions is also noticeable.

Jou et al. [52] presented a work on the phase equilibria in the system *n*-butane + water + methyldiethanolamine (MDEA), in which the authors included an analysis of the available literature data for the binary system *n*-butane + water. According to the authors, the various literature sources are in good agreement where the pressure and temperature along the three-phase line is concerned. However, significant differences are found in the results for the compositions of the different phases in equilibrium at the mentioned conditions, particularly in the compositions of the co-existing liquid phases.

Other noteworthy publications concerning mixtures of water and hydrocarbons, is for example, the work of Tsonopoulos [53], who presents an analysis on the mutual solubilities for systems of water and *n*-alkanes with a number of atoms of carbon between 2 and 16. Énglin et al. [54] presented an experimental work in which new data for the solubility of water in nearly 60 different hydrocarbons is presented, while McAuliffe [55] presented a work containing the results for the measurements of the solubilities of 65 hydrocarbons in water, at room temperature, by means of a gas-liquid partition

chromatographic technique. Also worth mentioning is the review of Wilhelm et al. [56], focusing on the low-pressure solubility of gases in liquid water.

For the systems containing hydrate inhibitors, a large number of references can be found for the systems containing methane or ethane + methanol, largely due to its application in the natural gas industry as hydrate inhibitor. Among the four glycols considered in this work, TEG was studied more frequently, a fact that can be justified by its wide application in the dehydration of natural gases and other hydrocarbons in general. Studies on mixtures involving methanol and heavier hydrocarbons such as *n*-hexane or *n*-heptane are also relatively common, due to the interest in these systems for fuel substitution, mainly in countries such as South Africa or Brazil for example, in which petrol is blended with methanol [57,58].

Nevertheless, and as verified before for the systems containing hydrocarbons and water mentioned in the last paragraphs, the existence of various sets of data does not necessarily imply a lower uncertainty in the knowledge of the systems in question, as often the existing data are in clear disagreement with each other. This was verified by Hradetzky and Lempe [57] who re-measured the LLE (liquid-liquid-equilibrium) for the system methanol + *n*-hexane after verifying the existence of divergences between the values previously presented [59] and literature data [60-62]. Also Cordray et al. [63] mention the existence of discrepancies for the literature values of the freezing line (SLE, solid-liquid equilibrium) of the system MEG + water at concentrations of glycol ranging from 55 wt% to 85 wt%, a type of measurements which, in principle, should be reasonably simple and exempt from problems.

In addition to the disparities between the existing data, another important feature of the analysis of the tables presented in Appendix I, is the limited existence of data for particular ranges of temperatures and pressures. This can be easily demonstrated if for instance, the study of the system methane + water at a temperature of 298.15 K and moderate pressures, between atmospheric pressure and 1 MPa, is considered. From the 56 references mentioned in Table A.3, only 4 of them can be used for comparison in the experimental conditions considered. Furthermore, the data available in the majority of the works mentioned in this table refer either to solubilities of water in the gas phase, or to the solubility of the gas in water. An analysis of the data available for other systems leads

frequently to the same conclusion, and this situation is even more significant for more complex systems, for which the number of existing data is reduced.

In conclusion, what the result of this thorough literature survey indicates, is the need for more experimental data, accurate, reliable, in extended ranges of experimental conditions, and whenever possible including a characterisation of the system in equilibrium as complete as possible.

## **References**

- [1] E. Hála, J. Pick, V. Fried, O. Vilím, Vapour Liquid Equilibrium, 2nd ed., Pergamon Press, 1967.
- [2] E. D. Sloan Jr., C. Koh, Clathrate Hydrates of Natural Gases, 3rd ed., CRC Press, Taylor and Francis Group, Boca Raton, 2008.
- [3] J. Carroll, Natural Gas Hydrates: A Guide for Engineers, 2nd ed., Elsevier, Oxford, 2009.
- [4] G. Maurer, Thermodynamic properties of complex fluid mixtures, John Wiley-VCH, Weinheim, 2004.
- [5] M. Christov, R. Dohrn, Fluid Phase Equilib. 202 (2002) 153-218.
- [6] R. Dohrn, G. Brunner, Fluid Phase Equilib. 106 (1995) 213-282.
- [7] R. Dohrn, S. Peper, J. M. S. Fonseca, Fluid Phase Equilib. 288 (2010) 1-54.
- [8] J. M. S. Fonseca, S. Peper, R. Dohrn, Fluid Phase Equilib., *In press*
- [9] R. E. Fornari, P. Alessi, I. Kikic, Fluid Phase Equilib. 57 (1990) 1-33.
- [10] K. D. Bartle, A. A. Clifford, S. A. Jafar, G. F. Shilstone, J. Phys. Chem. Ref. Data 20 (1991) 713-756.
- [11] Ö. Güçli-Üstündag, F. Temelli, Ind. Eng. Chem. Res. 39 (2000) 4756-4766.
- [12] Ö. Güçli-Üstündag, F. Temelli, J. Supercrit. Fluids 38 (2006) 275-288.

- [13] Ö. Güçli-Üstündag, F. Temelli, *J. Supercrit. Fluids* 36 (2005) 1-15.
- [14] H. Higashi, Y. Iwai, Y. Arai, *Chem. Eng. Sci.* 56 (2001) 3027-3044.
- [15] F. P. Lucien, N. R. Foster, *J. Supercrit. Fluids* 17 (2000) 111-134.
- [16] J. M. S. S. Esperanca, J. N. C. Lopes, M. Tariq, L. M. N. B. Santos, J. W. Magee, L. P. N. Rebelo, *J. Chem. Eng. Data* 55 (2010) 3-12.
- [17] S. Keskin, D. Kayrak-Talay, U. Akman, Í. Hortatsu, *J. Supercrit. Fluids* 43 (2007) 150-180.
- [18] K. N. Marsh, C. L. Young, D. W. Morton, D. Ambrose, C. Tsonopoulos, *J. Chem. Eng. Data* 51 (2006) 305-314.
- [19] K. N. Marsh, A. Abramson, D. Ambrose, D. W. Morton, E. Nikitin, C. Tsonopoulos, C. L. Young, *J. Chem. Eng. Data* 52 (2007) 1509-1538.
- [20] S. Sawamura, *Pure Appl. Chem.* 79 (2007) 861-874.
- [21] J. S. Loveday, R. J. Nelmes, *Phys. Chem. Chem. Phys.* 10 (2008) 937-950.
- [22] C. P. Hicks, *A Bibliography of Thermodynamic Quantities for Binary Fluid Mixtures*, in: *Chemical Thermodynamics*, The Chemical Society, London, 1978.
- [23] G. M. Schneider, *J. Supercrit. Fluids* 13 (1998) 5-14.
- [24] C. E. Schwarz, I. Nieuwoudt, J. H. Knoetze, *J. Supercrit. Fluids* 46 (2008) 226-232.
- [25] A. Toikka, M. Toikka, Y. Pisarenko, L. Serafimov, *Theor. Found. Chem. Eng.* 43 (2009) 129-142.
- [26] A. Ohashi, K. Ohashi, *Solvent Extr. Res. Dev. , Jpn.* 15 (2008) 11-20.
- [27] L. W. Diamond, N. N. Akinfiev, *Fluid Phase Equilib.* 208 (2003) 265-290.
- [28] N. Spycher, K. Pruess, J. Ennis-King, *Geochim. Cosmochim. Acta* 67 (2003) 3015-3031.

- [29] T. Loerting, C. G. Salzmann, K. Winkel, E. Mayer, *Phys. Chem. Chem. Phys.* 8 (2006) 2810-2818.
- [30] J. M. S. Fonseca, Phase equilibria on systems related with hydrate inhibition - Review, IVC-SEP (Center for Phase Equilibria and Separation Processes), Department of Chemical Engineering, Technical University of Denmark, Denmark, 2008.
- [31] E. Brunner, S. Maier, K. Windhaber, *J. Phys. E: Sci. Instrum.* 17 (1984) 44-48.
- [32] E. Brunner, *J. Chem. Thermodyn.* 17 (1985) 985-994.
- [33] E. Brunner, *J. Chem. Thermodyn.* 17 (1985) 871-885.
- [34] E. Brunner, *J. Chem. Thermodyn.* 17 (1985) 671-679.
- [35] E. Brunner, *J. Chem. Thermodyn.* 19 (1987) 823-835.
- [36] E. Brunner, W. Hultenschmidt, G. Schlichtharle, *J. Chem. Thermodyn.* 19 (1987) 273-291.
- [37] E. Brunner, *J. Chem. Thermodyn.* 20 (1988) 1397-1409.
- [38] E. Brunner, *J. Chem. Thermodyn.* 20 (1988) 273-297.
- [39] E. Brunner, W. Hultenschmidt, *J. Chem. Thermodyn.* 22 (1990) 73-84.
- [40] E. Brunner, *J. Chem. Thermodyn.* 22 (1990) 335-353.
- [41] V. Uribe-Vargas, A. Trejo, *Fluid Phase Equilib.* 238 (2005) 95-105.
- [42] R. Bunsen, *Liebigs Ann. Chem. Pharm.* 93 (1855) 1-50.
- [43] L. W. Winkler, *Ber. Dtsch. Chem. Ges.* 34 (1901) 1408-1422.
- [44] P. K. Frolich, E. J. Tauch, J. J. Hogan, A. A. Peer, *Ind. Eng. Chem.* 23 (1931) 548-550.
- [45] K. Lekvam, P. R. Bishnoi, *Fluid Phase Equilib.* 131 (1997) 297-309.

- [46] L. K. Wang, G. J. Chen, G. H. Han, X. Q. Guo, T. M. Guo, *Fluid Phase Equilib.* 207 (2003) 143-154.
- [47] A. H. Mohammadi, A. Chapoy, D. Richon, B. Tohidi, *Ind. Eng. Chem. Res.* 43 (2004) 7148-7162.
- [48] G. K. Folas, E. W. Froyna, J. Lovland, G. M. Kontogeorgis, E. Solbraa, *Fluid Phase Equilib.* 252 (2007) 162-174.
- [49] A. Chapoy, C. Coquelet, D. Richon, *Fluid Phase Equilib.* 214 (2003) 101-117.
- [50] N. E. Kosyakov, B. I. Ivchenko, P. P. Krishtopa, *Vopr. Khim. Tekhnol.* 47 (1982) 33-36.
- [51] K. Althaus, *Fortschr. -Ber. VDI Reihe 3* (1999) 350.
- [52] F. Y. Jou, J. J. Carroll, A. E. Mather, F. D. Otto, *Fluid Phase Equilib.* 116 (1996) 407-413.
- [53] C. Tsouopoulos, *Fluid Phase Equilib.* 156 (1999) 21-33.
- [54] B. A. Énglin, A. F. Platé, V. M. Tugolukov, M. A. Pryanishnikova, *Chem. Technol. Fuels Oils 1* (1965) 722-726.
- [55] C. McAuliffe, *J. Phys. Chem.* 70 (1966) 1267-1275.
- [56] E. Wilhelm, R. Battino, R. J. Wilcock, *Chem. Rev.* 77 (1977) 219-262.
- [57] G. Hradetzky, D. A. Lempe, *Fluid Phase Equilib.* 69 (1991) 285-301.
- [58] T. M. Letcher, S. Wootton, B. Shuttleworth, C. Heyward, *J. Chem. Thermodyn.* 18 (1986) 1037-1042.
- [59] G. Hradetzky, H. J. Bittrich, *Int. Data Ser.* 3 (1986) 216.
- [60] P. Alessi, M. Fermiglia, I. Kikic, *J. Chem. Eng. Data* 34 (1989) 236-240.
- [61] I. F. Hölscher, G. M. Schneider, J. B. Ott, *Fluid Phase Equilib.* 27 (1986) 153-169.

- [62] J. M. Sørensen, W. Artl, Liquid-liquid equilibrium data collection. DECHEMA Chemistry Data Series, Frankfurt (1979).
- [63] D. R. Cordray, L. R. Kaplan, P. M. Woyciesjes, T. F. Kozak, Fluid Phase Equilib. 117 (1996) 146-152.

## **Chapter 3**

# ***Experimental Methods for the Measurement of Phase Equilibria***

---

A wide variety of methods and techniques are currently available for application to experimental studies of phase equilibria. The author previously presented an extensive overview of methods and techniques available for the determination of very low vapour pressures, down to  $10^{-5}$  Pa [1]. The present work, however, focuses on the high-pressure range, as mentioned in the last chapter. Several reviews available in the literature, some of them mentioned in Chapter 2, include a description and classification of the different methods available for such experimental studies [2-18]. While most of these reviews are general, some others focus on specific types of methods, such as the work of Smith and Fang [5] focusing on the use of diamond anvil cells, or the review presented by Richon [4], centred on the equipments developed in his laboratory, using analytical methods with sampling. Robinson [19] has also presented a review on the experimental techniques used by him and his co-workers in their laboratories. Ruffine et al. [20] mention briefly a number of experimental set-ups used in phase equilibria studies at low temperatures and high pressures, in a work where the authors also present a new apparatus. Other reviews are directed to a specific type of study, such as the work presented by Mohammadi et al. [21] focusing on the experimental methods commonly used in the determination of the water content or water dew point in gases, or the work of Ng and Robinson [22,23], who reviewed the experimental methods commonly used in the determination of hydrate formation conditions.

Although focusing on moderate pressures, the work of Hála et al. [18] is worth mentioning. In addition to the description and classification of experimental methods, the

authors focus on important experimental details such as the correct measurement of temperature and pressure, presenting also a collection of experimental VLE data from a total of 2656 references, published up to May 1965. Obviously, being a work published in 1967, many of the considerations made by the authors concerning the measurements are currently out of date, due to technological progress and by the increase in the use of electronic systems, but nevertheless, some are still valid, and the work in general stands up for its completeness.

The existence of a wide variety of methods for phase equilibria studies at high pressure is related to the fact that there is not a single method that is suitable for all the different types of measurements. In some cases it is not even possible to assert which method is the most appropriate for a specific determination, with different methods presenting both advantages and disadvantages, as will be shown below. It is therefore helpful to make a categorisation of the experimental methods available. This is especially important in the present work, which involved the development of two new experimental set-ups, in order to allow a better understanding of the reasons behind the choices made for the new equipments.

The categorisation of the methods is not consensual, with different classifications proposed by different authors. Expressions such as “static” and “dynamic” are often used with different meanings by different authors, creating further confusion. Furthermore, the classification of a specific apparatus is not always straightforward, since combinations of different techniques may be used in different methods. The nomenclature adopted in this work, and represented schematically in Figure 3.1, is similar to that presented in two recent works [2,3], consisting in the refinement of the classification used in previous reviews of the same series [7,10].

Two fundamental classes of methods are considered, analytical and synthetic methods, depending on whether the composition of the phases in equilibrium are determined analytically or the system under study has a precisely known global composition, prepared (synthesised) previously to the experiment. The analysis of the phases in equilibrium can be performed with or without sampling, through the use of spectroscopic methods for example. As for the synthetic methods, a distinction can be made between experiments in which a phase change is observed and experiments where no phase change occurs.

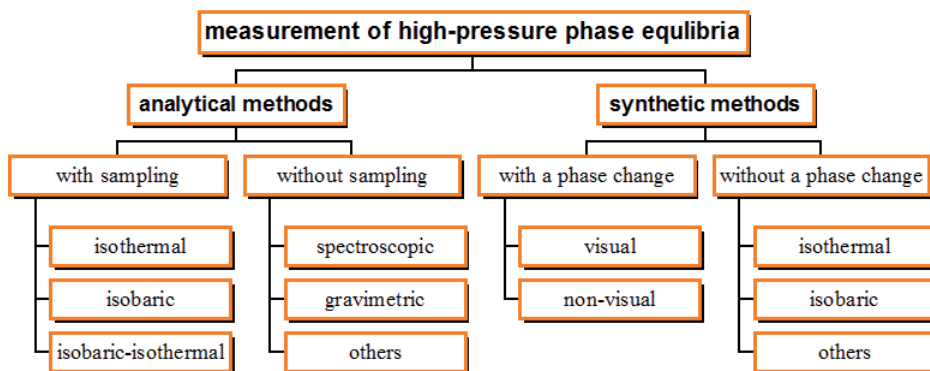


**Figure 3.1** – Categorisation of the experimental methods available for the measurement of high-pressure phase equilibrium.

In the present chapter, the various methods and techniques will be presented, together with short considerations on the main characteristics, advantages, disadvantages and common applications of each of the methods. Whenever possible, examples of applications found in recent literature are also provided.

### 3.1. Analytical Methods

In analytical methods, the equilibrium cell is charged with the components of the system to be studied without precise information of the total composition of the system, and the experimental conditions (temperature and pressure) are set. Once the equilibrium is achieved, the composition of the different phases is determined by withdrawing a sample for subsequent analysis, or by applying a suitable *in situ* physicochemical technique for analysis. The main advantage of analytical methods is the possibility of application to multi-component systems without significant complications, allowing the study of the “real-life” systems typical of industrial problems. The drawback is the necessary higher complexity of the apparatus, which must include an analytical part, often requiring calibrations and previous optimisations of the analytical technique(s).

The methods in which samples are withdrawn from the equilibrium cell can be classified, depending on the procedure used in the achievement of the equilibrium, into isothermal methods, isobaric methods and isobaric-isothermal methods. These methods are

notable for allowing a better understanding of the equilibrium systems under study, with the desirable characterisation of all the different phases involved.

One of the most important aspects to take into account with these methods is the possibility for the occurrence of significant pressure drop when the samples are withdrawn. There are however several techniques which can be used in order to avoid or reduce this issue. The use of a variable volume cell is probably one of the most common solutions to deal with this problem [24-26]. Variable volume cells have a wide application range, not only in analytical methods, but also in cells from where no sampling is performed (synthetic methods), readily allowing for isothermal changes in the pressure for the appearance of new phases, or the observation of critical phenomena, for example. The variation in the volume of the cell is usually made by using a solid moveable piston, whose position is regulated either by direct mechanical actuation [27], or through a pressure transmitter medium and a syringe pump [26,28]. This last technique can be especially efficient and practical if an electronic syringe pump is used [29]. Another possibility is the use of a “liquid piston”, using mercury that can be pumped into or out of the cell in order to change the volume available for the system under study [30-32]. This solution has the advantage of being leak proof, but it also has some drawbacks, such as the toxicity of the metal and the eventual possibility of reaction or solubilisation of some components of the system being studied. Another possible solution to avoid pressure drop is to use a buffer volume in combination with a syringe pump [33], or by blocking off the content of the cell from the sample before withdrawing it [34-38].

The pressure drops are directly related to the proportion between the total volume of the cell in which the system is in equilibrium and the volume of the withdrawn sample. It is therefore possible to minimise the problem by increasing the volume of the cell. Gozalpour et al. [39] for example, used an equilibrium cell with a volume of 9 dm<sup>3</sup> in the study of systems involving gas condensates.

The other obvious solution is, of course, to reduce the volume of the samples, and this can be achieved in several ways. A relatively common solution is the use of special valves, such as HPLC valves [40-43]. These valves allow the collection of the sample into a loop of a previously selected volume, and by actuation of the valve, insert the sample directly into the carrier gas flow of a gas chromatograph, for example. Another possibility is to perform the sampling through capillaries [44,45]. However, sampling through

capillaries can lead to differential vaporization, leading to a scattering in the results, especially in the case of mixtures composed of both light and heavy components, caused by a pressure drop all along the capillary [46]. This problem can be circumvented by means of an adequate experimental design, ensuring that most of the pressure drop occurs at the end of the capillary close to the chromatographic circuit.

The group of Richon, in the CENERG-TEP laboratory of the ENSMP (École Nationale Supérieure des Mines de Paris), developed a system where a micro-stem ending with a nose, enters inside the capillary to reduce the cross-sectional area at the end of the capillary. The system is associated to a fast-acting pneumatic or electromagnetic valve, the ROLSI™ sampler (Rapid On-Line Sampler Injector) [47-49]. These sampler-injectors were developed specifically for application in studies of phase equilibrium, with special attention to relevant details, making them a reference in the area, currently being used worldwide [49-57]. Figure 3.2 depicts an electromagnetic ROLSI™ sampler-injector.



**Figure 3.2** – Picture of an electromagnetic ROLSI™ sampler-injector, showing the actuator and the capillary through which sampling is made.

When special valves are used, the equilibrium cell can be coupled with analytical equipment, such as a high-performance liquid chromatograph [58], a supercritical fluid chromatograph [41], or in the most common solution, a gas chromatograph [50-52,59], usually allowing a sample of very small volume to be withdrawn and injected directly into a carrier gas flow, without any manipulation. It should be pointed out that, both in the case

of the HPLC-valves and of the ROLSI<sup>TM</sup> samplers, it is the reduced sample volume that simplifies the analytical processes, making possible the analysis of the whole sample by chromatography, without risk of saturation of the columns.

It is possible to find in the literature, however, experimental set-ups using an analytical method with sampling, where the volume of the equilibrium cell is considerably small, such as the one used by Bahramifar et al. [60], who used a cell with a total volume of just 0.5 cm<sup>3</sup>, with a loop of 23 mm<sup>3</sup> being used for sampling. Garmroodi et al. [61] used an equilibrium cell of 1 cm<sup>3</sup>, with a sample volume of 143 mm<sup>3</sup>, which accounts for more than 14% of the volume of the cell.

When working with high pressures, any connection to the cell, including sampling ports, is a possible source of leaks. To limit this problem, and to simplify the apparatus, some authors use a single sampling valve, with a mechanism that allows the sampler to move, allowing sampling from different phases. Laursen et al. [62] used a movable sampling needle in the study of VLLE systems. Reports of a cell equipped with a moveable ROLSI<sup>TM</sup> sampler can also be found in the literature [4]. Care should be taken that the movement of the sampler does not influence significantly the pressure in the cell.

A considerable advantage for most of the methods, although it can increase the price of an equilibrium cell, depending on the range of pressures demanded for the application, is the use of windows, for visual observation of the contents of the cell, interfaces between phases, among other phenomena. These windows can be made of thick glass [30,63] or quartz [64], but most commonly sapphire is used [28,65-69]. Although more expensive, sapphire is one of the hardest materials, being much stronger than glass and characterised by a good chemical resistance, thermal conductivity and thermal stability. The use of windows in the equilibrium cells can go from one single window [28,64,66,67] or two small parallel windows [62,70], up to a whole section of the equilibrium cell, making a 360° window [25,30,32,68,69]. It is worth mentioning the apparatus of Secuianu et al. [71], based on a variable volume cell with two sapphire windows where one of the windows is actually the piston.

Another approach for circumventing the problem of the pressure drop associated with sampling processes is, obviously enough, not to carry out any sampling, performing an analysis *in situ* through the use of a convenient physicochemical method. The most

common are spectroscopic methods, as in the case of Andersen et al. [72]. In this type of methods, the use of sapphire for the windows assumes a critical importance, due to the good transmission characteristics over the visible, near IR and near UV spectrum of this material, with a useful optical transmission range of wavelengths ranging from 200 nm to 5500 nm [73,74]. A disadvantage is that occasionally, these methods of analysis only allow the determination of the concentration of a particular compound in the different phases, which may be a limiting factor in the study of multi-component systems. Another aspect to consider is the requirement for time-consuming calibrations under different experimental conditions. Among analytical methods without sampling are also gravimetric methods, such as the used by Sato et al. [75], and other types of methods such as the one used by Boudouris et al. [76].

### ***3.1.1. Analytical Isothermal Methods***

In the isothermal methods, the temperature of the system is kept constant during the whole experiment, including throughout the equilibration process, while other equilibrium properties such as the pressure and the composition of the phases vary with time, until the achievement of the equilibrium values. The experiment starts by charging the equilibrium cell with the substances of interest. The initial value for the pressure is set under or above the desired value, taking into consideration the effect that the equilibration process will have on its value. Once the system is close to equilibrium, further adjustments in the pressure can be performed, by adding or withdrawing material, followed by a new equilibration process. When in equilibrium, the pressure reaches a stable value, and usually, additional time is given to the system without stirring, rocking or recirculation, before withdrawing any samples or performing any measurements, in order to have a good separation of the different phases, which otherwise might lead to non-homogeneous samples, where the sampled phase still contains material from another phase(s), such as droplets, bubbles or solid particles [71]. Figure 3.3 summarises these three fundamental steps, characteristic of the analytical isothermal methods.

In order to reduce the time necessary for the equilibration of the system, several techniques can be employed. The most common is probably the stirring of the mixture. This can be done through the use of a motor with a rotating axis passing through the wall

of the cell [62], making this an especially sensitive point for the occurrence of leaks, due to the wearing of the seals, or through the use of a magnetic system [25,30], that although less efficient under certain conditions, is far simpler, and does not interfere with the air tightness of the cell. The efficiency of magnetic stirring can however be inadequate, when the phases to be mixed have a high viscosity, or in the case of high temperature applications, since the magnets lose their strength with the increase of temperature. This last issue can be minimised by the use of a cooled magnetic stirring system, although this may have some negative impact on the homogeneity of the temperature of the equilibrium cell. In low temperature applications, care should also be taken so that the heat usually produced by the stirring motor does not interfere with the temperature of the equilibrium cell. In the study of systems with gas hydrates, or systems involving very viscous phases, rocking the equilibrium cell can be a good answer to promote faster achievement of the equilibrium [32,77,78]. It is an important requirement for this that all the connections to the cell should be flexible. These methods where stirring or rocking of the cell is performed are sometimes classified as “static-analytical method”.

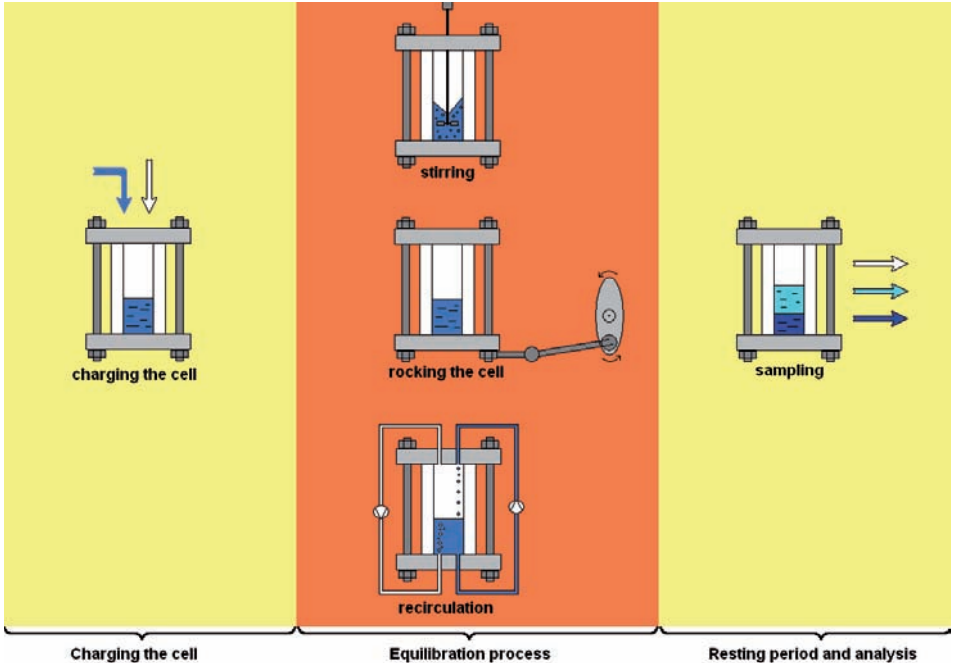


**Figure 3.3** – Schematic diagram showing the three fundamental steps in the application of analytical isothermal methods.

Another common technique is to promote the recirculation of one of the phases, by means of magnetic pumps, forcing the gas phase to be continuously bubbled through the liquid phase [63,79,80], or pumping the liquid phase to the top of the cell, where it re-enters through the gas phase [38,65]. Recirculation of both phases is also used by several authors [40,42,43,81-83]. This is a very effective method for expediting the equilibration process, although the further complexity in terms of connections and tubing can represent a problem, associated with the occurrence of pressure leaks. An additional aspect to take into account is the requirement for a good quality pump, characterised by a small pressure drop, and the need for a uniform temperature throughout the whole loop, so as to avoid partial condensation or vaporization in the recirculation line. Consequently, the application of recirculation methods is not recommended for studies in the region close to the critical point, where small changes in temperature and pressure have a strong influence on the phase behaviour [9]. Another drawback in using recirculation methods is the cost associated with good quality pumps.

Notwithstanding these aspects, recirculation methods may present advantages, when conveniently combined with specific sampling procedures, allowing for example the isobaric filling of a sample volume. Samples can be withdrawn by placing a sampling valve in the recirculation line [58], or by blocking off a determined volume between two valves in the recirculation loop [38,63]. Laursen et al. [84] proposed a simple VLE equipment for the measurement of gas solubility in substances with high stickiness and viscosity, such as wood resins, using recirculation of the vapour phase, and sampling from the liquid phase. The recirculation of both the vapour and the liquid phase, allows sampling from both phases without using capillaries [85,86]. Even in cases where only the liquid phase is circulated, this allows for example the blocking of a large liquid phase volume from the equilibrium cell before pressure reduction [37], in the study of LLE systems or the measurement of solubilities of gases in liquids [87].

Another possibility in the use of recirculation methods is the inclusion in the recirculation loop(s) of a vibrating-tube densitometer allowing the density of the circulated phase to be determined very easily [27,42,43,88,89]. Figure 3.4 presents a schematic drawing of the apparatus used by Tsivintzelis et al. [42,43], where both recirculation loops have been highlighted for easier visual identification. The apparatus presented by Kato et al. [88,89] has nothing less than three density meters, associated to an equal number of

recirculation loops, in a cell developed for the study of VLLE systems, allowing the determination of the density of all the phases. In such density measurements, it is important that the pumps are turned off during the density measurements, in order to avoid errors due to pulsation [86].

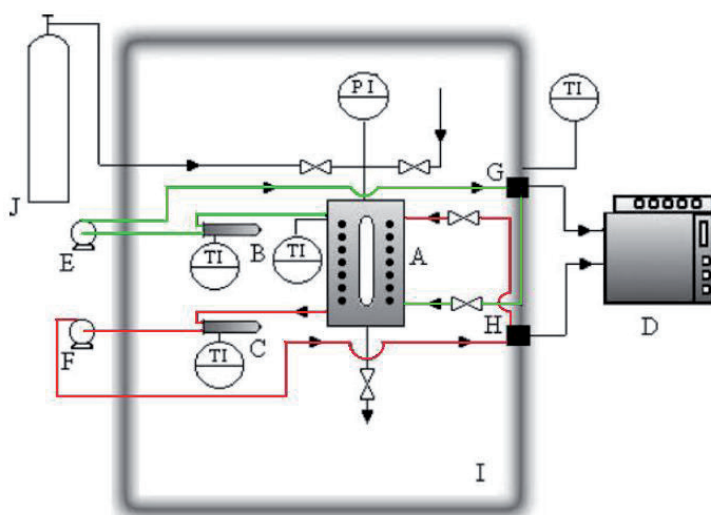


**Figure 3.4** – Schematic drawing of the apparatus used by Tsivintzelis et al. [42,43]. The recirculation loops for the liquid and the gas phase, containing the vibrating densitometers marked by “B” and “C”, were highlighted for easier identification.

In a particular application of blocking off a part of the system, the sampling volume is within the equilibrium cell. This method can be used for example in the measurement of the solubility of solids in supercritical fluids. Sherman et al. [90] put an excess amount of solute in a glass vial, capped with coarse filter paper, in the equilibrium cell. After equilibration and careful depressurization, the vial is removed and weighed. The solubility can be calculated from the difference of the initial and final mass of the solute in the vial and the difference of the volume of the equilibrium cell and the vial. As an alternative, Galia et al. [91] used three vials, of which only one was initially filled with the solute.

Nikitin et al. [92,93] used an alternative technique for measuring sorption of carbon dioxide in polystyrene, avoiding sampling from a high-pressure cell, according to the procedure represented in Figure 3.5.

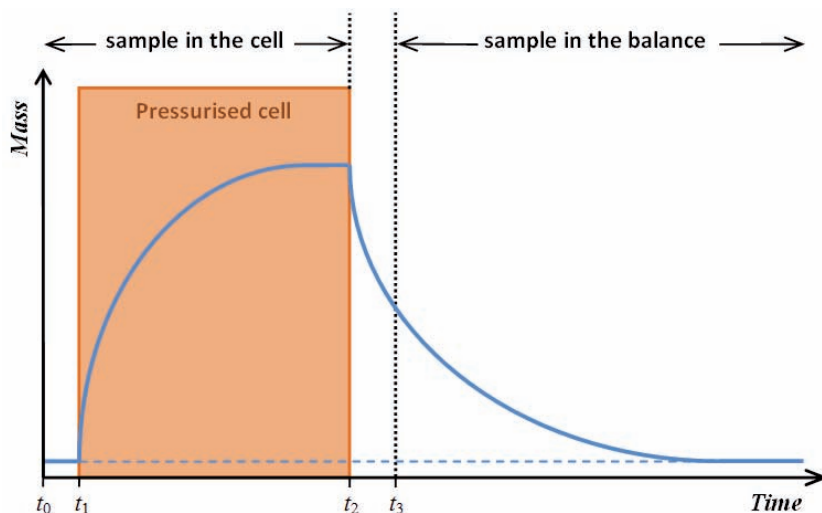


**Figure 3.5** – Schematic representation of the experimental procedure adopted by Nikitin et al. [92,93] in the study of sorption of carbon dioxide in polystyrene.

In the instant  $t_0$  the polymer is placed in the equilibrium cell, which is then pressurised up to the desired value,  $t_1$ . For several hours the volatile component is absorbed in the polymer, until equilibrium is achieved,  $t_2$ . Next, a fast depressurization procedure is performed in less than 10 seconds, followed by a quick transport of the sample to an analytical balance in less than 5 seconds. At instant  $t_3$ , the sample is placed in the analytical balance and the decreasing of the mass of the polymer sample due to desorption of carbon dioxide is recorded over time, allowing the initial value of sorbate mass to be determined by extrapolation of the desorption curve, to the beginning of the depressurization process, represented in the diagram of Figure 3.5 by instant  $t_2$ .

In the study of SLE in systems containing waxes, Pauly et al. [94] used an isobaric and isothermal filtration step, to ensure that the liquid phase to be sampled was free of solid particles. This was performed in an equilibrium cell with two variable-volume chambers connected via a filtration system using a disc of sintered steel with a pore size of 3  $\mu\text{m}$ .

In the analytical isothermal methods, the equilibration process can be followed over time, and sampling is only performed after equilibrium is achieved, which can be observed by the constant pressure value. This is an advantage when compared with analytical isobaric-isothermal methods, where there is the risk of an incomplete equilibration process

if the experimental conditions are not properly chosen. In the period from 2000 to 2008, 22.6% out of 4465 systems considered [2,3] were measured using an analytical isothermal method. In the period from 2000 to 2004 [2], this percentage was of 27.6%, showing that the use of this type of methods has decreased over the last years.

### **3.1.2. Analytical Isobaric-Isothermal Methods**

In isobaric-isothermal methods, sometimes called “dynamic methods”, one or more fluid streams are continuously pumped into a thermostated equilibrium cell. The pressure is kept constant during the whole experiment by controlling an effluent stream, most commonly the vapour phase, using a back-pressure regulator. One of the most important aspects to take into consideration in the application of these methods is related to the time needed for the full equilibration of the system to be attained, which should be sufficiently short, and imposes some limitations on the velocity of the flows. If the equilibration is too slow, there is the risk that the effluents will not correspond to the equilibrium state as desired. Previously to any set of experiments, it is recommended to carry out a number of tests under different flow conditions, in order to evaluate the limits for the systems under study. Analytical isobaric-isothermal methods were used in the study of 13.2% of the systems analysed in [2,3].

### **Continuous-flow methods**

In a typical design of a continuous-flow method, shown schematically in Figure 3.6, high-pressure metering pumps are used to supply a constant flow of the components, which after a pre-heating stage enter a mixer kept at a desired temperature, where the phase equilibrium is attained.

Often, static mixers are used [95,96]. The feed stream from the mixer is then separated in an equilibrium cell into a vapour and a liquid phase. To facilitate phase separation, a cyclone separator was used by Fonseca et al. [95]. Effluents from both phases are withdrawn continually, depressurized, accumulated and usually analysed after the experiment. The pressure in the system is adjusted by means of a back pressure regulator

that controls the effluent stream of the vapour phase. The interface level between the fluid phases in the equilibrium cell can be adjusted with a bottom-phase expansion valve, whereby the interface level is usually determined visually [97].

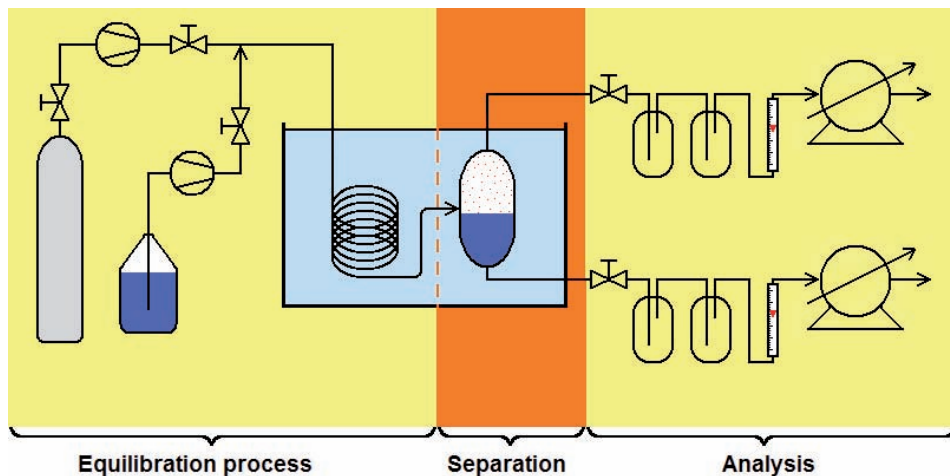


**Figure 3.6** – Schematic diagram showing a typical design of a continuous-flow method, showing the three fundamental steps of the method.

When compared with the isothermal methods described above, the continuous-flow methods present the important advantage that sampling can be done without disturbance of the equilibrium. Furthermore, if large samples are needed, for example to facilitate the analysis of traces of particular compounds in some phases, the run time of the experiment can just be extended in order to accumulate more material, without the need for increasing the volume of the equilibrium cell or the dimensions of the experimental set-up. Another great advantage of this type of method is related to the short residence time of the components in the apparatus, reducing the possibility for thermal decomposition or polymerization reactions when performing measurements at higher temperatures [98]. However the continuous-flow methods usually require the use of larger amounts of chemicals, which can be a disadvantage when compared with the isothermal analytical methods. Furthermore, the experimental procedure can be more complicated, due to the somewhat more complex process control involved.

Haruki et al. [99] used a continuous-flow method in the measurement of phase equilibria for systems water + hydrocarbon near the critical point of water. Hurst et al. [100] describe a continuous-flow cell equipped with large diameter optical ports suitable for visual observation, and for Raman spectroscopic studies of aqueous solutions at temperatures up to 770 K (500 °C). The cell was instrumented with a heated cylindrical insert (“hot finger”) that was employed for salt solubility, salt deposition and salt nucleation studies in near-critical aqueous solutions. The crystalline phases were observed using Raman spectroscopy.

### ***Semi-flow methods***

In semi-flow methods, only one of the phases is flowing while the other is stationary in an equilibrium cell. Semi-flow methods are also known as “single-pass flow methods”, “gas-saturation methods” or “pure-gas circulation methods”, depending on the authors. Typically, in these methods, a high-pressure stream of gas or of a supercritical fluid is passed through two cells connected in series, containing the low-boiling component in a condensed phase. The first cell is used as a pre-saturator while the second cell operates as an equilibrium cell. Upon equilibration, the effluent of the vapour phase is reduced in pressure and conducted through a trap, where the condensed component is collected. The quantity of gas can be determined volumetrically, by means of a gas meter, or using a flow meter such as a wet test meter [101,102]. Figure 3.7 presents a typical experimental set-up for the application of this method, with emphasis on the different steps of the measurement.

In most applications, only the composition of the vapour phase is analyzed, for example in the determination of the solubility of a low-boiling (liquid or solid) substance in a supercritical gas [102-104]. A wide variety of techniques are suitable for the determination of the composition of the vapour-phase effluent, through the use of a spectroscopic method [105,106], using a multi-port sampling valve and a subsequent HPLC analysis [107], using an absorption bath after previous expansion to atmospheric pressure using cold traps [102], or by means of a chromatography column filled with an appropriate adsorbent for the solute under study [108].

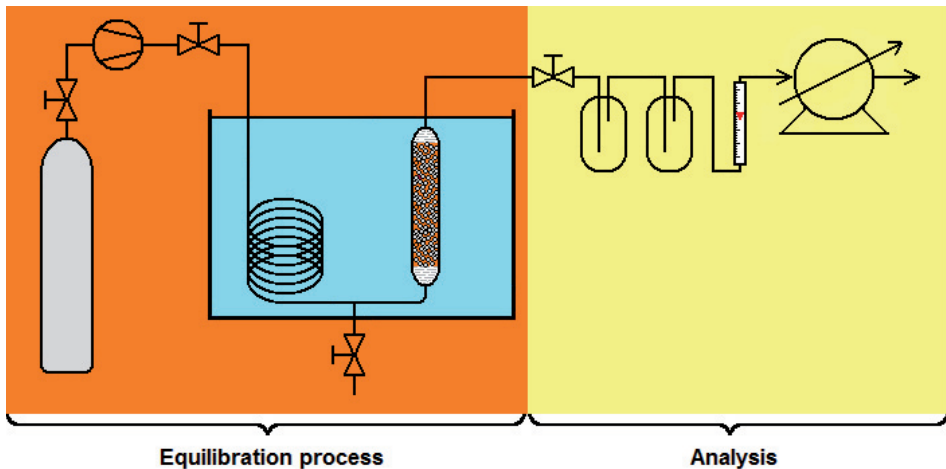


**Figure 3.7** – Schematic diagram showing a typical design of a semi-flow method, demonstrating the fundamental steps of the method.

In this type of solubility measurement, no samples from the stationary condensed phase need to be taken. However, when a semi-flow method is used in VLE studies, the composition of the condensed phase needs to be determined as well. A sample from the liquid phase can simply be withdrawn through a common valve and tubing and depressurized, before further analysis [109]. Furthermore, semi-flow methods can also be used in the measurement of the solubility of a gas in a liquid, as in the work presented by Tan et al. [110]. The experimental procedure is similar to the one just described for the vapour-liquid equilibria studies, but without the need to determine the composition of the effluent from the vapour phase.

In studies related with CO<sub>2</sub> capture, the solubility of this gas in a condensed phase (an amine solution, or a ionic liquid, for example) can also be determined using this method, for instance by passing a stream of a typical flue gas mixture of known composition through a solution, and continuously analysing the amount of carbon dioxide in the effluent flow. A typical experiment is characterised by an initial decrease in the amount of CO<sub>2</sub> in the effluent flow, followed by an increase back to its initial value, as the condensed phase becomes saturated with the gas.

Tuma et al. [111] used a modified supercritical fluid chromatograph (SFC) to measure the solubility of dyes in carbon dioxide. The column was filled with finely

pulverized dyestuff and the analysis of the vapour-phase stream was performed by means of Vis-spectroscopy.

As explained previously, the major source of uncertainty for all flow methods is the possible lack of attainment of equilibrium. To deal with this problem, Sauceau et al. [112] used an equilibrium cell with 3 compartments, equivalent to 3 cells in series. Another possible source of problems is the eventual occurrence of partial condensation of the solute from the saturated vapour stream in the tubing, in particular inside and immediately after the expansion valve. This undesired variable hold-up of the solute can lead to a scattering in the results in the order of 10% [113]. To collect precipitated solute at the end of an experiment from the tubing and from the expansion valve, Takeshita and Sato [114] used a stream of carbon dioxide after having blocked off the equilibrium cell.

Ferri et al. [115] describe an experimental technique that allows the measurement of high concentrations of dyestuff in a supercritical fluid. The authors use a second pump to stabilise the flow rate of the fluid in the extractor, damping the pulses of the first pump. Glass wool before and after the packed bed guarantees a uniform flow distribution and prevents particle entrainment. A line bypassing the extractor allows solubility measurements at high concentrations. It dilutes the saturated fluid stream with clean carbon dioxide and reduces the risk of valve clogging and flow rate instability.

In order to overcome the problems related with the depressurization process, Pauchon et al. [116] developed a semi-flow method that works without pressure reduction. The effluent vapour-phase flows into the top part of an autoclave which is filled with mercury. The use of mercury, acting as a piston, allows obtaining a precise adjustment of the vapour flow and avoids pressure changes that produce solute precipitation. Sampling at isobaric conditions is performed with a six-port valve. As mentioned for other cases, special attention is required during the regeneration of mercury and cleaning of the apparatus, due to the high toxicity of this metal.

### ***Chromatographic methods***

In the chromatographic methods, the retention of a solute in a chromatographic column is measured, and related to the Gibbs energy of solute transfer between the

stationary and the mobile phase. Roth [117] gives a review on applications of supercritical fluid chromatography (SFC) for the determination of the relative values of solute solubilities in supercritical fluids, and on the determination of solute partition coefficients between a supercritical fluid and the stationary phase. In SFC, the thermodynamic analysis of solute retention is more challenging than in common gas chromatography since the uptake of the mobile phase fluid by the stationary phase is no longer negligible. The main advantage of the chromatographic methods is the possibility to determine equilibrium properties and diffusion coefficients simultaneously, in one experiment [118].

Sato et al [119] used a chromatographic method in the study of the vapour-liquid equilibrium ratio of *n*-hexane at infinite dilution in propylene + impact polypropylene copolymer, while for the determination of the solubility of propylene in the copolymer the authors made use of a synthetic isothermal method, a type of method described later in this chapter.

Chester [120] reviewed a chromatographic technique, which he calls “flow injection peak-shape method”, that allows the determination of the pressure and temperature coordinates of the vapour-liquid critical locus of binary systems. This technique can be implemented using open-tubular SFC instrumentation, by replacing the SFC column with several meters of fused-silica tube. This tube may be deactivated but is not coated with a stationary phase. The procedure to map a critical locus involves selecting a temperature, then making injections at various pressures while looking for the pressure where the peaks change from their rectangular appearance (liquid phase and vapour phase present in the column) to distorted Gaussian (single homogeneous phase in the column). This transition pressure provides an estimate of the mixture critical pressure, corresponding to the oven temperature.

### **3.1.3. Analytical Isobaric Methods**

One of the most common methods for the measurement of vapour pressures of pure compounds in the pressure range from 10 kPa to 100 kPa is ebulliometry (from Latin *ebullio* “to boil, to bubble up”) [1]. The method can however be extended to the study of mixtures and to high pressures. In this method, the boiling temperature of a mixture is measured under isobaric conditions and the phase compositions are determined after

sampling and analysis. The experimental apparatus, an ebulliometer, is fundamentally a one-stage total-reflux boiler equipped with a vapour-lift pump to spray slugs of equilibrated liquid and vapour onto a thermometer well. As opposed to the more frequently used synthetic isobaric method described later in this chapter, vapour and liquid streams are separated, collected and analyzed. The compositions of the liquid and the vapour phase vary with time, towards a stable value that should not differ significantly from the true equilibrium value. This analytical isobaric method is still frequently used in measurements of low-pressure data, being often referred by some authors as “dynamic VLE method”.

### **3.1.4. Analytical Spectroscopic Methods**

Spectroscopic methods allow the analysis of the phase composition at high pressures, without the need to withdraw any samples. A number of techniques can be used in these methods, such as near infrared spectroscopy [72,121], or the  $^2\text{H}$  NMR technique combined with light microscopy used by Cruz Francisco et al. [122] in the study of the phase behaviour of lecithin + water + hydrocarbon + carbon dioxide mixtures. Pasquali et al. [123] used attenuated total reflection infrared (ATR-IR) spectroscopy to simultaneously measure the sorption of  $\text{CO}_2$  in polyethylene glycol (PEG) and the polymer swelling.

Aizawa et al. [124] developed a high-pressure optical cell for the investigation of absorption and fluorescence phenomena using a "totsu" (denoting the shape) type window. In this particular application, the protruding part of the window acts as a light-guide and enhances the laser power imparted onto the sample in the monitoring light. Shieh and co-workers [125] studied the effect of carbon dioxide on the morphological structure of compatible crystalline/amorphous polymer blends by means of small angle X-ray scattering (SAXS) with the measurement of absolute scattering intensity.

Rondinone et al. [126] developed a single-crystal sapphire cell, for performing neutron-scattering experiments on gas hydrates. Since the sapphire crystal only contains aluminium and oxygen, it possesses a low incoherent neutron scattering and absorption cross section, having a low contribution to the background signal.

Some articles found in the literature, using Raman spectroscopy for the detection of gas hydrates [127,128], or laser scattering techniques [129-131], are not included in the analytical spectroscopic methods, since the techniques are used in the detection of a new phase, rather than in the quantitative analysis of the phase compositions. Such methods will be discussed later in this chapter.

In the analytical spectroscopic methods, the advantage of avoiding the sampling process is often outweighed by the inherent disadvantages. In addition to the inability to perform a complete characterisation of the composition of the phases, as already mentioned, it is also necessary to consider the requirement of time consuming calibrations at various pressures.

From the 4465 systems considered in the period between 2000 and 2008 [2,3], only 1.7% were studied through the use of an analytical spectroscopic method.

### **3.1.5. Analytical Gravimetric Methods**

Gravimetric methods are based in the monitoring of the mass of a non-volatile condensed phase, such as a polymer [75,132-136] or an ionic liquid [137], in phase equilibrium with a fluid phase. Using additional information, like the density of the phases, the phase compositions can be determined. Figure 3.8 shows a schematic representation of the apparatus used by von Solms et al. [134-136].

Palamara et al. [138] placed an entire high-pressure equilibrium cell on a balance, and performed the equilibration under isobaric conditions. A very important aspect to consider in such application is the weight of the cell and the attached valve, since for commercially available analytical balances, a higher sensitivity is synonymous with a lower maximum load capacity. In the study of Palamara et al. [138], the cell and the attached valve have an approximate weight of only 190 g.

Cutugno et al. [139] and Moore and Wanke [140], placed a quartz spring balance and an electro microbalance, respectively, within a high-pressure cell, in order to measure the sorption of gases in polymers.

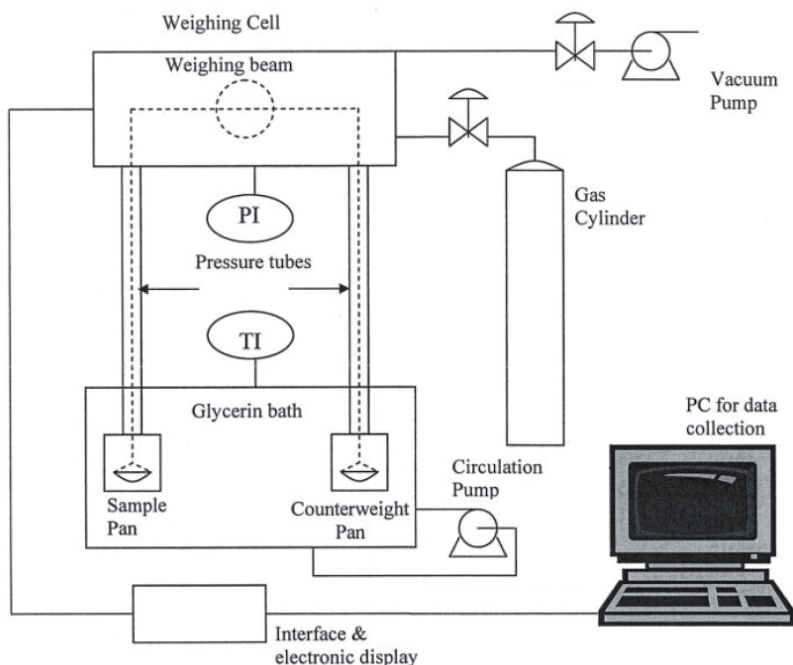


**Figure 3.8** – Schematic representation of the analytical gravimetric apparatus employed by von Solms et al. [134-136].

Kleinrahm and Wagner [141] developed a unique balance, a so-called magnetic suspension balance, intended for accurate measurements of fluid densities, with the main advantage that both the sample and the balance are isolated. An electronically controlled magnetic suspension coupling is used to transmit the measured force from the sample enclosed in a pressure vessel to a microbalance. The suspension magnet, which is used for transmitting the force, consists of a permanent magnet, a sensor core and a device for decoupling the measuring-load. An electromagnet attached at the under-floor weighing hook of a balance, maintains the freely suspended state of the suspension magnet by means of an electronic control unit. Using this magnetic suspension coupling, the measuring force is transmitted without contact from the measuring chamber to the microbalance, located outside the chamber under ambient atmospheric conditions. To better illustrate this concept, a schematic diagram of a magnetic suspension balance is shown in Figure 3.9.

Several researchers used a magnetic suspension balance to measure the solubility and diffusivity of volatile components in polymers, such as the case of Sato et al. [142].

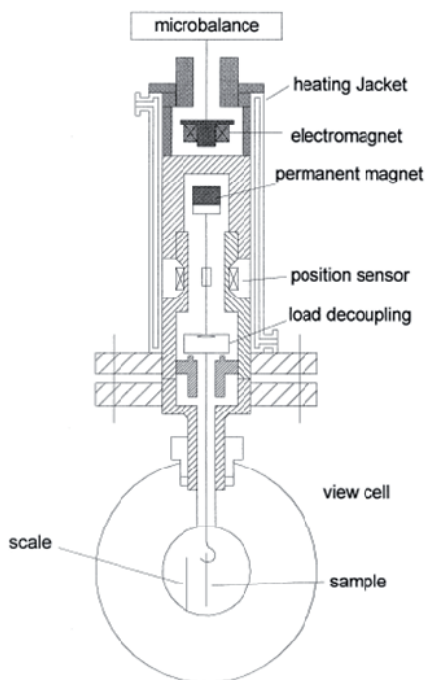


**Figure 3.9** – Schematic representation of a magnetic suspension balance. Source: Dohrn et al. [143].

Gravimetric methods require corrections for buoyancy effects and, consequently, the exact information on the density of the fluid phase and on the density and volume of the condensed phase is essential, particularly at high pressures. These methods were used in the study of 3.4% of the 4465 phase equilibrium systems considered in the aforementioned reviews [2,3].

### **3.1.6. Other Analytical Methods**

Just as in gravimetric methods, quartz crystal microbalances can be used in the determination of the solubility of a gas in a polymer, by measuring the mass of the polymer in equilibrium with the gas. From the basic principle, it is not a gravimetric measurement, so that buoyancy effects play a different role. Quartz crystal microbalances are usually based on the piezoelectric effect observed in an AT-cut quartz crystal. The crystal under the influence of an applied alternating electric voltage undergoes a shear deformation, with a maximum at a specific frequency known as the resonance frequency [76]. This resonance

frequency is dependent on the mass, and thus any mass change will result in an associated frequency shift. Sorption experiments are based in the measurement of the resonance frequency of the bare (clean) crystal, of the same crystal coated with polymer, and finally, of the coated crystal after the equilibrium between the polymer and the gas is attained, all at the same controlled temperature. The resonance frequency of a reference crystal is also measured at the same conditions of the experiments, in order to compensate any temperature or pressure effects. Park et al. [144] examined the effect of temperature deviation and pressure change on the frequency shift by measuring the frequency change of an uncoated crystal under high-pressure carbon dioxide.

Further developments to the quartz crystal technique, were performed by Guigard et al. [145], who applied the method in the measurement of low solubilities of metal chelates in supercritical fluids. A small mass of solute is deposited on the crystal and the solubility is measured by observing the change in the frequency of the crystal as the solute dissolves in the supercritical fluid.

Mohammadi et al. [146] used a quartz crystal balance as an extremely sensitive detector for the appearance of hydrates. A change of mass of merely 1 ng results in a change of frequency of 1 Hz. However, this is not considered to be an analytical method, since the balance is used merely for the detection of a new phase, being included in the category of the synthetic methods, discussed later in the chapter.

When compared to conventional methods, such as the gravimetric or the pressure decay technique, a synthetic isothermal method presented later, the quartz crystal microbalance provides a much higher sensitivity in the determination of mass changes, meaning that smaller samples are necessary to perform the experiments, which in turn accounts for a faster equilibration process and faster experiments [147], since equilibration time is inversely proportional to the square of the film thickness. However, the quartz crystal microbalance technique also has some drawbacks. The preparation and loading of the sample onto the crystal can be very challenging, and the system tends to be highly sensitive to small changes in electrical current, air flow or motion in the surroundings, or any other interference occurring in the same room or even next door [148]. Errors rise with temperature and pressure, due to dampening and viscous dissipation upon entering the glass transition and rubbery state [132,144].

Another analytical method was used by Morris et al. [149], who made use of a palladium/hydrogen electrical resistance sensor for the determination of the hydrogen content in the liquid phase, in studies of the low gas solubilities of hydrogen in water.

Abbott et al. [150] presented a capacitive method (dielectric constant method, or in accordance with the term designated by IUPAC, relative permittivity method), in the measurement of the solubility of low-volatile substances in supercritical gases. The authors used a 25 cm<sup>3</sup> high-pressure cell, lined with a layer of Teflon. A capacitor consisting of two parallel rectangular stainless steel plates, with an area of 6.6 cm<sup>2</sup> and held 1 mm apart by Teflon spacers was placed in the vapour phase. The dielectric constant of the saturated vapour phase was measured at different pressures. In order to calculate the concentration of the solute in the vapour phase from the dielectric constant, the permanent dipole moments and the molecular polarizabilities of the different components of the mixture need to be known.

### **3.2. Synthetic Methods**

The idea behind the synthetic methods is again to avoid the need for sampling, this time by using a mixture with a precisely known composition, and subsequently observing its phase behaviour in an equilibrium cell, measuring only properties such as pressure and temperature in the equilibrium state. The application of synthetic methods can be based in a phase transition, where the appearance of a new phase is detected, or not. But in both cases, a mixture with a precisely known composition has to be prepared (synthesised), and the challenge of analysing fluid mixtures is substituted by the challenge of carefully preparing them [14].

Equilibrium cells for synthetic methods are usually smaller than cells used with analytical methods, since no sampling is necessary. But also for synthetic methods, a larger cell volume can be advantageous. When developing a new high pressure equilibrium cell, Nieuwoudt et al. [151] increased the internal volume from the 40 cm<sup>3</sup> of the old cell to 80 cm<sup>3</sup> for the new cell. The larger volume allows for increased accuracy on the composition, particularly in studies involving low concentrations of solutes.

In the case of synthetic methods with a phase transition, the initial conditions are selected in order to promote the existence of one single homogeneous phase in the system. During the experiment, the pressure and/or temperature conditions are altered, leading to the appearance of a new phase. These experiments can be used merely to know the pressure and temperature coordinates of a specific transition, but inferring the composition of one of the phases is also possible. The moment when the second phase appears, and while it is still very small, the composition of the large phase can be considered to be equal to the global composition of the system, each experiment yielding one point of the  $pTx$  phase envelope.

But not only variations on pressure and temperature can be used to promote the phase transition. This effect can also be achieved by a change in the overall composition of the system, as in the work presented by Wubbolts et al. [152] who used a method sometimes designated as “vanishing-point method“ or “clear-point method”, in the study of solid-liquid equilibrium. In this method, a clear solution of a given solute concentration is added to a known amount of anti-solvent until the last crystal disappears. The composition of the mixture at this vanishing point corresponds to the solubility of the mixture. Repeating the procedure with solutions of different concentrations leads to additional points for the solubility curve.

The detection of a phase transition can be done by visual means, in which case the methods are classified as visual synthetic methods, or non-visually, in the case of non-visual synthetic methods. The application of synthetic methods without the occurrence of a phase transition is dependent on the measurements of a number of equilibrium properties, such as pressure, temperature, phase volumes and densities, which are subsequently used in calculations involving material balances for the characterisation of the phase compositions. These methods can be divided in isothermal, isobaric and other methods.

Synthetic methods with a phase transition are by far more common than synthetic methods without a phase transition, but this last type has been going through an expansion over the last years. In the period of 2000 to 2008, 46.0% of the 4465 systems considered in [2,3] were studied by a synthetic method involving a phase transition. As for the synthetic methods without a phase transition, they were used in the study of 12.3% of the 4465 systems considered. These numbers show the extensive application of synthetic methods,

used in 58.3% of the systems reviewed in the period 2000 to 2008. Furthermore, the application of synthetic methods in the period from 2000 to 2004 was 53.3% of the systems considered [2], while in the period from 2005 to 2008 synthetic methods accounted for 63%, almost two thirds, of the reviewed systems [3], meaning not only that the synthetic methods are predominant, but also that this predominance is increasing significantly. Analytical methods where all the phases are analysed may be preferable, due the completeness of the information they can provide, but they are often not preferred, given the number of advantages of the synthetic methods.

Synthetic methods can be used where the application of analytical methods becomes more problematic, as in situations where phase separation is difficult due to similar densities of the coexisting phases, or near or even at critical points and in barotropic systems, where at certain conditions the coexisting phases have the same density. Kodama and his co-workers [81] recently presented a study on the phase equilibrium of the binary system ethylene + butanol, in which they used an analytical method for the majority of the measurements, but a synthetic method for determinations near the critical region.

Often, the experimental procedure is easy and quick [16], and since no sampling is required, the experimental set-up can be much simpler and rather inexpensive, without the sampling and the analytical equipment. The equilibrium cell can be more compact, of a smaller volume, as there are no pressure drop problems associated with sampling, allowing the development of equipment suitable for extreme conditions, where temperature and pressure are concerned [66]. Cohen-Adad [153] describes a diamond anvil cell that can be used for pressures up to 135 GPa. Fang et al. [154] have presented experimental data obtained at pressures up to 2.6 GPa, also using a diamond anvil cell. Smith and Fang [5] recently presented a review on the use of this type of cell, emphasising the advantages of this technique for application at high pressure and high temperature conditions. According to the authors, the very small volume of this type of cell also facilitates the study of supercritical systems at high density, from  $400 \text{ kg.m}^{-3}$  to  $1\,200 \text{ kg.m}^{-3}$ , which can otherwise be difficult or expensive with other methods.

Figure 3.10 shows a schematic diagram of a diamond anvil cell, as presented by Cohen-Adad [153], which can be used from cryogenic temperatures up to 4000 K. In this cell, the two diamond anvils are forced together by means of spring-loaded screws or using a standard arm-lever block. The diamond anvils are cemented in place through a rigidly

mounted sample gasket. The sample is placed inside the gasket hole, together with a pressure transmitting fluid and small ruby chips which are used to measure the pressure by excitation of their fluorescence. While for cryogenic temperatures the cell can be suspended in a liquid helium cryostat, to achieve temperatures up to 4000 K a CO<sub>2</sub> or a YAG laser can be used.

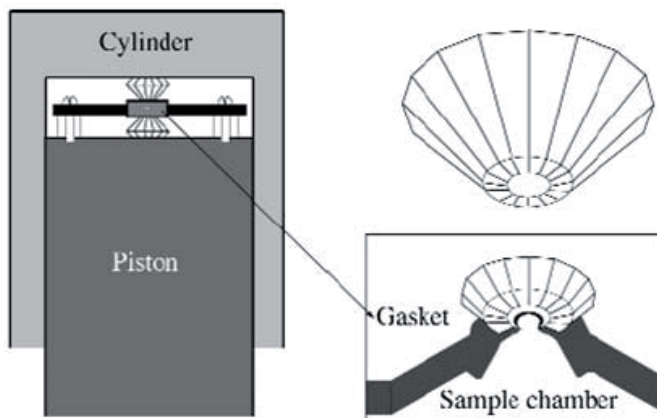


**Figure 3.10** – Schematic diagram of a generic diamond anvil cell, as presented by Cohen-Adad [153].

The limited information that synthetic methods can provide in the study of multi-component systems, for which the tie lines cannot be determined without additional experiments, constitutes perhaps the most important drawback of these methods. Furthermore, in some experiments the phase compositions in equilibrium are calculated based on approximations and rely on the results of equations of state or other prediction methods. Nevertheless, synthetic methods are still a powerful solution for the study of simpler systems.

### **3.2.1. Visual Synthetic Methods**

In the most common of the synthetic methods, the appearance of a new phase is detected by visual observation of the resulting turbidity or the appearance of a meniscus in a view cell. Limitations exist in the cases of isooptic systems, where the coexisting phases have approximately the same refractive index, making visual observation unfeasible. The

visual synthetic method has a wide application range, and it can be used not only for the determination of simple vapour-liquid equilibria, but also in the study of more complex phase behaviour, such as multi-phase equilibria [155], solid-liquid equilibria [156], critical curves of mixtures [157], gas hydrate formation [158], cloud-point determinations [130] or phase equilibria in polymer-solvent systems [159].

The Cailletet apparatus of TU Delft [30], named after the French physicist and inventor Louis-Paul Cailletet (1832 – 1913), is the most frequently used type of apparatus using a synthetic visual method. It consists of a thick-walled Pyrex glass tube (500 mm long, 3 mm inner diameter) with the open end placed in an autoclave and immersed in mercury. The mercury confines the sample in the Cailletet tube and a stainless steel ball driven by reciprocating magnets provides the stirring of the sample. Daridon et al. [160] used a very small cell with a volume of just 0.03 cm<sup>3</sup>, for the visual observation of synthetic waxes at high pressures, placed within a polarizing microscope, allowing the visual observation of crystals of 2 µm.

When only small quantities of a sample are used in the experiment, for example in the observation of solid-liquid-gas equilibria, a glass capillary can be placed inside the high-pressure view cell [161,162]. Veiga et al. [163] used glass capillary helixes not only to investigate the high pressure behaviour of pure compounds but also at negative pressures, as far down as minus 20.8 MPa.

To improve the detection of phase transitions, some authors use special techniques such as laser light scattering [129,130]. Jager and Sloan [127] used Raman spectroscopy in order to detect the appearance of gas hydrates, while Dong et al. [164], made use of additional small angle X-ray scattering measurements in the determination of the median micelle size of the water in carbon dioxide micro emulsions.

Synthetic visual methods are by far the most frequent type of method found in the literature during the preparation of two recent reviews [2,3], having been used in the study of 35.8% of the 4465 systems covered by these reviews, in the period between 2000 and 2008.

### 3.2.2. Non-Visual Synthetic Methods

As an alternative to visual inspection, other physical properties can be monitored in order to detect the occurrence of phase transitions. Minicucci et al. [165] for example, made use of transmitted X-rays instead of visible light, as the basis for phase detection, while Drozd-Rzoska et al. [166] used measurements of the relative dielectric permittivity for liquid-liquid equilibrium measurements at high, low and at negative pressures.

In cases where the volume of a variable-volume cell can be known accurately at any instant, the appearance of a new phase can be obtained from the abrupt change in slope on the pressure-volume plot more accurately than by visual observation [167,168]. The apparatus used by Kodama et al. [168], represented schematically in Figure 3.11, has the particularity of being one of the few experimental set-ups found in the recent literature, equipped with two density meters in the recirculation loops, for measuring the density of different phases. It also employs a very simple system for the variation of the volume of the cell, in which a piston is manually and directly actuated, without the use of a pressure transmitter medium. This allows the exact position of the piston to be determined with a higher precision, and consequently the total volume of the cell, at any instant during the experiment.

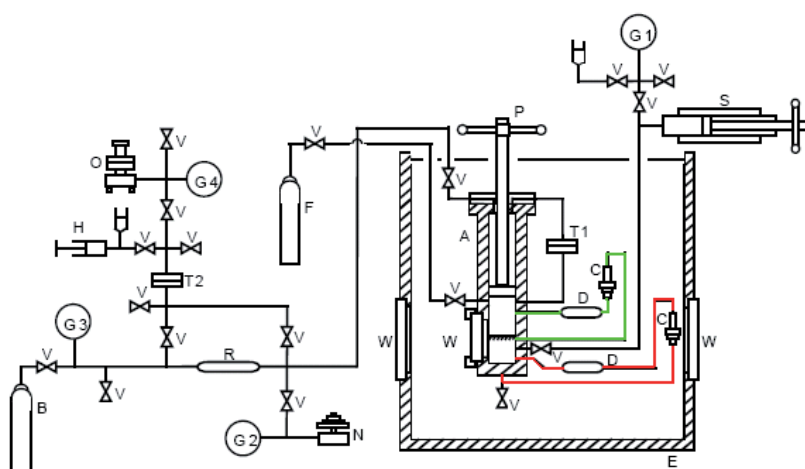


**Figure 3.11** – Schematic diagram of the apparatus used by Kodama et al. [168]. The recirculation loops for the liquid and the gas phase, containing the densitometers, were highlighted for easier identification.

As an alternative,  $pVT$  measurements can be performed, and the intersection of isochors can be used to determine points on the coexistence curve, whenever a sharp change in the  $(dp/dT)$  slope occurs at the phase boundary. This is one of the most used methods in the determination of hydrate formation conditions. Ivanic et al. [169] monitored the pressure and temperature in a hydrate-bearing system and identified equilibrium at the conditions where the last hydrate crystal in the system dissociates at the cross point of the  $pT$  curves from cooling and from heating. Figure 3.12 shows a graph of a typical result for this type of measurements applied to the determination of hydrate formation conditions, adapted from the plot presented in the work of Mohammadi et al. [170].

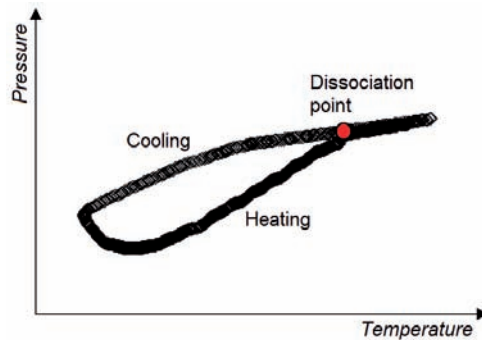


**Figure 3.12** – Typical result obtained in the determination of hydrate formation conditions using the change in the  $(dp/dT)$  slope method.

In a variation of this method, the temperature is lowered in order to promote a faster appearance of the hydrate phase, and subsequently increased in small steps for recording of the  $pT$  curves [171,172]. In this technique, only the heating is considered for the construction of the  $pT$  curves, since in the case of hydrates, the existence of a significant sub-cooling associated with induction and growth times make the cooling  $pT$  lines less useful [173], a fact also observable in Figure 3.12.

May et al. [174] used a microwave re-entrant resonator in the detection of dew and bubble points in hydrocarbon systems. Takagi et al. [175] measured bubble point pressures using an ultrasonic speed apparatus. The excited acoustic wave used for the measurement of the speed of sound in the sample is strongly absorbed in the gas phase as compared to the absorption in the liquid phase, and so the appearance of the gas phase can be perceived by the occurrence of a change in the acoustic echo signal. For searching critical points of

pure fluids, acoustic methods have the advantage that even for temperatures several degrees above the critical point, the sound velocity exhibits a minimum when measured isothermally as a function of pressure [176].

To measure the critical temperature of a thermally unstable substance, it is possible to use the pulse-heating method, as described by Nikitin and co-workers [177]. It is based on measuring the pressure dependence of the temperature of the attainable superheat (spontaneous boiling-up) of a liquid with the help of a thin wire probe heated by pulses of electric current. When the pressure in the liquid approaches the critical pressure, the temperature of the attainable superheat approaches the critical temperature.

In the determination of critical points of thermally unstable or reactive components, VonNiederndorfer et al. [178] used a method in which a sample of precisely known composition is continuously displaced and heated in a capillary tube, in order to achieve very short residence times. Although resembling an analytical continuous-flow method, it is in fact a synthetic non-visual method since no analysis takes place. To determine the critical point by this method, several temperature scans must be made in the vicinity of the critical point. Below the critical point, the temperature scan will show a flat, horizontal region indicative of isothermal boiling, while above the critical point, the transition region is no longer flat and horizontal. The critical point is inferred by the temperature and pressure where isothermal boiling is no longer observed.

Valyashko et al. [179] used jumps of the isochoric heat capacity to detect the appearance of a vapour phase or a second liquid phase. Würflinger and Urban [180] studied the phase behaviour of liquid crystals with high-pressure differential thermal analysis (DTA).

Manara et al. [66] investigated the melting point of uranium dioxide at high pressures, using helium as pressurising medium. Temperatures of almost 3200 K were needed for the measurements. Such high temperatures can be measured optically by pyrometry, as in the experimental set-up used by Manara et al. [66], schematically represented in Figure 3.13.

In this set-up, two pulsed Nd-YAG laser beams are mixed through a suitable optical system in the same fibre and then focused onto the sample surface. The pulse with the higher power peak is used to heat the sample above the melting point, while the other one,

less powerful but of longer duration, is used in the control of the cooling rate of the sample surface. This procedure leads to an enhanced definition of the freezing plateau.

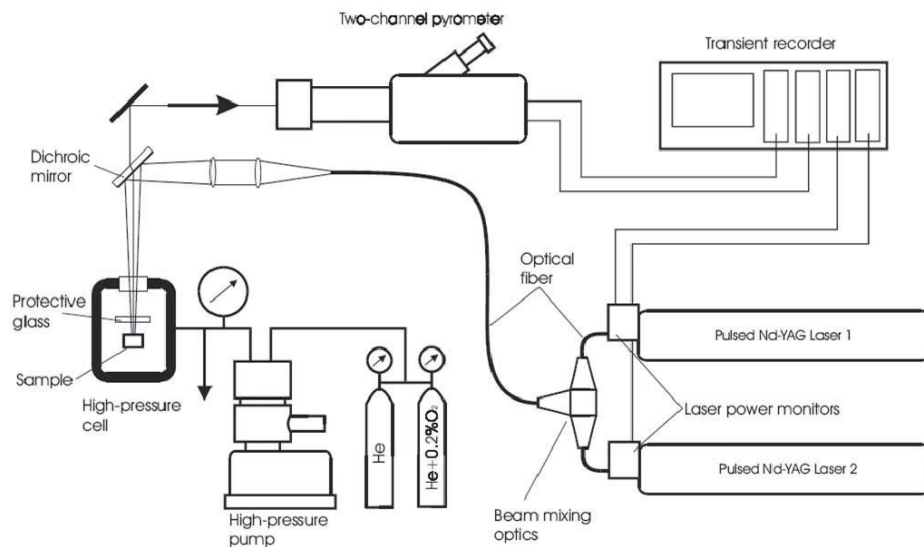


**Figure 3.13** – Schematic representation of the experimental apparatus employed by Manara et al. [66].

Diamond anvil cells are particularly suitable for non-visual measurements at very high pressures [153], and the selective transparency of diamond for IR to X-ray and  $\gamma$ -ray radiations, allows *in situ* measurements during experiments.

Ngo et al. [181] used a synthetic non-visual method for the determination of the solubility of solids in carbon dioxide. In the adopted procedure, the cell is initially charged with the solid, and subsequently pressurized with carbon dioxide under permanent stirring. By periodically taking spectra (UV absorbance) of the solution, the equilibrium state is identified *in situ*. The pressure is then raised stepwise, until no further significant increase in the peak absorbance is observed, meaning that all the solids had been dissolved in the fluid phase.

Randzio [182] presented a new transitiometric method in the investigation of the solid phase behaviour in asymmetric binary systems. Transitiometry is based on a simultaneous recording of both mechanical and thermal variables of a thermodynamic transition induced by scanning one independent variable, either pressure, temperature or

volume, while the other independent variable is kept constant. The three-phase curve (solid-liquid-vapour) has been determined for the binary system tetracosane + methane, used as a test example. The apparatus, a “transitiometer”, consists essentially of a high pressure calorimeter and a  $pVT$  system, and allows the recording of both the heat flux and the volume variations during isobaric temperature scans.

In measurements of solid-liquid equilibria at high pressures, the dead-volume of the apparatus can have a large negative influence [153]. The volatility of constituents changes the nominal composition of a sample and can induce an incorrect apparent retrograde solubility curve.

Non-visual methods can be particularly advantageous in studies of phase behaviour in porous media. Zatsepina and Buffett [183] used electrical resistance measurements to monitor the appearance and growth of carbon dioxide hydrate crystals in the pore fluid. Omi et al. [184] used a high pressure NMR probe to investigate the pressure and the pore size dependence of the critical behaviour of xenon in mesopores.

Oag et al. [119] describe an apparatus where the determination of phase transitions and critical points can be carried out with different methods: visually, by measuring the laser reflectance of the fluid, which is at its maximum at the critical point, and the sound velocity by using vibrating shear mode sensors.

### **3.2.3. Synthetic Isothermal Methods**

Experiments using synthetic isothermal methods are performed without a phase transition, by measuring the pressure of a synthesized multi-phase mixture at isothermal conditions, being the phase compositions calculated through the application of a material balance. The most common application of this type of methods is in the determination of solubilities of gases in condensed phases.

At the beginning of an experiment, the equilibrium cell is charged with an exactly known amount of the first component, usually the condensed phase, and then evacuated, before setting the system to the desired temperature. Subsequently, a precisely known amount of the second component, the gas, is added to the cell, leading to an increase of the

pressure of the system. As this component dissolves into the condensed phase, the pressure inside the equilibrium cell will decrease, eventually reaching an equilibrium value. For this reason, this method is often referred to as “pressure decay method” by some authors.

After equilibration of the system, the pressure and temperature are registered, and the composition of the vapour phase can then be calculated by means of a phase equilibrium model, or alternatively, it is assumed to only contain the pure gas, if it is considered that the condensed phase is non-volatile or has a negligible volatility at the temperature of the measurements. This is usually valid in measurements of solubility of gases in polymers, in ionic liquids, or in other compounds with negligible volatility. To a certain extent, the same assumption can be made for the study of solubilities in aqueous solutions, providing that the temperature of the measurements is sufficiently low and the pressure in equilibrium sufficiently high, in order for the pressure of water vapour to be negligible. The composition of the liquid phase is calculated using the material balance from the known total composition, the composition of the vapour phase and the phase densities and volumes [185]. More experimental points along the boiling point line can be measured by repeating the experiment with a different amount of gas, or just by repeating the addition of the second component into the cell.

In low pressure studies, this method is often called “static method” or “isothermal  $pTx$  method”. When used for a pure component, the synthetic isothermal method delivers the vapour pressure, as in the case of the work by Funke et al. [186]. In this case, it is usually called the “static” vapour-pressure method, and its application can be extended to pressures as low as 0.1 Pa using high-precision capacitance manometers [187,188]. Synthetic isothermal methods are very commonly used [189-202]. Examples of the use of the synthetic isothermal methods at high pressures can be given for the determination of the solubility of low-boiling substances in polymers [203,204], or the solubility of gases in ionic liquids [191-201,205-209], in oils [210] or in electrolyte solutions as in the case of the work presented by Gmehling et al. [211].

Very often, synthetic isothermal methods are used with equilibrium cells equipped with windows. This is extremely useful for the visual determination of the volumes of the liquid and the vapour phase [205,206,208,210], and increases the versatility of the cell, which can also be used with a synthetic visual method [212]. Additionally, it is an advantage in the detection of unusual behaviours, such as foaming. Fukné-Kokot et al.

[162] for example, measured solid-liquid-gas equilibria using the synthetic isothermal method to determine the carbon dioxide content in liquid, and the synthetic visual method to detect solid formation.

Despite the fact that frequently the synthetic isothermal methods make use of models for the calculations of the phase compositions, thus not yielding “pure experimental values”, they can produce results of identical quality as the analytical methods, as shown by Krüger et al. [213], who compared results obtained with the synthetic isothermal method in the study of VLE for the system *n*-pentane + poly(dimethylsiloxane), with the results obtained through the gravimetric sorption method and through the use of inverse gas chromatography. These three methods differ greatly in the underlying experimental principles as well as in the complexity of the data analysis, but notwithstanding these differences, the agreement of the measured VLE data was excellent.

### **3.2.4. Synthetic Isobaric Methods**

Typical isobaric experiments are performed in an ebulliometer as described in section 3.1.3 of this chapter. In these methods the boiling temperature of a synthesised mixture is measured at isobaric conditions, and the phase compositions are calculated by means of a material balance. As opposed to analytical isobaric methods described before, no sampling or analysis is performed, and just as it was verified for the synthetic isothermal methods, these methods are also performed without a phase transition.

Ebulliometry, is frequently used with pure components, in the determination of vapour pressures, as in the case of the work by Weber et al. [214]. An ebulliometer was first used to determine the molecular weights of substances, by measuring the changes of the boiling point of water caused by the presence of the unknown substance. Twin ebulliometry can be used to determine the activity coefficient at infinite dilution. The temperature difference between an ebulliometer filled with the first (pure) component and a second ebulliometer (under the same pressure) filled with the first component and with a small amount of a second component (diluted solution) is measured. From the difference of the boiling temperatures, the activity coefficient at infinite dilution can be calculated.

As mentioned before, ebulliometry has a wide application in the determination of vapour pressures in the range under 100 kPa, being sometimes designated by “dynamic” vapour pressure method. The use of comparative ebulliometry allows the extension of the range of applicability of the method, up to higher pressures, as demonstrated by Ewing and Ochoa [215], who used comparative ebulliometry to precisely determine the vapour pressure of pure components at high pressures. The sample and a reference fluid are boiled in separate ebullimeters under a common pressure of gas such as helium or nitrogen, and the condensation temperatures of the sample and of the reference fluid are measured. The common pressure is calculated from the known vapour pressure of the reference fluid. The method presents several advantages: direct measurement of pressure is avoided, the fluids are degassed by boiling, and the ebullimeters act as heat pipes to provide high-performance thermostats. The corresponding disadvantages are the considerable demands on thermometry, the solubility of the buffer gas at high pressures, and thermal gradients due to pressure heads. But the greatest advantage is speed of measurement, with a pressure-temperature point typically being obtained in one hour.

### **3.2.5. Other Synthetic Methods**

Properties measured in the homogenous or heterogeneous region can be used in the calculation of phase boundaries. Abdulagatov et al. [216] used two-phase isochoric heat capacity measurements in the determination of values of the critical pressure and slope of the vapour-pressure curve at the critical point of 18 pure components.

For systems with two degrees of freedom, e.g. a binary two-phase equilibria or ternary three-phase equilibria, the compositions are fixed when temperature and pressure are given. Luks and co-workers [217] took phase volume and overall composition raw data for a set of three experimental runs at the same temperature and pressure. In each run a different phase is caused to be volumetrically dominant relative to the other two phases. With the use of mass balance, the compositions and molar volumes of the three phases were determined from the three conjugate measurements [218].

Di Nicola et al. [219] used isochoric  $p/T_x$  measurements in the single phase region to fit the binary interaction parameters of an equation of state. Subsequently, the compositions of the coexisting phases are calculated using the equation of state model.

## References

- [1] José M. S. Fonseca, Graduation Thesis, Department of Chemistry of the Faculty of Sciences of the University of Porto, Porto, Portugal, 2002.
- [2] R. Dohrn, S. Peper, J. M. S. Fonseca, *Fluid Phase Equilib.* 288 (2010) 1-54.
- [3] J. M. S. Fonseca, S. Peper, R. Dohrn, *Fluid Phase Equilib.*, *In press*
- [4] D. Richon, *Pure Appl. Chem.* 81 (2009) 1769-1782.
- [5] J. Smith, Z. Fang, *J. Supercrit. Fluids* 47 (2009) 431-446.
- [6] D. E. Knox, *Pure Appl. Chem.* 77 (2005) 513-530.
- [7] M. Christov, R. Dohrn, *Fluid Phase Equilib.* 202 (2002) 153-218.
- [8] J. D. Raal, A. L. Muehlbauer, *Phase Equilibria: Measurement and Computation*, Taylor & Francis, Washington, D.C., 1998.
- [9] K. Nagahama, *Fluid Phase Equilib.* 116 (1996) 361-372.
- [10] R. Dohrn, G. Brunner, *Fluid Phase Equilib.* 106 (1995) 213-282.
- [11] S. Saito, *J. Supercrit. Fluids* 8 (1995) 177-204.
- [12] K. D. Bartle, A. A. Clifford, S. A. Jafar, G. F. Shilstone, *J. Phys. Chem. Ref. Data* 20 (1991) 713-756.
- [13] R. E. Fornari, P. Alessi, I. Kikic, *Fluid Phase Equilib.* 57 (1990) 1-33.
- [14] U. K. Deiters, G. M. Schneider, *Fluid Phase Equilib.* 29 (1986) 145-160.
- [15] P.T. Eubank, K.R. Hall, J.C. Holste, A Review of Experimental Techniques for Vapor-Liquid Equilibria at High Pressures in: H.Knapp, S.I.Sandler (Eds.), 2nd Int. Conf. Phase Equilibria and Fluid Properties in the Chem. Ind., Dechema, 1980.
- [16] G.M. Schneider, *Phase Equilibria of Liquid and Gaseous Mixtures at High Pressures* in: B.LeNeindre, B.Vodar (Eds.), *Experimental Thermodynamics*, Vol. II, pp. 787-801 Butterworth, 1975.

- [17] D. S. Tsiklis, *Handbook of Techniques in High-Pressure Research and Engineering*, Plenum, New York, 1968.
- [18] E. Hála, J. Pick, V. Fried, O. Vilím, *Vapour Liquid Equilibrium*, 2nd ed., Pergamon Press, 1967.
- [19] D. B. Robinson, *Pure Appl. Chem.* 65 (1993) 971-976.
- [20] L. Ruffine, A. Barreau, I. Brunella, P. Mougin, J. Jose, *Ind. Eng. Chem. Res.* 44 (2005) 8387-8392.
- [21] A. H. Mohammadi, A. Chapoy, D. Richon, B. Tohidi, *Ind. Eng. Chem. Res.* 43 (2004) 7148-7162.
- [22] H. J. Ng, D. B. Robinson, *New Developments in the Measurement and Prediction of Hydrate Formation for Processing Needs*, 1994. ISBN: 0077-8923.
- [23] H. J. Ng, D. B. Robinson, *New Developments in the Measurement and Prediction of Hydrate Formation for Processing Needs*, 1994. ISBN: 0077-8923.
- [24] C. Secuianu, V. Feroiu, D. Geana, *Fluid Phase Equilib.* 261 (2007) 337-342.
- [25] G. K. Folas, O. J. Berg, E. Solbraa, A. O. Fredheim, G. M. Kontogeorgis, M. L. Michelsen, E. H. Stenby, *Fluid Phase Equilib.* 251 (2007) 52-58.
- [26] S. Sawamura, N. Egoshi, Y. Setoguchi, H. Matsuo, *Fluid Phase Equilib.* 254 (2007) 158-162.
- [27] M. Kato, K. Sugiyama, M. Sato, D. Kodama, *Fluid Phase Equilib.* 257 (2007) 207-211.
- [28] H. S. Byun, N. S. Jeon, *Fluid Phase Equilib.* 167 (2000) 113-122.
- [29] A. Sane, S. Taylor, Y. P. Sun, M. C. Thies, *J. Supercrit. Fluids* 28 (2004) 277-285.
- [30] A. Shariati, C. J. Peters, *J. Supercrit. Fluids* 23 (2002) 195-208.
- [31] A. L. Ballard, M. D. Jager, K. Nasrifar, M. M. Mooijer-van den Heuvel, C. J. Peters, E. D. Jr. Sloan, *Fluid Phase Equilib.* 185 (2001) 77-87.

- [32] K. K. Ostergaard, B. Tohidi, A. Danesh, R. W. Burgass, A. C. Todd, *Fluid Phase Equilib.* 169 (2000) 101-115.
- [33] O. Pfohl, J. Petersen, R. Dohrn, G. Brunner, *J. Supercrit. Fluids* 10 (1997) 95-103.
- [34] A. P. Bünz, N. Zitko-Stemberger, R. Dohrn, *J. Supercrit. Fluids* 7 (1994) 43-50.
- [35] O. Pfohl, J. Timm, R. Dohrn, G. Brunner, *Fluid Phase Equilib.* 124 (1996) 221-233.
- [36] K. Sue, T. Mizutani, T. Usami, K. Arai, H. Kasai, H. Nakanishi, *J. Supercrit. Fluids* 30 (2004) 281-285.
- [37] G. Raabe, J. Janisch, J. Koehler, *Fluid Phase Equilib.* 185 (2001) 199-208.
- [38] M. A. Marcelino Neto, J. Barbosa, *ÿÿ* 31 (2008) 34-44.
- [39] F. Gozalpour, A. Danesh, A. C. Todd, B. Tohidi, *Fluid Phase Equilib.* 208 (2003) 303-313.
- [40] K. Jeong, J. Im, S. Lee, H. Kim, *J. Chem. Thermodyn.* 39 (2007) 531-535.
- [41] C. M. M. Duarte, M. Crew, T. Casimiro, A. Aguiar-Ricardo, M. N. Nunes da Ponte, *J. Supercrit. Fluids* 22 (2002) 87-92.
- [42] I. Tsivintzelis, D. Missopolinou, K. Kalogiannis, C. Panayiotou, *Fluid Phase Equilib.* 224 (2004) 89-96.
- [43] D. Missopolinou, I. Tsivintzelis, C. G. Panayiotou, *Fluid Phase Equilib.* 238 (2005) 204-209.
- [44] C. Lu, Y. Tian, W. Xu, D. Li, R. Zhu, *J. Chem. Thermodyn.* 40 (2008) 321-329.
- [45] J. Yu, S. Wang, Y. Tian, *Fluid Phase Equilib.* 246 (2006) 6-14.
- [46] G. Brunner, J. Teich, R. Dohrn, *Fluid Phase Equilib.* 100 (1994) 253-268.
- [47] A. Valtz, C. Coquelet, D. Richon, *Thermochim. Acta* 443 (2006) 245-250.
- [48] A. Valtz, M. Hegarty, D. Richon, *Fluid Phase Equilib.* 210 (2003) 257-276.

- [49] A. Valtz, C. Coquelet, A. Baba-Ahmed, D. Richon, *Fluid Phase Equilib.* 207 (2003) 53-67.
- [50] H. Madani, A. Valtz, C. Coquelet, A. H. Meniai, D. Richon, *J. Chem. Thermodyn.* 40 (2008) 1490-1494.
- [51] F. Garcia-Sánchez, G. Eliosa-Jiménez, G. Silva-Oliver, A. Godínez-Silva, *J. Chem. Thermodyn.* 39 (2007) 893-905.
- [52] M. Grigante, P. Stringari, G. Scalabrin, E. C. Ihmels, K. Fischer, J. Gmehling, *J. Chem. Thermodyn.* 40 (2008) 537-548.
- [53] O. Elizalde-Solis, L. A. Galicia-Luna, S. I. Sandler, J. G. Sampayo-Hernández, *Fluid Phase Equilib.* 210 (2003) 215-227.
- [54] S. Mokraoui, C. Coquelet, A. Valtz, P. E. Hegel, D. Richon, *Ind. Eng. Chem. Res.* 46 (2007) 9257-9262.
- [55] D. Seredynska, G. Ullrich, G. Wiegand, N. Dahmen, E. Dinjus, *J. Chem. Eng. Data* 52 (2007) 2284-2287.
- [56] Catinca Secuianu, Department of Applied Physical Chemistry and Electrochemistry, "Politehnica" University of Bucharest, Romania, Personal Communication, 2009.
- [57] Even Solbraa, Statoil ASA, Research and Development Centre, Trondheim, Norway, Personal Communication, 2009.
- [58] K.-D. Wagner, N. Dahmen, E. Dinjus, *J. Chem. Eng. Data* 45 (2000) 672-677.
- [59] A. Valtz, C. Coquelet, D. Richon, *Fluid Phase Equilib.* 258 (2007) 179-185.
- [60] N. Bahramifar, Y. Yamini, A. Ramazani, N. Noshiranzadeh, *J. Chem. Eng. Data* 48 (2003) 1104-1108.
- [61] A. Garmroodi, J. Hassan, Y. Yamini, *J. Chem. Eng. Data* 49 (2004) 709-712.
- [62] T. Laursen, P. Rasmussen, S. I. Andersen, *J. Chem. Eng. Data* 47 (2002) 198-202.

- [63] C. N. Kim, E. H. Lee, Y. M. Park, J. Yoo, K. H. Kim, J. S. Lim, B. G. Lee, *Int. J. Thermophys.* 21 (2000) 871-881.
- [64] Y. Tian, H. G. Zhu, Y. Xue, Z. H. Liu, L. Yin, *J. Chem. Eng. Data* 49 (2004) 1554-1559.
- [65] M. Brass, T. Pritzel, E. Schulte, J. U. Keller, *Int. J. Thermophys.* 21 (2000) 883-898.
- [66] D. Manara, C. Ronchi, M. Sheindlin, *Int. J. Thermophys.* 23 (2002) 1147-1156.
- [67] S. B. Kiselev, J. F. Ely, M. Abdulagatov, A. R. Bazaev, J. W. Magee, *Ind. Eng. Chem. Res.* 41 (2002) 1000-1016.
- [68] M. V. da Silva, D. Barbosa, P. O. Ferreira, J. Mendonça, *Fluid Phase Equilib.* 175 (2000) 19-33.
- [69] P. Guilbot, P. Théveneau, A. Baba-Ahmed, S. Horstmann, K. Fischer, D. Richon, *Fluid Phase Equilib.* 170 (2000) 193-202.
- [70] S. P. Kang, H. Lee, C. S. Lee, W. M. Sung, *Fluid Phase Equilib.* 185 (2001) 101-109.
- [71] C. Secuianu, V. Feroiu, D. Geana, *J. Chem. Eng. Data* 48 (2003) 1384-1386.
- [72] W. C. Andersen, R. E. Sievers, A. F. Lagalante, T. J. Bruno, *J. Chem. Eng. Data* 46 (2001) 1045-1049.
- [73] *Handbook of Optical Materials*, M. J. Weber (ed.), CRC Press, 2002.
- [74] F. Gervais, *Handbook of Optical Constants of Solids, Volume 2*, E. D. Palik (ed.), Elsevier, 1998.
- [75] Y. Sato, T. Takikawa, A. Sorakubo, S. Takishima, H. Masuoka, M. Imaizumi, *Ind. Eng. Chem. Res.* 39 (2000) 4813-4819.
- [76] D. Boudouris, J. Prinos, M. Bridakis, M. Pantoula, C. Panayiotou, *Ind. Eng. Chem. Res.* 40 (2001) 604-611.

- [77] A. J. Mesiano, R. M. Enick, E. J. Beckman, A. J. Russell, *Fluid Phase Equilib.* 178 (2001) 169-177.
- [78] L. C. Draucker, J. P. Hallett, D. Bush, C. A. Eckert, *Fluid Phase Equilib.* 241 (2006) 20-24.
- [79] L. Fedele, S. Bobbo, R. Camporese, M. Scattolini, *Fluid Phase Equilib.* 251 (2007) 41-46.
- [80] F. Y. Jou, A. Mather, *Int. J. Thermophys.* 28 (2007) 490-495.
- [81] D. Kodama, T. Seki, M. Kato, *Fluid Phase Equilib.* 261 (2007) 99-103.
- [82] J. Im, G. Lee, Y. J. Lee, H. Kim, *J. Chem. Thermodyn.* 39 (2007) 1164-1167.
- [83] M. Kato, D. Kodama, M. Sato, K. Sugiyama, *J. Chem. Eng. Data* 51 (2006) 1031-1034.
- [84] T. Laursen, S. I. Andersen, S. Dahl, O. Henriksen, *J. Supercrit. Fluids* 19 (2001) 239-250.
- [85] K. Chylinski, M. J. Cebola, A. Meredith, G. Saville, W. A. Wakeham, *J. Chem. Thermodyn.* 34 (2002) 1703-1728.
- [86] J. Freitag, M. T. S. Diez, D. Tuma, T. V. Ulanova, G. Maurer, *J. Supercrit. Fluids* 32 (2004) 1-13.
- [87] H. S. Phiong, F. P. Lucien, *J. Chem. Eng. Data* 47 (2002) 474-477.
- [88] K. Ishihara, H. Tanaka, M. Kato, *Fluid Phase Equilib.* 144 (1998) 131-136.
- [89] H. Tanaka, M. Kato, *J. Chem. Eng. Jpn.* 28 (1995) 263-266.
- [90] G. Sherman, S. Shenoy, R. A. Weiss, C. Erkey, *Ind. Eng. Chem. Res.* 39 (2000) 846-848.
- [91] A. Galia, A. Argentino, O. Scialdone, G. Filardo, *J. Supercrit. Fluids* 24 (2002) 7-17.

- [92] L. N. Nikitin, M. O. Gallyamov, R. A. Vinokur, A. Y. Nikolaev, E. E. Said-Galiyev, A. R. Khokhlov, H. T. Jespersen, K. Schaumburg, *J. Supercrit. Fluids* 27 (2003) 131.
- [93] L. N. Nikitin, M. O. Gallyamov, R. A. Vinokur, A. Y. Nikolaev, E. E. Said-Galiyev, A. R. Khokhlov, H. T. Jespersen, K. Schaumburg, *J. Supercrit. Fluids* 26 (2003) 263-273.
- [94] J. Pauly, J. L. Daridon, J. A. P. Coutinho, *Fluid Phase Equilib.* 187 (2001) 71-82.
- [95] J. Fonseca, P. C. Simoes, M. N. Nunes da Ponte, *J. Supercrit. Fluids* 25 (2003) 7-17.
- [96] R. M. Ruivo, A. Paiva, P. C. Simoes, *J. Supercrit. Fluids* 29 (2004) 77-85.
- [97] A. Bamberger, G. Sieder, G. Maurer, *J. Supercrit. Fluids* 17 (2000) 97-110.
- [98] S. Mahmood, Q. Zhao, V. N. Kabadi, *J. Chem. Eng. Data* 46 (2001) 994-999.
- [99] M. Haruki, Y. Iwai, S. Nagao, Y. Yahiro, Y. Arai, *Ind. Eng. Chem. Res.* 39 (2000) 4516-4520.
- [100] W. S. Hurst, M. S. Hodes, W. J. Bowers, V. E. Bean, J. E. Maslar, P. Griffith, K. A. Smith, *J. Supercrit. Fluids* 22 (2002) 157-166.
- [101] K. W. Cheng, M. Tang, Y. P. Chen, *Fluid Phase Equilib.* 181 (2001) 1-16.
- [102] R. Eustaquio-Rincón, A. Trejo, *Fluid Phase Equilib.* 185 (2001) 231-239.
- [103] A. Berna, A. Chafer, J. B. Montón, S. Subirats, *J. Supercrit. Fluids* 20 (2001) 157-162.
- [104] K. W. Cheng, M. Tang, Y. P. Chen, *Fluid Phase Equilib.* 201 (2002) 79-96.
- [105] D. Fu, X. Sun, Y. Qiu, X. Jiang, S. Zhao, *Fluid Phase Equilib.* 251 (2007) 114-120.
- [106] A. Kordikowski, M. Siddiqi, S. Palakodaty, *Fluid Phase Equilib.* 194-197 (2002) 905-917.
- [107] I. Goodarznia, F. Esmailzadeh, *J. Chem. Eng. Data* 47 (2002) 333-338.

- [108] P. Alessi, I. Kikic, A. Cortesi, A. Fogar, M. Moneghini, J. Supercrit. Fluids 27 (2003) 309-315.
- [109] K. W. Cheng, S. J. Kuo, M. Tang, Y. P. Chen, J. Supercrit. Fluids 18 (2000) 87-99.
- [110] Z. Q. Tan, G. H. Gao, Y. X. Yu, C. Gu, Fluid Phase Equilib. 180 (2001) 375-382.
- [111] D. Tuma, B. Wagner, G. M. Schneider, Fluid Phase Equilib. 182 (2001) 133-143.
- [112] M. Sauceau, J. Fages, J.-J. Letourneau, D. Richon, Ind. Eng. Chem. Res. 39 (2000) 4609-4614.
- [113] H. Sovova, R. P. Stateva, A. A. Galushko, J. Supercrit. Fluids 20 (2001) 113-129.
- [114] Y. Takeshita, Y. Sato, J. Supercrit. Fluids 24 (2002) 91-101.
- [115] A. Ferri, M. Banchemo, L. Manna, S. Sicardi, J. Supercrit. Fluids 30 (2004) 41-49.
- [116] V. Pauchon, Z. Cissé, M. Chavret, J. Jose, J. Supercrit. Fluids 32 (2004) 115-121.
- [117] M. Roth, J. Chromatogr. A 1037 (2004) 369-391.
- [118] T. Funazukuri, C. Y. Kong, N. Murooka, S. Kagei, Ind. Eng. Chem. Res. 39 (2000) 4462-4469.
- [119] Y. Sato, A. Tsuboi, A. Sorakubo, S. Takishima, H. Masuoka, T. Ishikawa, Fluid Phase Equilib. 170 (2000) 49-67.
- [120] T. L. Chester, J. Chromatogr. A 1037 (2004) 393-403.
- [121] A. H. Haines, D. C. Steyler, C. Rivett, J. Supercrit. Fluids 44 (2008) 21-24.
- [122] J. d. Cruz Francisco, D. Topgaard, B. Sivik, B. Bergenstahl, J. Supercrit. Fluids 31 (2004) 255-262.
- [123] I. Pasquali, J. M. Andanson, S. G. Kazarian, R. Bettini, J. Supercrit. Fluids 45 (2008) 384-390.
- [124] T. Aizawa, M. Kanakubo, Y. Ikushima, N. Saitoh, K. Arai, R. L. Smith, J. Supercrit. Fluids 29 (2004) 313-317.

- [125] Y. T. Shieh, K. H. Liu, T. L. Lin, *J. Supercrit. Fluids* 28 (2004) 101-112.
- [126] A. J. Rondinone, C. Y. Jones, S. L. Marshall, B. C. Chakoumakos, C. J. Rawn, E. Lara-Curzio, *Canadian Journal of Physics* 81 (2003) 381-385.
- [127] M. D. Jager, E. D. Jr. Sloan, *Fluid Phase Equilib.* 185 (2001) 89-99.
- [128] S. Hashimoto, S. Murayama, T. Sugahara, H. Sato, K. Ohgaki, *Chem. Eng. Sci.* 61 (2006) 7884-7888.
- [129] H. C. de Sousa, L. P. N. Rebelo, *J. Chem. Thermodyn.* 32 (2000) 355-387.
- [130] V. Najdanovic-Visak, J. M. S. S. Esperanca, L. P. N. Rebelo, M. N. Nunes da Ponte, H. J. R. Guedes, K. R. Seddon, H. C. de Sousa, J. Szydowski, *J. Phys. Chem. B* 107 (2003) 12797-12807.
- [131] J. R. Trindade, A. M. A. Dias, M. Blesic, N. Pedrosa, L. P. N. Rebelo, L. F. Vega, J. A. P. Coutinho, I. M. Marrucho, *Fluid Phase Equilib.* 251 (2007) 33-40.
- [132] M. Pantoula, C. G. Panayiotou, *J. Supercrit. Fluids* 37 (2006) 254-262.
- [133] M. Pantoula, J. von Schnitzler, R. Eggers, C. G. Panayiotou, *J. Supercrit. Fluids* 39 (2007) 426-434.
- [134] N. von Solms, J. K. Nielsen, O. Hassager, A. Rubin, A. Y. Dandekar, S. I. Andersen, E. H. Stenby, *J. Appl. Polym. Sci.* 91 (2004) 1476-1488.
- [135] N. von Solms, N. Zecchin, A. Rubin, S. I. Andersen, E. H. Stenby, *Eur. Polym. J.* 41 (2005) 341-348.
- [136] N. von Solms, A. Rubin, S. I. Andersen, E. H. Stenby, *Int. J. Thermophys.* 26 (2005) 115-125.
- [137] J. L. Anthony, E. J. Maginn, J. F. Brennecke, *J. Phys. Chem. B* 106 (2002) 7315-7320.
- [138] J. E. Palamara, P. K. Davis, U. Suriyaphadilok, R. P. Danner, J. L. Duda, R. J. Kitzhoffer, J. M. Zielinski, *Ind. Eng. Chem. Res.* 42 (2003) 1557-1562.

- [139] S. Cotugno, E. Di Maio, C. Ciardiello, S. Iannace, G. Mensitieri, L. Nicolais, *Ind. Eng. Chem. Res.* 42 (2003) 4398-4405.
- [140] S. J. Moore, S. E. Wanke, *Chem. Eng. Sci.* 56 (2001) 4121-4129.
- [141] R. Kleinrahm, W. Wagner, *J. Chem. Thermodyn.* 18 (1986) 739-760.
- [142] Y. Sato, T. Takikawa, S. Takishima, H. Masuoka, *J. Supercrit. Fluids* 19 (2001) 187-198.
- [143] R. Dohrn, S. Peper, and J. M. S. Fonseca, High-pressure fluid-phase equilibria: Experimental methods and systems investigated, 24th ESAT, European Symposium on Applied Thermodynamics, Santiago de Compostela, Spain, 2009.
- [144] K. Park, M. Koh, C. Yoon, H. Kim, H. Kim, *J. Supercrit. Fluids* 29 (2004) 203-212.
- [145] S. E. Guigard, G. L. Hayward, R. G. Zytner, W. H. Stiver, *Fluid Phase Equilib.* 187-188 (2001) 233-246.
- [146] A. H. Mohammadi, B. Tohidi, R. W. Burgass, *J. Chem. Eng. Data* 48 (2003) 612-616.
- [147] N. S. Oliveira, J. Oliveira, T. Gomes, A. Ferreira, J. Dorgan, I. M. Marrucho, *Fluid Phase Equilib.* 222-223 (2004) 317-324.
- [148] M. D. A. Saldaña, L. Sun, S. E. Guigard, F. Temelli, *J. Supercrit. Fluids* 37 (2006) 342-349.
- [149] D. R. Morris, L. Yang, F. Giraudeau, X. Sun, F. R. Steward, *Phys. Chem. Chem. Phys.* 3 (2001) 1043-1046.
- [150] A. P. Abbott, S. Corr, N. E. Durling, E. G. Hope, *J. Chem. Eng. Data* 47 (2002) 900-905.
- [151] F. C. Fourie, C. E. Schwarz, J. H. Knoetze, *J. Supercrit. Fluids* 47 (2008) 161-167.
- [152] F. E. Wubbolts, O. S. L. Bruinsma, G. M. van Rosmalen, *J. Supercrit. Fluids* 32 (2004) 79-87.
- [153] M. Th. Cohen-Adad, *Pure Appl. Chem.* 5 (2001) 771-783.

- [154] Z. Fang, R. L. Smith, H. Inomata, K. Arai, J. Supercrit. Fluids 16 (2000) 207-216.
- [155] E. Franceschi, M. B. Grings, C. D. Frizzo, J. V. Oliveira, C. Dariva, Fluid Phase Equilib. 226 (2004) 1-8.
- [156] M. Yang, E. Terakawa, Y. Tanaka, T. Sotani, S. Matsuo, Fluid Phase Equilib. 194-197 (2002) 1119-1129.
- [157] A. Diefenbacher, M. Türk, Fluid Phase Equilib. 182 (2001) 121-131.
- [158] D. D. Link, E. P. Ladner, H. A. Elsen, C. E. Taylor, Fluid Phase Equilib. 211 (2003) 1-10.
- [159] H. S. Byun, M. A. McHugh, Ind. Eng. Chem. Res. 39 (2000) 4658-4662.
- [160] J. L. Daridon, J. Pauly, M. Milhet, Phys. Chem. Chem. Phys. 4 (2002) 4458-4461.
- [161] R. Dohrn, E. Bertakis, O. Behrend, E. Voutsas, D. Tassios, J. Mol. Liq. 131-132 (2007) 53-59.
- [162] K. Fukné-Kokot, A. König, Z. Knez, M. Skerget, Fluid Phase Equilib. 173 (2000) 297-310.
- [163] H. I. M. Veiga, L. P. N. Rebelo, M. N. Nunes da Ponte, J. Szydlowski, Int. J. Thermophys. 22 (2001) 1159-1173.
- [164] X. Dong, C. Erkey, H. J. Dai, H. C. Li, H. D. Cochran, J. S. Lin, Ind. Eng. Chem. Res. 41 (2002) 1038-1042.
- [165] D. Minicucci, X.-Y. Zou, J. M. Shaw, Fluid Phase Equilib. 194-197 (2002) 353-360.
- [166] A. Drozd-Rzoska, S. J. Rzoska, A. R. Imre, Phys. Chem. Chem. Phys. 6 (2004) 2291-2294.
- [167] U. Domanska, P. Morawski, Phys. Chem. Chem. Phys. 4 (2002) 2264-2268.
- [168] D. Kodama, J. Miyazaki, M. Kato, T. Sako, Fluid Phase Equilib. 219 (2004) 19-23.
- [169] J. Ivanic, Z. Huo, E. D. Jr. Sloan, Fluid Phase Equilib. 222-223 (2004) 303-310.

- [170] A. H. Mohammadi, W. Afzal, D. Richon, *J. Chem. Thermodyn.* 40 (2008) 1693-1697.
- [171] N. Gnanendran, R. Amin, *Fluid Phase Equilib.* 221 (2004) 175-187.
- [172] R. Masoudi, B. Tohidi, R. Anderson, R. W. Burgass, J. Yang, *Fluid Phase Equilib.* 219 (2004) 157-163.
- [173] R. Ohmura, S. Matsuda, S. Takeya, T. Ebinuma, H. Narita, *Int. J. Thermophys.* 26 (2005) 1515-1523.
- [174] E. F. May, T. J. Edwards, A. G. Mann, C. Edwards, R. C. Miller, *Fluid Phase Equilib.* 185 (2001) 339-347.
- [175] T. Takagi, K. Fujita, D. Furuta, T. Tsuji, *Fluid Phase Equilib.* 212 (2003) 279-283.
- [176] R. M. Oag, P. J. King, C. J. Mellor, M. W. George, J. Ke, M. Poliakoff, V. K. Popov, V. N. Bagratashvili, *J. Supercrit. Fluids* 30 (2004) 259-272.
- [177] E. D. Nikitin, A. P. Polov, N. S. Bogatishcheva, Y. G. Yatluk, *J. Chem. Eng. Data* 47 (2002) 1012-1016.
- [178] D. M. VonNiederhausen, G. M. Wilson, N. F. Giles, *J. Chem. Eng. Data* 45 (2000) 157-160.
- [179] V. M. Valyashko, I. M. Abdulagatov, J. M. H. L. Sengers, *J. Chem. Eng. Data* 45 (2000) 1139-1149.
- [180] A. Würflinger, S. Urban, *Phys. Chem. Chem. Phys.* 3 (2001) 3727-3731.
- [181] T. T. Ngo, D. Bush, C. A. Eckert, C. L. Liotta, *Aiche J.* 47 (2001) 2566-2572.
- [182] S. L. Randzio, C. Stachowiak, J. P. E. Grolier, *J. Chem. Thermodyn.* 35 (2003) 639-648.
- [183] O. Y. Zatsepina, B. A. Buffett, *Fluid Phase Equilib.* 192 (2001) 85-102.
- [184] H. Omi, B. Nagasaka, K. Miyakubo, T. Ueda, T. Eguchi, *Phys. Chem. Chem. Phys.* 6 (2004) 1299-1303.

- [185] K. Fischer, M. Wilken, *J. Chem. Thermodyn.* 33 (2001) 1285-1308.
- [186] M. Funke, R. Kleinrahm, W. Wagner, *J. Chem. Thermodyn.* 34 (2002) 735-754.
- [187] José M. S. Fonseca, M.Sc. Thesis, Department of Chemistry of the Faculty of Sciences of the University of Porto, Porto, Portugal, 2004.
- [188] M. J. S. Monte, L. M. N. B. Santos, M. Fulem, J. M. S. Fonseca, C. A. D. Sousa, *J. Chem. Eng. Data* 51 (2006) 757-766.
- [189] R. Dohrn, O. Pföhl, *Fluid Phase Equilib.* 194-197 (2002) 15-29.
- [190] O. Pföhl, R. Dohrn, *Fluid Phase Equilib.* 217 (2004) 189-199.
- [191] J. Kumelan, Á. P.-S. Kamps, I. Urukova, D. Tuma, G. Maurer, *J. Chem. Thermodyn.* 37 (2005) 595-602.
- [192] J. Kumelan, Á. P.-S. Kamps, D. Tuma, G. Maurer, *Fluid Phase Equilib.* 228-229 (2005) 207-211.
- [193] J. Kumelan, Á. P.-S. Kamps, D. Tuma, G. Maurer, *J. Chem. Eng. Data* 51 (2006) 11-14.
- [194] J. Kumelan, D. Tuma, G. Maurer, *J. Chem. Eng. Data* 51 (2006) 1802-1807.
- [195] J. Kumelan, Á. P.-S. Kamps, D. Tuma, G. Maurer, *J. Chem. Eng. Data* 51 (2006) 1364-1367.
- [196] J. Kumelan, Á. P.-S. Kamps, D. Tuma, G. Maurer, *J. Chem. Thermodyn.* 38 (2006) 1396-1401.
- [197] J. Kumelan, Pérez-Salado Kamps, I. Urukova, D. Tuma, G. Maurer, *J. Chem. Thermodyn.* 39 (2007) 335.
- [198] J. Kumelan, Á. P.-S. Kamps, D. Tuma, G. Maurer, *Fluid Phase Equilib.* 260 (2007) 3-8.
- [199] J. Kumelan, Á. P.-S. Kamps, D. Tuma, G. Maurer, *Ind. Eng. Chem. Res.* 46 (2007) 8236-8240.

- [200] J. Kumelan, Á. P.-S. Kamps, D. Tuma, G. Maurer, *J. Chem. Eng. Data* 52 (2007) 2319-2324.
- [201] J. Kumelan, Á. P.-S. Kamps, D. Tuma, A. Yokozeki, M. B. Shiflett, G. Maurer, *J. Phys. Chem. B* 112 (2008) 3040-3047.
- [202] J. Kumelan, D. Tuma, S. P. Verevkin, G. Maurer, *J. Chem. Eng. Data* 53 (2008) 2844-2850.
- [203] O. Pfohl, C. Riebesell, R. Dohrn, *Fluid Phase Equilib.* 202 (2002) 289-306.
- [204] Y. Sato, T. Takikawa, M. Yamane, S. Takishima, H. Masuoka, *Fluid Phase Equilib.* 194-197 (2002) 847-858.
- [205] X. Yuan, S. Zhang, Y. Chen, X. Lu, W. Dai, R. Mori, *J. Chem. Eng. Data* 51 (2006) 645-647.
- [206] S. Zhang, X. Yuan, Y. Chen, X. Zhang, *J. Chem. Eng. Data* 50 (2005) 1582-1585.
- [207] L. A. Blanchard, Z. Gu, J. F. Brennecke, *J. Phys. Chem. B* 105 (2001) 2437-2444.
- [208] X. Yuan, S. Zhang, J. Liu, X. Lu, *Fluid Phase Equilib.* 257 (2007) 195-200.
- [209] S. Zhang, Y. Chen, R. X. F. Ren, Y. Zhang, J. Zhang, X. Zhang, *J. Chem. Eng. Data* 50 (2005) 230-233.
- [210] S. Bobbo, L. Fedele, M. Scattolini, R. Camporese, R. Stryjek, *Fluid Phase Equilib.* 256 (2007) 81-85.
- [211] J. Kiepe, S. Horstmann, K. Fischer, J. Gmehling, *Ind. Eng. Chem. Res.* 41 (2002) 4393-4398.
- [212] R. A. Harris, M. Wilken, K. Fischer, T. M. Letcher, J. D. Raal, D. Ramjugernath, *Fluid Phase Equilib.* 260 (2007) 60-64.
- [213] K. M. Krüger, O. Pfohl, R. Dohrn, G. Sadowski, *Fluid Phase Equilib.* 241 (2006) 138-146.
- [214] L. A. Weber, *J. Chem. Eng. Data* 45 (2000) 173-176.

- [215] M. B. Ewing, J. C. S. Ochoa, *J. Chem. Eng. Data* 49 (2004) 486-491.
- [216] A. I. Abdulagatov, G. V. Stepanov, I. M. Abdulagatov, *Fluid Phase Equilib.* 209 (2003) 55-79.
- [217] L. E. Gutiérrez, K. D. Luks, *Fluid Phase Equilib.* 205 (2003) 89-102.
- [218] A. Hassan, K. L. Levien, J. J. Morrell, *Fluid Phase Equilib.* 179 (2001) 5-22.
- [219] G. Di Nicola, G. Giuliani, F. Polonara, R. Stryjek, *Fluid Phase Equilib.* 210 (2003) 33-43.

# **Chapter 4**

## ***New Experimental Set-up, Analytical Method***

---

The comprehensive review of existing phase equilibria data for the systems under consideration in this work, presented in Chapter 2, revealed the need for new accurate and reliable data, preferably with full characterization of all the phases present in equilibrium. While for some systems the data is very scarce, especially in particular ranges of pressure and temperature, for some better studied systems there are still considerable divergences in the results obtained by different research groups, as it was recently demonstrated in the work of Folas et al. [1], for the solubility of methane in water. In the analysis of the articles in the literature survey presented in Chapter 2, it was also found that often, a considerable part of the information available from the experiments is simply disregarded. Examples of this are several studies of solubility of one compound in another phase, disregarding the determination of mutual solubilities, sometimes easily available with small changes in the experimental setup and in the procedure.

Other problems are related to experimental limitations in the complete analysis of some of the phases, mostly due to very low concentrations, such as in the determination of the water and glycol content in the gas phase. But as in many other areas, continuous technological developments have led to significant advances in the available instrumentation, with increased sensitivity, promoting the development of new methods and the enhancement of the existing ones, thus allowing not only the measurement of new data but also the evaluation of the existing values.

With this as motivation, we set out to develop a new experimental apparatus, and to work in the improvement and modernisation of a previously existing one, as an effort to enhance the existing experimental methods available in our laboratory. In this chapter, the description of both apparatus is presented.

#### ***4.1. Development of a New Experimental Set-up – Preliminary Steps***

The development of a new experimental set-up entails a series of preliminary steps which usually go unnoticed when looking at the final result. These preliminary studies are often time consuming, but they should not be disregarded, as they are of prime importance for the accomplishment of a high quality for the new assembly.

The first step is, naturally, to have a clear idea of the goals to achieve, i.e., what properties ought to be measured, what type of compounds are involved, their toxicity, possibility of corrosion, temperature and pressure ranges, always considering the necessary thermodynamic background. After this, a critical evaluation of existing apparatus, in the laboratories of the group or described in literature, should be performed, with special attention to the existing problems, limitations, possible sources of errors and aspects which could be improved. Similarly, good ideas are frequently found, which can serve as inspiration for the future installation. Ultimately, combining existing good ideas, some innovation, and avoiding the errors committed by others, an improved apparatus can be developed.

After this is done, a creative process can then start, with the design of the apparatus through inspiration and innovative ideas. The result is only a first sketch that should undergo a maturation process, through the exchange of ideas with specialists from different areas, about what materials to use, the difficulty involved in machining the necessary parts, etc. This will most certainly lead to some changes and refinements. Further improvements can also emerge with the foreseeing of possible problems with the future installation. This is a very important stage that consists in simulating the operation of the apparatus, carefully looking at every step of the procedure. A distraction at this stage, or the disregarding of some aspects may lead to severe consequences once the apparatus is ready,

the desired experimental procedure may be impossible to carry out and solutions have to be improvised, often at the expense of the precision of the results.

Another important point to take into account, from a management point of view, is the fact that projects do not last forever, and due to the cost and complexity of some experimental set-ups, the possibility of adapting the apparatus for other applications in the future should be considered, such as the study of different systems, or even for different types of measurements. With this in mind, a modular construction presents unique advantages, either when some parts need to be substituted, or in improving the versatility of the apparatus. In the last case, the eventual decommissioning of the apparatus should ensure the possibility of using all, or almost all its parts in other different applications.

Having taken all these aspects into account, a selection of the materials and of the instrumentation to use should be performed, based on factors such as cost, quality, precision, previous experience with manufacturers, etc., and whenever possible, making a good use of available technological advancements. Nowadays, this will surely involve a considerable knowledge of electronics, especially for data acquisition and process automation. It is likely that this step will also lead to further small changes to the design.

If the planning was careful, and the necessary parts were manufactured according to the design, the stage of assembly of all the parts should proceed without further complications. In this aspect, computer-aided design (CAD) has become an invaluable tool, allowing to virtually build the apparatus and to “travel” through it using three dimensional applications, even before the parts have been manufactured or acquired. Currently, modern equipment used by workshops in the machining of parts also uses this type of software, making the process easier and less susceptible of errors.

In summary, the development of a new experimental set-up is a multidisciplinary process, requiring knowledge in different areas, from metrology to material science, electronics or CAD software, in addition to the necessary knowledge in the area of application of the apparatus.

## 4.2. *New Experimental Set-up, Analytical Method*

The aforementioned need for new accurate and reliable data, as well as the demand for a full characterization of all the phases present in a system, including the quantification of residual amounts of non-volatile compounds in the gas phase, has been confirmed in discussions with industry [2]. Furthermore, there is industrial interest in measurements at very low temperatures, down to 213 K, so as to replicate polar conditions for example.

With this in mind, it became obvious that the better suited method for the study of phase equilibrium in the systems under consideration in this work, would be an analytical method. This implies a higher complexity of the equipment, with the necessary development of a sampling procedure, as well as of an analytical method. Nevertheless, analytical methods allow a better understanding of the equilibrium systems under study, with the desirable characterisation of all the phases involved, from a purely experimental approach, without referring to mass balances, use of equations of state or other approximations. These methods also allow the study of more complex systems, analogous to the “real-life” systems typical of industrial problems. This is an undeniable advantage of the method.

As mentioned in Chapter 3, one of the main problems with the analytical methods has to do with the possible occurrence of pressure drops associated with the sampling process. Exempt from this problem are of course the analytical methods in which an *in-situ* analysis is performed. The problem of pressure drops can usually be dealt with by two means, either by using special sampling valves, capable of withdrawing very small sample volumes with negligible influence on the pressure of the system, or by using a variable volume cell, where a piston can reduce the volume of the cell during sampling, keeping the inner pressure constant. Both solutions have also additional advantages. The use of special valves can simplify greatly the sampling procedure, making it possible to perform online sampling, where the entire sample is inserted directly into, for example, a gas chromatograph (GC) carrier gas line, without the need for dilutions or any other manipulation. This is possible only through the use of very small samples; otherwise a saturation of the GC column might occur. The use of a variable volume cell simplifies the operation of the apparatus extensively, allowing a very simple pressure regulation without changing the overall composition of the system, in order to get a desired value of pressure,

or to drive the system to the appearance of new phases, for the observation of critical phenomena, etc.

Another great advantage in an equilibrium cell, as already mentioned in the previous chapter, is the use of windows, for visual observation of the contents of the cell, interfaces between phases, among other phenomena. Among possible materials, sapphire is likely to be the most obvious choice. Despite its cost, a sapphire single crystal is one of the hardest materials, being much stronger than glass and representing a good solution for viewing windows in high pressure and vacuum applications. It possesses a high mechanical strength, chemical resistance, thermal conductivity and thermal stability. Furthermore, sapphire presents good transmission characteristics over the visible, near IR and near UV spectrum, with an useful optical transmission range of wavelengths in the range from 200 nm to 5500 nm [3,4], which can also constitute an advantage if spectroscopic or other *in-situ* methods are considered for analysis. Rondinone et al. [5] developed a sapphire cell for the study of gas hydrates using neutron-scattering experiments, taking advantage of the special characteristics of this material. Gorbaty and Bondarenko [6] presented an apparatus for Raman studies in corrosive liquids suitable for measurements at pressures up to 100 MPa and temperatures up to 800 K, in which the liquids under study could only come in contact with sapphire and gold.

Besides some of the apparatus already mentioned in Chapter 3, other examples of experimental set-ups specially designed for operation at low temperatures and high pressures can be found in the literature [5,7,8]. In addition to a careful evaluation of many equipments found in the literature, the preliminary stage of this work also included a visit to the Research and Development Centre of Statoil ASA, in Trondheim, Norway, providing an opportunity for accompanying the operation of some of the existing apparatus and the exchange of ideas with people working in this area. One of these apparatus, a commercial set-up developed by Sanchez Technologies, France, and previously described in the literature [9], served as inspiration and as a starting point for the design of the new cell presented in this work.

After a number of contacts with different companies for the supply of an equilibrium cell or an apparatus, it became clear that the use of a commercial model would always, invariably, imply some limitations, either in the temperature range of application, in the selection of parts, in the quality of the instrumentation, or in the main characteristics of the

cell itself. Taking this into consideration, and considering the high costs associated with the commercial versions available, a decision was made to develop an apparatus based on a cell designed specifically for this purpose, and therefore meeting all the desired requirements.

The most immediate challenges were directly related with the desired temperature range of application of the apparatus. Working at temperatures below 230 K imposes severe limitations on the parts and components to be used in the apparatus. The most commonly used polymers used in valve sealings for example, are not suitable for such conditions, and the same is valid for motors, pumps and other electric or electronic systems. Special attention is therefore required in the selection of parts, with the necessity for extended testing, in order to take the components to the limit, which are not always in agreement with the specifications publicised by the suppliers.

The resulting apparatus is presented next, first with an overall presentation and afterwards focusing the attentions in the most important parts and components, underlining for each one the grounds for its design or for its selection.

#### ***4.2.1. Description of the Apparatus***

In this section of the work, a new experimental set-up is presented, that although priming for its versatility, was specially designed for the measurement of multi-phase equilibria in hydrocarbon-water-hydrate inhibitor systems, at temperatures ranging from 213 K to 353 K and at pressures up to 40 MPa. The apparatus depicted in Figure 4.1 and schematically represented in Figure 4.2, is based on an analytical isothermal method, what some authors would call a static analytical method. However, as mentioned in Chapter 3, the term “static” is avoided in this work due to some ambiguity in its use.

According to the classification proposed and described in two recent works [10,11], this method would be classified as “AnTCapValVarVis”, i.e., it uses an isothermal analytical method, where special capillary valves are used for sampling, from a cell of variable volume, with a view window.



**Figure 4.1** – General aspect of the new developed experimental set-up for the measurement of multi-phase equilibria, showing the cell inside the temperature chamber and the GC unit.

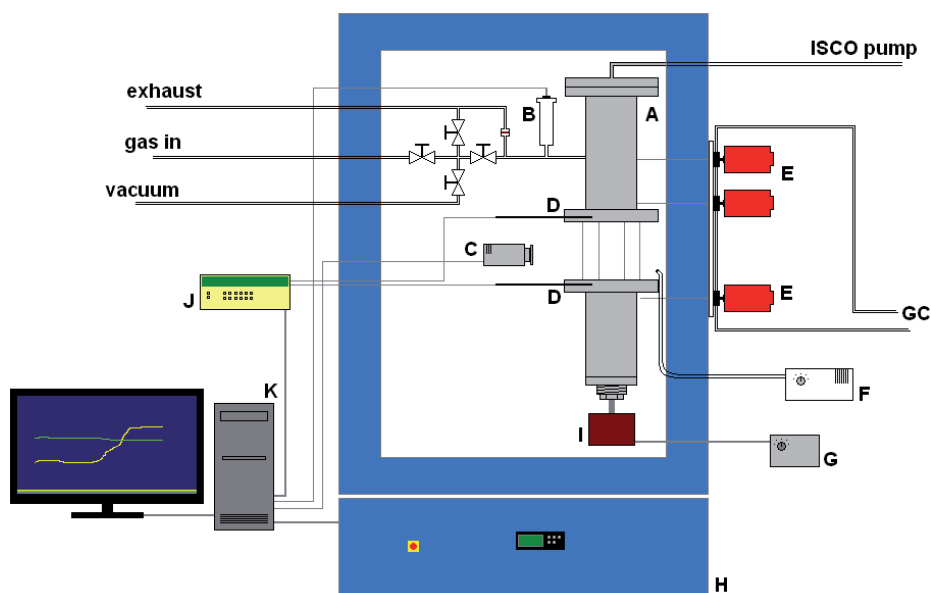


**Figure 4.2** – Schematic representation of the new experimental set-up for the measurement of multi-phase equilibria. – A: High pressure cell with 360° sapphire window. B: Temperature compensated high precision pressure sensor. C: Video camera. D: Platinum resistance thermometers Pt100. E: ROLSI™ samplers. F: Cold light source with optical fibre. G: Remote control for the stirring motor. H: Low temperature chamber. I: Stirring motor. J: Data logger. K: Computer.

The apparatus can, however, be easily adapted to a recirculation method, through very small changes in the system, when a thorough mixing of the different components is necessary for a faster achievement of the equilibrium, or for example, in cases where the high viscosity of the lower phase may interfere with the efficiency of the magnetic stirring.

The main part of the apparatus is the variable-volume high-pressure equilibrium cell, specially designed for this application and equipped with a 360° sapphire window. The volume of the cell can be varied manually and automatically by means of a high pressure syringe pump. The temperature, measured in different points of the cell by platinum resistance thermometers is monitored and recorded over time through a computer, to which is also connected the temperature compensated pressure sensor. The same computer controls the temperature chamber inside which the cell is contained.

Connected to the cell are three automatic ROLSI™ sampler-injectors, which allow the withdrawing of very small samples from the different phases directly to the carrier gas stream of a gas chromatograph (GC), where the samples are then analysed. In the current configuration, the GC analysis was made using an Agilent 6890 GC System (Agilent Technologies, Inc., USA), equipped with an Agilent 7683B automatic injector, a HP-PLOT Q capillary column, and a thermal conductivity detector (TCD) coupled in series with a flame ionisation detector (FID), although the apparatus was designed accounting for the possibility of connecting a second gas chromatograph associated with mass spectroscopy (GC-MS), for more complex analysis and a lower detection limit. A second computer using the software GC ChemStation (Agilent Technologies, Inc., USA) is used for the acquisition and treatment of the GC data. The possibility of using columns for automated thermal desorption columns (ATD columns) and/or other methods such as coulometric Karl-Fischer titration for the analysis of non-volatile compounds in the gas phase were also considered.

Figure 4.3 shows the equilibrium cell mounted on a structure specially designed and constructed for this application, inside the temperature chamber. The picture also illustrates the connection to the stirring motor, all the valves and the platinum resistance thermometers. The luminosity around the sapphire window is noticeable, provided by the cold light source connected to the optical fibre placed under the valves.

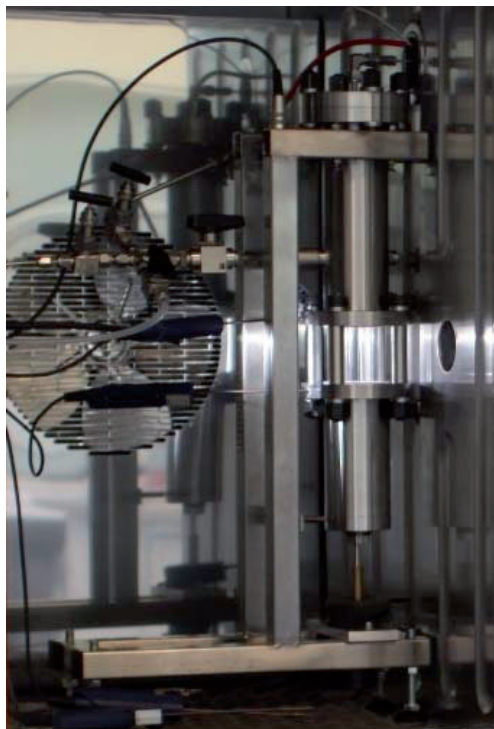


**Figure 4.3** – Image of the equilibrium cell mounted on a structure specially designed and constructed for this application, inside the temperature chamber.

The position of the cell close to the side wall of the temperature chamber is necessary due to the sampling system, in order to keep the connections to the ROLSI™ samplers, placed outside the chamber, as short as possible, since the thickness of the temperature chamber is already considerable, around 150 mm.

The total cost of this apparatus, excluding the gas chromatograph and the high pressure syringe pump already available in our laboratory, was under 308 000 DKK (approximately 41 350 EUR), a value considerably lower than the amounts usually involved in the acquisition of available commercial versions, despite the use of high quality parts only.

## ***The cell***

The core of this apparatus is the high pressure cell, entirely designed and built “in house”, in Stainless Steel 316, equipped with a 360° sapphire window, and with an operating volume variable from approximately 116 cm<sup>3</sup> to 207 cm<sup>3</sup>. The cell was planned and designed by the author, through the use of SolidWorks 3D CAD Design Software, which was used to produce the files that were subsequently handed to the workshop of the department for the building process.

The body of the cell can be seen in more detail in Figure 4.4, where a three dimensional computer generated image is presented, as well as an image with a cut of the cell, showing its interior.



**Figure 4.4** – Three-dimensional computer generated images of the high pressure cell. – **On the left:** View of the cell. **On the right:** Cut of the cell showing its interior.

The cell is constituted by two stainless steel segments connected through a tube of sapphire that acts as a 360° window. The inner diameter of the cell varies from a maximum of 40 mm for the stainless steel segments to a minimum of 20 mm for the inner diameter of the sapphire tube. Although the resulting hourglass-like shape may impose some limits on the effectiveness of the stirring system, the dimensioning of the sapphire segment was conditioned by its tensile strength and by the price of this material.

The sapphire has a wall thickness of 15 mm and it was dimensioned according to the properties of the material provided by the supplier, to cope with pressures of 40 MPa for extended periods of time, but also to pass the safety tests imposed by the internal rules at the department, according to which, the cell had to be tested for a pressure of approximately 133% of the maximum operating pressure (54 MPa). The synthetic sapphire single crystal ( $\text{Al}_2\text{O}_3$ , 99.9%) was acquired from Goodfellow Cambridge Ltd., UK, with a polishing better than  $0.1\mu\text{m}$   $R_a$  (the average radius of the irregularities or cavities in the surface is inferior  $0.1\mu\text{m}$ ).

Each of the stainless steel segments contains a piston in its interior, for regulation of the volume of the cell. As visible in the cut-view of the cell in Figure 4.4, in the lower segment of the cell there is a hollow piston, designed to comprise in its interior the magnetic stirring system, as described later. This piston, of manual operation, is capable of inducing a  $24\text{ cm}^3$  difference in the volume of the cell, and it is intended to be adjusted in the beginning of a series of experiments, influencing the range of volumes available for those experiments. It can, however, be regulated at anytime, allowing for example the height of the interface between two phases to be conveniently positioned on the sapphire window, or the adjustment of the position of the sampling points relatively to the different phases. This piston is connected to the bottom of the cell through a thread, and its position is adjusted by means of its six-sided tip like a regular bolt. Care should be taken when operating this piston, in order not to damage the extensible telescopic connection of the magnetic system.

Inside the upper segment of the cell, there is a floating piston, which has a displacement of 535 mm between its extreme positions, accounting for a variation in the volume of the cell of approximately  $67\text{ cm}^3$ . It is understood that the length of the piston constitutes a limit to the extension of its displacement, influencing also the external size of the whole equilibrium cell, but the dimensions of the piston are intended to provide the necessary stability during its displacement inside the cell, in order to minimize possible deviations from its axial position, which could result in a blockage of the piston and/or in the damaging of the cell's inner wall surface, polished electrochemically for a better performance of the seals. Its massive design makes it heavier, but on the other hand contributes to the thermal inertia of the cell, which is an important factor in equilibrium measurements.

The piston has the purpose of compensating for any pressure drops that might result from the sampling process, although it can also be used to set a specific value of pressure in the cell, for example to promote the appearance of a new phase, or the observation of critical phenomena, as mentioned before. The position of the piston is set by the balance between the pressure inside the cell and the pressure imposed by a high pressure syringe pump ISCO 100DX (Teledyne Isco, Inc., USA), using as pressure transmitting medium the thermal fluid Julabo Thermal HL80 (JULABO Labortechnik GmbH, Germany). This fluid, based on polydimethylsiloxanes and polyphenylmethylsiloxanes, was originally designed to be used as a cooling fluid in thermal baths with recirculation, at temperatures down to 188 K (maximum temperature 443 K). Its characteristic low viscosity even at low temperatures, 70 cSt at 193 K ( $1 \text{ cSt} = 1 \times 10^{-6} \text{ m}^2 \cdot \text{s}^{-1}$ ; as a reference, at 293 K, the kinematic viscosity of water is about 1 cSt, while for glycerine is 648 cSt) makes it ideal for this particular application, since the transmission of the pressure to the cell is done through a pipe of reduced dimensions and an increase in the viscosity of the medium could lead to delays in the piston actuation or even to its inoperability [12].

This viscosity problem could be easily avoided by the use of a gas as a pressure transmitter medium, but this would lead to several other problems. The high thermal expansion and compressibility of the gas would cause a considerable instability in the pressure generated with the high pressure syringe pump. It is expected that the equilibrium cell will frequently be operated at a temperature which differs greatly from the temperature of the syringe pump, meaning that the injection or withdrawing of gas would lead to changes in its temperature, with a consequent expansion or contraction, making necessary further adjustments from the syringe pump, eventually leading to pressure oscillations in the cell. Furthermore, the amount of gas necessary to promote a certain pressure is always much higher than the amount of liquid necessary for the same process, due to the much lower compressibility factor of the last. This means that the use of a gaseous fluid for pressure transmission would imply the use of an intermediate reservoir of some type, since the syringe pump has a limited capacity. The use of a liquid is also recommended where safety is concerned.

The total weight of the cell, including bolts and nuts, is over 15 kg, and although this affects its practicality, it provides the cell a high thermal inertia, related directly to the mass of the cell and the heat capacity of its constituent materials. A higher thermal inertia

will contribute to a slower achievement of the programmed temperature, but this is largely compensated by the fact that once in equilibrium, the cell will attenuate the inevitable temperature oscillations inside the temperature chamber, especially when working at temperatures that differ greatly from the ambient temperature.

The air tightness of the cell is assured by Mupu seals, both in the case of static seals such as those between the sapphire and the stainless steel segments, as in the case of the dynamic seals in the outer walls of the pistons. Mupu seals, showed in Figure 4.5, are high performance seals consisting of a jacket of Kefloy<sup>®</sup> energized by a metal spring. This type of sealing overcomes the limitations of the more traditional sealing materials, being suitable for pressures up to 60 MPa and temperatures as low as 200 K or even lower, depending on the polymers used. The material initially used in this work was acquired from M-SEALS A/S, Denmark, but due to a series of unsatisfactory results, new parts were acquired from DICHTA SA, Switzerland. Similar parts are also available from other suppliers, for example, from Sealco International Ltd, USA, or from TEST Systemy Uszczelniające, Poland.

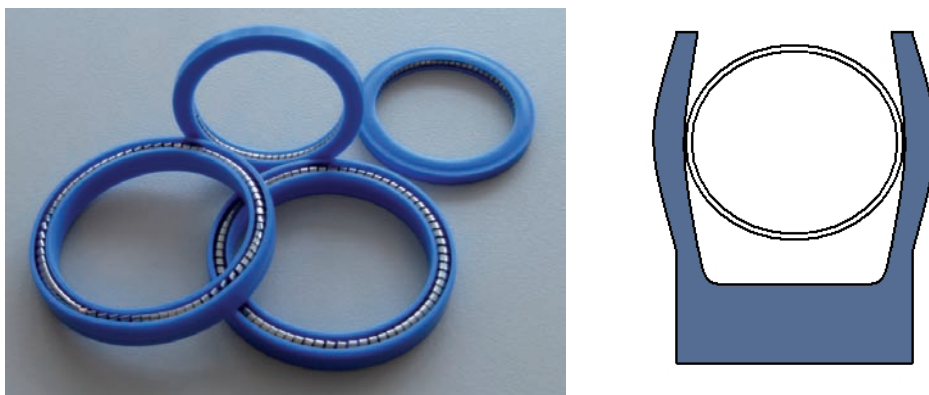


**Figure 4.5** – Mupu seals. – **On the left:** Examples of Mupu seals. **On the right:** Schematic drawing of a Mupu seal.

### ***Thermostatisation of the cell***

One of the main goals for this apparatus is its extensive temperature range of operation, reaching values as low as 213 K. To accomplish this, different solutions were considered for the thermostatisation of the cell.

The first choice was made between the use of either liquid, or air thermal baths. While the first type can usually provide better temperature stability, air baths are far more practical, requiring no special concerns about the position of electronic components that might not be air tight and cannot be submersed. Liquid baths can also be less effective when the temperature of operation differs greatly from the ambient temperature, and unless special fluids are used, with high costs associated, the same fluid cannot be used in an extensive range of temperatures.

After this, contacts were established with companies working in the cooling / refrigeration area, for discussions regarding the use of either cryogenic or mixed (cryogenic plus mechanical) cooling as an alternative to mechanical refrigeration. Both methods have their advantages and disadvantages. Especially when such low temperatures need to be achieved and maintained for long periods, cryogenic cooling has lower energetic requirements. Additionally, cryogenic coolants such as nitrogen or carbon dioxide are less harmful to people and to the environment than the refrigerants used in mechanical cooling. However, this option would require the design and building of a temperature chamber, and its practicality is limited due to the inevitable need to refill a reservoir with the cryogenic liquid regularly. Mechanical refrigeration is therefore more practical, it is better established and readily available in commercial solutions. Moreover, there has been a substantial increase in the energetic efficiency of the modern commercial units making them more environmentally friendly.

The final choice for thermostatisation of the equilibrium cell was a temperature chamber WEISS WT 240/70, specially customized by the manufacturer, Weiss Umwelttechnik GmbH, Germany, for this application. With an internal working volume of 240 dm<sup>3</sup> and equipped with a relatively large window in its front, this temperature chamber is designed to promote a stable temperature on its interior, in the range from 203 K to 453 K with a temperature constancy better than  $\pm 0.7$  K over time, according to the manufacturer. Preliminary tests have shown, however, that the temperature stability inside the chamber is better than this value, around  $\pm 0.5$  K even for very low temperatures, leading subsequently to a temperature stability of the cell better than 0.005 K, due to its thermal inertia. The temperature chamber is equipped with a 32-bit MINCON<sup>®</sup> controller and it has a RS-232 C interface for connection to a computer, allowing the chamber to be controlled through the software SIMPATI<sup>®</sup>, also supplied by the manufacturer.

## ***Temperature and pressure measurements***

Probably the most important parameters in any thermodynamic measurement are temperature and pressure. In phase equilibria this is evident, regardless of the experimental method used.

The temperature of the cell is monitored with a resolution of 0.001 K and a precision of 0.01 K, through two four-wire platinum resistance thermometers Pt100 class 1/10 DIN, acquired from Dostmann Electronic GmbH, Germany, placed horizontally over and under the sapphire window, perpendicularly to each other, meaning that one of the sensors has its tip in the front side of the cell, while the other sensor has its tip in the back of the cell. This configuration is intended to readily detect any problems with the temperature uniformity in the cell. The thermometers, with a diameter of 3 mm, are inserted in specially cavities with thermal paste, in order to improve the thermal contact. In the absence of standard thermometry equipment in the laboratory, the temperature sensors were calibrated according to the International Temperature Scale ITS-90, at the triple point of water, through the careful measurement of their electrical resistance at that temperature,  $R_0$ .

The thermometers are connected to a data acquisition system Agilent 34970A (Agilent Technologies, Inc., USA) which is in turn connected to a computer via a RS-232 connection, for monitoring and recording of the experimental conditions through the software Agilent BenchLink Data Logger 3 from the same manufacturer. During the period of tests, additional platinum resistance thermometers were placed in different points of the temperature chamber in order to monitor the temperature stability and its uniformity in space.

One of the main sources of errors in pressure measurements has to do with the change in the response of the sensor with the temperature at which it operates. In the measurement of very low pressures, in the order of 1 Pa for example, where extreme precision and accuracy are crucial, it is common that the electronics are placed separately from the sensor itself, in a compartment with an independent temperature control. The most common solution to this problem is to place the pressure sensor outside the thermostated area, consequently further from the equilibrium cell. However, this can create areas where accumulation of residues may occur with time, for example due to condensation. Another way to circumvent this problem, although with an extra cost

associated, is to use temperature compensated pressure sensors. For the apparatus under consideration, this was thought to be the best solution.

The pressure inside the cell is monitored by means of a temperature compensated, high precision, pressure transmitter Keller 33X (KELLER AG für Druckmesstechnik, Switzerland), for measurements up to 50 MPa with an accuracy of 0.1% of the full scale (0.05 MPa) over the whole temperature range of operation. This transmitter is equipped with a floating piezoresistive transducer and an internal microprocessor with an integrated 16-bit A/D converter. The thermal compensation is calculated mathematically by the microprocessor with reference to the calibration data matrix stored in an internal non-volatile memory and determined during calibration in the factory. These calculations are performed approximately every 2 ms, using the temperature readings from the transmitter's internal temperature sensor, yielding a pressure value independent of the operation temperature. To the higher precision of the transmitter contributes the digital output, allowing a direct connection to the computer via a RS-485 to RS-232 adaptor, with the monitoring and recording of the pressure being made through the software READ30, also supplied by the manufacturer. The option for an analogue output was also available from the supplier, which would allow the connection of the pressure transmitter to the Agilent 34970A data logger to which the temperature sensors are also connected. This would allow the use of a single program for data acquisition, but with a compromise in the accuracy of the pressure measurements. In any case, the collection and recording of temperature and pressure values during the experiments can be set to occur simultaneously, and afterwards, the data from both programs can be exported to data analysis software such as Microsoft Office Excel<sup>TM</sup> or Origin (OriginLab Corporation, USA) for a combined evaluation. The zero of the sensor was adjusted against a Crouzet quartz mano 2100, last calibrated in May 2009 by Buhl & Bønsøe A/S, a company accredited by DANAK, The Danish Accreditation and Metrology Fund.

Although being the best available option, there are still some limitations regarding this pressure transmitter. Its range of operability goes from 233 K to 393 K, but the effectiveness of the temperature compensation is limited to the interval between 263 K and 353 K. Nevertheless, and similarly to what was found for the temperature chamber, the preliminary tests showed that the results were in fact better than what was claimed by the manufacturer. Although this may seem somewhat strange, it is in fact quite usual, and it

relates to the safety margins that the manufacturing companies usually use when publicising the specifications for their products. Unfortunately the opposite is also frequently found to be the case.

### ***The sampling system***

The sampling system consists of three automatic electromagnetic capillary ROLSI™ samplers, a product developed by the CENERG-TEP laboratory of the ENSMP (École Nationale Supérieure des Mines de Paris), with a patent registered to Armines and commercialised by Transvalor, France, already mentioned in the third chapter of this work. Developed specifically for the purpose of phase equilibria studies, The ROLSI™ samplers have been establishing themselves as a reference worldwide, being currently used in many universities as well as in industry, in many research groups considered as a reference for phase equilibria and petroleum related studies [13-22].

These sampler-injectors, shown previously in Figure 3.2 and illustrated in Figure 4.6, are electromagnetic valves that allow taking samples from each of the phases without the disturbance of the other phases in equilibrium, and vaporising them directly to the carrier gas stream of a gas chromatograph, without any manipulation of the samples.

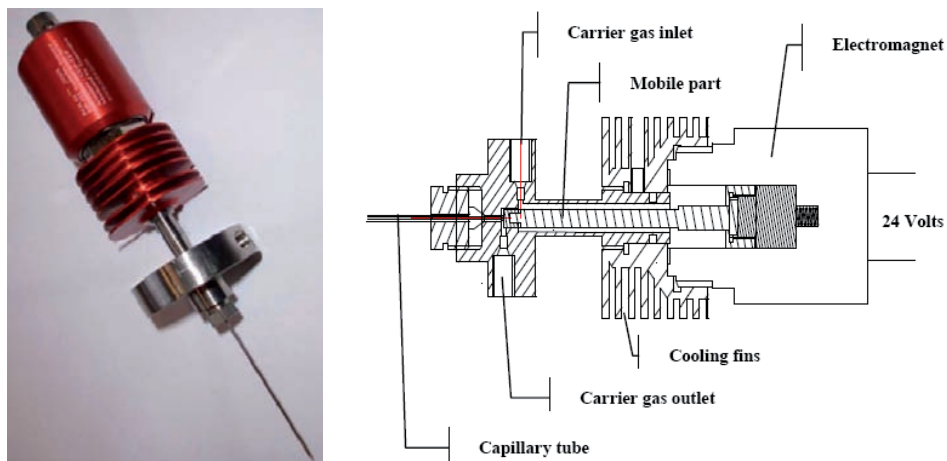


**Figure 4.6** – Electromagnetic ROLSI™ sampler. – **On the left:** picture of the sampler. **On the right:** Schematic drawing of a sampler.

This is possible due to the extremely small sample volumes that these samplers can withdraw through Monel<sup>®</sup> 400 capillary tubes with an internal diameter varying from 0.10 mm to 0.15 mm, reducing the possibility of eventual pressure drops in the cell (which in any case would be compensated by the automatic piston), and accounting for an increase in the number of samples that can be taken for each equilibrium stage. The samplers act as magnetically actuated on/off valves and the sampling itself happens through the difference of pressure inside the equilibrium cell and the carrier gas line, meaning that the amount of sample withdrawn for the specific opening time will depend on the equilibrium pressure, and that the applicability of this sampling system is limited to pressures at least 0.03 MPa (approximately) above the pressure in the carrier gas line.

Another parameter to influence the amount of withdrawn sample is the internal diameter of the capillaries tubes. Very thin capillaries, appropriate for sampling at pressures around 40 MPa, will not be adequate for sampling at pressures less than 1 MPa. For this work, the acquired samplers were supplied with two different sets of capillaries, one for working up to 6 MPa and another to be used with pressures between 5 MPa and 40 MPa.

The opening time of the samplers is controlled by a Crouzet Top 948 timer (Crouzet Automatismes SAS, France), and can be reduced to a minimum of 0.05 seconds. When a sample is withdrawn, an electronic signal is sent to the gas chromatograph in order for this unit to start recording a new chromatogram. The time between samplings can also be programmed so that a series of samplings can be programmed and run in a fully automated way. Both the ROLSI<sup>™</sup> samplers and the GC carrier gas line can be heated up to 523 K, through the use of West P6100 1/16 Din process controllers (West Instruments, UK). Besides promoting the immediate vaporisation of the samples, the heating has also the purpose of avoiding, or at least minimising, the possible adsorption of the analytes in the carrier gas line, which would constitute a serious source of errors in the analysis, especially when dealing with samples containing very low amounts of some compounds. The segment of tubing that conducts the samples to the GC unit is made of deactivated fused-silica, much like an empty GC column, in an attempt to further minimise possible adsorption problems. Both the timer and the PID temperature controllers are supplied together with the samplers, in a control box whose front panel is shown in Figure 4.7.



**Figure 4.7** – Control panel for the ROLSI™ samplers, with the timer, the temperature controllers, and additional switches to chose from which valve to use at a given time.

The position of the samplers relatively to the equilibrium cell was already illustrated in Figure 4.2. The connection to the GC is done by diverting the carrier gas line through the valves, before the injector, as represented in Figure 4.8.

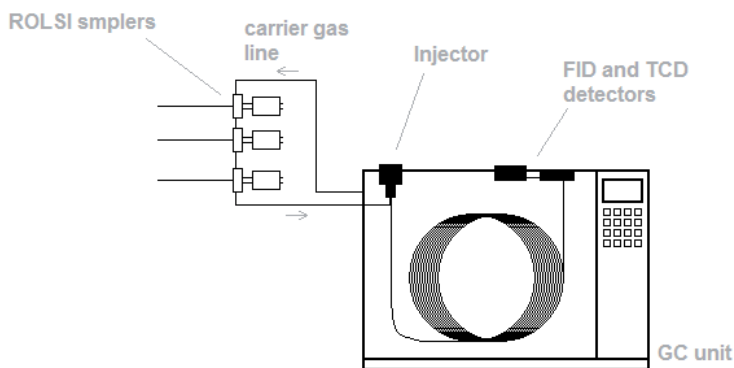


**Figure 4.8** – Schematic drawing of the connection of the ROLSI™ samplers with the gas chromatograph.

## ***The analytical method***

As mentioned before, there are several methods or techniques planned to be used with this apparatus, depending on the type of systems under study and on the requirements in terms of detection limits.

Gas chromatography is a powerful and versatile method, well established in the petroleum industry, which has proven its effectiveness in the study of the type of systems considered in this project. Nevertheless, the lack of GC expertise in our research group made the development of the analytical method not as straightforward as initially thought.

Gas chromatography can be divided in two parts, separation of the analytes and detection. For a good separation it is crucial to select an appropriate column. For a typical ternary system of interest for this work, containing water, a hydrocarbon and either methanol or glycol, the choice of the right column already entails a certain degree of complexity, since although relatively simple, such a system contains both polar and non-polar compounds, and usually the columns adequate for the first type of compounds are not suitable for the second. Based on the specifications given by manufacturers and on previous works found in the literature focusing the same type of mixtures, all of them already cited in Chapter 2, three chromatographic capillary columns were tested experimentally in the separation of synthesised mixtures, using an Agilent 6890 GC System (Agilent Technologies, Inc., USA), equipped with an Agilent 7683B automatic injector, from the same manufacturer, connected to a computer equipped with the software GC ChemStation, also from Agilent Technologies, Inc. The most satisfactory results were achieved with a HP-PLOT Q capillary column (Agilent Technologies, Inc.), which appeared to be sufficient for a good separation of all the compounds, without the use of another column in parallel, a solution adopted in some of the works found in the literature [23-27].

As for detection, the flame ionisation detector (FID) is the most widely used and presents a very good sensibility to hydrocarbons. However, it is unable to detect water. Also very common is the thermal conductivity detector (TCD), in principle, a universal detector based on the difference in the thermal conductivities of the analytes and that of the carrier gas, at the temperature of the detector. It is a frequently used solution for detection of water and it can also detect hydrocarbons, although with a lower sensitivity when

compared to the FID. Both detectors can however be used together, and coupled in series, since the TCD is non-destructive. These two detectors were used in the current configuration of the apparatus. On account of a higher sensitivity, the use of GC-MS may help to improve the characterisation of phases with very low concentrations of some compounds. This technique can be adopted very easily, with minimal changes in the apparatus, as it is enough to conduct the carrier gas of the GC-MS unit through one or all of the ROLSI<sup>TM</sup> samplers.

Other methods such as ATD columns or coulometric Karl-Fischer titration can bring a further improvement concerning detection limits, but the implementation of these methods requires additional changes in the apparatus and implies sacrificing the automated sampling process and analysis. These two solutions could be of special interest in the analysis of the gas phase, in the quantification of traces of water and glycols. ATD columns can be used together with a gas meter. A certain amount of the gas phase is sampled through a regular valve and is passed through an ATD tube and into a gas meter for determination of the sample volume. Inside the ATD tube glycol is adsorbed and accumulated, until a measurable amount is collected. The ATD columns are then connected to a GC unit and heated, promoting desorption of the glycol, which is then quantified by gas chromatography.

Karl-Fischer titration is one of the most common methods for determination of traces of water or moisture. Its applicability, in the case of coulometric titrations, goes from 1 ppm to 5% of water content, and there is currently a wide selection of commercial set-ups for the application of the method. The theory associated with this method can be found elsewhere, in almost any analytical chemistry text book.

As stated before, the use of these methods was considered during the development of the apparatus, but they have not yet been implemented.

### **Valve configuration**

The valve configuration in the apparatus was also carefully planned. Although *prima facie* this does not seem like a critical matter, the fact is that most of the problems when working with high pressures or vacuum are related to leaks and failures of the air tightness

of the systems, and the positioning of the valves is often critical in locating the origin of the problem. Even during regular operation, the correct configuration of the valves can facilitate the experimental procedure. As can be seen in Figure 4.2, and in more detail in Figure 4.9, all the connections to the cell are centralised in one of the valves, represented as “V1” in Figure 4.9. By reducing the number of direct connections to the cell, the chance of leaks that can interfere with the experiments is decreased.

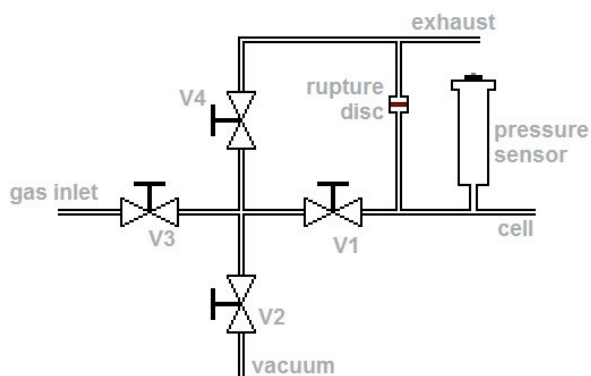


**Figure 4.9** – Schematic representation of the valve configuration showing the existence of one single connection to the equilibrium cell.

Furthermore, not only the layout of the valves is important, but also the type of valves used. V1 in Figure 4.9 is a ball valve that although having the disadvantage of being an on/off valve, presents several advantages when compared to other types. When open, this valve behaves like a section of straight tubing, without any resistance or influence in the flow. In this apparatus, this allows loading the equilibrium cell by means of a syringe with a long needle, without the need to disconnect the valve from the cell. To empty the cell, a similar procedure is adopted, using a long thin flexible tube connected to a liquid pump. Another characteristic of these valves is that the higher the pressure differential, the more thoroughly they will close, since the pressure presses the ball against its seat in the body of the valve. Valve V2 is also a ball valve, in order to prevent bottlenecks and minimise dead volumes in the tubing, factors that could affect the vacuum in the cell during its evacuation for cleaning. Valves V3 and V4 are needle valves, to allow a slow and progressive opening, either for pressurising the cell, in the case of V3, or for depressurising it through valve V4. All valves were acquired from Swagelok Company,

USA, and are equipped with PCTFE (polychlorotrifluoroethylene) seats, for a temperature range from 233 K to 310 K, and pressures up to 41 MPa.

### ***Additional systems***

A key factor in phase equilibria measurements has to do with the celerity with which the state of equilibrium is achieved, and as described in Chapter 3, there are different options to expedite the process, through recirculation of one or more phases, through mechanical stirring, etc. One of the possibilities to accelerate the attainment of equilibrium is the use of magnetic stirring. Arguably less efficient than some of the other solutions, it presents the advantage of not requiring any additional port to the cell, which would always constitute another possibility for the occurrence of leaks.

In this work, several types of magnets were tested in association with the stirring motor, with different strengths and with different shapes, in conjunction with different magnetic bars inside the cell. A magnetic bar with an oval shape provided the best results for the hourglass-like shape of the cell. The stirring is promoted through a Neodymium-Iron-Boron magnet, produced by Supermagnete / Webcraft GmbH, Switzerland, placed inside the lower piston on the cavity observable in Figure 4.4, and connected by an telescopic connection to a low temperature motor Maxon EC 45 flat (Maxom Motor AG, Switzerland) with remote controls, recommended for temperatures down to 233 K, 30 Watts of power and with a speed variable between 40 rpm and 1300 rpm after a 5:1 reduction of speed through a Spur Gearhead Maxon GS 45 A, from the same manufacturer. Not only is this motor suitable for operation at low temperatures, as it is also characterised by low heat dissipation that otherwise might interfere with the thermal homogeneity inside the temperature chamber. Furthermore, there is no direct contact between the cell and the stirring system, by means of avoiding any friction, and the motor is placed under a metallic plate with a thickness of 5 mm, which shields the equilibrium cell, deflecting any heat that might be irradiated from the motor.

The use of the gear head has to do with the original speed range of the motor being too high for this application. If the rotation of the magnet inside the piston is too fast for the magnetic bar inside the cell to cope with, the stirring loses its efficiency.

It is possible that, under specific experimental conditions, the magnetic stirring system may lose some of its effectiveness. It is suspected for example, that the study of systems containing triethylene glycol (TEG) at very low temperatures, where the glycol rich phase is characterised by a high viscosity, may lead to such problems. However, and as mentioned before, the apparatus can be easily adapted to a recirculation method, where one phase is circulated and forced through other phase(s) for a quicker achievement of equilibrium in the system, as explained in the third chapter of this work. This can be done through the use of “T” connections placed where the ROLSI™ samplers are connected to the cell. In last instance it would be possible to create two circulation loops, using also a similar “T” connection close to the rupture disk (see Figure 4.9), however, even in the case of VLLE, using the connections for the upper and lower ROLSI™ samplers for promoting the bubbling of the gas phase through the heavy liquid phase, and consequently through the light liquid phase as well, would improve greatly the rate of equilibrium achievement.

An external light source Schott KL 200 LED (Schott AG, Germany), making use of LED technology and connected to a 1 meter long optical fibre, was used to illuminate the 360° window of the equilibrium cell, for better visualisation of its interior. It was also considered to use a digital video camera inside the temperature chamber, connected to the computer, for monitoring and eventually recording some images, but until now this has not been implemented, although it is represented in Figure 4.2. The existence of the window in the door of the temperature chamber allows a normal camera to be used, since it can be placed outside the chamber and it does not have to be exposed to low temperatures.

#### **4.2.2. Experimental Procedure**

The apparatus can be used in different configurations, or even using different methods. However, some fundamental steps of the experimental procedure are common to all possibilities. In the following description, the schematic diagram of Figure 4.9 should be considered.

One of these steps is the loading of the cell with the different components to be studied. As mentioned before, this can be performed using a syringe with a long needle, through the valve represented as V1 in Figure 4.9, making possible to determine the volume of the liquid compounds injected, either volumetrically, through the graduation in

the syringe, or gravimetrically, by weighing the cell before and after the injection of the compound.

After this, the remaining of the valve system can be reconnected to valve V1 and the degassing of the components can be performed. With valves V1, V3 and V4 closed, valve V2 is open connecting the valve system to vacuum. Subsequently, valve V1 can be open for short intervals, evacuating the gas in equilibrium with the liquid phases and letting them to new equilibration. After a number of cycles, the pressure inside the cell should be stable after closing V1, and close to the vapour pressure of the most volatile component in the cell. The lost of material originated in the process should be negligible due to the relatively small volume of the cell. However, in cases where a precise knowledge of the composition is required, the temperature of the cell can be lowered in order to reduce the volatility of the components in the cell and this way reducing the losses.

In normal conditions of operation, the cell will be operated at high pressure, in order to allow the operation of the sampling system. This means that almost invariably, a pressurised gas will be load into the equilibrium cell. Once the interior of the cell is free from any air, the compressed gas can be loaded through valve V3, or alternatively through the use of a gas cylinder, directly connected to V1. This last option allows the knowledge of the exact amount of gas inserted into the system.

After loading the cell, the equilibration process can take place, after programming the temperature of the chamber in the computer. The collection and recording of temperature and pressure values over time can be done with any desired frequency. However it should be considered that some studies may last for several days, and that a high frequency in the collection of values may lead to a substantial amount of data, and consequently to files that will be more difficult to handle in a posterior analysis. In general, in this work, values of pressure and temperature were collected for recording every 10 minutes. In order to improve simplicity in a later analysis of the experiment conditions, it is useful if pressure and temperature are recorded in coincident points in time.

In the end of an experiment, V1 can be opened, keeping all other valves closed. V4 can then be opened slowly for depressurisation of the system. After depressurisation, the valve system can be disconnected from V1 and the liquid phases can be pumped out through a thin flexible tube.

Before further experiments, the cell should be carefully cleaned several times with an adequate solvent(s), and placed under vacuum for some hours, in order to evaporate possible traces of solvent before the preparation of a new experiment.

### **4.3. Testing of the New Apparatus**

After assembling any new apparatus, it becomes necessary to perform a series of tests, which will attest the quality of the results to be produced. This can be done by performing measurements on reference systems, or on systems that have been studied frequently and by different authors. But before these first measurements, other preliminary tests are of prime importance, in order to verify that no electronic errors or interferences are affecting the results, and to get acquainted with the limits of the apparatus in terms of stability, etc.

Nowadays electronics play a great role in the quality of experimental results. Modern apparatus for the measurement of thermodynamic properties are not conceivable without the use of electronic systems in high-quality measurements, for temperature, pressure or any other property. And the output of any common sensor is invariably an electric property, either being resistance, capacitance, current or potential difference, therefore susceptible to be affected by a number of electric and electromagnetic interferences.

There are of course, a series of rules that ought to be followed, with the purpose of avoiding electronic errors and sources of noise, but the ultimate confirmation of the absence of problems can only be given by testing. This should, therefore, be the objective of the first set of tests.

#### **4.3.1. Preliminary Tests**

This first series of tests, focusing on electronic aspects, did not reveal the existence of major problems, concerning the cables manufactured in our labs or interferences from the electrical supply to the instruments. No excessive noise was found, nor any evidence of periodical interferences in several hours of measurements, performed using different frequencies for the collection of values.

The pressure readings, at atmospheric pressure, were characterised by a short time stability better than  $\pm 0.15$  kPa (0.0015 bar) and a long time stability around  $\pm 0.25$  kPa. As for the temperature, from the four platinum resistance thermometers tested initially, three provided readings with a stability better than  $\pm 0.0025$  K while the fourth presented stability values in the order of  $\pm 0.005$  K. This thermometer had been used for some time in another project, in a 2-wire configuration and some changes had been performed on its cables, although there is no evidence that this fact was the origin of the problem. This thermometer was not used to measure the temperature of the cell, being used only to monitor the temperature inside the temperature chamber, for which the precision requirements are less significant.

After these basic electronic tests, the temperature compensation of the pressure sensor was investigated, by recording the deviation of the values yielded under atmospheric pressure as a function of the operation temperature. The results of this test are shown in Figure 4.10, where a print screen from the software READ30 shows both the temperature of the electronics inside the transmitter (in green, corresponding values on the right side of the graph), and the value of the pressure baseline (in red, corresponding values on the left side of the graph), as a function of time.

It was verified that in the temperature range from 263 K to 303 K, inside the temperature compensation range of the transmitter, the maximum variation in the pressure was 7 kPa (0.07 bar). When the temperature was decreased down to 229 K (-44 °C) the deviation in the pressure values went up to 46 kPa (0.46 bar), a value that in any case is still inside the 50 kPa value corresponding to the accuracy limit of this particular transmitter. It should be noticed that at these lower temperatures, the temperature of the electronics inside the transmitter is around 4 K to 5 K higher than the temperature measured in the cell. This fact was expected and it is due to the heat inevitably produced by the electronic components. It was also verified with these tests that when the temperature of the electronics goes below 230 K, the pressure transmitter stops supplying values with physical meaning.

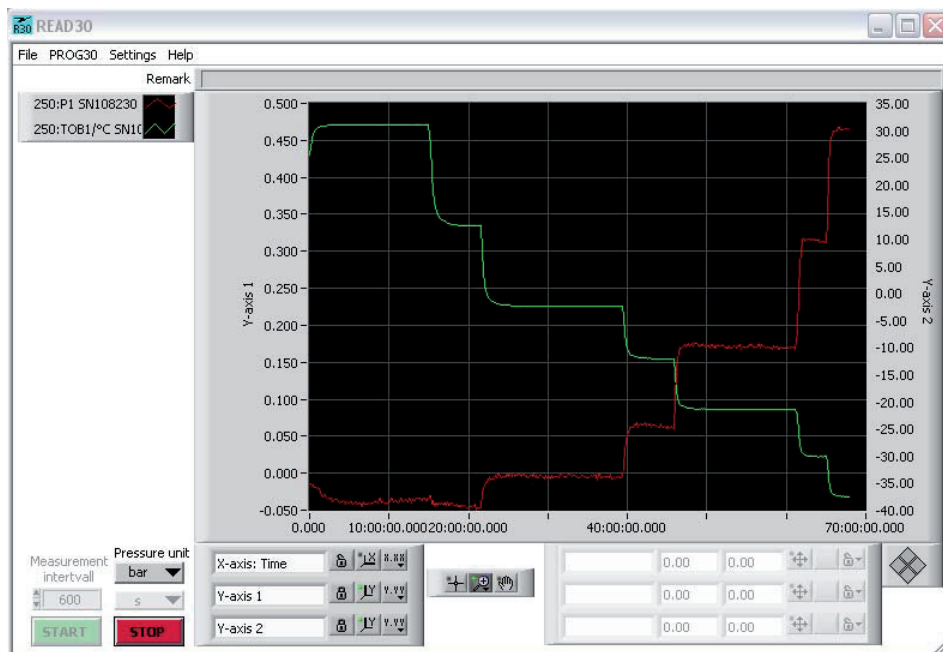


**Figure 4.10** – Print screen of the program READ30 showing the deviation of the pressure readings (red line, left axis) as a function of the temperature of the electronics of the pressure transmitter (green line, right axis).

After this, tests involving the cell started. The air tightness of the cell and the ability of the sapphire crystal to withstand high pressures for prolonged periods were successfully tested, submitting the cell to a pressure of around 30 MPa for 72 hours at 298 K.

A small number of measurements performed along the vapour-liquid equilibrium line of pure carbon dioxide, confirmed the stability of the pressure and temperature obtained in the first tests, which had been carried out without the equilibrium cell. Furthermore, the thermal contact between the cell and the platinum resistance thermometers and the relative response times of the pressure and temperature sensors were examined, with very satisfactory results, as the graph in Figure 4.11 attests, where the reflection in the pressure values of small oscillations in the temperature values is shown. The difference between the temperature values yielded by the two thermometers was, for this case, 0.03 K on average, a value within the precision of the temperature sensors.

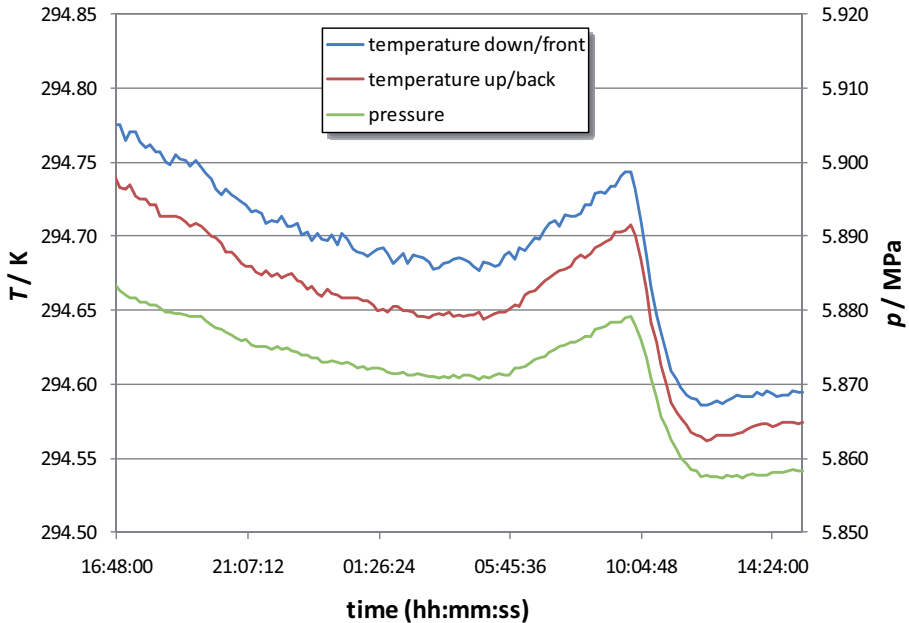


**Figure 4.11** – Influence of small oscillations in the temperature of the cell in the pressure values, evidence of a good thermal contact between the cell and the platinum resistance thermometers. The values were obtained during a series of tests with liquid carbon dioxide in equilibrium with its vapour phase.

### **4.3.2. Measurements on Reference Systems**

After the successful preliminary tests, the next stage is the validation of the apparatus, with study of reference systems or of other systems that have been studied frequently and by different authors.

As mentioned before, temperature and pressure are probably the most important parameters in any thermodynamic study. For temperature measurements, the calibration of platinum resistance thermometers in conformity with the DIN 43760 standard is simple to perform, and it can be repeated at any time. However, the same does not apply to pressure measurements. The calibration of a pressure sensor is often more time consuming and requires the use of different additional equipment, depending on the type of calibration performed. The pressure transmitters used in this work, not only for this apparatus, have been previously calibrated in the factory for the whole range of pressure and along the complete range of temperature compensation. The transmitters are delivered with a

calibration certificate which includes a plot of the deviations observed in the calibration, showing that the transmitter is in accordance with its specifications in terms of accuracy.

Nevertheless, as a part of the validation of the apparatus, it is necessary to perform some measurements, at this stage, merely to confirm the quality of the temperature and pressure values yielded by the apparatus, leaving for a subsequent stage the validation of the analytical method. The results will attest to the quality of both pressure and temperature measurements.

### ***Binary system methanol + ethane***

The first measurements were performed on the study of the three-phase coexisting line for the binary system methanol + ethane, for temperatures around 298 K and 280 K. This system has been studied in the past by different groups in various occasions and through different methods. Data is available in the literature not only regarding pressure and temperature values, but also concerning phase compositions, with values that can be used as a reference for different phases.

Methanol (CH<sub>3</sub>OH, Methanol for HPLC, Merck KGaA, Germany) with a minimum purity of 99.8% as determined by the supplier using gas chromatography, was used together with ethane (C<sub>2</sub>H<sub>6</sub>, purity of 99.95%, supplied by AGA Gas AB, Sweden). The reduced amount of results obtained in the study of this binary system are presented in Table 4.1 and in the diagram in Figure 4.12, in which experimental data found in the literature [28-33] are also represented. It should be pointed out that the data given by Ma and Kohn [30] are smoothed values rather than raw experimental points.

**Table 4.1** – Results obtained during the study of the three-phase coexisting line for the binary system methanol + ethane, using the new cell.

<i>T</i> / K	<i>p</i> / MPa
298.39	4.141
298.48	4.174
279.80	2.789
279.85	2.791

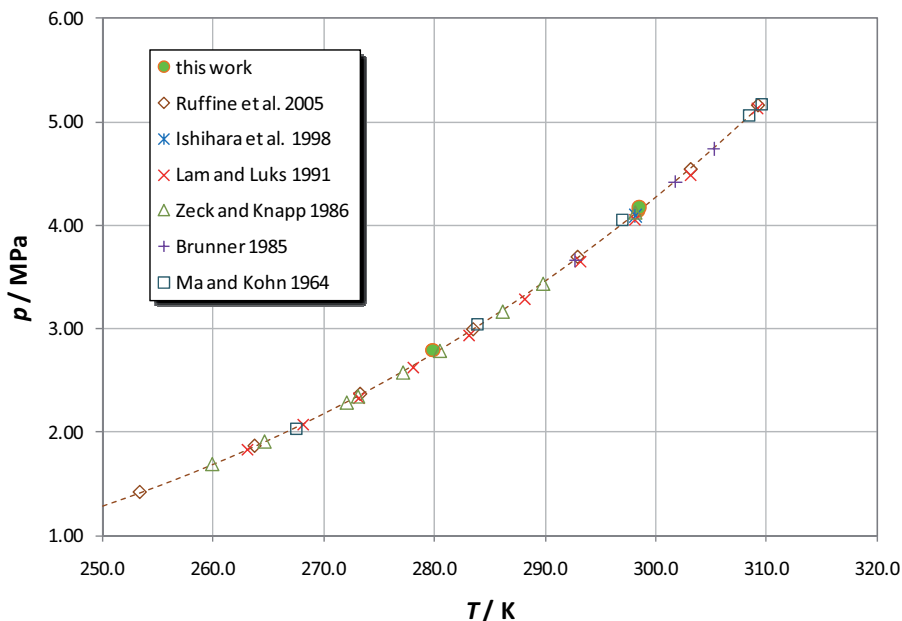


**Figure 4.12** – Results obtained in the study of the three-phase (vapour-liquid-liquid) coexisting line for the binary system methanol + ethane, and comparison with values found in the literature [28-33].

The graph in Figure 5.12 shows what seems to be a good agreement between the values obtained in this work and the literature, however, and in order to quantify this agreement, a reference equation is needed. The dashed line in the graph is given by equation 4.1, which was calculated from fitting of the equation of Clarke and Glew truncated to three parameters [34], to the experimental data published by Ruffine and his co-workers [31], in a work where a new experimental apparatus for the measurement of phase equilibria at low temperatures is presented. This set of literature data is not only the most recent, but also the most extensive, with measurements from 194 K up to the upper critical end point of the system methanol + ethane, at 309 K.

$$R \ln(p/\text{MPa}) = \frac{3509.3}{298.15} + 15286 \left( \frac{1}{298.15} - \frac{1}{T} \right) + 12.092 \left[ \left( \frac{298.15}{T} \right) - 1 + \ln \left( \frac{T}{298.15} \right) \right] \quad (4.1)$$

The equation of Clarke and Glew [34] has been widely used in the representation of the variation of pressure with temperature in equilibrium systems, especially in the representation of vapour pressures of pure compounds, in which case it allows the

determination of thermodynamic quantities [35-45]. Its deduction and the application to pressure-temperature relations was presented in detail by the author in a previous work [35]. It should not be confused with the Clarke-Glew-Weiss equation [34,46,47] also used repeatedly in the analysis of equilibrium data. The Clarke and Glew equation has fitted the data of Ruffine et al. [31] with a value of  $r^2 = 0.99996$  and an average deviation for the 13 experimental points of  $7 \times 10^{-3}$  MPa.

Figure 4.13 shows, the deviations from the experimental points to the values given by Equation 4.1, for all the data sets. Besides the relative deviations, which can be read in the vertical axis of the graph, additional lines referring to the absolute deviations were also added to the plot, allowing inferring this parameter as well.

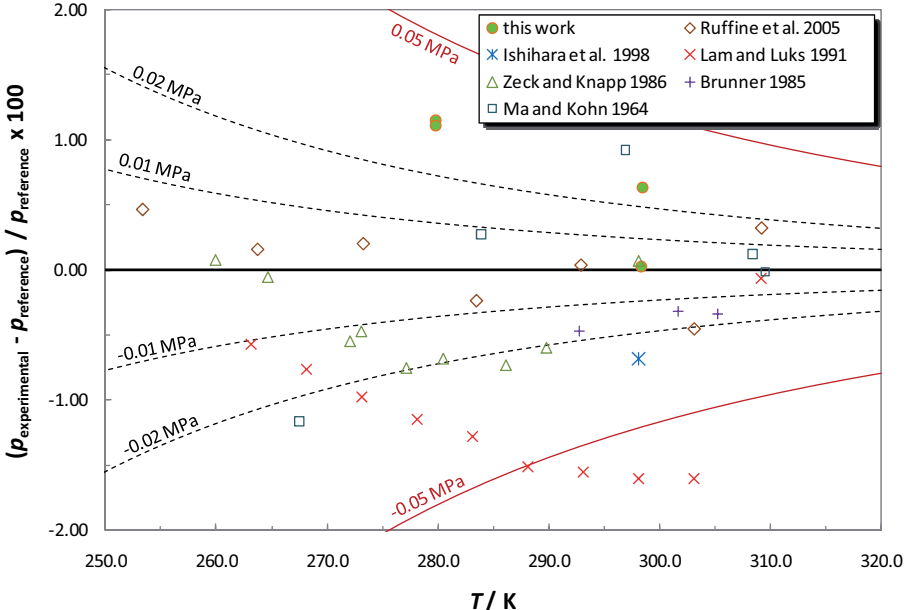


**Figure 4.13** – Deviations from the experimental points to the values given by Equation 4.1, for the results obtained in this work and the values found in literature [28-33] in the study of the three-phase coexisting line for the binary system methanol + ethane.

The results obtained in this work are up to 1.1% higher than the values provided by the fitting to the data of Ruffine et al. [31]. However, the maximum absolute deviation observed is around 0.03 MPa, which is well below the accuracy of 0.05 MPa which characterises the pressure transmitter used.

It is also noticeable in the graph that most of the other data sets have values lower than those presented by Ruffine and his co-workers [31]. Although some data sets, such as the values of Ma and Kohn [30] seem to present a higher dispersion, the values from Zeck and Knapp [32] not only look internally consistent, but also more in agreement with the results from Brunner [33] and from Ishihara [28].

Fitting the data from Zeck and Knapp [32] to the equation of Clarke and Glew [34], results in Equation 4.2, presented below. The result of the fitting was  $r^2 = 0.99988$  with an average deviation for 11 experimental points of  $7 \times 10^{-3}$  MPa.

$$R \ln(p/\text{MPa}) = \frac{3506.3}{298.15} + 15615 \left( \frac{1}{298.15} - \frac{1}{T} \right) + 28.142 \left[ \left( \frac{298.15}{T} \right) - 1 + \ln \left( \frac{T}{298.15} \right) \right] \quad (4.2)$$

The comparison of the results obtained in this work with the values provided by this equation, is given in the plot in Figure 4.14.

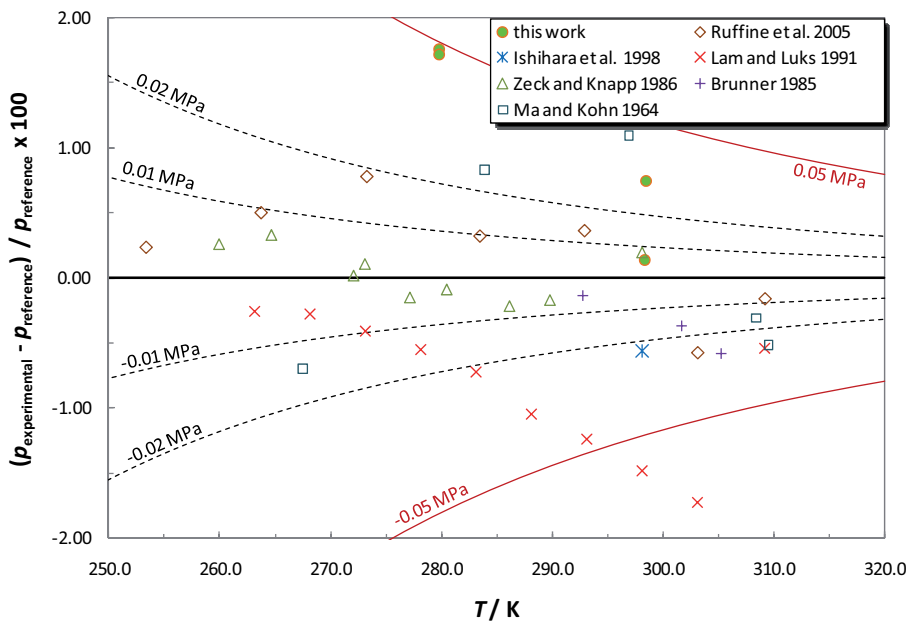


**Figure 4.14** – Deviations from the experimental points to the values given by Equation 4.2, for the results obtained in this work and the values found in literature [28-33] in the study of the three-phase coexisting line for the binary system methanol + ethane.

In this graph it is possible to observe a more even distribution of all the data sets, but the results obtained in this work appear associated with higher errors, although still inside the accuracy limit defined for the transmitter, 0.05 MPa.

Another possibility for the analysis of the results is to apply the equation of Clarke and Glew [34] to all the data series combined, avoiding the arbitrary choice of a particular data set to be taken as reference. This results in Equation 4.3, with the fitting presenting a value of  $r^2 = 0.99977$  and an average residual for 45 experimental points of  $1.5 \times 10^{-2}$  MPa.

$$R \ln(p/\text{MPa}) = \frac{3499.2}{298.15} + 15408 \left( \frac{1}{298.15} - \frac{1}{T} \right) + 15.408 \left[ \left( \frac{298.15}{T} \right) - 1 + \ln \left( \frac{T}{298.15} \right) \right] \quad (4.3)$$

The comparison of the present results with the reference values from this equation is illustrated in the graph of Figure 4.15.

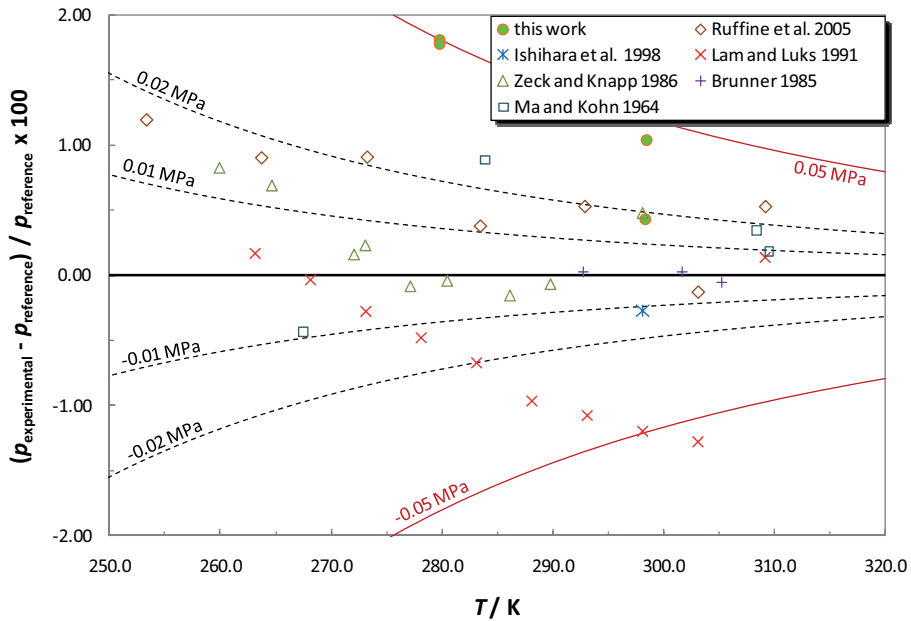


**Figure 4.15** – Deviations from the experimental points to the values given by Equation 4.3, for the results obtained in this work and the values found in literature [28-33] in the study of the three-phase coexisting line for the binary system methanol + ethane.

The deviations of the values found in this work are very similar to the obtained considering the data of Zeck and Knapp [32] as a reference, showing that the first choice of

considering the data of Ruffine et al. [31] might lead to some bias in the analysis of the results. Despite the higher deviations, the data obtained is still inside the accuracy limit defined for the transmitter, 0.05 MPa.

The results of these first tests were not completely satisfactory, considering the high quality of results aimed at. However, it is necessary to take into account that these were the very first measurements with the apparatus, and it is practice that generally leads to a refinement of the experimental procedure and a better knowledge of the apparatus by the experimentalist, resulting in an improvement on the quality of the results.

During the measurements with the binary system methanol + ethane, and although the analytical method was not yet fully developed and optimised, some qualitative GC analysis was performed in order to test the ROLSI<sup>TM</sup> samplers. Figure 4.16 presents a chromatogram of the analysis of one sample withdrawn from the methanol rich phase, where a good separation between the two peaks is visible. The shape of the peaks on the other hand is far from optimal, but as mentioned, the analytical method was not yet fully developed.

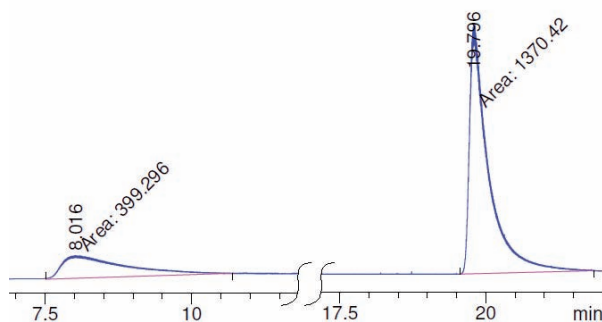


**Figure 4.16** – Chromatogram of the analysis of one sample withdrawn from the methanol rich phase during the study of the three-phase coexisting line for the binary system methanol + ethane.

Figure 4.17 shows a picture of the sapphire window of the equilibrium cell during the experiments, where the three phases are visible. The picture was taken from outside the temperature chamber, through the window in its door.

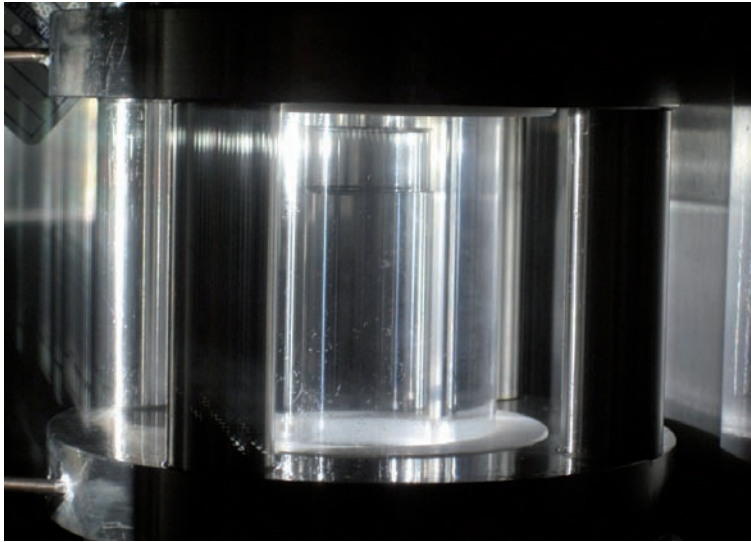


**Figure 4.17** – Image of the sapphire window in the equilibrium cell during the study of the three-phase coexisting line for the binary system methanol + ethane, where the three phases are visible.

Before the measurements in this binary system could be continued, an incident led to the damaging of the pressure transmitter, which had to be replaced. The new transmitter was in every detail similar to the previous, already described. Nevertheless, new tests were necessary, to verify the influence of the temperature on its output values, under atmospheric pressure. The results of these tests were pretty much similar to the verified for the first pressure transmitter used. Inside the temperature compensation range, from 263 K to 303 K, the deviation on the output values was lower than 5.5 kPa (0.055 bar), while for a temperature around 243 K the deviation went up to 11 kPa (0.11 bar).

### ***Carbon dioxide***

The vapour-liquid equilibrium line for pure carbon dioxide was extensively studied in order to, not only evaluate the quality of the pressure measurements provided by the new transmitter, but also to evaluate the influence of temperature on these measurements. This compound has been the object of many studies over the years, and its vapour-liquid equilibrium line is well defined. For comparison of the present measurements, a reference equation is used, rather than an arbitrary selection of data from the literature.

The carbon dioxide (CO<sub>2</sub>), with a purity of 99.995%, was produced by Linde AG, Germany, and supplied by AGA A/S, Denmark. A total of 75 experimental points were measured from 239 K up to a temperature of 303 K, close to the critical point of the compound. The results are presented in Table 4.2, where the order of the experiments is also indicated.

**Table 4.2** – Experimental results obtained in the study of the vapour-liquid equilibrium line for pure carbon dioxide. The first column in the table refers to the order of the measurements.

n.	<i>T</i> / K	<i>p</i> / MPa	n.	<i>T</i> / K	<i>p</i> / MPa	n.	<i>T</i> / K	<i>p</i> / MPa
43	239.17	1.260	50	264.62	2.760	58	284.37	4.630
44	239.17	1.260	26	264.66	2.800	74	285.26	4.733
19	239.27	1.299	51	269.69	3.171	75	285.30	4.738
18	239.29	1.300	52	269.69	3.171	73	285.47	4.756
46	244.37	1.500	53	269.73	3.174	38	288.92	5.172
45	244.39	1.501	11	269.73	3.215	37	288.92	5.174
21	244.43	1.537	12	269.76	3.220	7	289.13	5.245
22	244.43	1.537	72	273.10	3.474	6	289.18	5.251
20	244.51	1.542	71	273.11	3.476	8	289.18	5.252
41	249.54	1.768	27	274.66	3.659	64	293.46	5.759
42	249.57	1.770	39	274.74	3.629	63	293.51	5.764
16	249.60	1.809	67	279.51	4.102	62	293.51	5.765
15	249.60	1.809	66	279.52	4.103	3	294.58	5.959
17	249.60	1.809	9	279.55	4.148	4	294.58	5.959
24	254.56	2.098	68	279.56	4.107	5	294.58	5.959
47	254.56	2.062	10	279.56	4.150	1	294.66	5.972
48	254.56	2.063	54	279.58	4.109	2	294.72	5.980
23	254.57	2.099	55	279.59	4.111	32	298.28	6.444
40	259.57	2.391	56	279.62	4.113	33	298.28	6.444
14	259.65	2.435	28	284.23	4.656	60	298.28	6.436
13	259.67	2.436	30	284.23	4.656	61	298.29	6.438
69	264.60	2.759	31	284.23	4.656	34	302.28	7.056
70	264.60	2.758	29	284.25	4.658	65	302.29	7.044
25	264.62	2.797	57	284.37	4.630	35	302.30	7.059
49	264.62	2.760	59	284.37	4.630	36	303.30	7.217

These results are represented in Figure 4.18, together with the reference values from the DIPPR database [48], defined by Equation 4.4.

$$\ln(p/\text{Pa}) = 140.54 + \frac{-4735}{T} - 21.268 \cdot \ln(T) + 0.040909 \cdot T \quad (4.4)$$

According to the database, this equation is valid in the temperature range from 256.58 K to 304.21 K and it has been derived by fitting a general equation (Equation 101 in the database) with five parameters to the values from sets of experimental data, with an associated error estimated to be lower than 1%.

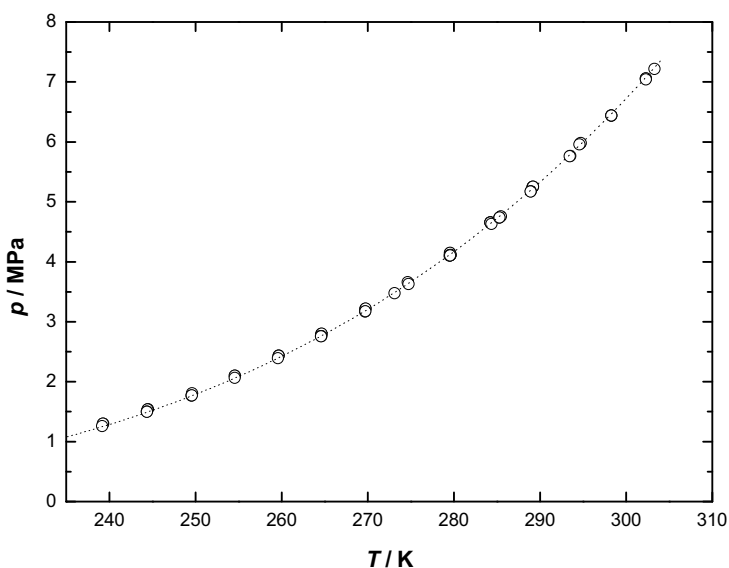


**Figure 4.18** – Results obtained in the study of the vapour-liquid equilibrium line for pure carbon dioxide. The dotted line refers to the reference values recommended by the DIPPR database [48].

The deviations from the results obtained in this work comparatively to the reference values are given in Figure 4.19. As before, both relative and absolute deviations can be inferred, the first through the vertical axis of the graph, and the second by means of reference lines, two of which are represented in red, relative to the accuracy of the pressure transmitter.

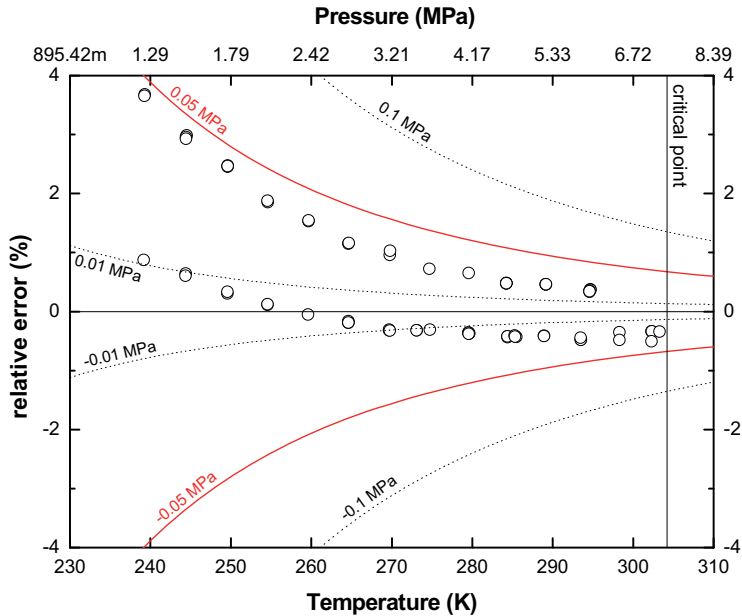


**Figure 4.19** – Relative and absolute deviations from the data points obtained in this work for the vapour-liquid equilibrium line for pure carbon dioxide, to the reference values recommended by the DIPPR database [48] and defined by Equation 4.4.

Concerning the results, two groups of data points are easily identified, with one set of values having higher errors associated, but nevertheless still inside the accuracy limits of the sensor. A careful analysis of the values revealed that this group of data points correspond to the first thirty one measurements performed. Given the order in which the experiments were conducted, it is certain that hysteresis is not the source of the problem.

Inside the temperature compensation range of the pressure transducer, above 263 K, the agreement of the results with the reference data is better than 1%, which is the error associated to Equation 4.4 according to the DIPPR database [48], but for the lower temperatures, the points in the first set of data present deviations up to 4%. However, if only the second set of data values is considered, all the points in the studied temperature range are inside the 1% margin, with the data points obtained above 263 K presenting deviations under 0.5%, as shown in Figure 4.20, where only the points relative to the second set of data are presented. Additionally, the absolute deviations for this data set is never superior to values around 0.01 MPa (0.1 bar), even at the lowest temperature studied.

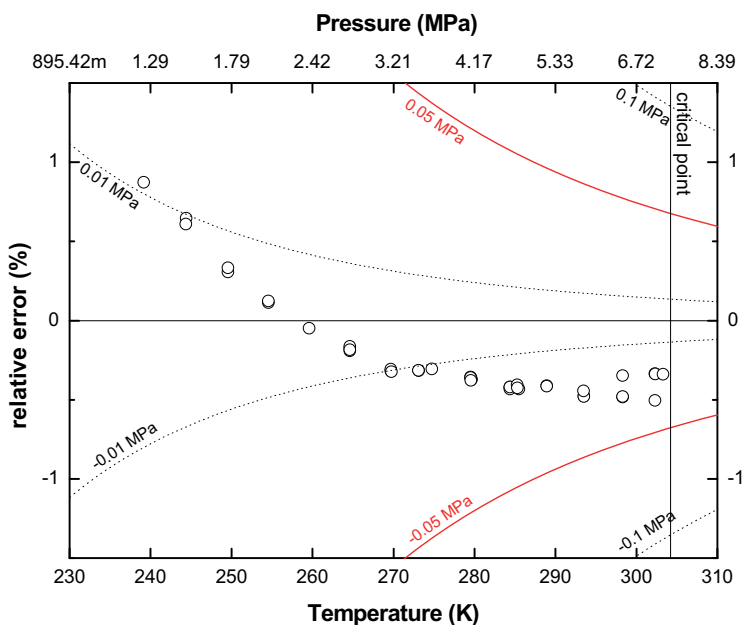


**Figure 4.20** – Relative and absolute deviations from the second set of data points obtained in this work in the study of the vapour-liquid equilibrium line for pure carbon dioxide, to the reference values recommended by the DIPPR database [48] and defined by Equation 4.4.

The deviations in the pressure values obtained at lower temperatures, outside the temperature compensation range of the sensor, i.e., under 263 K, seem to indicate that the cause for these errors might be related to the response of the pressure transmitter. Any errors associated to the temperature measurements would affect the results in a different manner, either with a constant error along the whole range of the measurements, or by deviations presenting symmetry relatively to 273.15 K.

Nevertheless, another aspect should be considered when debating the source of the errors affecting the measurements at lower temperatures, which is the fact that they correspond to lower values of pressure, and in this particular case, to pressures in the lower 4% of the full scale of the transmitter. One of the most important questions in the choice of a pressure sensor is its pressure range vs. the precision in the measurement of pressures at the lower edge of its pressure range. Pressure sensors usually have the same electronic output regardless of the pressure range they are suited for. Even digital pressure transmitters such as the one used in this work, have an initial analogue output that is later converted to a more reliable digital signal by an internal A/D converter. Obviously there is

a limit to the smallest quantity measurable from this electronic output, and that is why manufacturers usually guarantee a minimum absolute accuracy rather than a relative precision. This means that, higher relative errors are expected at the lower limit of the scale of the sensor.

The present apparatus is devised for working mostly at high pressures, and therefore only one pressure transmitter was acquired. However, if at some point it should be frequently used for measurements at lower pressures, the use of a second pressure transmitter with a more limited pressure range is highly recommended. The use of different sensors in the same apparatus is a common solution for improving the quality in pressure measurements, and it can be found in several descriptions of apparatus available in the literature [49-55].

### **Ethane**

In order to attain a better characterisation of the response of the pressure transmitter with temperature for a reliable quantification of the deviations, and also with the aim of clarifying the existence of the two observed sets of points, further measurements of a different system were required.

The tests of the apparatus continued with study of the vapour-liquid equilibrium line for pure ethane (C<sub>2</sub>H<sub>6</sub>, purity of 99.95%, supplied by AGA Gas AB, Sweden) was extensively studied, with a total of 84 measured equilibrium points, in a temperature range from 234 K up to the critical point of this compound, around 305 K. The obtained results are listed in Table 4.3, with an indication of the order of the experiments, and are represented graphically in Figure 4.21, together with the reference values recommended by the DIPPR database [48], calculated from Equation 4.5, applicable in the temperature interval from 90.35 K to 305.32 K. Its five adjustable parameters have been calculated from different sets of experimental and predicted data, with an error associated estimated to be less than 1%.

$$\ln(p/\text{Pa}) = 51.857 + \frac{-2598.7}{T} - 5.1283 \cdot \ln(T) + 0.000014913 \cdot T^2 \quad (4.5)$$

**Table 4.3** – Experimental results obtained in the study of the vapour-liquid equilibrium line for ethane. The first column in the table refers to the order of the measurements.

n.	$T / \text{K}$	$p / \text{MPa}$	n.	$T / \text{K}$	$p / \text{MPa}$	n.	$T / \text{K}$	$p / \text{MPa}$
75	233.86	0.807	78	264.57	1.926	3	288.76	3.414
76	233.86	0.808	29	264.58	1.926	4	288.76	3.413
77	233.87	0.808	27	264.60	1.927	36	289.46	3.457
21	233.94	0.810	12	269.77	2.195	38	289.47	3.457
20	233.95	0.810	11	269.78	2.195	37	289.48	3.458
48	239.10	0.951	45	273.14	2.379	33	289.50	3.460
47	239.12	0.953	46	273.24	2.385	35	289.50	3.460
18	239.13	0.954	31	274.55	2.463	34	289.54	3.462
19	239.16	0.955	32	274.56	2.463	51	293.32	3.769
22	244.38	1.115	30	274.61	2.466	81	293.36	3.768
23	244.38	1.115	41	279.36	2.752	80	293.37	3.768
50	249.47	1.289	42	279.39	2.753	52	293.46	3.780
16	249.48	1.290	8	279.46	2.763	53	293.46	3.780
17	249.49	1.291	66	279.48	2.768	82	293.47	3.776
49	249.49	1.290	67	279.48	2.769	2	295.27	3.932
25	254.48	1.480	65	279.49	2.769	1	295.28	3.932
26	254.48	1.480	9	279.56	2.772	58	298.30	4.198
24	254.52	1.482	10	279.57	2.772	57	298.30	4.197
72	254.58	1.484	6	279.58	2.774	56	298.30	4.198
73	254.62	1.487	64	279.59	2.775	68	298.30	4.191
74	254.62	1.487	7	279.59	2.775	69	298.31	4.191
43	259.45	1.688	40	283.95	3.057	83	298.31	4.179
44	259.47	1.689	39	283.95	3.057	84	298.31	4.180
13	259.53	1.694	71	284.33	3.093	55	303.30	4.646
14	259.54	1.694	70	284.34	3.093	54	303.30	4.646
15	259.54	1.694	63	288.74	3.412	60	304.78	4.788
28	264.57	1.926	62	288.75	3.414	61	304.78	4.788
79	264.57	1.926	5	288.76	3.413	59	304.78	4.788

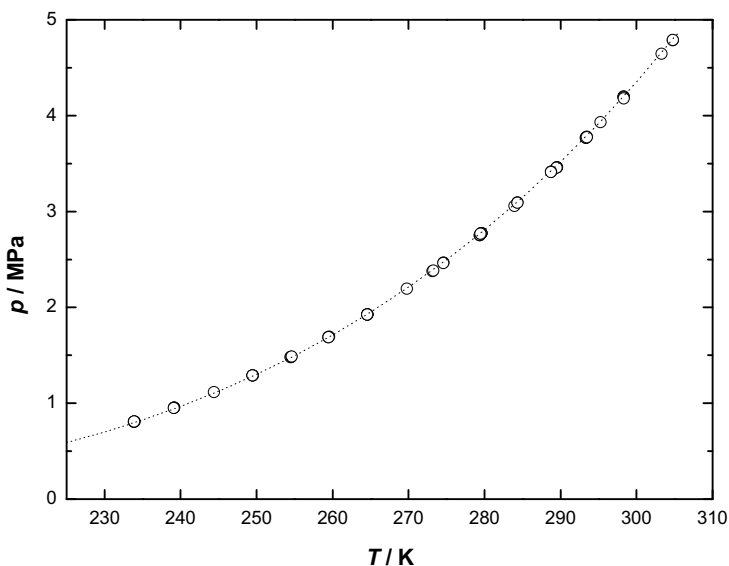


**Figure 4.21** – Results obtained in the study of the vapour-liquid equilibrium line for pure ethane. The dotted line corresponds to the reference values recommended by the DIPPR database [48].

Figure 4.22 presents the deviations of the results relatively to the reference values given by Equation 4.5. As before, the results are well inside the accuracy limit of the pressure transmitter, with the higher deviations observed for the lower temperatures studied. The results relative to temperatures above 263 K are within a range of 0.6 % of the reference values. For a temperature around 240 K, the errors are slightly above 0.01 MPa, much as what had been verified for the second set of data in the study of carbon dioxide.

These results shed no light into the problem of the existence of two tendencies in the results obtained for carbon dioxide. One can only speculate that perhaps that had to do with the first time the sensor was being used.

If the first values for carbon dioxide are ignored, a combined analysis of the deviations verified in the study of both carbon dioxide and ethane, reveals a parallel between the errors verified in the measurements performed on the two systems, as shown in Figure 4.23 and Figure 4.24, for the absolute and relative deviations, respectively.

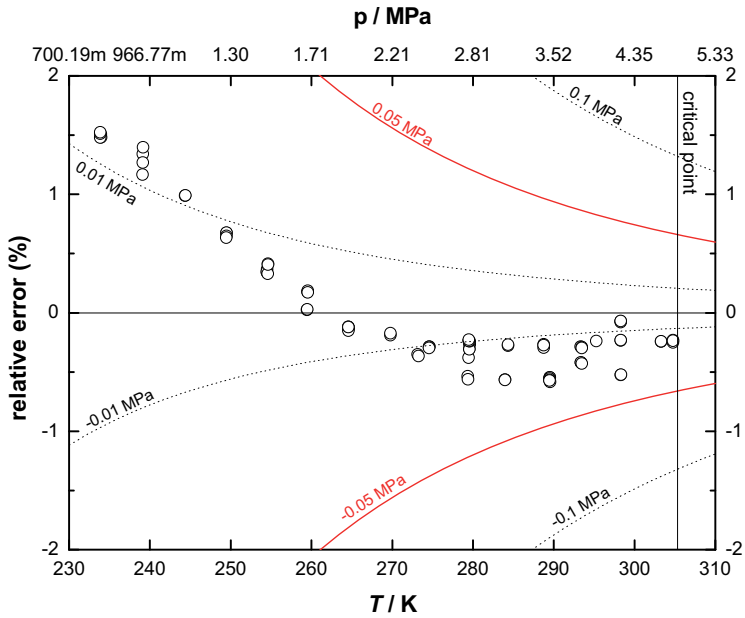


**Figure 4.22** – Relative and absolute deviations from the results obtained in this work for the vapour-liquid equilibrium line for pure ethane, to the reference values recommended by the DIPPR database [48] and defined by Equation 4.5.

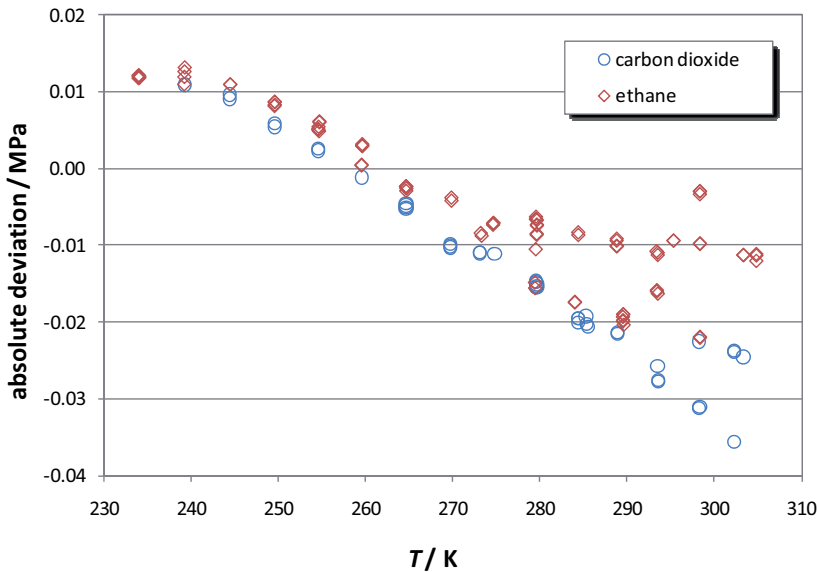


**Figure 4.23** – Similarity between the absolute deviations verified for the results obtained for the vapour liquid equilibrium line for carbon dioxide and ethane, relatively to reference values.

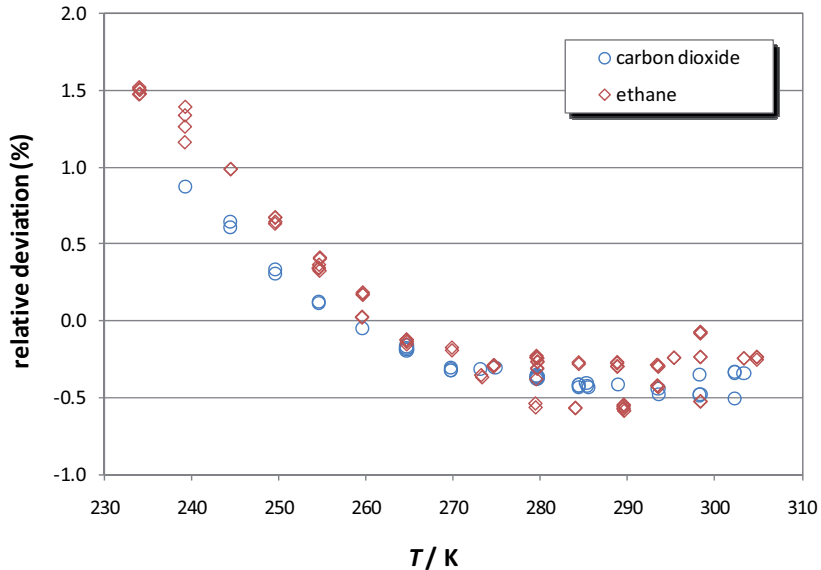


**Figure 4.24** – Similarity between the relative deviations verified for the results obtained for the vapour liquid equilibrium line for carbon dioxide and ethane, relatively to reference values.

This similarity could be the basis for the development of a calibration equation, in order to correct the values for the lower temperatures. Taking as example the relative deviations, it is possible to establish a correction based on two linear equations, for the two temperature ranges below and above 263 K, according to Figure 4.25.

It is arguable, however, that this is the most appropriate approach. There are several points to take into account. On one hand, the deviations for the lower temperatures are almost certainly the result of the influence of temperature in the response of the pressure transmitter legitimising a correction. On the other hand, the maximum deviations observed were of 1.5%, and the equations used as reference are characterised by an error margin of 1%. Furthermore, it is imperative to keep in mind the specifications of the pressure transmitter used. It is one of the best available in the market in terms of accuracy with 0.1% of the full scale over a wide range of temperatures, but nevertheless it has a range of 50 MPa and this implies that when used to measure pressures around 1 MPa considerable relative errors are expected. Still, the observed performance of the sensor is outstanding, with maximum absolute deviations less than 0.015 MPa, even outside the temperature compensation range, a value much lower than the accuracy limit of  $\pm 0.05$  MPa of the

sensor used. As mentioned before, for an improved accuracy at lower pressures, a pressure transmitter with a more limited scale should be used.

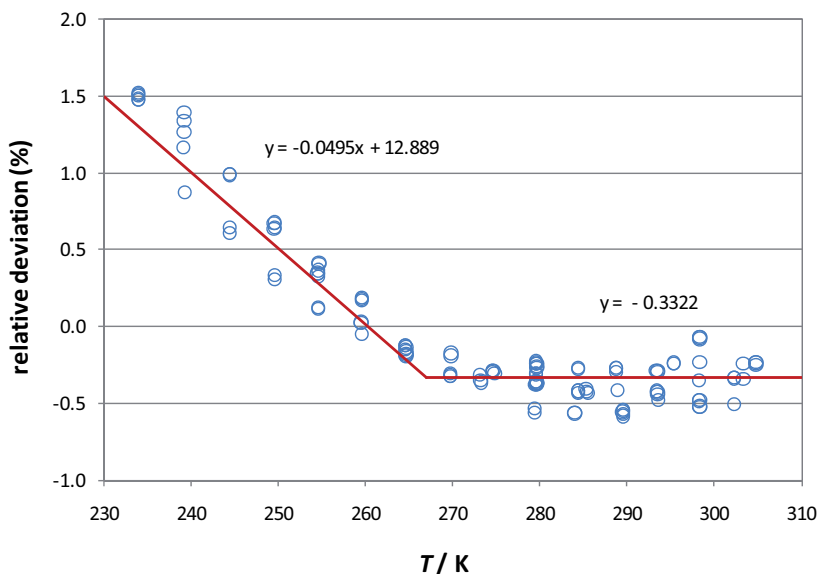


**Figure 4.25** – Combined analysis of the relative deviations of the results obtained for the vapour liquid equilibrium line for carbon dioxide and ethane relative to reference values, and proposed equations for correction of the raw experimental values.

In conclusion, the ideal is to avoid the application of this particular pressure transmitter for the measurement of low pressures at low temperatures. When that is not possible, the considerations written above should be taken into account.

Another curious point, is that in the study of both compounds, the maximum absolute deviations were less than 0.015 MPa, even for temperatures as low as 234 K, where the print screen in Figure 4.10, in which the influence of the temperature in the zero of the sensor was studied, shows a deviation greater than 0.03 MPa for a temperature of 243 K of the electronics of the transmitter, corresponding approximately to a temperature of 239 K in the cell.

## **4.4. Gas Chromatography**

In Figure 4.16, a chromatogram of the analysis of a sample from the methanol rich phase during the study of the binary system methanol + ethane, obtained in a stage where the analysis method was not yet fully developed and optimised, was already shown. The purpose at that stage was to confirm the good functioning of the sampling system.

As previously mentioned, the analysis of a typical ternary or multi-component system of interest for this work using gas chromatography involves some complexity, due to the mixed polar and non-polar nature of the compounds. Another challenge is related to the very small concentrations to be determined in most of the measurements, such as the concentrations of hydrocarbons in the aqueous liquid phase, or the amounts of water in the gas phase. As also stated previously, the lack of expertise within the research group regarding this analytical area, contributed to an increase in the significance of these challenges.

Two different aspects of the application of gas chromatography should be considered. Firstly, it is necessary to achieve a good separation between the different components of the systems under study, which on its own allows only a qualitative analysis. This is related to the development of an appropriate chromatographic method, through the selection of an adequate column and the optimisation of a number of experimental parameters. After this first stage, with the development of the separation process, it is then necessary to establish the relations between the area of the chromatographic peaks and the amount of each substance injected in the GC column, in order to create the basis for the desired quantitative analysis. These relations, usually linear in a specific range of conditions, are dependent on the nature of the compounds to be analysed and on the type of detector used, and can be determined by means of calibrations, which can be performed in relative or absolute terms, giving rise respectively, to more restricted or more universal calibrations.

### **4.4.1. Development of the Chromatographic Method**

The development of the chromatographic method consisted not only in the experimentation of different columns, but also in the development and testing of different

experimental conditions such as the inlet temperature, detector temperature, column temperature and temperature program, nature of the carrier gas, carrier gas flow rates, etc., in order to optimise the separation of all the compounds in a typical multi-component system. The aim of this optimisation is to obtain well defined, narrow and symmetrical peaks for all the compounds involved. Parallel to this, it is desirable to reduce as much as possible the time necessary for each analysis, meaning that the retention times for all the components should be as low as possible, without causing an overlapping of the respective peaks in the chromatogram.

Firstly, the Agilent 6890 GC System previously existing in our laboratory, until then equipped with a flame ionisation detector (FID) only, was upgraded with a thermal conductivity detector (TCD) essential in this work for the detection of water. Synthesised mixtures of water, ethylene glycol and *n*-hexane or *n*-pentane were used in the evaluation of three different chromatographic capillary columns, listed in Table 4.4 together with their main characteristics, length, internal diameter, film thickness and temperature of applicability. All the columns were acquired from Agilent Technologies, Inc., USA.

**Table 4.4** – List of the different chromatographic capillary columns tested in the present work and their main characteristics: length, internal diameter, film thickness and temperature of applicability.

Column	Manufacturer	Length / m	I.D. / mm	Film / $\mu\text{m}$	Temperature / K
HP-1	Agilent	30	0.53	5	213 K – 533 K
HP-5	Agilent	30	0.32	0.25	213 K – 588 K
HP-PLOT/Q	Agilent / J&W	30	0.320	20.00	213 K – 543 K

The first results obtained with the HP-PLOT/Q column were characterised by a strong tailing effect in all the peaks, as shown in Figure 4.16, relative to the analysis of methanol and ethane, and observable in Figure 4.26, corresponding to FID output during the analysis of a mixture of water, ethylene glycol and *n*-pentane. The temperature program used is also observable in the figure.

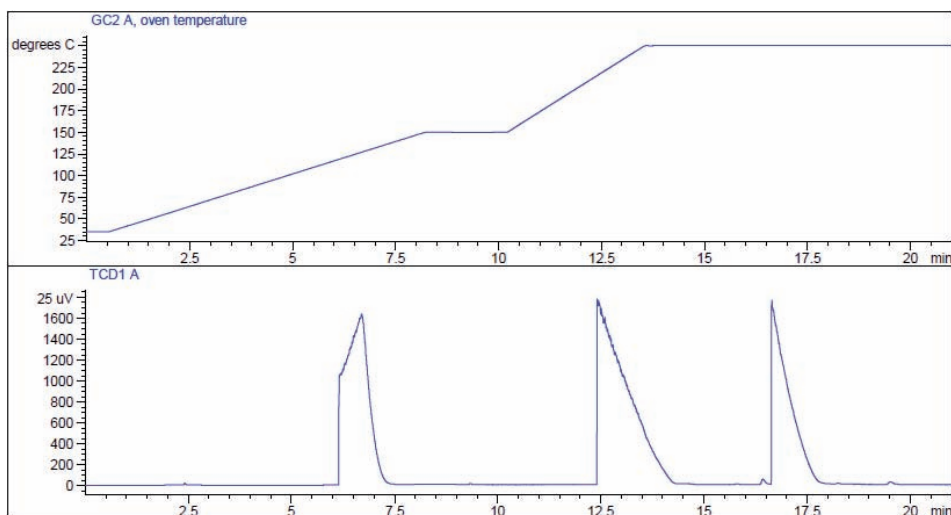


**Figure 4.26** – Chromatogram (TCD) of the analysis of a mixture of water, *n*-pentane and ethylene glycol, and respective temperature program.

The problem of the tailing effect observed in the chromatograms persisted for some time, despite several attempts to solve the problem. The other two chromatographic columns were used in a number of analyses, with very good results in the separation of complex mixtures of hydrocarbons, but proved to be inadequate for the study of systems containing polar compounds such as water or methanol.

After an extensive number of tests, characterised by a long learning process and several “trial and error” stages, mainly due to the lack of expertise in the area of chromatography within the research group, a suitable method for the analysis of the type of mixtures considered in this project was eventually established. The most important parameters of this method are listed in Table 4.5. The temperature program consisted in a 5 minutes plateau at a temperature of 60 °C (333 K), followed by an increase in the temperature, at 20 K.min<sup>-1</sup> (9.5 minutes), before a new plateau at 250 °C (523 K) for another 15 minutes, accounting for a total time of approximately 30 minutes.

**Table 4.5** – List of the most important parameters of the generic chromatographic method developed for the analysis of the mixtures of interest for this work.

Parameter	Setting
Temperature of the injector	200 °C / 473 K
Split ratio	25:1
Total flow	53 mL.min <sup>-1</sup>
Carrier gas	He
Temperature of the TCD	250 °C / 523 K
Temperature of the FID	250 °C / 523 K

Figure 4.27 shows a chromatogram obtained in the analysis of a prepared solution of *n*-pentane, *n*-hexane, water and MEG in methanol, in which methane was bubbled before the injections. In Figure 4.28, the result of an analysis of a solution of *n*-pentane, *n*-hexane, water and methanol, in which ethanol was used as solvent is presented. For this chromatogram, the temperature program used differs slightly from that mentioned above, as a temperature ramp of 25 K.min<sup>-1</sup> was applied here. This is noticeable in the retention times of *n*-pentane and *n*-hexane, which changed respectively from 20.1 min and 23.7 min in Figure 4.27 to 18.4 min and 21.5 min in Figure 4.28. Table 4.6 presents a synthesis of the approximate retention times observed for the compounds involved in these analyses.

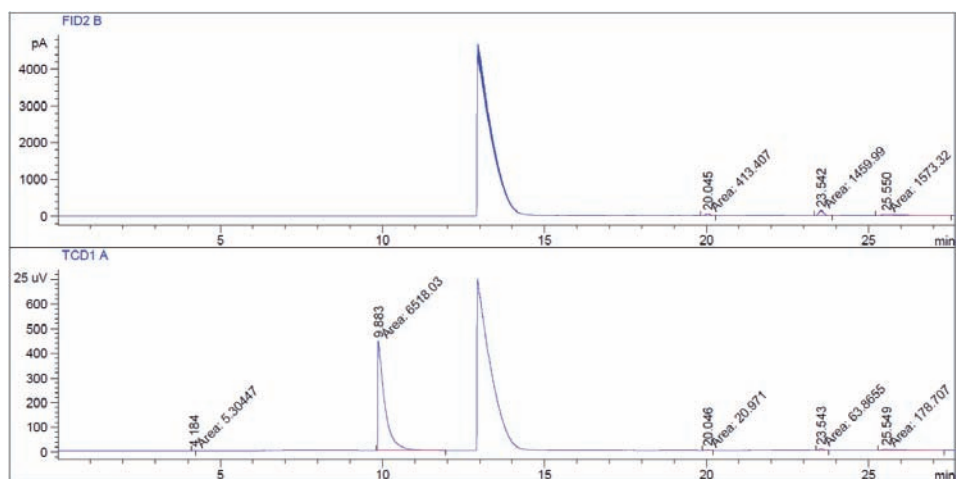


**Figure 4.27** – Chromatogram (FID and TCD) of the analysis of a mixture of solution of methane, *n*-pentane, *n*-hexane, water and MEG in methanol.

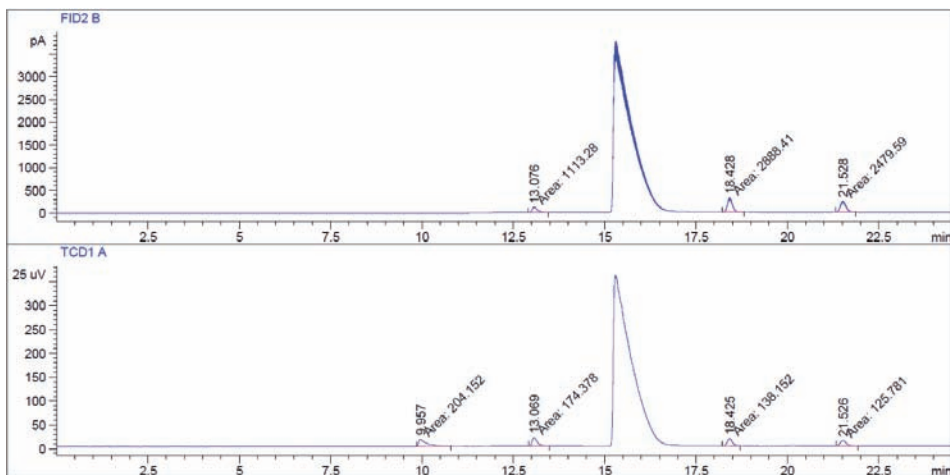


**Figure 4.28** – Chromatogram (FID and TCD) of the analysis of a mixture of solution of *n*-pentane, *n*-hexane, methanol and water in ethanol.

**Table 4.6** – Approximate retention times observed for the compounds involved in these analyses presented in Figure 4.27 and 4.28, according with the chromatographic method developed.

Compound	Retention time / min
methane	4.2
<i>n</i> -pentane	20.2 / 18.4 <sup>a</sup>
<i>n</i> -hexane	23.7 / 21.5 <sup>a</sup>
water	9.9
methanol	13.1 – 13.5
ethanol	15.3
MEG	25.7

<sup>a</sup> – retention times for a temperature ramp of 25K.min<sup>-1</sup>.

Both chromatograms show a good separation between the different constituents of the mixtures analysed, with a total time of analysis less than 30 min. This analysis time can obviously still be reduced, just by changing the temperature program. This would be especially useful in studies of only two or three compounds. However, it should be taken into consideration that the chromatographic method presented is a generic method, developed to provide a basis for the generality of the analysis to be performed in the study of the type of systems under consideration in this work, and therefore a good separation was prioritised. The intention is to facilitate the identification of peaks in the study of

compounds different from those included in the analysed mixtures, leaving open the possibility for further improvements in the analyses of particular systems. As an example, in the study of the binary system methane + water, the analysis is completed after 12 minutes under the presented conditions, so there would be no need for prolonging the analysis for the whole 25 or 30 minutes.

#### **4.4.2. Calibration of the Gas Chromatograph**

With the separation achieved by means of the chromatographic method presented, it is only necessary to perform a calibration, in order to perform quantitative analyses from the phases in equilibrium in the cell. In general, two types of calibration can be considered, one relatively simpler, the other more complex, but supplying a greater amount of information, and valid regardless of the system under study.

Often in phase equilibria studies, the knowledge of the mole fractions in each phase is sufficient to characterise the system. In order to obtain such information from a chromatogram, it is only necessary to know the relative sensibility of the detectors to each of the components, and the information of the mole fraction is given by the ratio between the areas of the peaks. For such measurements, a calibration can be easily performed using two or three different solutions of the constituents of the system under study, in order to correlate the ratio between the areas with the known molar fractions of the solutions. If a different system is then studied, a new calibration is required, even if only one of the components is different.

Another way to perform a calibration, more time consuming, but more effective in the long term, is to calibrate independently each compound, obtaining a relation between the area of the peak in the chromatogram and the amount of compound injected. These calibrations are recommended, being valid for that particular compound regardless of the system under study. This means that, when a new system is placed under study, containing one or more components for which a calibration was previously made, a considerable amount of time can be saved since there is no need to calibrate for those compounds.

It should be understood however, that a few injections of standard solutions should always be performed, in order to confirm that the previously made calibration is still valid.

This is necessary due to the possibility of long time changes in the response of the chromatographic detectors. For the same reason, and despite an initial calibration, it is recommended to perform some additional injections during a series of measurements on a particular system, for instance, during the time necessary for the mixture inside the cell to achieve a new state of equilibrium after a change in the pressure or in the temperature. This will provide additional points to the existing calibration, contributing to its refinement and allowing the detection of the aforementioned possible changes in the response of the detectors, and the monitoring of the rate at which these changes occur.

This type of calibration presents further advantages, given that when an analysis is performed, it allows the knowledge of the exact amount of each substance present in the sample, which in the particular case of this work is undoubtedly an advantage, allowing to better understand how the magnitude of the sample withdrawn by the automatic ROLSI™ sampler-injectors is related with the sampling time and with the pressure of the system inside the equilibrium cell, since as opportunely explained before, the sampling process is controlled merely by the opening time of the sample-injectors and by the difference of pressure inside the equilibrium cell and in the GC carrier gas line.

To perform such a calibration, different amounts of a compound are injected, usually using diluted solutions with a precisely known concentration so that smaller amounts of the component of interest can be injected. To increase the quality of the calibration, it is necessary that the volume of each injection is precisely known, and that the same exact volume is injected a number of times, which can be difficult for an inexperienced analyst, due to partial vaporisation, and the irreproducibility of the injection procedure. In order to deal with these limitations and improve the calibration process, as well as making it considerably more practical, an automatic injector can be used, such as the Agilent 7683B automatic injector employed in the present work.

The calibration for gaseous compounds is usually performed manually, either by the use of gas-tight syringes, or using different loops of an exact known volume in the carrier gas line. This last solution offers a higher reproducibility in terms of the volumes injected, when compared with manual injection, but it implies a higher complexity in the procedure, since different loops have to be disconnected and re-connected to the carrier gas line. In the present work, and due to the connections already existing in this line for the ROLSI™ samplers, the use of loops could be especially complex.

## **4.5. Analytical Measurements on Reference Systems**

As mentioned before, an important step in the validation of the apparatus involves the study of reference systems or of other systems that have been studied frequently and by different authors. In the present case, the binary system methane + water was selected for the first measurements. Although being a simple system, its study entails a number of challenges. Previous to the actual measurements, it is necessary to perform a calibration for the two components involved. This involves the calibration for a liquid and the calibration for a gas, which can be somewhat challenging, since none of the persons involved in the project had any previous experience in doing so. Additionally to this, the study of the samples withdrawn during the measurements on this binary system will involve the analysis of very low concentrations, constituting a serious test for the capability of the gas chromatography, in terms of detection limits, the influence of noise in the signals, reproducibility of the values, etc.

This also means that some difficulties are likely to be encountered, and the solution for eventual problems will have to be found, but ultimately this will allow a better knowledge of the performance and limitations of the analytical part of this new experimental set-up, contributing to a reduction in the number of possible “new problems” that might be encountered in the future, during the use of the apparatus.

### **4.5.1. Calibration for Water and Methane**

Following is a description of the process of calibration for water and methane, a system that has been measured various times by different authors, and which will be used in the validation of the current experimental analytical method. Furthermore, it comprises the calibration for a liquid and a gaseous compound, constituting therefore a perfect example to be given in this work.

The calibration process started with the calibration for water, using the automatic injector. Seven solutions of water in ethanol, with concentrations varying between  $3.997 \times 10^{-2} \text{ mol.dm}^{-3}$  and  $4.541 \text{ mol.dm}^{-3}$ , were carefully prepared and placed in vials in the automatic injector. A vial containing pure solvent was also included. Ten injections of a volume of  $1 \mu\text{L}$  were performed from the vial containing the solvent, and from each

solution, corresponding to a range in the number of moles of water injected between  $3.997 \times 10^{-8}$  mol and  $4.541 \times 10^{-6}$  mol. The results are presented in Figure 4.29, where the areas of the chromatographic peaks yielded by the TCD are represented as a function of the number of moles of water injected.

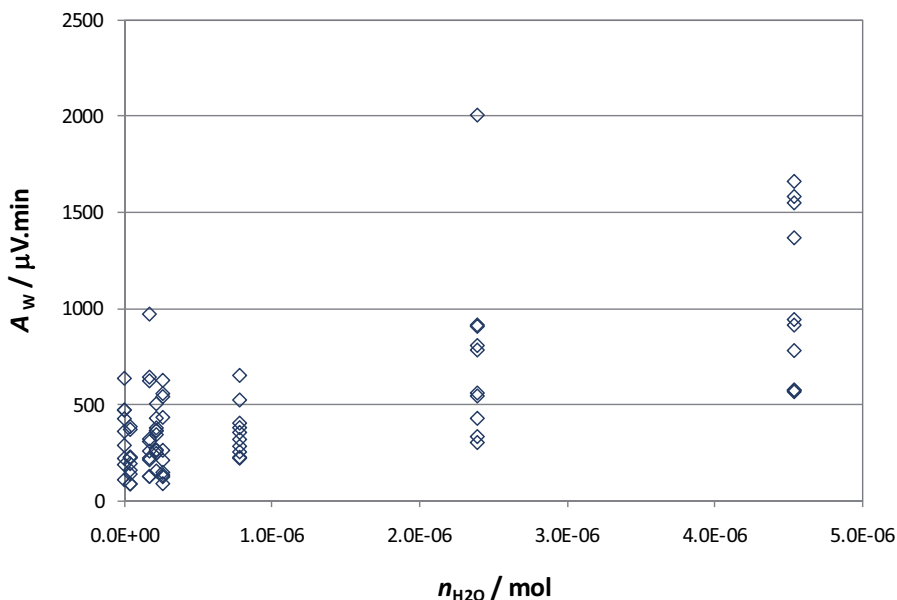


**Figure 4.29** – Areas of the chromatographic peaks yielded by the TCD as a function of the number of moles of water injected, relative to the GC calibration of water using an automatic injector.

The extremely large scattering found for the area values, was obviously unexpected. Among the possible causes for such disparity in the values, is the occurrence of oscillations in the response from the sensor, or the fact that a different amount of sample is reaching the column and the detectors.

In Figure 4.30 a similar representation is made, but using the percentage of the peaks for water relative to the total area of the two peaks, from water and from the solvent. The improvement in the aspect of the plot is noticeable, with most of the scattering decreasing to more acceptable amounts. This shows that whenever the peak of water is smaller, the peak of the solvent also decreases, by the same proportion, showing that the problem is most likely related to the amount of sample injected, or at least, reaching the detectors.

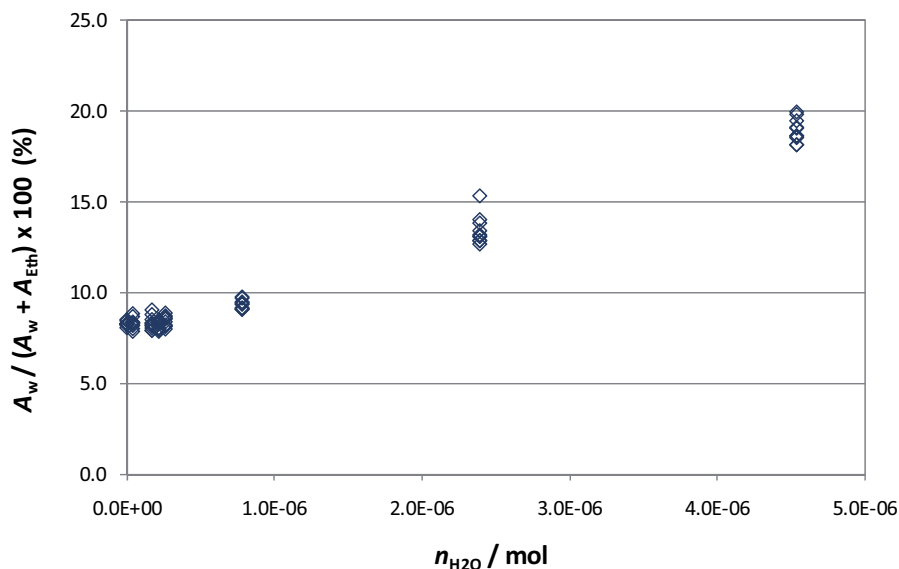


**Figure 4.30** – Percentage of the water peak area from the total areas yielded by the TCD (water + solvent), as a function of the number of moles of water injected, relative to the GC calibration of water using an automatic injector.

Another aspect worth noting in this plot is that the solutions with the lowest concentrations present a percentage of the water peak similar to that from the solvent, indicating that the solvent itself already contains some amount of water, a fact which is not surprising since the solvent is ethanol. Furthermore, the amount of water present in the solvent is of such magnitude that the quantity of water used in the preparation of the most diluted solutions seems to have a negligible effect on its overall concentration. This problem and the approach necessary to deal with it will be discussed later.

As for the issues related to the amount material reaching the detectors, the source of the problem could be related to the volumes injected, or with a non-uniform split of the sample in the injector. The chromatographic method was changed to a “splitless” configuration, and the injections repeated, yielding similar results to the ones presented in last two graphs. A number of injections of 5  $\mu\text{L}$  were performed, also without perceptible improvement. As a consequence, the next step was to perform manual injections, in order to verify whether the problem was related to the inconsistency of the volumes of sample injected by the automatic injector, acquired specifically to perform the calibration avoiding the occurrence of this type of problems, more common in manual injections.

Based on the previous results, five new solutions were prepared, with water concentrations varying between  $9.769 \times 10^{-2} \text{ mol.dm}^{-3}$  and  $25.103 \text{ mol.dm}^{-3}$ . Ethanol from a different source was used as solvent, expected to contain a lower amount of water. A minimum of seven injections were performed from each solution and from the solvent, all with a volume equal to  $1 \mu\text{L}$ . Figure 4.31 presents a chromatogram obtained from one of these injections.

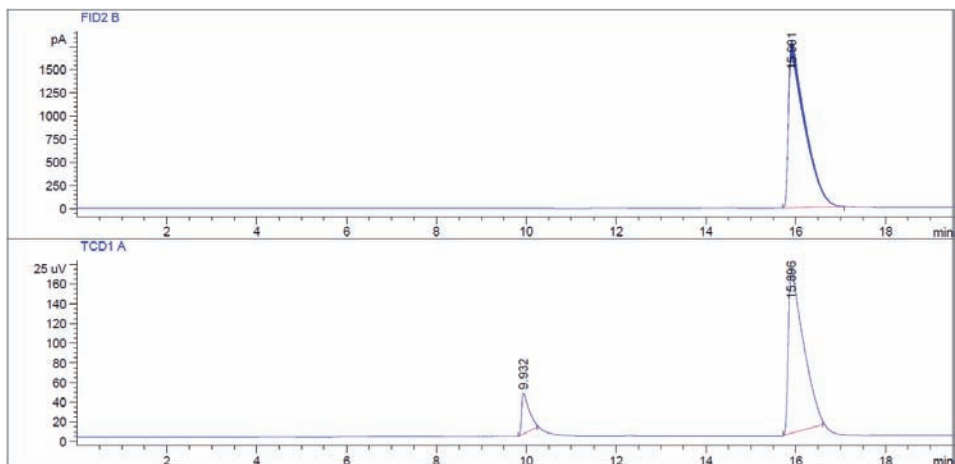


**Figure 4.31** – Chromatogram (FID and TCD) obtained during the calibration for water, using solutions of this compound in ethanol.

The results of the calibration are presented graphically in Figure 4.32. In this plot it is still possible to observe a considerable scattering of the area values relative to the more concentrated solutions, however, the same is not true for the more diluted, and as a consequence, the general aspect was considerably improved by the adoption of the manual injection, confirming the suspicion that the automatic injector was not functioning properly in terms of the injection volume. This fact was later confirmed by comparison of the results obtained with this automatic injector, and a different one borrowed from another research group. In Figure 4.33, a presentation similar to the one in Figure 4.32 is made, exhibiting not all the experimental points, but rather the average area relative to each of the solutions used in the calibration.

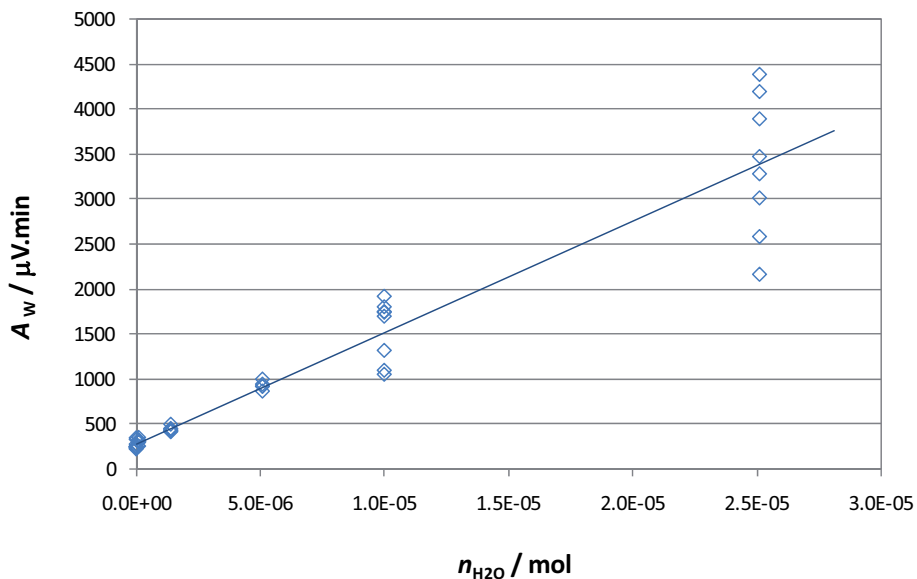


**Figure 4.32** – Areas of the chromatographic peaks yielded by the TCD as a function of the number of moles of water injected, relative to the GC calibration of water through manual injection.

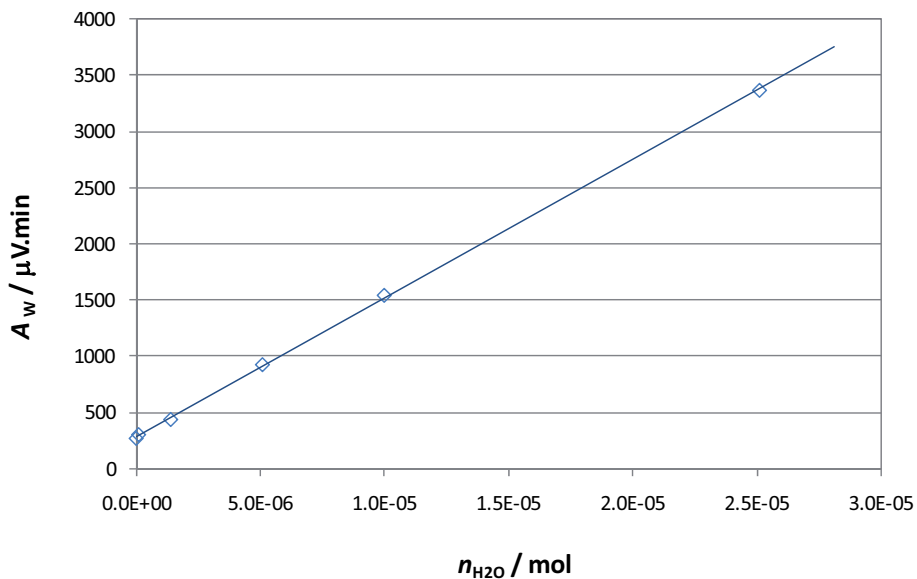


**Figure 4.33** – Average areas of the chromatographic peaks yielded by the TCD as a function of the number of moles of water injected, relative to the GC calibration of water through manual injection.

The quality of the results is in this case more obvious, with the observance of an almost perfect linear relation ( $r^2 = 0.9998$ ). It is also observable however, that a considerable amount of water is still present in the solvent, with a concentration similar to the one from the most diluted solution, being therefore necessary to perform a correction in the actual concentration of the solutions.

At this point, the suitability of ethanol as a solvent for the water solutions may be questioned. The hygroscopic character of ethanol is indeed a disadvantage, but other aspects must be taken into account in the choice of an adequate solvent. It is advisable that the solvent is of the same nature as the compounds to be used in the phase equilibria studies, as components of a different nature may interact with the analyte and lead to changes in the instrumental response. This limits the choice of available solvents to alcohols and hydrocarbons. Due to the limited miscibility between water and light hydrocarbons, the most adequate choice was ethanol, despite the problems its use involves.

Dealing with this problem requires a correction in the concentrations of the solutions used. The solutions were all prepared in a short interval, so the concentration of water in the solvent may be assumed to be equal for all the solutions. Each solution was prepared independently, simultaneously gravimetrically and volumetrically, from a pre-determined amount of water and ethanol, rather than preparing the more concentrated solution and subsequently the others by dilution. This means that for each of the prepared solutions, the amounts of water and of solvent added are known precisely.

In order to apply the necessary corrections, two methods can be used. The first method, with a more simple and fast application, implies the assumption that the amount of water present in the solutions with its origin in the solvent is the same for all the solutions prepared, based on the facts that, similar volumes of each solution were prepared, the relatively low volume of water used relative to the volume of solution prepared, meaning that the volume of ethanol was also nearly constant, and the unknown but relatively low concentration of water in the solvent.

Based on this assumption, the correction of the concentrations can be calculated by subtracting from all the areas the value of the area obtained in the analysis of "pure" ethanol. This should correspond approximately to the areas that would have been produced if the solvent contained no water. From these new values, a relation between the number of

moles of water and the area of the chromatographic peaks can be established, and subsequently be applied to the area of the peak obtained for ethanol, for determination of its concentration. The knowledge of this parameter allows the correction of the values of concentration of all the solutions, and a calibration curve is then obtained using the areas measured for the solutions and for the solvent, which is now regarded as just another solution, as a function of the number of moles injected.

Another method consists in the use of the exact amounts of water and solvent used in the preparation of each solution, as explained next. From the plots of Figure 4.32 and Figure 4.33, it is expected the relation between the number of moles and the chromatographic areas to be linear. It can then be considered the following expression:

$$Area = A \cdot n_{inj} + B \quad (4.6)$$

In this equation,  $n_{inj}$  refers to the amount of water injected, which can be defined in the following manner:

$$n_{inj} = (n_{add} + n_{eth}) \frac{V_{inj}}{V_{sol}} \quad (4.7)$$

where  $n_{add}$  is the quantity of water added in the preparation of the solution,  $n_{eth}$  refers to the amount of water in the solution originating in the solvent,  $V_{inj}$  is the volume of the injection, in the case of this work equal to 1  $\mu\text{L}$ , and  $V_{sol}$  refers to the volume of the solution prepared.

Equation 4.7 can be re-written as a function of the concentration of water in ethanol,  $C$ , and the volume of this solvent used in the preparation of the solution,  $V_{eth}$ :

$$n_{inj} = (n_{add} + C \cdot V_{eth}) \frac{V_{inj}}{V_{sol}} \quad (4.8)$$

Substituting in equation 4.6:

$$Area = (A \cdot n_{add} + A \cdot C \cdot V_{eth}) \frac{V_{inj}}{V_{sol}} + B \quad (4.9)$$

This equation can be written independently for each of the solutions prepared for this calibration, and also for ethanol, in which case it simplifies into expression 4.10, given that  $V_{eth} = V_{sol}$  and  $n_{add} = 0$ .

$$Area = A \cdot C \cdot V_{inj} + B \quad (4.10)$$

These equations can be used in the simultaneous determination of the parameters  $A$  and  $B$ , and of the concentration of water in the ethanol, represented by  $C$ . The values determined in the present calibration, are presented in Table 4.7.

**Table 4.7** – Determined values for the parameters  $A$  and  $B$ , and for the concentration of water in the solvent,  $C$ , relative to Equation 4.9, in the calibration for water.

Parameter	Determined value
$A$	$1.2790 \times 10^8 \mu\text{V} \cdot \text{min} \cdot \text{mol}^{-1}$
$B$	$33.977 \mu\text{V} \cdot \text{min}$
$C$	$1.9589 \times 10^{-3} \text{mol} \cdot \text{mL}^{-1}$

The plot in Figure 4.34 illustrates a comparison between the non-corrected calibration curve, and the curves obtained applying the two described correction methods. It is noticeable that the simplified correction method works very well for the solutions of lower concentrations, but fails for the higher values, in which a smaller amount of ethanol was added in the preparation of the solutions, leading to an overcorrection of the values.

The average areas of the chromatographic peaks obtained during the calibrations, and the corresponding number of moles injected, corrected by means of the second and more exact correction method presented, are given in Table 4.8. It should be noticed that the values in the first line of the table, correspond to the results obtained with the injections of ethanol, which after the corrections is regarded as just another solution.

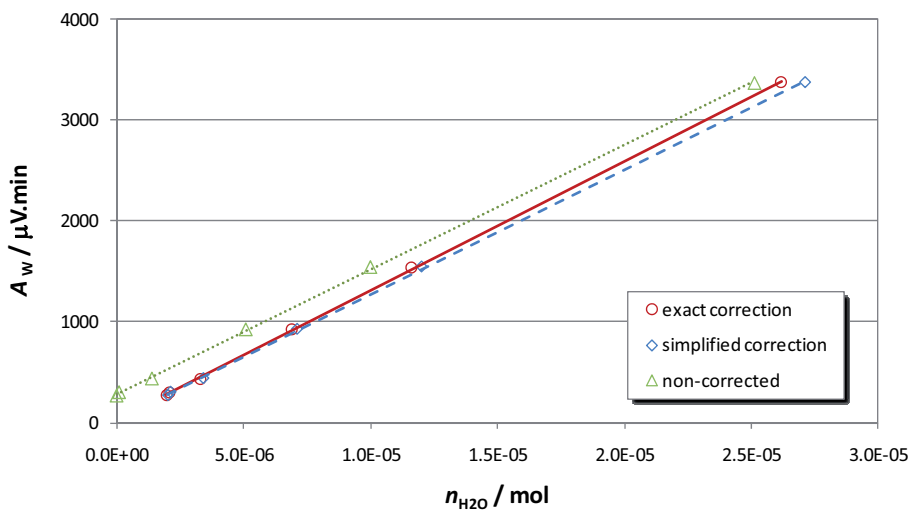


**Figure 4.34** – Comparison between the non-corrected calibration curve, and the curves obtained applying the two described correction methods.

**Table 4.8** – Average areas of the chromatographic peaks obtained in the calibration of the GC for water, and number of moles injected.

Area / $\mu\text{V}\cdot\text{min}$	Moles injected / mol
268.78	$1.959 \times 10^{-6}$
302.51	$2.053 \times 10^{-6}$
437.84	$3.300 \times 10^{-6}$
925.90	$6.864 \times 10^{-6}$
1543.61	$1.160 \times 10^{-5}$
3369.61	$2.618 \times 10^{-5}$

The correlation of the values presented in the table, leads to equation 4.11.

$$Area = 1.2790 \times 10^8 \cdot n_{water} + 33.977 \quad (4.11)$$

However, according to equation 4.11, even the absence of water would correspond to a chromatographic peak of area equal to  $33.977 \mu\text{V}\cdot\text{min}$ . This fact can become problematic in the study of low concentrations of water, for instance, in determining the solubility of water in a gas at high-pressure, where it is expected the quantity of water analysed to be

extremely small using the ROLSI<sup>TM</sup> sampler-injectors. A constraint may then be imposed, forcing the equation to yield a value of zero for the area, when the amount of water is also zero. The resulting expression, equation 4.12, is regarded as the final calibration curve to be used in this work, according to which the response of the TCD detector is characterised for the analysis of water.

$$Area = 1.2989 \times 10^8 \cdot n_{water} \quad (4.12)$$

Despite the implementation of this last constraint, the square linear correlation coefficient for the equation is given by  $r^2 = 0.9997$ . Further calibrations for even lower amounts of water could still be performed using for example dilute solutions of water in *n*-hexane or in *n*-heptane, at concentrations in which the complete miscibility of the two compounds is observed. Nonetheless, it was decided to first verify the applicability of the current calibration in the study of the binary system already mentioned.

Regarding the calibration for methane, the procedure consisted in the manual injection of different volumes of the pure gas, using two gas-tight syringes of different volumes. Methane with a purity of 99.9995%, supplied by AGA Gas AB, Sweden, and prepared by Linde Gas UK Ltd, UK, was initially transferred from the pressurised bottle to a Tedlar® SKC sampling bag, of one litre of capacity and equipped with a valve and a septum containing a syringe port, supplied by SKC Gulf Coast Inc, USA. The Tedlar® film is composed mostly from polyvinyl fluoride, and it is characterised by a high chemical inertia and resistance to gas permeation, assuring the sample integrity. From the sample bag, a number of samples of different volumes, between 0.02 mL and 1.0 mL were withdrawn for injection. The amount of substance injected, was calculated using values for the density of the gas at the temperature of the room and at atmospheric pressure, taken from NIST Standard Reference Data, Thermophysical Properties of Fluid Systems [56].

A minimum of seven injections were performed for each volume. Since methane is detected by both the TCD and the FID, it is possible to establish a double calibration, using the results of both detectors. It should be pointed out however, that if a choice has to be made, the FID output should be selected, since it is characterised by a higher sensitivity in the analysis of hydrocarbons. The results obtained in this calibration are presented in Figure 4.35 and Figure 4.36, relative to the outputs of the TCD and of the FID respectively.

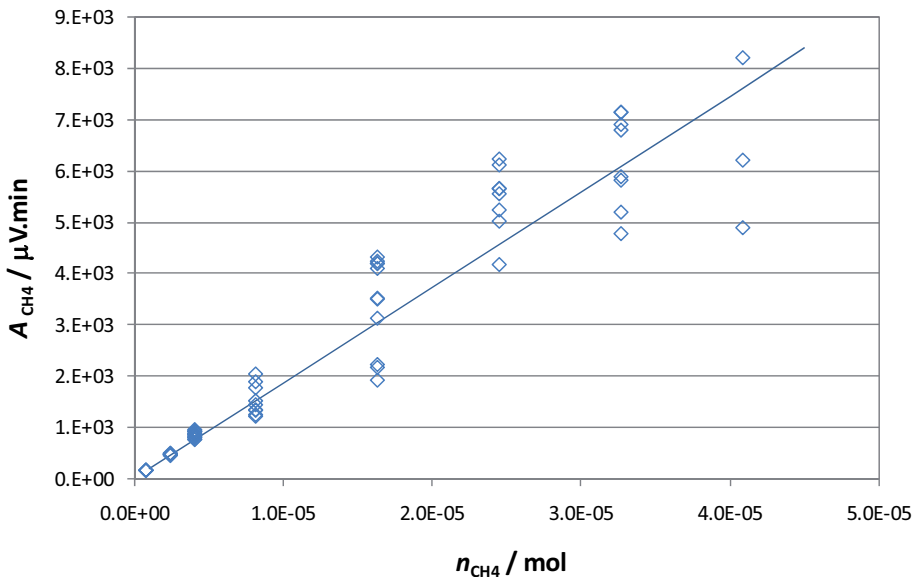


**Figure 4.35** – Areas of the chromatographic peaks yielded by the TCD as a function of the number of moles of methane injected, during the GC calibration of this gas.

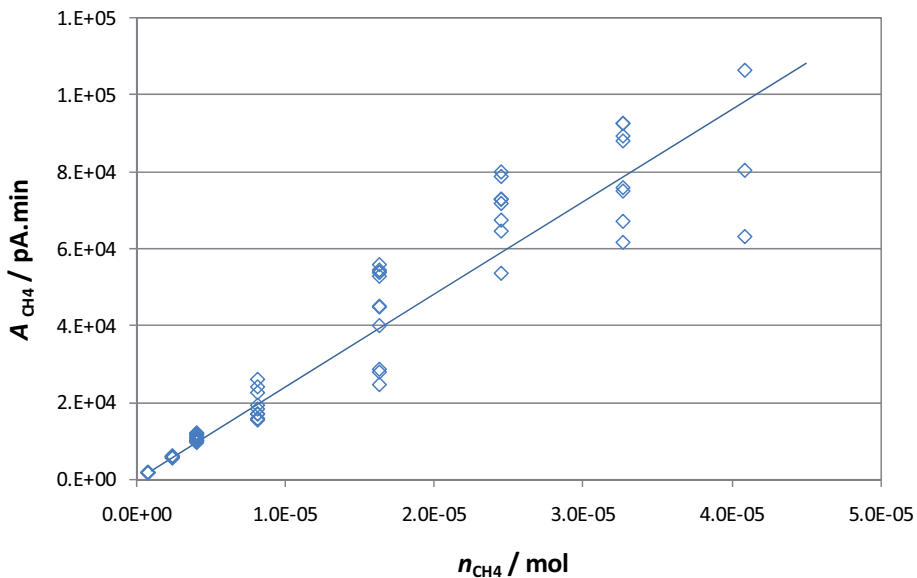


**Figure 4.36** – Areas of the chromatographic peaks yielded by the FID as a function of the number of moles of methane injected, during the GC calibration of this gas.

The results are characterised by a higher scattering and a poorer linearity than the calibration for water. The similarity between the two figures is noteworthy, showing that the scattering is not a product of the response of the detectors, but that it is rather related to an inconsistency in the injected volumes. The scattering for the higher volumes, for which the injections were performed using a gas-tight syringe with 1 mL of capacity, is related to the high internal diameter of the syringe, contributing to a considerable uncertainty in the volume of gas injected, which ultimately translates into the observed dispersion of values.

The lines shown in the graphs are considered as the calibration lines for methane. As before, a constraint was imposed forcing the equations to an intercept of zero, therefore yielding a value of zero for the area when no gas is injected, for the reasons explained previously. The resulting equations, relative to the TCD and the FID, respectively, are given by the following expressions:

$$Area_{TCD} = 1.8642 \times 10^8 \cdot n_{\text{methane}} \quad (4.13)$$

$$Area_{FID} = 2.4046 \times 10^9 \cdot n_{\text{methane}} \quad (4.14)$$

It can be argued whether the calibration lines should in fact be given by a straight line. In this particular case, the adoption of a second order polynomial might seem to be more appropriate, due to an apparent deviation of the area values for the higher numbers of moles represented in the graph. However, it is necessary to take into account that the representation in the graph is limited in terms of the range of the number of moles of methane, and that an extrapolation has to be considered during the study of the systems in equilibrium. It is therefore not recommended to perform an adjustment to a second order equation for the calibration points, as such equation would lead to severe deviations for higher amounts of gas, achieving a maximum value and then starting to decrease again.

#### **4.5.2. Analytical Results for the System Methane + Water**

After completing the calibrations for both components, measurements on this binary system were performed at temperatures of 298 K and 303 K, and pressures between 5 MPa and 13 MPa. The mixture was prepared using deionised water and methane with a

purity of 99.9995%, supplied by AGA Gas AB, Sweden, and prepared by Linde Gas UK Ltd, UK. Firstly, the equilibrium cell was cleaned with toluene, water and with ethanol several times, before being placed under vacuum for a period of 24 hours. The cell was then re-opened, and the deionised water was placed inside for degassing. After the successful degassing, methane was added to the cell directly from a high pressure bottle, taking care to rinse the previously evacuated tubing. After equilibration through stirring, samples from the gas and liquid phases were withdrawn and analysed. A series of 6 measurements were made for each of the experimental conditions studied, in order to evaluate the repeatability of the sampling and of the analysis. The first series of samplings were used to optimise experimental details such as the sampling times, and some characteristics of the analytical method.

Concerning the opening times of the samplers, a balance has to be reached. Low opening times allow sharper chromatographic peaks and a chromatogram with a better definition, but of lower area and therefore more susceptible of being affected by errors in the integration of the peaks, which in the determination of lower concentrations can be critical. On the other hand, larger sampling times help reduce this problem and permit the measurement of lower concentrations, but can lead to a significant broadening of the peaks. Additionally, it should be considered that in the case of the measurement of lower concentrations, as in the case of the binary system under study, one of the components will be present in almost residual amounts while the other is predominant, and the resulting chromatogram will show a very small peak and a very large peak. The sampling volume should be large enough to allow a reliable evaluation of the small peak, but not too large that will affect the quality of the peak corresponding to the predominant component. Finally, it should also be taken into account that the relation between the volume of sample and the opening time of the ROLSI<sup>TM</sup> valves is dependent on the viscosity of the phases and on the pressure inside the cell.

The generic chromatographic method developed before and presented in Section 4.4.1, also needs to be optimised. Its length needs to be adjusted to the compounds under study, by means of increasing the frequency with which samples can be withdrawn from the equilibrium cell. It was also verified that a “splitless” configuration for the GC would yield results accompanied by a lower degree of scattering.

The results obtained in the analytical study of VLE in the binary system methane + water are presented in Table 4.9, where  $x_{\text{methane}}$  and  $y_{\text{water}}$  correspond to the molar fractions of methane in the liquid phase, and of water in the gas phase, respectively. Each value presented in the table is the result of at least of 6 measurements, the individual data points are given in Appendix 2.

**Table 4.9** – Results obtained in the analytical study of the system methane + water.  $x_{\text{methane}}$  and  $y_{\text{water}}$  correspond to the molar fractions of methane in the liquid phase, and of water in the gas phase, respectively.

$T / \text{K}$	$p / \text{MPa}$	$x_{\text{methane}} \times 10^3$	$y_{\text{water}} \times 10^3$ (FID)	$y_{\text{water}} \times 10^3$ (TCD)	$y_{\text{water}} \times 10^3$ (av.)
298.28	5.430	1.135	--	--	--
298.21	5.527	--	0.570	0.581	0.576
298.31	7.344	1.392	--	--	--
298.30	7.638	1.544	--	--	--
298.29	7.934	--	0.378	0.385	0.382
298.29	8.218	1.612	--	--	--
298.28	8.447	1.676	--	--	--
298.30	11.340	2.026	--	--	--
298.30	11.452	--	0.270	0.279	0.275
303.27	5.340	0.908	--	--	--
303.28	5.246	--	0.838	0.850	0.844
303.27	6.692	1.141	--	--	--
303.28	7.175	1.306	--	--	--
303.28	7.241	--	0.635	0.648	0.642
303.28	12.232	1.919	--	--	--
303.28	12.345	--	0.389	0.398	0.394

The values referring to the mole fraction of water in the gas phase were calculated twice for each sample, since the number of moles of methane can be calculated based both on the TCD signal and on the FID signal. It was verified in all the cases that the results obtained from both signals were in a good agreement with each other, as observable in the table, where a column with the average value was also included. As for the values of methane in water, only the results from the FID peak for methane were considered, since the lower sensitivity of the TCD associated to the very small amounts of methane present

in the samples, lead to significant errors in the determination of its mole fraction on the aqueous phase.

The results obtained in the analysis of the different phases are compared separately with values found in literature. Therefore, Figure 4.37 presents the values relative to the solubility of methane in water, making a comparison to several literature sources [57-61]. In the plot, the individual data points are presented, rather than average values, making possible to infer the scattering in the experiments. The lines presented are given merely for eye guidance, and were drawn based on the values of Chapoy et al. [57]. A good agreement between the results obtained in this work and the literature values can be observed, confirming not only the quality of the apparatus developed, but also the validity of the performed calibrations. The scattering of the data obtained is comparable to the scattering of the data presented by Yang et al. [61].

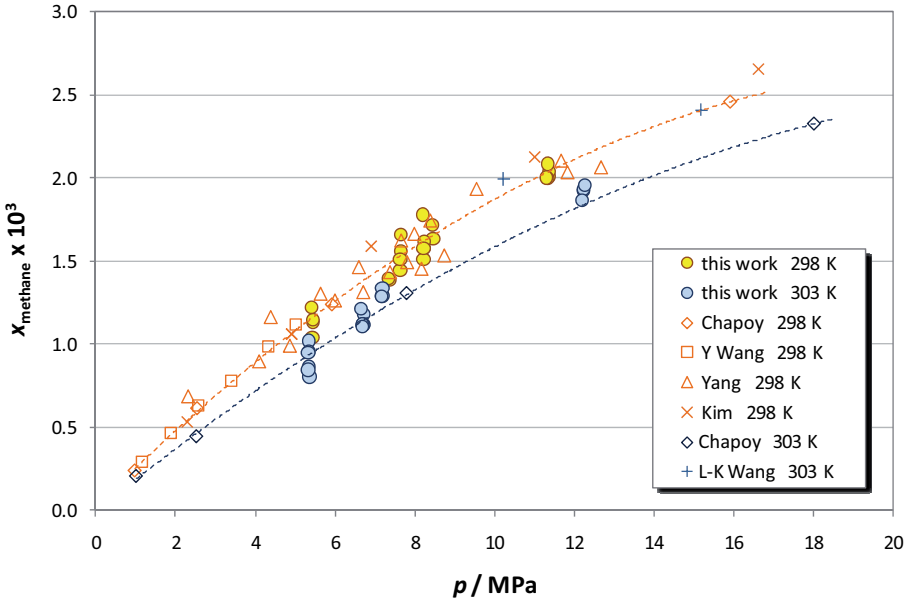


**Figure 4.37** – Individual data points obtained for the liquid phase in the analytical study of the system methane + water, and comparison with values found in the literature [57-61]. The lines in the graph are given merely for eye guidance.

In order to better evaluate the conformity between the results and the literature values, Figure 4.38 presents only the average value for each series of results. For the

temperature of 298 K, the agreement is close to perfect, with the exception of one point. As for the results obtained at 303 K, the results differ slightly from the line drawn based on the values of Chapoy et al. [57], but a good agreement can still be considered, especially when taking into account the dispersion between the different data sources observable for the temperature of 298 K.

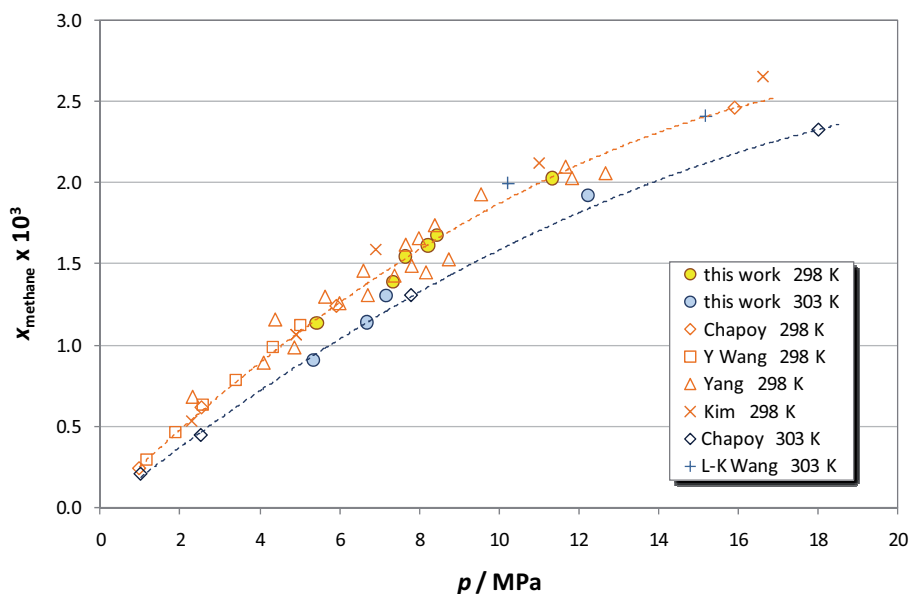


**Figure 4.38** – Results (average values) obtained for the liquid phase in the analytical study of the system methane + water, and comparison with values found in the literature [57-61]. The lines in the graph are given merely for eye guidance.

Figure 4.39 presents the results obtained for the solubility of water in methane, and the comparison with values from literature [62]. These results are considered to be an important test for the quality of the apparatus, since they entail the determination of very low concentrations. The plot in the figure shows once again the excellent agreement between the data from this work and the literature, an agreement better than the one observed in the study of the liquid phase. It is also observable that these results are characterised by a lower amount of scattering, when compared with those obtained in the study of the aqueous phase.

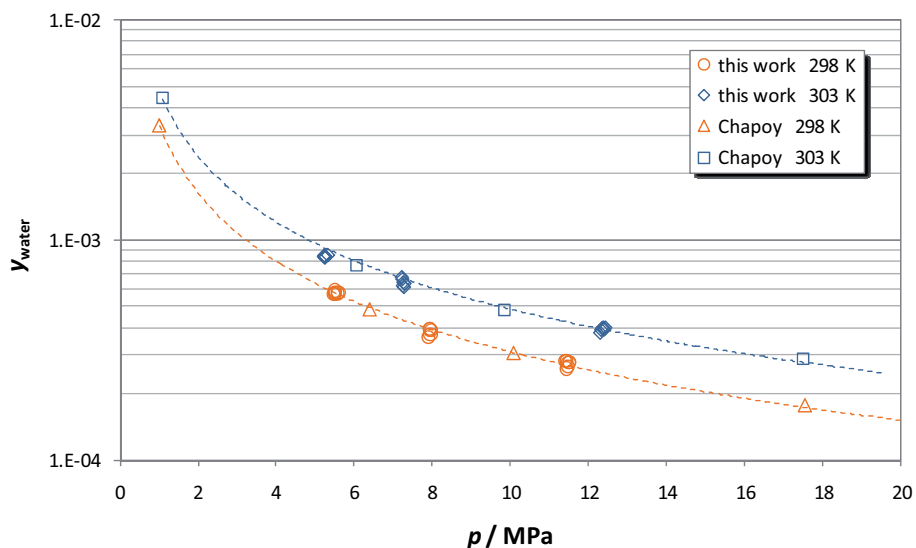


**Figure 4.39** – Individual data points obtained for the gas phase in the analytical study of the system methane + water, and comparison with values found in the literature [62]. The lines in the graph are based on the literature values and are given merely for eye guidance.

One of the major concerns in this type of analysis was the possibility of adsorption of traces of water in the line assuring the connection between the sample-injectors and the GC unit. As mentioned before, this line is made of deactivated fused-silica, much like an empty GC column, in order to minimise adsorption problems, and it can be heated up to 523 K. Before the experiments which led to the results presented, a series of tests were performed in order to evaluate how the temperature of the samplers and of the line can influence the results.

Once again, a fine balance is required. The temperature of the line should be high enough to avoid adsorption problems, and the temperature of the samplers should be sufficiently elevated in order to avoid partial condensation caused by the pressure drop of the sample. Conversely, a high difference between the temperature of the samplers and the temperature of the equilibrium cell can lead to temperature gradients, which might have a negative impact in the thermal homogeneity of the cell.

In the analysis of both phases, it was noticed that the integration of the chromatographic peaks is a critical step, which can have a serious influence the final results. The combination of low sample volumes with low concentrations, result in an

extremely small peak for the solute (water in the gas phase, or methane in the aqueous phase), where a small error in the integration translates into a considerable relative error in the mole fraction value.

The results gathered in the analytical study of this binary system confirm the correct performance of the analytical part of the apparatus, even in challenging conditions such as these, with the determination of very low concentrations.

In combination with the tests previously presented, which confirmed the quality of the temperature and pressure measurements and of their control systems, these results confirm the high quality of the analytical apparatus designed and built in this project, representing the achievement of an important objective of the present work.

#### **4.6. Conclusions**

In this chapter, a new high-quality experimental set-up for the study of phase equilibrium in multi-component systems at high pressures and low temperatures was presented. Based on an analytical method with sampling, the apparatus uses a variable volume cell designed and built “in house”, equipped with a 360° sapphire window. This relatively complex apparatus was completely planned, designed and built for a current project, with an overall cost several times less than the commercial solutions available. Furthermore, this allowed a higher degree of customisation, avoiding the need for compromises, always inevitable where commercial equipment is concerned.

A complete description of the apparatus was given, first in a more general manner, and subsequently presenting a detailed description of all of its main parts and components, underlining in each case the arguments for its design or for its selection.

The quality of the apparatus was confirmed by the extensive testing performed to all the systems involved, from the temperature and pressure measurements to the analytical aspects. These tests revealed the high precision and accuracy of the results which can be achieved with the apparatus.

## References

- [1] G. K. Folas, E. W. Froyna, J. Lovland, G. M. Kontogeorgis, E. Solbraa, *Fluid Phase Equilib.* 252 (2007) 162-174.
- [2] Even Solbraa, Statoil ASA, Research and Development Centre, Trondheim, Norway, Personal Communication, 2007.
- [3] F. Gervais, *Handbook of Optical Constants of Solids, Volume 2*, E. D. Palik (ed.), Elsevier, 1998.
- [4] *Handbook of Optical Materials*, M. J. Weber (ed.), CRC Press, 2002.
- [5] A. J. Rondinone, C. Y. Jones, S. L. Marshall, B. C. Chakoumakos, C. J. Rawn, E. Lara-Curzio, *Canadian Journal of Physics* 81 (2003) 381-385.
- [6] Y. E. Gorbaty, G. V. Bondarenko, *Review of Scientific Instruments* 66 (1995) 4347-4349.
- [7] L. Ruffine, A. Barreau, I. Brunella, P. Mougin, J. Jose, *Ind. Eng. Chem. Res.* 44 (2005) 8387-8392.
- [8] H. Reisig, K. D. Wisotzki, G. M. Schneider, *Fluid Phase Equilib.* 51 (1989) 269-283.
- [9] G. K. Folas, O. J. Berg, E. Solbraa, A. O. Fredheim, G. M. Kontogeorgis, M. L. Michelsen, E. H. Stenby, *Fluid Phase Equilib.* 251 (2007) 52-58.
- [10] R. Dohrn, S. Peper, J. M. S. Fonseca, *Fluid Phase Equilib.* 288 (2010) 1-54.
- [11] J. M. S. Fonseca, S. Peper, R. Dohrn, *Fluid Phase Equilib.*, *In press*
- [12] Ole J. Berg, Statoil ASA, Research and Development Centre, Trondheim, Norway, Personal Communication, 2007.
- [13] H. Madani, A. Valtz, C. Coquelet, A. H. Meniai, D. Richon, *J. Chem. Thermodyn.* 40 (2008) 1490-1494.

- [14] F. Garcia-Sánchez, G. Eliosa-Jiménez, G. Silva-Oliver, A. Godínez-Silva, *J. Chem. Thermodyn.* 39 (2007) 893-905.
- [15] M. Grigante, P. Stringari, G. Scalabrin, E. C. Ihmels, K. Fischer, J. Gmehling, *J. Chem. Thermodyn.* 40 (2008) 537-548.
- [16] O. Elizalde-Solis, L. A. Galicia-Luna, S. I. Sandler, J. G. Sampayo-Hernández, *Fluid Phase Equilib.* 210 (2003) 215-227.
- [17] A. Valtz, C. Coquelet, A. Baba-Ahmed, D. Richon, *Fluid Phase Equilib.* 207 (2003) 53-67.
- [18] S. Mokraoui, C. Coquelet, A. Valtz, P. E. Hegel, D. Richon, *Ind. Eng. Chem. Res.* 46 (2007) 9257-9262.
- [19] D. Seredynska, G. Ullrich, G. Wiegand, N. Dahmen, E. Dinjus, *J. Chem. Eng. Data* 52 (2007) 2284-2287.
- [20] Catinca Secuianu, Department of Applied Physical Chemistry and Electrochemistry, "Politehnica" University of Bucharest, Romania, Personal Communication, 2009.
- [21] Even Solbraa, Statoil ASA, Research and Development Centre, Trondheim, Norway, Personal Communication, 2009.
- [22] D. Richon, *Pure Appl. Chem.* 81 (2009) 1769-1782.
- [23] T. Jiang, C. J. Liu, M. F. Rao, C. D. Yao, G. L. Fan, *Fuel Process. Technol.* 73 (2001) 143-152.
- [24] M. Jia, W. Li, H. Xu, S. Hou, Q. Ge, *Appl. Catal. , A* 233 (2002) 7-12.
- [25] R. Susilo, J. D. Lee, P. Englezos, *Fluid Phase Equilib.* 231 (2005) 20-26.
- [26] S. O. Derawi, G. M. Kontogeorgis, E. H. Stenby, T. Haugum, A. O. Fredheim, *J. Chem. Eng. Data* 47 (2002) 169-173.
- [27] G. K. Folas, G. M. Kontogeorgis, M. L. Michelsen, E. H. Stenby, E. Solbraa, *J. Chem. Eng. Data* 51 (2006) 977-983.

- [28] K. Ishihara, H. Tanaka, M. Kato, *Fluid Phase Equilib.* 144 (1998) 131-136.
- [29] D. H. Lam, K. D. Luks, *J. Chem. Eng. Data* 36 (1991) 307-311.
- [30] Y. H. Ma, J. P. Kohn, *J. Chem. Eng. Data* 9 (1964) 3-5.
- [31] L. Ruffine, A. Barreau, I. Brunella, P. Mougin, J. Jose, *Ind. Eng. Chem. Res.* 44 (2005) 8387-8392.
- [32] S. Zeck, H. Knapp, *Fluid Phase Equilib.* 25 (1986) 303-322.
- [33] E. Brunner, *J. Chem. Thermodyn.* 17 (1985) 871-885.
- [34] E. C. W. Clarke, D. N. Glew, *Trans. Faraday Soc.* 62 (1966) 539-547.
- [35] José M. S. Fonseca, M.Sc. Thesis, Department of Chemistry of the Faculty of Sciences of the University of Porto, Porto, Portugal, 2004.
- [36] J. M. S. Fonseca, L. M. N. B. Santos, M. J. S. Monte, *J. Chem. Eng. Data* 55 (2010) 2238-2245.
- [37] M. J. S. Monte, L. M. N. B. Santos, M. Fulem, J. M. S. Fonseca, C. A. D. Sousa, *J. Chem. Eng. Data* 51 (2006) 757-766.
- [38] M. J. S. Monte, L. M. N. B. Santos, J. M. S. Fonseca, C. A. D. Sousa, *J. Therm. Anal. Calorim.* 100 (2010) 465-474.
- [39] V. K. Abrosimov, G. V. Sibrina, *J. Struct. Chem.* 31 (1990) 423-427.
- [40] M. F. Bailey, B. E. Davidson, J. Haralambidis, T. Kwok, W. H. Sawyer, *Biochemistry* 37 (1998) 7431-7443.
- [41] J. G. Blok, A. C. G. van Genderen, P. R. van der Linde, H. A. J. Oonk, *J. Chem. Thermodyn.* 33 (2001) 1097-1106.
- [42] M. Fulem, P. Moravek, J. Pangrac, E. Hulicius, T. Simecek, K. Ruzicka, V. Ruzicka, B. Kozyrkin, V. Shatunov, *J. Chem. Eng. Data* 55 (2010) 362-365.
- [43] C. Klofutar, N. Segatin, *J. Solution Chem.* 36 (2007) 879-889.

- [44] A. C. G. van Genderen, J. C. van Miltenburg, J. G. Blok, M. J. van Bommel, P. J. van Ekeren, G. J. K. van den Berg, H. A. J. Oonk, *Fluid Phase Equilib.* 202 (2002) 109-120.
- [45] A. C. G. van Genderen, H. A. J. Oonk, *Colloids Surf. , A* 213 (2003) 107-115.
- [46] D. N. Glew, *J. Phys. Chem.* 66 (1962) 605-609.
- [47] R. F. Weiss, *Deep-Sea Res. Oceanogr. Abstr.* 17 (1970) 721-735.
- [48] DIADEM Professional, DIPPR Interface and Data Evaluation Manager, version 3.0.0, 2000, using DIPPR Design Institute for Physical Property Data Database 2009.
- [49] J. Xia, Á. P.-S. Kamps, G. Maurer, *Fluid Phase Equilib.* 207 (2003) 23-34.
- [50] A. Valtz, M. Hegarty, D. Richon, *Fluid Phase Equilib.* 210 (2003) 257-276.
- [51] J. Kumelan, Á. P.-S. Kamps, D. Tuma, G. Maurer, *Fluid Phase Equilib.* 260 (2007) 3-8.
- [52] C. Descamps, C. Coquelet, C. Bouallou, D. Richon, *Thermochim. Acta* 430 (2005) 1-7.
- [53] P. Théveneau, C. Coquelet, D. Richon, *Fluid Phase Equilib.* 249 (2006) 179-186.
- [54] J. Freitag, M. T. S. Diez, D. Tuma, T. V. Ulanova, G. Maurer, *J. Supercrit. Fluids* 32 (2004) 1-13.
- [55] Y. Anoufrikov, Á. P.-S. Kamps, B. Rumpf, N. A. Smirnova, G. Maurer, *Ind. Eng. Chem. Res.* 41 (2002) 2571-2578.
- [56] E.W. Lemmon, M.O. McLinden, D.G. Friend, *Thermophysical Properties of Fluid Systems in: P.J.Linstrom, W.G.Mallard (Eds.), NIST Chemistry WebBook, NIST Standard Reference Database Number 69, National Institute of Standards and Technology, Gaithersburg MD, 20899, <http://webbook.nist.gov>, 2009.*
- [57] A. Chapoy, A. H. Mohammadi, D. Richon, B. Tohidi, *Fluid Phase Equilib.* 220 (2004) 111-119.

- [58] Y. S. Kim, S. K. Ryu, S. O. Yang, C. S. Lee, *Ind. Eng. Chem. Res.* 42 (2003) 2409-2414.
- [59] L. K. Wang, G. J. Chen, G. H. Han, X. Q. Guo, T. M. Guo, *Fluid Phase Equilib.* 207 (2003) 143-154.
- [60] Y. Wang, B. Han, H. Yan, R. Liu, *Thermochim. Acta* 253 (1995) 327-334.
- [61] S. O. Yang, S. H. Cho, H. Lee, C. S. Lee, *Fluid Phase Equilib.* 185 (2001) 53-63.
- [62] A. Chapoy, C. Coquelet, D. Richon, *Fluid Phase Equilib.* 214 (2003) 101-117.

## **Chapter 5**

# ***Re-commission of an Existing Equilibrium Cell, Synthetic Method***

---

Prior to the development of the new experimental set-up, already presented in the previous chapter, an attempt was made to re-commission an old existing apparatus for the study of VLLE systems, described in 2002 by Laursen et al. [1] and later used in other works by the same authors [2,3]. Internal reports show that the apparatus was still used until the end of 2003 although no publications were found in the literature.

### ***5.1. Limitations of the Existing Apparatus***

This apparatus, already mentioned in Chapter 3, was also described, although very briefly, by Laursen in his PhD thesis [4]. It was based on an analytical method, with samples taken directly to a GC carrier gas flow by means of a moveable syringe and two Rheodyne injection valves, equipped with different sample loops for the gas phase and for the liquid phases. Figure 5.1 shows the apparatus as it was by the end of 2003 [5]. In the centre of the picture it is possible to see the cell involved in an isolation jacket. The motor for stirring can be observed on top of the cell, with the moveable syringe on its right side. On the right side in the picture, two stainless steel cylinders are visible, containing the heated loops, part of the sampling system.

The main component of this apparatus was a stainless steel high pressure cell with an internal volume of 570 cm<sup>3</sup>, produced by Top Industrie, France, equipped with two parallel sapphire windows and a moveable syringe that allowed the withdrawing of samples from

different liquid phases during the study of vapour-liquid-liquid equilibrium (VLLE) systems [1]. The gas chromatograph associated with the cell was a Carlo Erba HRGC 5300, already used by other authors in previous works [6-8].

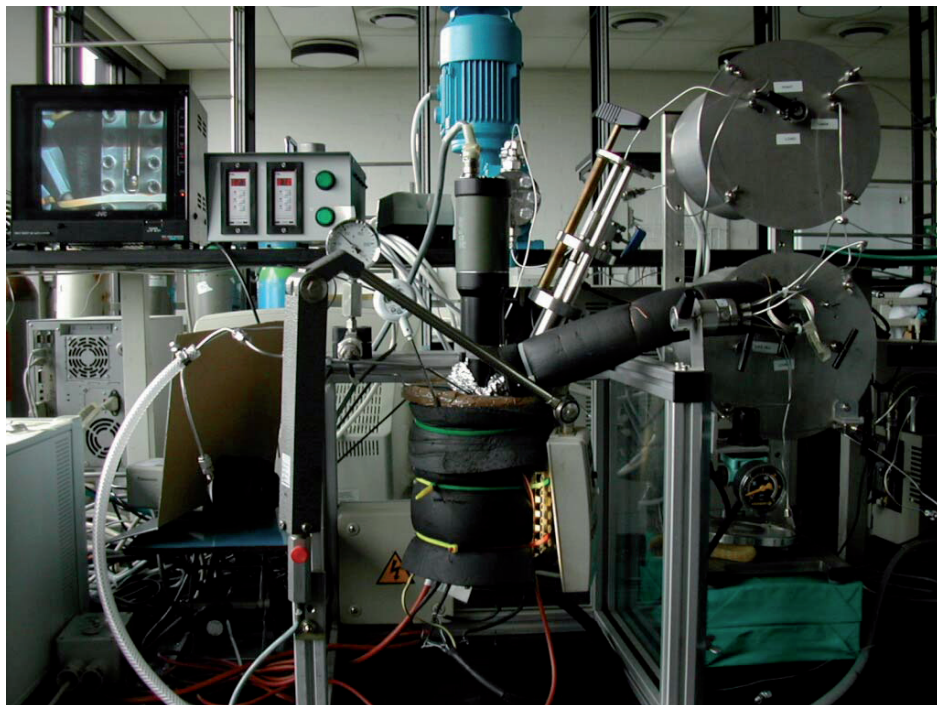


**Figure 5.1** – Picture of the old experimental set-up as it was by 2003. Picture extracted from an internal presentation by Sautédé, from 10 of October, 2003 [5].

A careful analysis of the available literature in which the set-up and the experimental procedure were described [1,4], revealed, together with the first tests performed in this work, several important limitations, not only related with the apparatus itself but also associated with the experimental procedure.

The poor condition of the gas chromatograph, was in any case not surprising, from a GC apparatus around twenty years old. The high amount of noise on the baseline accompanied by a severe drift that was encountered during the preliminary tests carried out in this work, had been already noticed and pointed out by Laursen [4] as being one of the causes for the high uncertainty (up to 30%) estimated by this author on the analysis of heavier components in the gas phase.

Problems with temperature control were also found. Originally, the temperature of the cell was regulated through the use of four heating rods mounted from below, into the sides of the cell, inside its thick walls. These rods were connected, together with a platinum resistance thermometer placed in a well existing in the lid of the cell, to a Eurotherm 2416 PID controller. It was noted by Laursen [4] that at temperatures above 308 K (35 °C), condensation could be observed on the top of the cell, in its interior. This was due to the fact that the lid of the cell was at a lower temperature, since the heating was promoted on the walls of the cell only. In an attempt to overcome this problem, the authors used a second, independent temperature control system for the lid of the cell, using a Eurotherm 2216 PID controller. In his thesis, Laursen claims a control of the temperature of the cell within  $\pm 0.1$  K, stating however, that the top of the cell has a “slightly higher temperature than the rest of the cell” [4].

Besides this unquantified temperature gradient in the cell, caused by the use of two independent controllers, other issues can also be pointed out with this arrangement. From an instrumental point of view, and regardless of the quality of the temperature controller used, it is highly recommended to monitor the temperature by means of a thermometer or sensor independent of that used with the temperature control system. This should allow a more precise monitoring of the values, when compared to the readings performed in the display of the temperature controller, with limited decimal places, and which will almost invariably, be equal to the programmed set point.

Issues were also found in the sampling procedure described by Laursen [4]. According to the author, when a liquid sample was taken, after the convenient positioning of the aforementioned moveable syringe, the loop was filled with sample through the use of a pump, which would be left running for two minutes before the injection valve was turned and the sample in the loop injected into the carrier gas flow. During these two minutes, the liquid phase was recirculated from the bottom of the cell, through the loop, and entering the cell at its top. Such a procedure can obviously lead to a perturbation of the phases in equilibrium, especially when the separation of the phases is not fast enough, and droplets or bubbles from the lighter phases may exist in the withdrawn sample. Any experimental procedure where the recirculation of one or more phases is used to promote a faster attainment of the equilibrium state includes a recirculation period, followed invariably by a resting period, preceding the sampling or other *in-situ* measurements, in

which the system is left to ensure a good separation of the coexisting phases. Moreover, the same applies to the analytical methods where the mixing of the components is promoted by other means such as stirring or rocking of the cell, otherwise the sample might not be homogeneous, containing material from another phase in the form of droplets, bubbles or solid particles [9,10].

Concerning the sampling from the gas phase, Laursen [4] stated that the withdrawing of a single sample would lead to a pressure drop in the cell between 0.01 MPa and 0.2 MPa, meaning that between the two samples taken and analysed for every set of conditions, there was a considerable change in the equilibrium conditions. Still according to the author, the pressure drop was not considered to be relevant since the results obtained from the pairs of samples have always been consistent within 1% to 2%.

It should be pointed out that the goal is not to vilify the existing apparatus, but rather to present the limitations that justified and provided the motivation for the subsequent improvements performed during the course of this work. In addition, it is arguable whether these inaccuracies did in fact influence the results, but when such imprecisions exist in a process and are not taken into account, great precision and accuracy of the final results can hardly be claimed.

The validation of the apparatus was presented in a work already mentioned [1], through the study of the binary systems carbon dioxide + methanol at 298.2 K and carbon dioxide + dimethyl ether at 320.2 K, and the comparison of the obtained values with data available in the literature. For the first system, the results obtained can be considered in agreement with the values presented by Brunner et al. [11], with differences going up to 1%. However, they differ significantly from the other three sets of data used for comparison, all in close agreement with each other [12-14], with differences that go up to 5% in the values of pressure, when a mole fraction of 0.5 in the liquid phase is considered. For the system carbon dioxide + dimethyl ether, the pressures obtained by Laursen and his co-workers, for a mole fraction of carbon dioxide in the liquid phase around 0.4 or 0.5 are about 6% higher than the values from the literature [7,15]. Despite these results the authors considered that there was a good agreement between the obtained values and the literature data.

Later, in an internal presentation made by Sautédé [5], new results for the binary system carbon dioxide + dimethyl ether were reported for a temperature of 320.2 K, with differences, according to the author, up to 5% for the vapour phase and up to 3.5% for the liquid phase when compared with the literature [1,6,15]. For a more complex system, of nitrogen, dimethyl ether and water, at 308 K, the differences between the results presented by the author and the literature [1], were superior to 8% concerning the molar fractions of nitrogen and dimethyl ether in the vapour phase. As for the results relative to the upper and lower liquid phases, the divergences are around 2% and 4%, respectively, for the mole fractions of both water and dimethyl ether.

Finally, in addition to all these points, the apparatus offered no possibility for recording the experimental conditions over time, and both pressure and temperature values had to be noted down manually, after reading from the respective displays (in the case of the temperature, from the display of the PID controllers), requiring a frequent human presence. Furthermore, the automated and constant recording of the experimental conditions presents great advantages, for instance following of the evolution of the system towards equilibrium, the evaluation of the temperature and pressure stability of the apparatus, or the detection of leaks and other types of failures, even transient ones. As for the precision of the measurements, the pressure display could only be read with one decimal place (0.1 bar), while temperature could be read with a maximum of 2 decimal places.

## ***5.2. Re-commissioning the Apparatus – A First Approach***

In addition to the mentioned limitations, the apparatus was not in use for three years, and several parts needed repair. It was therefore decided to make some small changes to the apparatus, in order to, at least, overcome or minimise some of the perceived limitations.

The existing gas chromatograph was immediately abandoned, after the high amount of noise on the baseline and the strong drift observed in the preliminary tests, together with the sampling system associated with it. As for the problems with the temperature homogeneity, they were overcome by placing the cell inside a decommissioned temperature chamber that existed in our laboratory, with the advantage of allowing experiments to be carried out at low temperatures, down to 233 K. A new manual sampling

procedure was adopted, still based on the moveable syringe, but without the connection to the gas chromatograph, and with the limitation of only permitting the sampling from the liquid phase(s).

This new configuration however, raised new problems, and did not constitute an effective answer for some of the existing ones. The placement of the cell inside a closed temperature chamber meant that several parts such as the pressure sensor or the video camera had to undergo the same temperature conditions as the cell, and although the camera could cope very well with the low temperatures, the response of the pressure sensor was severely affected by the temperature to which it was exposed.

After recognizing this problem, the following step was to calibrate the response of the pressure sensor as a function of temperature, first at atmospheric pressure, in order to quantify the influence of the temperature in the baseline, and then with measurements in a reference system, or in other systems that have been studied frequently and by different authors, for comparison of the results.

After the successful calibration at atmospheric pressure, a number of measurements were performed in the study of the three-phase coexisting line for the binary system methanol + ethane. The results were partly satisfactory, despite the uncertainty of some of the assumptions made when correcting the measured values of pressure, as explained later in this chapter, where these results are presented.

Before further tests were possible, the cell revealed problems related to its air tightness, and a considerable amount of time was spent in solving successive leaks, the last one occurring inside the stirrer that went through the lid of the cell. Problems with the air tightness of the cell had in fact been a constant since the first tests with the equilibrium cell. At this point, it was also recognised that the moveable syringe was touching the rotating axis of the stirrer, inside the cell.

In conclusion, additional modifications were imperative in order to deal with the existing problems, preferably involving not only simple changes in the configuration of the apparatus, but also a strong effort in the modernisation of the whole set-up, with the purpose of increasing the quality and precision of the results it could produce, and facilitating its operation with the inclusion of a proper data acquisition and recording system, since up to this point all the experimental conditions still had to be noted down

manually. The outcome of these further and deeper modifications in the apparatus is presented below, with the description of the resulting experimental set-up, the second developed and used in this work.

### **5.3. *Re-commissioning the Apparatus – Final Configuration***

This second configuration of the set-up makes use of a synthetic method, and is intended for the study of simpler systems, without the need for sampling.

As presented in the third chapter of this work, synthetic methods can be used in the detection of phase changes, such as dew point measurements or the study of the appearance of new phases, as well as in the measurement of gas solubilities in non-volatile phases, in which the composition is determined indirectly, provided that the overall composition of the synthesised mixture is precisely known. In any cases, the synthetic methods allow the use of simpler apparatus, simpler operation and maintenance, which justifies their broad use despite of some limitations, accounting for more than 58% of the systems considered in recent reviews focusing on high pressure phase equilibria [9,16]. For this project in particular, and since another experimental set-up was developed based on an analytical method, the option for a synthetic method seemed adequate, opening a possibility for faster, complementary measurements when necessary, and allowing the more complex apparatus to be reserved for more complex measurements. Furthermore, from an experimental point of view, the use of two apparatus based on different methods is clearly interesting, allowing not only to infer the consistency of the results produced by both apparatus through the study of common systems, but also by putting emphasis on the advantages and limitations of both methods.

#### **5.3.1. *Description of the Apparatus***

As a foreword for the description of this apparatus, it should be pointed out the different philosophy involved in its development. Rather than the exhaustive work that was the development of the analytical apparatus already presented, where all the different parts were carefully planned, the process of development of this experimental set-up had more to

do with improvisation and readapting existing parts in our laboratory that, together with the acquirement of a few new parts, crucial to improve the quality of the yielded results, led to an apparatus capable of producing quality results, spending less than 28 000 DKK (approx. 3 750 EUR). It is therefore natural that some opportunities for further improvements can be found, but most probably these would represent deeper changes and higher costs.

The new experimental set-up is suitable for measurements at temperatures ranging from 233 K to 353 K, at pressures up to 20 MPa. In Figure 5.2, a schematic representation of the apparatus is presented. The central part of the apparatus is the high pressure equilibrium cell, equipped with two parallel sapphire windows, one of them containing a scale.

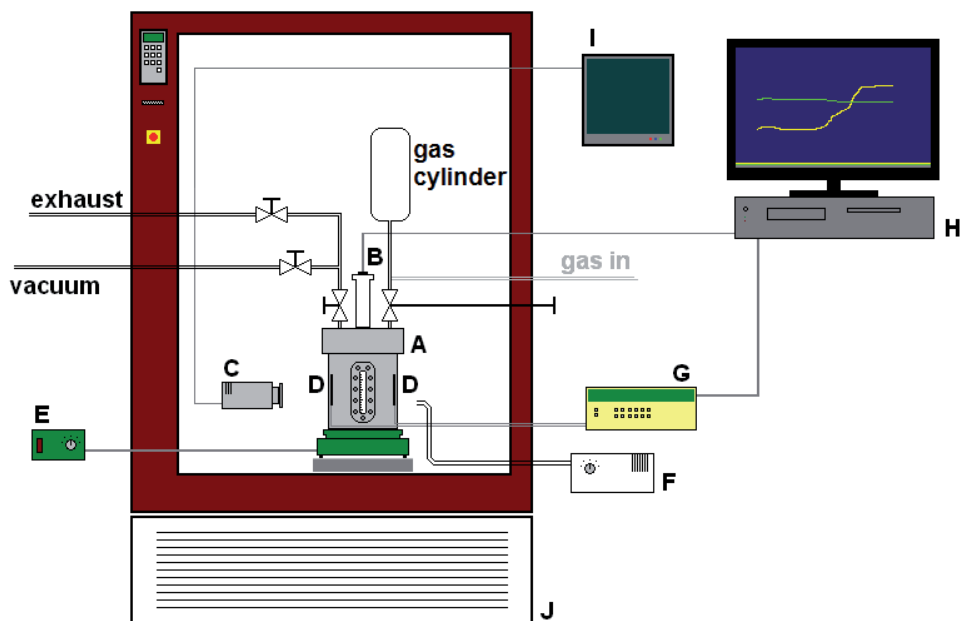


**Figure 5.2 – Schematic representation of the new experimental set-up for the measurement of phase equilibria.** – A: High pressure cell with two parallel sapphire windows. B: Temperature compensated high precision pressure sensor. C: Video camera. D: Platinum resistance thermometers Pt100. E: Remote control for the magnetic stirrer. F: Cold light source with optical fibre. G: Data logger. H: Computer. I: Video monitor. J: Temperature chamber.

The temperature is measured in opposite sides of the cell, by means of platinum resistance thermometers placed inside the walls of the cell and connected to a computer

through a data logger. A temperature compensated pressure sensor is connected to the same computer, used for monitoring and recording of the experimental conditions. The stirring is promoted magnetically, and an independent video system is used to monitor the interior of the equilibrium cell, with the help of a cold light source.

### ***The cell***

The nucleus of this apparatus is the high pressure view cell, originally built by Top Industrie, France, in stainless steel 316Ti, to withstand pressures up to 20 MPa, with an internal volume around 570 cm<sup>3</sup> and equipped with two, 10 mm wide, parallel sapphire windows.

The main problem with the original cell was related with its air tightness, a consequence of the many connections it had on its lid, one of them comprising a rotating part, the axis of the stirrer. The implementation of a synthetic method allows a decrease in the number of necessary connections, since no sampling is required, and the adoption of a magnetic stirring system is another significant modification, acquitting one more connection. With this in mind, a new lid for the cell was designed by the author, with the help of SolidWorks 3D CAD Design Software, containing just three connections, instead of the previous seven, therefore reducing the possibility for leaks. Figure 5.3 shows a picture of the new lid, after being built at the workshop of the department, as well as the old one for comparison.

Another modification in the cell is that one of the sapphire windows is now equipped with a scale, which after calibration, allows the knowledge of the volume occupied by each of the phases, through the observation of the position of the phase interface in the scale, by means of a video camera conveniently placed in front of the sapphire window.

The thickness of the bottom of the cell was also reduced in 8 mm, since its excessive dimensions would have a negative impact in the implementation of the new magnetic stirring system.



**Figure 5.3** – Lid of the cell. – **On the left:** new lid, with three connections in total, two Swagelok ¼” connections and one connection for the pressure sensor. The two additional small holes visible on top are merely for the support of the cell in its structure. **On the right:** old lid, with seven connections.

Concerning the volume of the system, it should be underlined that most of the experiments should be carried out with a gas cylinder containing a precisely known amount of gas connected to cell, in which a precisely known quantity of the other component(s) was previously placed. The total volume available for the system in equilibrium is therefore dependent on the volume of the cylinder, which can go from 150 cm<sup>3</sup>, accounting for a total volume around 820 cm<sup>3</sup>, up to 1000 cm<sup>3</sup>, resulting in a total volume close to 1570 cm<sup>3</sup>. The total volume should always be carefully determined for each cylinder using a reference gas, for instance nitrogen or carbon dioxide. The possibility of adapting the total volume of the system to the type of experiments presents itself as a great advantage, since for example, in the measurement of solubilities, the total volume of the system has a serious influence in the reduction of the relative uncertainty when estimating the volume of the gas phase involved in the equilibrium through the position of the gas-liquid interface. On the other hand, employing a larger gas cylinder, which is necessarily heavier, may impose the use of an analytical balance with a lower sensitivity, therefore limiting the precision with which the amount of gas introduced into the system is known.

Figure 5.4 shows a picture of the cell inside the temperature chamber, connected to a 150 cm<sup>3</sup> detachable gas cylinder. In the picture it is also possible to observe the valve

system, the magnetic stirrer with an elevation system and other parts. The needle valve connected to the gas cylinder is equipped with a safety rupture disc, and its handle can be extended in order to be operated from outside the temperature chamber, through a port on its side wall.



**Figure 5.4** – Image of the high-pressure equilibrium cell together a gas cylinder and other parts, inside the temperature chamber.

### ***Thermostatisation of the cell***

The cell is placed inside a temperature chamber WTB Binder MK 720 (BINDER GmbH, Germany), with an internal volume of 720 dm<sup>3</sup>, for applications in the temperature range from 233 K to 423 K, with a stability of  $\pm 0.5$  K according to preliminary tests. The temperature stability of the cell is of course better than this value, due to its own thermal inertia. According to the preliminary tests, the long time temperature stability of the cell is better than 0.007 K, with short time oscillations of around 0.0015 K.

Due to excessive internal volume of the temperature chamber, when setting a new temperature, a long time is needed for the cell to achieve a stable temperature value. This constitutes one good example of what was mentioned before regarding the room for improvements and the philosophy associated with the development of this apparatus, focusing on the reuse of existing parts, as the temperature chamber used existed previously in our laboratories, and was also re-commissioned.

### ***Temperature and pressure measurements***

The temperature of the cell, measured with a resolution of 0.001 K and a precision of 0.01 K, is monitored through two platinum resistance thermometers Pt100 class 1/10 DIN, with 3 mm of diameter and 40 mm long, supplied by OMEGA Engineering Limited, UK., and calibrated in accordance to the International Temperature Scale ITS-90, at the triple point of water, 273.16 K, through the careful measurement of their electrical resistance at that temperature,  $R_0$ , in the absence of standard thermometry equipment in the laboratory. These thermometers are positioned inside the thick walls of the high pressure cell, in opposite sides of the cell, in two holes made specifically for them. They are connected to a data acquisition system Agilent 34970A (Agilent Technologies, USA), which is in turn connected to a computer via a RS-232 connection, for monitoring and recording of the experimental conditions through the software Agilent BenchLink Data Logger 3 (Agilent Technologies, USA). Two type J (iron–constantan) thermocouples connected to the same data acquisition system are used to follow the temperature in other points inside the temperature chamber, in order to monitor, among other things, the temperature uniformity in space.

The pressure inside the cell is monitored by a temperature compensated pressure transmitter Keller 33X (KELLER AG für Druckmesstechnik, Switzerland), for measurements up to 20 MPa with an accuracy of 0.1% FS (0.02 MPa). This transmitter is similar to the used in the analytical apparatus, previously described. It is connected directly to the computer through a Keller K104B RS-485 to USB adaptor (KELLER AG für Druckmesstechnik, Switzerland), being the data acquisition made by means of the software READ30, supplied by the same manufacturer. Again, the option for an analogical output

was also available from the supplier, but this would imply a compromise in the accuracy of the sensor.

### **Valve configuration**

The configuration of the valve system was again, just like in the first apparatus described, carefully chosen. Thus, the valve represented on the left of the cell, “V1” in Figure 5.5, is a ball valve suitable for low temperatures. This valve has a critical role, like the ball valve used in the first apparatus, allowing the passage of a syringe to charge up the cell with a known amount of liquid, and allowing a small tube to be inserted down to the bottom of the cell when we want to pump out the liquid phases after the experiments. It also avoids the creation of bottlenecks that might influence the quality of the vacuum in the cell while this is being cleaned before a set of experiments.

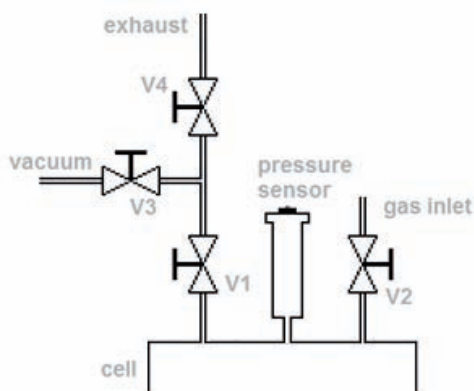


**Figure 5.5** – Schematic representation of the valve configuration and positioning of the pressure sensor on the top of the equilibrium cell.

The connection to the vacuum is also made through a ball valve for the same reasons, while the valve in the exhaust tubing is a needle valve, in order to permit a slow depressurising of the cell. Similarly, the valve on the right side in Figure 5.5 is a needle valve, to permit a slow pressurising of the cell, which has the particularity of being operated from outside the temperature chamber, in order not to disturb the thermal equilibrium inside. This can be extremely useful, as shown later when the experimental

procedure is explained. As mentioned before, when using a gas cylinder instead of a direct gas inlet from a high pressure gas bottle, the needle valve associated with the gas cylinder is also equipped with a safety rupture disc, for protection of the cylinder when filling it from high-pressure bottles, since its use is limited to a maximum pressure of around 12 MPa.

All valves are appropriate for the use at low temperatures, being equipped with polychlorotrifluoroethylene (PCTFE) seats, serviceable between 233 K and 310 K, and pressures up to 41 MPa.

### ***Additional systems***

As mentioned before, the stirring is now promoted magnetically, by means of a simple commercial magnetic stirrer Heidolph MR1000 (Heidolph Instruments GmbH, Germany), with variable speed, up to 2200 rpm, placed under the cell. This stirrer, previously existing in our lab, was adapted so it can now be controlled remotely, from outside the temperature chamber. This was done by simply relocating the controls in a customized box outside the temperature chamber, connected to the stirrer through a 2 meters cable. Although there are commercial versions of magnetic stirrers with remote control available in the market, they are extremely expensive when compared to regular stirrers, showing once more that, what is a small and simple task for a workshop can help reducing significantly the costs of development of an experimental set-up. The shape and size of the magnetic bar inside the cell was carefully chosen after performing various tests with several bars, of different sizes and shapes.

A video camera conveniently placed in front of one of the sapphire windows and connected to a colour video monitor, allows the observation of the interior of the cell, with the aid of an external cold light source Schott KL 200 LED (Schott AG, Germany) connected to a 1 meter long optical fibre.

## **5.4. Testing of the Re-commissioned Cell**

The tests with the re-commissioned equilibrium cell started with the evaluation of different parts under its initial configuration, similar to that described in previous works [1,4,5] and already presented in Figure 5.1. Most of these tests are not relevant as some of the parts involved were immediately abandoned, such as the gas chromatography unit or the thermostatisation system, so the results will not be presented in this work.

### **5.4.1. Measurements with the intermediate configuration**

As mentioned in section 5.2 of the present chapter, some tests were performed in the intermediate stage of the re-commissioning process of the existing equilibrium cell. The first tests dealt with the calibration of the response of the pressure sensor as a function of temperature under atmospheric pressure, in order to quantify the influence of the temperature in the baseline.

The calibration at atmospheric pressure was performed at temperatures between 244 K and 313 K, with the output of the sensor varying from -1.7 barg to 0.5 barg, as shown in Figure 5.6. These values show a strong dependence of the output of the sensor on the temperature of operation. Around room temperature, for example, a change in temperature of 10 K will lead to a variation of the output of the sensor around 0.2 barg to 0.3 barg. It is important to remember that the values yielded by the pressure sensor can only be read with one decimal place, with a precision of 0.1 bar.

After this calibration, measurements on the study of the three-phase coexisting line for the binary system methanol + ethane were performed at temperatures between 253 K and 300 K. As earlier, methanol (CH<sub>3</sub>OH, Methanol for HPLC, Merck KGaA, Germany) with a minimum purity of 99.8% as determined by the supplier using gas chromatography, was used together with ethane (C<sub>2</sub>H<sub>6</sub>), with a purity of 99.95%, supplied by AGA Gas AB, Sweden.

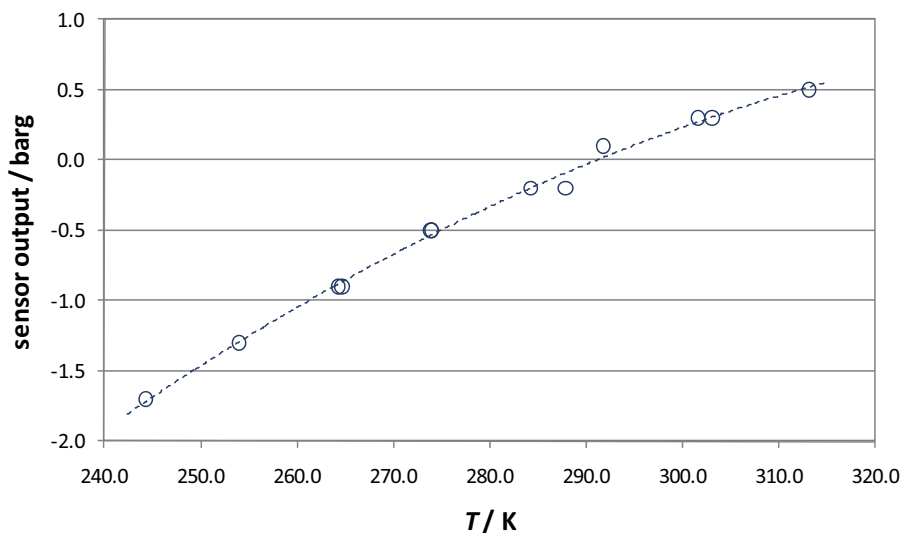


**Figure 5.6** – Output of the pressure sensor at atmospheric pressure, as a function of its temperature of operation. The dashed line is represented merely for eye guidance.

The values obtained from the pressure sensor for each temperature were corrected using the results of the calibration performed, by means of the values presented in Figure 5.6, in the (not proven) assumption that deviations verified in the measurements under atmospheric pressure would be exclusively dependent on the temperature, and not influenced by the pressure in the system. Table 5.1 presents the results of these measurements, including the corrected values of pressure, as well as the original values read in the display of the sensor.

**Table 5.1** – Results obtained during the study of the three-phase coexisting line for the binary system methanol + ethane, using the re-commissioned cell.

$T / \text{K}$	$p / \text{barg}$	$p_{\text{corrected}} / \text{MPa}$
252.95	11.2	1.35
263.75	16.7	1.86
273.35	22.1	2.36
283.65	28.7	2.99
298.45	40.3	4.12
299.85	41.6	4.25

These corrected results were compared with the literature values already mentioned in Chapter 4 of this work [17-22]. Figure 5.7 shows the deviations of the obtained results relatively to Equation 4.3, result of the fitting of the equation of Clarke and Glew to all the data sets available. The deviations of the results obtained with the new analytical cell described in Chapter 4, are also presented in the graph.

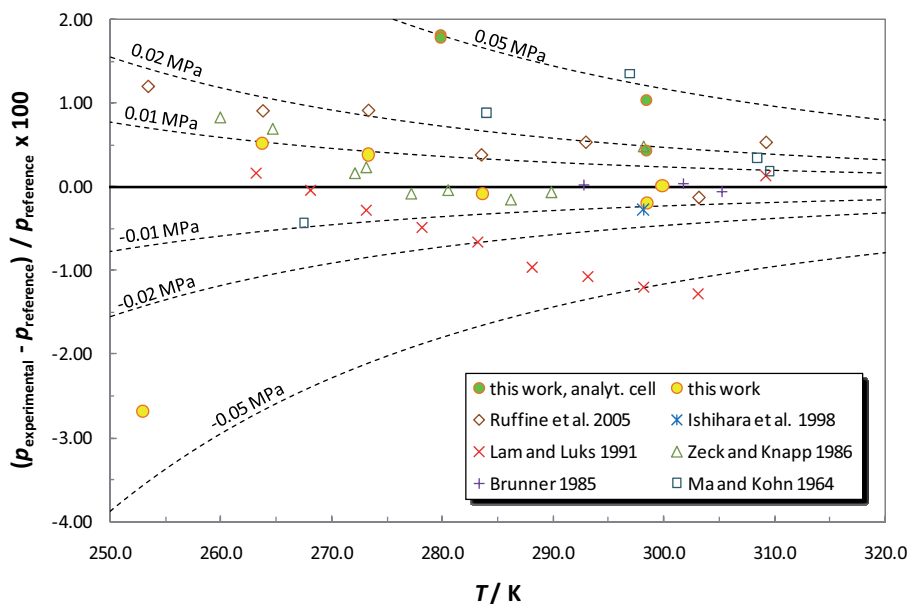


**Figure 5.7** – Deviations from the experimental results obtained in this work and from the literature values [17-22] to Equation 4.3, in the study of the three-phase coexisting line for the binary system methanol + ethane.

Except for the data point at to the lowest temperature, 253 K, the results are in close agreement with the literature exhibiting a surprisingly good accuracy, especially taking into account that the corrections to the pressure values have been based merely on an assumption. And here resides the main problem concerning the confidence on these results. The error associated to the data point at the lowest temperature studied raises some doubts as to the legitimacy of the corrections. Further measurements of different systems would be necessary, preferably at different pressure ranges in order to ascertain any influence of the pressure in the deviations caused by the temperature of operation of the sensor.

But as mentioned in the last chapter, several problems related to the air tightness of the equilibrium cell prevented the completion of more tests using this configuration, and additional modifications were made in the apparatus, including its modernisation. With this process, the pressure sensor used in these measurements was excluded as it still required taking note of the pressure values by hand, and with limited precision.

### **5.4.2. Preliminary Tests**

As discussed for the first apparatus described, following the conclusion of the assembling of the apparatus, it is necessary to perform a series of tests, for evaluation of the quality of its measurements. As earlier, the initial tests should focus on the electronic aspects of the apparatus.

This first sequence of tests did not reveal the existence of any problems, concerning the cables used, some of them prepared in our labs, or possible interferences from the electrical supply to the instruments. Pressure and temperature values were collected for extended periods of time, at different frequencies, showing neither evidence of excessive noise nor the existence of periodical interferences. The short time stability of pressure readings, at atmospheric pressure, revealed to be better than  $\pm 0.2$  kPa (0.002 bar) with a long time stability of  $\pm 0.25$  kPa. As for the temperature, the platinum resistance thermometers provided readings in which the stability was around  $\pm 0.002$  K.

After these tests, the temperature compensation of the pressure sensor was examined, by recording the deviation of the values yielded by the transmitter under atmospheric pressure for different temperatures of operation of the transmitter. In a temperature range between 233 K and 313 K, the total deviation in the pressure values was less than 15 kPa (0.15 bar), a value under the accuracy limit of  $\pm 20$  kPa, characteristic of the transmitter tested.

A number of measurements performed along the vapour-liquid equilibrium line of pure carbon dioxide confirmed the stability of the pressure and temperature obtained in the first tests, carried out without the equilibrium cell.

In Figure 5.8, it is possible to observe a response in the pressure values of even the slightest oscillations in the temperature values, an indication of an optimal thermal contact between the platinum resistance thermometers and the system in equilibrium in the interior of the cell, and of good response times of the pressure and temperature sensors.

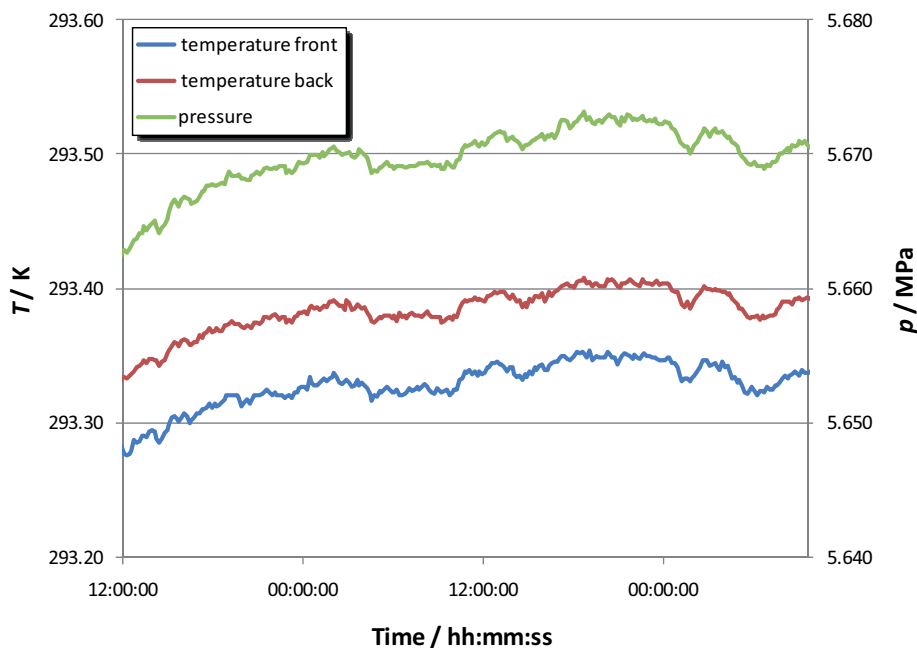


**Figure 5.8** – Reflexion in the pressure values of small oscillations in the temperature of the cell, showing a good thermal contact between the cell and the platinum resistance thermometers. The values were obtained during a series of tests performed along the vapour-liquid equilibrium line of carbon dioxide.

Also noticeable in the figure is the difference between the temperature values measured by the two platinum resistance thermometers, with the temperature measured in front of the cell being 0.06 K lower on average than the temperature registered on the back of the cell. This small difference is within the precision of the thermometers, and since the two thermometers were calibrated simultaneously, it is expected that the differences in the values are due to real differences in the temperature of the two sides of the cell, possibly resulting from the convection pattern of the air inside the temperature chamber. When performing measurements, the average of the values yielded by the two platinum resistance

thermometers should be considered, as shown below, with the analysis of the results obtained in the study of some reference systems.

During these tests, it was verified that a long time is required for the cell to achieve a stable temperature, after a new temperature has been set. This is most likely due to the substantial internal volume of the temperature chamber (720 dm<sup>3</sup>), and the localisation of the temperature sensor associated with the controller of the chamber, far from the equilibrium cell, causing it to monitor a stable temperature inside the temperature chamber, different from the actual temperature of the cell.

It was also noticed during the preliminary tests with carbon dioxide, that the stirring system has an effect on the temperature of the cell, causing it to increase by approximately one degree, regardless of the speed of the stirring. This influence in the temperature may or may not be critical to the phase equilibria results, depending on the method being used. When working only with the volume of the cell, the convection promoted by the stirring should provide a uniform temperature in the whole cell. However, when using a gas cylinder connected to the cell, some problems may arise, due to the bottle neck between the two volumes, leading to the existence of different temperatures for the two parts of the gas phase, in the cylinder and in the cell.

### **5.4.3. Measurement of Reference Systems**

After the preliminary tests, the validation of the apparatus proceeded with the study of reference systems, in order to confirm simultaneously the quality of the temperature and pressure measurements. As before, special attention is given to the influence of the temperature in the values yielded by the pressure transmitter, even though the transmitters used in this project are delivered with the certificate of the calibration made in the factory.

#### ***Ethane***

During air tightness tests, after substitution of the seals in the cell, a single measurement was performed in the vapour-liquid equilibrium line of ethane. This gas was used with a purity of 99.95%, as supplied by AGA Gas AB, Sweden.

For a temperature of 298.39 K, the vapour-liquid equilibrium pressure was found to be 4.218 MPa, a value 0.2% higher than the reference value given by the DIPPR database [23], according Equation 4.5.

### **Carbon dioxide**

Experiments along the vapour-liquid equilibrium line of pure carbon dioxide were performed in a temperature interval between 258 K and 299 K. As in the tests performed with the first apparatus described, carbon dioxide with a purity of 99.995% produced by Linde AG, Germany, and supplied by AGA A/S, Denmark, was used in the experiments. The results are presented in Table 5.2 and in Figure 5.9, where reference values from the DIPPR database [23], defined by Equation 4.4, are also represented.

**Table 5.2** – Experimental results obtained in the study of the vapour-liquid equilibrium line for carbon dioxide, using the re-commissioned cell. The first column in the table refers to the order of the measurements.

n.	$T / \text{K}$	$p / \text{MPa}$	n.	$T / \text{K}$	$p / \text{MPa}$
15	258.15	2.294	6	283.46	4.546
16	258.17	2.295	2	293.35	5.770
9	265.31	2.819	1	293.36	5.772
10	265.37	2.824	17	297.09	6.294
13	268.48	3.077	4	298.16	6.449
14	268.60	3.088	3	298.18	6.452
7	273.35	3.509	12	299.09	6.588
8	273.38	3.512	11	299.12	6.593
5	283.42	4.542			

The deviations of the obtained results from the reference values, are given in Figure 5.10, where the graph denotes an almost linear increase of the deviations from literature with the decrease of the temperature, up to a maximum of 0.8% verified for 258 K. This value, however, corresponds to an absolute deviation of 0.018 MPa, a value inside the accuracy limit of the transmitter used (0.02 MPa). In any case, it should be considered that the error associated with Equation 4.4, here taken as reference, is 1%.

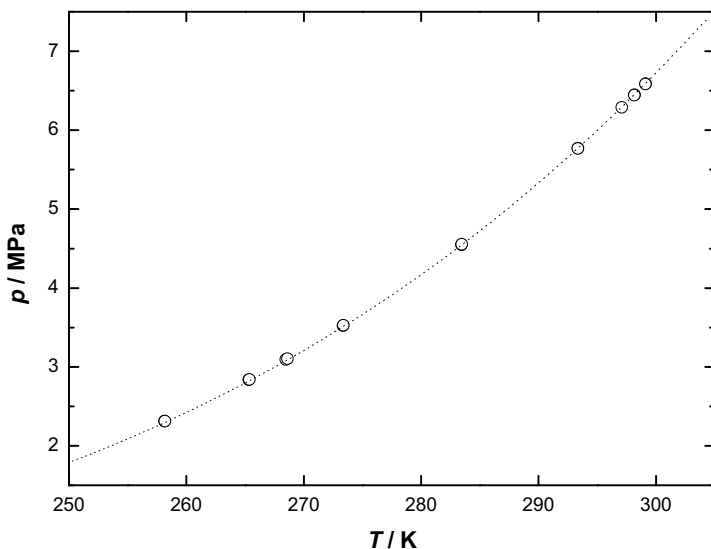


**Figure 5.9** – Results obtained in the study of the vapour-liquid equilibrium line for carbon dioxide. The dotted line refers to the reference values recommended by the DIPPR database [23].

At the moment, the plans for the use of this apparatus are restricted to temperatures between 273 K and 313 K. In this range of temperatures, the deviations of the results are under 0.5%. Should this cell be used at lower temperatures in the future, further measurements with a reference system are recommended.

Relative to the possible non-uniformity of the temperature in the cell, discussed in the analysis of the graph in Figure 5.8, in which a difference between the temperature registered by the two thermometers positioned in different sides of the cell was observed, it should be pointed out that no influence of such problem is noticeable on the obtained results. It should be mentioned that the temperature values presented in Table 5.2 are obviously the average of the values yielded by the two platinum resistance thermometers, in a similar manner to what is done for the first cell described.

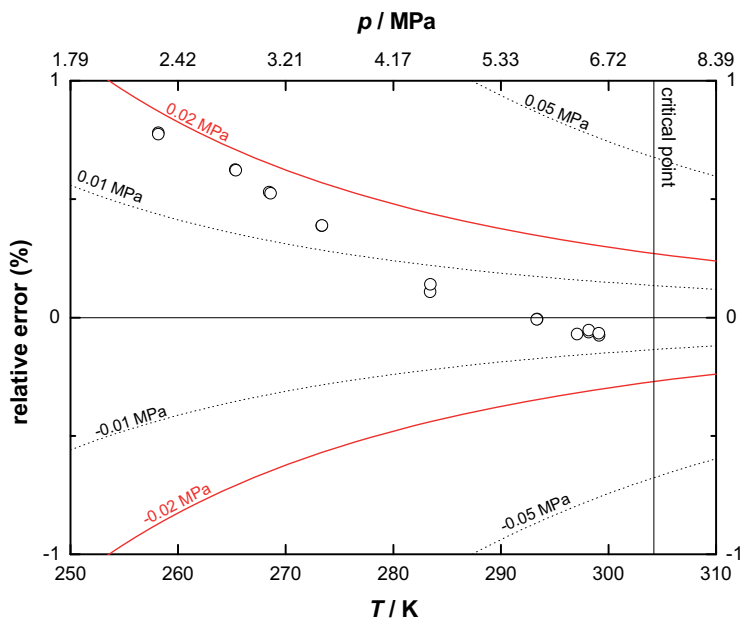


**Figure 5.10** – Relative and absolute deviations from the results obtained in this work for the vapour-liquid equilibrium line for carbon dioxide, to the reference values recommended by the DIPPR database [23] and defined by Equation 4.4.

#### 5.4.4. Validation of Experimental Methods

As described in the third chapter of this work, there is a variety of synthetic methods that, in principle, can be applied with this apparatus. However, in practice, the characteristics of the set-up and in particular of the equilibrium cell may impose some limitations in the practicability of some of the experimental procedures. Some of the methods are also dependent on further calibrations.

After confirming the quality of the pressure and the temperature measurements, essential parameters to any phase equilibria study, tests were performed in order to assess the applicability of this apparatus to some types of measurements.

## ***Formation of gas hydrates***

The equilibrium conditions for the formation of gas hydrates can be determined by means of a very simple synthetic method, based on the slopes of  $pT$  curves [24-27], according to a procedure previously explained on Chapter 3. The suitability of this apparatus to the application of this method was tested by performing a set of experiments on the well defined binary system methane + water.

The cell was initially charged with a volume of approximately 150 cm<sup>3</sup> of deionised water, which was subsequently degassed under controlled vacuum, before pressurising the cell with pure methane (CH<sub>4</sub>, purity of 99.9995%, supplied by AGA Gas AB, Sweden and prepared by Linde Gas UK Ltd, UK) up to a pressure close to 9 MPa. The first step of the experiment was to set the system to a temperature 5 K lower than the known equilibrium conditions for the formation of hydrates, in order to afterwards, promote the increase of the temperature by small steps. During the cooling of the cell, its contents were observed through the monitor connected to the video camera, and the formation of the first hydrate crystals was noticed around the expected temperature and pressure conditions, taking into consideration the sub-cooling always associated with a fast cooling of the system. The starting point of formation of hydrates is also noticeable in the pressure and temperature profiles of the experiment, presented in Figure 5.11. After three hours and a half of experiment, a severe change in the pressure decrease is observable, also accompanied by a change in the cooling rates, especially noticeable in the temperature of the pressure transmitter, represented in the graph of the figure as “temperature Keller”. This occurred at a pressure of 7.875 MPa and a temperature of 278.52 K.

Also visible in the graph, is the fact that after seventy hours of experiment the pressure of the system was still decreasing, revealing that the equilibrium conditions had not yet been achieved. The variation in the pressure during the last hour of experiment was very small, only 2.4 kPa, demonstrating that the system was very close to the equilibrium. However, this was only the first step of the experiment, a succession of equilibrium stages would be necessary to collect an experimental point for the hydrate forming conditions. The conclusion is that it is not feasible to carry out this type of measurements in this apparatus.

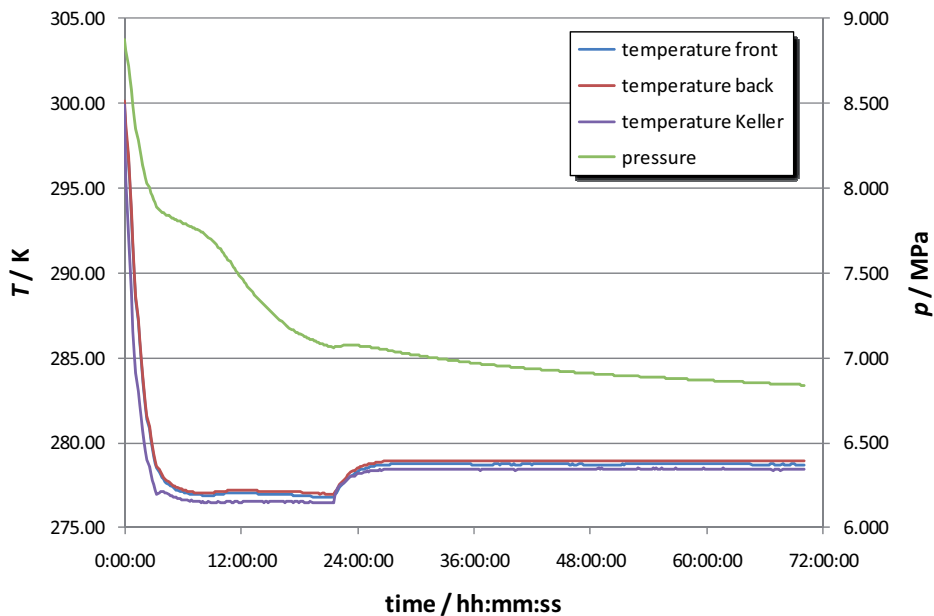


**Figure 5.11** – Pressure and temperature profiles registered during the cooling process for the promotion of methane hydrates in the system methane + water.

The observation of the interior of the cell during the experiment helps to understand the reasons for such a slow equilibrium. Once the hydrates start forming, their crystals accumulate at the surface of the liquid phase, due to the lower density. After some time, when the hydrate crystals reach a thickness of around two centimetres, the stirring loses its effectiveness, in the sense that although the liquid phase is being stirred, there is no contact between this phase and the gas phase, and the formation of more hydrate becomes dependent on the diffusion of the methane gas through the hydrate phase, in order to reach the aqueous phase where the new crystals are formed.

One of the conclusions to withdraw from these observations is that in the study of hydrate formation, a simple magnetic stirring system is not adequate to promote an effective mixing of the different phases for the fast achievement of equilibrium. Better options would be rocking the cell, recirculation of the gas phase through the liquid phase, or eventually, stirring through a more complex system of blades inside the cell. The use of a cell with a considerably smaller volume would also be an advantage.

### ***Solubility of gas in a non-volatile condensed phase***

As mention in Chapter 3, a very common method to determine the solubility of a gas in a condensed phase, such as a polymer [28,29], an ionic liquid [30-45], an oil [46] or an aqueous solution [47], consists in adding to an equilibrium cell, containing a determined amount of the condensed phase and previously evacuated, a precisely known amount of gas. After the establishment of the equilibrium in the cell, the pressure of the system can then be used to calculate the solubility of the gas, as described before.

In the experimental procedure adopted, a known amount of the condensed phase is initially placed inside the cell, and the level of the liquid in the scale in the window of the cell is registered. A gas cylinder is first placed under vacuum and weighed, then charged with gas and weighed once more, for the exact determination of the mass of gas inside. After attaching the gas cylinder to the cell, the condensed phase is degassed in a succession of short periods under controlled vacuum. Once the temperature of the cell is stable, the valve separating the gas from the cell is opened and the peak value of the pressure noted down. The system is then left to equilibrate, first with stirring in order to accelerate the process, and then letting the system rest. Once a stable value of pressure has been reached, the level of the liquid phase is registered and used to infer the volume of the gas phase, knowing the total volume of the system (cell + cylinder), previously calibrated. Through the gas density values derived from a reference equation of state or correlation, the amount of gas in the gas phase is determined, and by difference, the amount of gas in the liquid phase, at the pressure and temperature of the equilibrium.

The first step for the implementation of this method was the calibration of the total volume of the system, cell plus gas cylinder. This was made following a procedure similar to the one just described, but without the condensed phase in the cell. The gas cylinder is charged with a precisely known amount of gas, and subsequently connected to the evacuated equilibrium cell. Once the temperature and pressure of the system are stable, the volume of the system is calculated through the density of the gas at the equilibrium pressure and temperature, given by a reference equation of state.

In the present case, methane was used in the calibration, and the values for the gas density at equilibrium conditions were obtained from NIST Standard Reference Data, Thermophysical Properties of Fluid Systems [48]. Six measurements were performed, at

pressures varying from 0.9 to 2.1 MPa, using a gas cylinder of 150 cm<sup>3</sup>. The calibration resulted in a value of (742 ± 1) cm<sup>3</sup> for the total volume of the cell and the gas cylinder.

The next preliminary step was to calibrate the scale in the window of the cell, since it is through it that the volume of both liquid and gas phases is calculated at the equilibrium conditions. The calibration was performed with the help of a burette, using pure water at a temperature of 298 K. The results, presented in the graph of Figure 5.12, are characterised by a great linearity, as expected considering the shape of the cell. The first two points registered, marked in red in the graph, deviate from linearity due to the round shape of the window at its lower extreme.

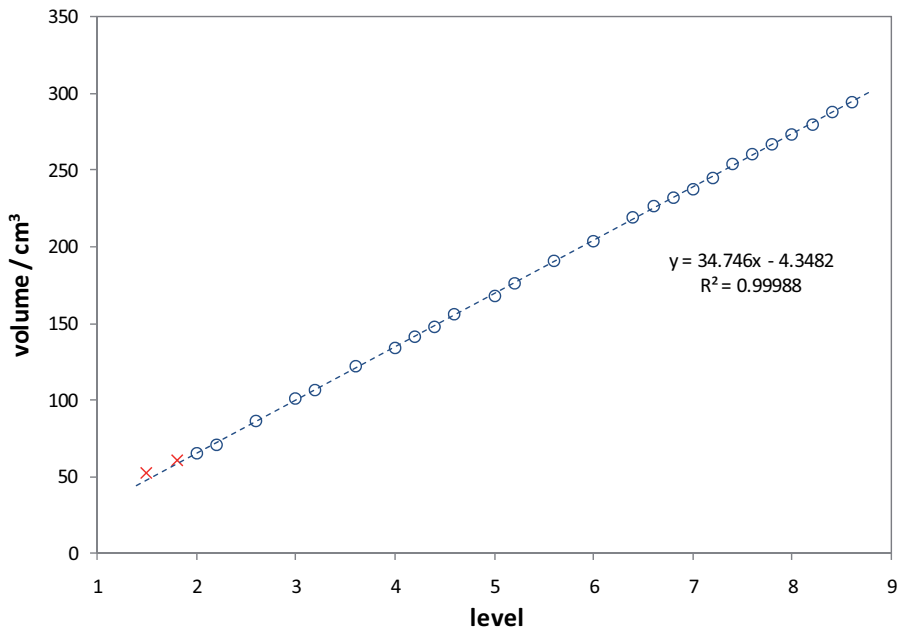


**Figure 5.12** – Results obtained during the calibration of the scale in the window of the equilibrium cell.

The volume of liquid phase, inside the linearity range, can then be calculated from the level readings through Equation 5.1, with an associated uncertainty of ± 0.46 cm<sup>3</sup>.

$$V / \text{cm}^3 = (34.746 \pm 0.076) \cdot l - (4.35 \pm 0.45) \quad (5.1)$$

After the calibration, the experimental method was finally implemented, in the measurement of the solubility of methane in water.

### ***Binary system water + methane***

Several experimental conditions may have a significant influence in the precision of the results obtained by this method. The volume of the gas phase is determined by the level of liquid phase through the position of the interface in the scale. A larger volume of the gas phase in equilibrium translates into a smaller relative error in its determination. It should therefore be favourable to use a lower quantity of condensed phase in the cell. On the other hand, the volume of the condensed phase should be enough to allow the minimisation of possible errors that may arise from mass losses associated to its degassing process, prior to the addition of the gas to the cell. In addition, the amount of solubilised gas is directly dependent on the amount of condensed phase, and in cases of low solubility of the gas, it is necessary to ensure that the amount of dissolved gas is enough to be determined with sufficient precision.

The precision with which the total mass of gas used in the experiment is known is obviously dependent on the amount of gas charged into the cylinder. A higher amount of gas means a higher charging pressure, which in some cases can imply a high complexity of the charging process, or of a higher volume of the cylinder, consequently heavier and probably requiring the use of a less precise balance in the determination of the mass of gas.

Adding to these aspects, the influence of the pressure on the density of the gas phase for a particular temperature is not constant, and therefore the error involved in the determination of the mass of gas in the equilibrium gaseous phase is lower for values of pressure where its influence on the density is smaller.

In conclusion, the analysis of the uncertainty associated with the solubility measurements is far from straightforward, depending on various aspects, some of them influencing more than one source of errors. Therefore, in order to evaluate the influence of different experimental conditions in the precision of the results obtained by this method, a number of experiments were performed, using deionised water and methane with a purity of 99.9995%, supplied by AGA Gas AB, Sweden, and prepared by Linde Gas UK Ltd,

UK, under different experimental conditions. The amount of methane charged into the cylinder was determined gravimetrically, according to the experimental procedure described above, using an analytical balance Mettler-Toledo PR1203 with a precision of 0.001 g.

The experiments were separated in two series. In the first series, the already discussed experimental conditions were chosen according to which was thought to be the optimal conditions. Six measurements were performed using a low amount of water, between 90 and 100 cm<sup>3</sup>, at temperatures close to 298.2 K and pressures between 1.0 and 2.1 MPa. The results are presented in Table 5.3, and in the graph of Figure 5.13, where values from five different literature sources are also presented [49-53]. In the plot, the dashed line is based on the literature values, and given merely for eye guidance.

**Table 5.3** – Results obtained in the first series of measurements of the solubility of methane in pure water, at 298 K.

$T / \text{K}$	$p / \text{MPa}$	$x_{\text{methane}} \times 10^3$
298.14	1.03	0.245
298.20	1.03	0.249
298.32	1.03	0.248
298.15	1.03	0.252
298.12	2.12	0.513
298.30	2.11	0.514

The results show a very good internal consistency, and are in excellent agreement with the values presented by Wang et al. [51], and with the values of Chapoy et al. [53], obtained by means of an analytical method. This agreement corroborates the applicability of this particular experimental method for this type of measurement. No corrections were made for the vapour pressure of water, which was considered negligible at the temperature of the experiments, when compared with the experimental equilibrium pressures.

Among the literature sources used for comparison, the deviation of the data obtained by Yang et al. [52] is noteworthy, when compared to the values presented by other authors.

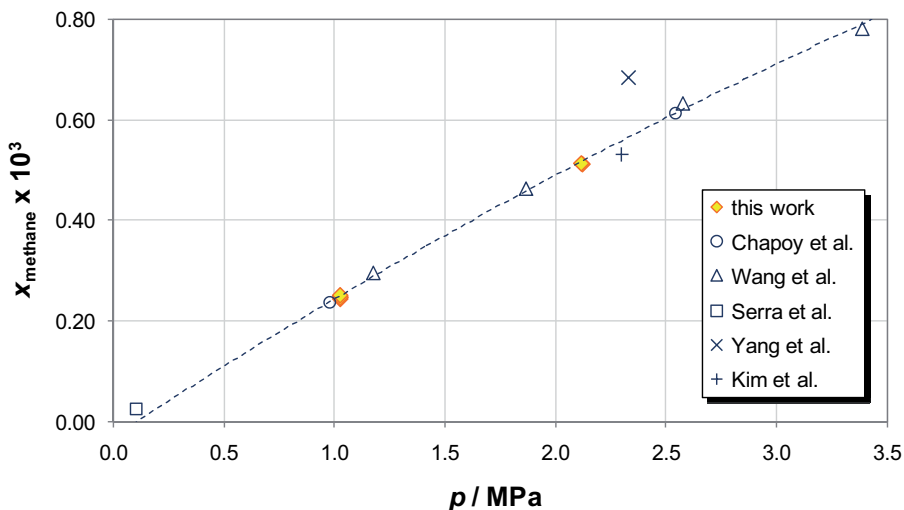


**Figure 5.13** – Results obtained in the first series of measurements of the solubility of methane in pure water, at 298 K, and comparison with values found in the literature [49-53]. The line in the graph is based on the literature data and it is given merely for eye guidance.

On the second series of measurements, the aforementioned experimental parameters were altered, in order to evaluate the respective influence in the quality of the results. The influence of the stirring during equilibrium was also established. For such a binary system, the stirring should have no effect on the equilibrium itself, however, as mentioned already, preliminary tests showed an influence of the stirring on the temperature of the cell, leading to an increase of approximately one degree. Although the temperature of the components inside the cell should be uniform, precisely due to the stirring, it is possible that the limited convection between the internal volume of the cell and the internal volume of the cylinder, caused by the presence of a needle valve, leads to a temperature gradient, with the temperature of the gas inside the cylinder being slightly lower than for the gas inside the equilibrium cell.

A number of measurements were performed at temperatures around 298.2 K and 283.3 K, with pressures ranging from 0.3 MPa to 2.1 MPa. The volume of condensed phase (water) used in all the experiments was around 214 cm<sup>3</sup>, with the exception of one experiment in which a volume of 222 cm<sup>3</sup> was used. The results obtained are given in Table 5.4, and presented in Figure 5.14, where values from several data sets found in the literature for the two temperatures studied are also provided [49-54].

**Table 5.4** – Results obtained in the second series of measurements of the solubility of methane in pure water, at 298 K and at 283 K.

$T / \text{K}$	$p / \text{MPa}$	$x_{\text{methane}} \times 10^3$
298.17	1.17	0.289
299.63	2.05	0.482
298.21	0.32	0.068
298.22	0.32	0.069
298.13	1.78	0.445
298.30	0.62	0.202
298.33	0.50	0.164
298.18	0.89	0.207
283.26	0.48	0.135
283.28	0.48	0.134
283.26	0.84	0.271
283.26	0.84	0.244

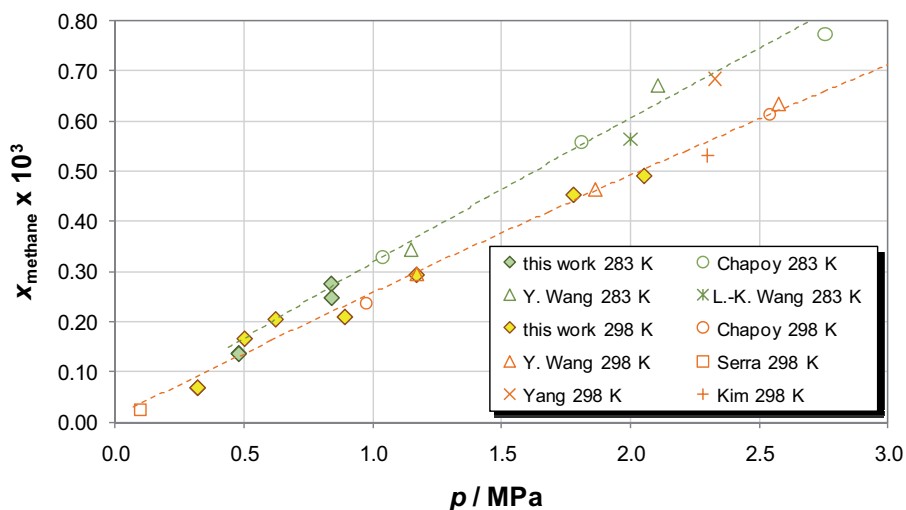


**Figure 5.14** – Results obtained in the second series of measurements of the solubility of methane in pure water, at 283 K and 298 K, and comparison with values found in the literature [49-54]. The lines are based on the literature data and are given merely for eye guidance.

The consistency of the results is not at the same level as that observed in the first series of results, something that was expected due to the experimental conditions chosen. For the majority of the points, the deviations to the lines presented in the graph, that although given for eye guidance, are based on the literature sets that appear more reliable [50,51,53], are under  $2 \times 10^{-5}$  for the mole fraction of methane in the liquid phase. Furthermore, it should be mentioned that some of the results in this work were obtained at a temperature somewhat different than the 298.15 K from the literature, such as the case of the experimental point at the highest pressure, which is for a temperature of 299.6 K, and therefore expected to be somewhat lower than the reference.

An important consideration to make is that no systematic error is observed in the results. The higher scattering relative to the first series of results obtained, is associated with an increase in the uncertainty of the experiments, most probably related to the relative errors in the calculations of the volume of the gas phase, something that was in fact predicted.

The influence of the stirring was verified to be very small, or insignificant within the precision of the results. This can be easily understood under the consideration that the equilibrium process is defined by the temperature inside the cell, which is necessarily uniform due to the stirring. The aforementioned possibility that the gas inside the cylinder might be at a slightly lower temperature, would only influence the calculations of the amount of gas in the gas phase, due to an error arising from the different density of the fraction of gas in the cylinder. The variation of the density of methane with the temperature is however very small, around 0.3% /K at 0.2 MPa, and up to 0.4% /K at 2 MPa, for temperatures around 298 K.

As a conclusion, the tests performed confirmed the applicability of the experimental method in question to the quantification of the solubility of a gas in a condensed phase, by showing that it is possible to achieve very good results, provided that the choice of the experimental conditions is the most appropriate, and also by yielding some information on what these conditions are.

It was stated in Chapter 3, when the synthetic methods were presented, that the application of these methods presents unequivocal advantages in simpler studies. It should be understood that the use of such simple apparatus in experiments regarding obtaining

more complex results, such as the characterisation of phases in equilibrium, relies necessarily on assumptions and approximations which will undoubtedly contribute to an increase in the uncertainty of the results. It is up to the experimentalist then, to perform an adequate selection of the experimental conditions, as well as of the experimental procedure, by means of minimising these sources of errors. Besides a careful analysis of the apparatus and the method, this often involves some preliminary experiments using reference systems.

The role of the experimentalist in these steps is a good example of the importance of the know-how mentioned in Chapter 1, which can provide the necessary sensitivity for some experimental aspects, and that can only be acquired by experience.

## **5.5. Conclusions**

In the current chapter, a second experimental apparatus is described, developed using decommissioned material previously existing in the laboratory. Contrary to the apparatus described in the previous chapter, relatively complex and specially planned and developed for a particular project, the set-up presented in this chapter is much simpler, making use of a synthetic method, and developed at an extremely low price. As in Chapter 4, a complete description of the apparatus is made, and the results obtained in the study of reference systems presented, verifying the applicability of the apparatus in different types of studies, and confirming the high quality of the equipment developed, provided that a correct and careful operation is assured, with special attention to possible sources of errors

## **References**

- [1] T. Laursen, P. Rasmussen, S. I. Andersen, *J. Chem. Eng. Data* 47 (2002) 198-202.
- [2] T. Laursen, S. I. Andersen, *J. Chem. Eng. Data* 47 (2002) 1173-1174.
- [3] T. Laursen, S. I. Andersen, *J. Chem. Eng. Data* 48 (2003) 1085-1087.
- [4] Torben Laursen, Ph.D. Thesis, Technical University of Denmark, Department of Chemical Engineering, Kgs. Lyngby, Denmark, 2002.

- [5] Julien Sautédé, Internal presentation, Technical University of Denmark, Department of Chemical Engineering, 10 Oct. 2003.
- [6] A. Jonasson, O. Persson, A. Fredenslund, J. Chem. Eng. Data 40 (1995) 296-300.
- [7] A. Jonasson, O. Persson, P. Rasmussen, J. Chem. Eng. Data 40 (1995) 1209-1210.
- [8] M. Teodorescu, P. Rasmussen, J. Chem. Eng. Data 46 (2001) 640-646.
- [9] R. Dohrn, S. Peper, J. M. S. Fonseca, Fluid Phase Equilib. 288 (2010) 1-54.
- [10] C. Secuianu, V. Feroiu, D. Geana, J. Chem. Eng. Data 48 (2003) 1384-1386.
- [11] E. Brunner, W. Hultenschmidt, G. Schlichtharle, J. Chem. Thermodyn. 19 (1987) 273-291.
- [12] C. J. Chang, C. Y. Day, C. M. Ko, K. L. Chiu, Fluid Phase Equilib. 131 (1997) 243-258.
- [13] T. Katayama, K. Ohgaki, G. Maekawa, M. Goto, T. Nagano, J. Chem. Eng. Jpn. 8 (1975) 89-92.
- [14] K. Ohgaki, T. Katayama, J. Chem. Eng. Data 21 (1976) 53-55.
- [15] C. Y. Tsang, W. B. Streett, J. Chem. Eng. Data 26 (1981) 155-159.
- [16] J. M. S. Fonseca, S. Peper, R. Dohrn, Fluid Phase Equilib., *In press*
- [17] K. Ishihara, H. Tanaka, M. Kato, Fluid Phase Equilib. 144 (1998) 131-136.
- [18] D. H. Lam, K. D. Luks, J. Chem. Eng. Data 36 (1991) 307-311.
- [19] Y. H. Ma, J. P. Kohn, J. Chem. Eng. Data 9 (1964) 3-5.
- [20] L. Ruffine, A. Barreau, I. Brunella, P. Mougin, J. Jose, Ind. Eng. Chem. Res. 44 (2005) 8387-8392.
- [21] S. Zeck, H. Knapp, Fluid Phase Equilib. 25 (1986) 303-322.
- [22] E. Brunner, J. Chem. Thermodyn. 17 (1985) 871-885.

- [23] DIADEM Professional, DIPPR Interface and Data Evaluation Manager, version 3.0.0, 2000, using DIPPR Design Institute for Physical Property Data Database 2009.
- [24] R. Ohmura, S. Matsuda, S. Takeya, T. Ebinuma, H. Narita, *Int. J. Thermophys.* 26 (2005) 1515-1523.
- [25] N. Gnanendran, R. Amin, *Fluid Phase Equilib.* 221 (2004) 175-187.
- [26] R. Masoudi, B. Tohidi, R. Anderson, R. W. Burgass, J. Yang, *Fluid Phase Equilib.* 219 (2004) 157-163.
- [27] A. H. Mohammadi, W. Afzal, D. Richon, *J. Chem. Thermodyn.* 40 (2008) 1693-1697.
- [28] O. Pfohl, C. Riebesell, R. Dohrn, *Fluid Phase Equilib.* 202 (2002) 289-306.
- [29] Y. Sato, T. Takikawa, M. Yamane, S. Takishima, H. Masuoka, *Fluid Phase Equilib.* 194-197 (2002) 847-858.
- [30] X. Yuan, S. Zhang, Y. Chen, X. Lu, W. Dai, R. Mori, *J. Chem. Eng. Data* 51 (2006) 645-647.
- [31] S. Zhang, X. Yuan, Y. Chen, X. Zhang, *J. Chem. Eng. Data* 50 (2005) 1582-1585.
- [32] L. A. Blanchard, Z. Gu, J. F. Brennecke, *J. Phys. Chem. B* 105 (2001) 2437-2444.
- [33] X. Yuan, S. Zhang, J. Liu, X. Lu, *Fluid Phase Equilib.* 257 (2007) 195-200.
- [34] J. Kumelan, Á. P.-S. Kamps, I. Urukova, D. Tuma, G. Maurer, *J. Chem. Thermodyn.* 37 (2005) 595-602.
- [35] J. Kumelan, Á. P.-S. Kamps, D. Tuma, G. Maurer, *Fluid Phase Equilib.* 228-229 (2005) 207-211.
- [36] J. Kumelan, Á. P.-S. Kamps, D. Tuma, G. Maurer, *J. Chem. Eng. Data* 51 (2006) 11-14.
- [37] J. Kumelan, D. Tuma, G. Maurer, *J. Chem. Eng. Data* 51 (2006) 1802-1807.

- [38] J. Kumelan, Á. P.-S. Kamps, D. Tuma, G. Maurer, *J. Chem. Eng. Data* 51 (2006) 1364-1367.
- [39] J. Kumelan, Á. P.-S. Kamps, D. Tuma, G. Maurer, *J. Chem. Thermodyn.* 38 (2006) 1396-1401.
- [40] J. Kumelan, Pérez-Salado Kamps, I. Urukova, D. Tuma, G. Maurer, *J. Chem. Thermodyn.* 39 (2007) 335.
- [41] J. Kumelan, Á. P.-S. Kamps, D. Tuma, G. Maurer, *Fluid Phase Equilib.* 260 (2007) 3-8.
- [42] J. Kumelan, Á. P.-S. Kamps, D. Tuma, G. Maurer, *Ind. Eng. Chem. Res.* 46 (2007) 8236-8240.
- [43] J. Kumelan, Á. P.-S. Kamps, D. Tuma, G. Maurer, *J. Chem. Eng. Data* 52 (2007) 2319-2324.
- [44] J. Kumelan, Á. P.-S. Kamps, D. Tuma, A. Yokozeki, M. B. Shiflett, G. Maurer, *J. Phys. Chem. B* 112 (2008) 3040-3047.
- [45] S. Zhang, Y. Chen, R. X. F. Ren, Y. Zhang, J. Zhang, X. Zhang, *J. Chem. Eng. Data* 50 (2005) 230-233.
- [46] S. Bobbo, L. Fedele, M. Scattolini, R. Camporese, R. Stryjek, *Fluid Phase Equilib.* 256 (2007) 81-85.
- [47] J. Kiepe, S. Horstmann, K. Fischer, J. Gmehling, *Ind. Eng. Chem. Res.* 41 (2002) 4393-4398.
- [48] E.W. Lemmon, M.O. McLinden, D.G. Friend, *Thermophysical Properties of Fluid Systems in: P.J.Linstrom, W.G.Mallard (Eds.), NIST Chemistry WebBook, NIST Standard Reference Database Number 69, National Institute of Standards and Technology, Gaithersburg MD, 20899, <http://webbook.nist.gov>, 2009.*
- [49] Y. S. Kim, S. K. Ryu, S. O. Yang, C. S. Lee, *Ind. Eng. Chem. Res.* 42 (2003) 2409-2414.

- [50] M. C. Serra, F. L. P. Pessoa, A. M. F. Palavra, *J. Chem. Thermodyn.* 38 (2006) 1629-1633.
- [51] Y. Wang, B. Han, H. Yan, R. Liu, *Thermochim. Acta* 253 (1995) 327-334.
- [52] S. O. Yang, S. H. Cho, H. Lee, C. S. Lee, *Fluid Phase Equilib.* 185 (2001) 53-63.
- [53] A. Chapoy, A. H. Mohammadi, D. Richon, B. Tohidi, *Fluid Phase Equilib.* 220 (2004) 111-119.
- [54] L. K. Wang, G. J. Chen, G. H. Han, X. Q. Guo, T. M. Guo, *Fluid Phase Equilib.* 207 (2003) 143-154.



## **Chapter 6**

# ***Modelling of Phase Equilibrium in Hydrate Inhibitor Systems Using Simplified PC-SAFT***

---

Notwithstanding the considerable progresses attained over the last years, present thermodynamic models for prediction of phase equilibrium still face a number of challenges, specifically concerning equilibrium at very high pressures, in multi-component systems or in systems containing associating compounds, as pointed out in chapter one of this work. The typical systems considered in this work, consisting of hydrocarbons, water and a hydrate inhibitor, include associating compounds, making them of great interest from a theoretical point of view, for evaluating the extent of the association and the ability of these models to correctly describe the phase equilibria, as these associating species forming hydrogen bonds often exhibit a highly non-ideal thermodynamic behaviour.

In pure fluids, strong attractive interactions between similar molecules, such as hydrogen bonds or Lewis acid-base interactions result in the formation of molecular clusters that considerably affect their thermodynamic properties. When mixtures are considered, such interactions can occur not only between molecules of the same species (self-association), but also between molecules of different species (cross-association). It is, therefore, desirable for any thermodynamic model to account correctly for this association term. Examples of applicable equations of state (EoS) are the Cubic Plus Association EoS (CPA) [1,2], or the various variations of the Statistical Associating Fluid Theory EoS (SAFT) [3-8], some of them compared in a number of publications [9,10].

In the present chapter, a simplified version of the PC-SAFT EoS (Perturbed-Chain Statistical Associating Fluid Theory), proposed by von Solms et al. [8] and already applied to a number of complex systems [11,12], was used in the modelling of binary mixtures containing water, hydrocarbons and methanol as a thermodynamic hydrate inhibitor. The results are compared with the data existing in the literature presented in Chapter 2. This work focused on a number of representative systems containing methane, *n*-hexane, *n*-octane, water and methanol, and is intended to have a complementary character to the experimental work performed.

## **6.1. Introduction**

As mentioned before, computational methods have an important role in modern day chemical engineering, from the simple correlation models which may account for a reduction in the number of experimental points to be measured for a particular system, to more complex methods with more physical significance, but still approximate, and with potential to be used as predictive methods. Common to all the methods is the desire for a balance between simplicity and the accuracy.

A variety of equations of state (EoS) are widely used in engineering, the more common being variations of the van der Waals equations. These equations, such as the cubic EoS, can be thought of as based on the hard-sphere model to account for repulsive interactions, and can be very flexible in correlating phase equilibrium data for simple, nearly spherical molecules such as low molecular mass hydrocarbons, and simple inorganic compounds, but they are not adequate for systems with polar or associating compounds that present high deviations from ideality in the liquid phase. This is due to the fact that in most cubic EoS attractive interactions occur only as dispersive forces.

In order to overcome this drawback, the cubic plus association (CPA) equations of state have been developed [1,2]. They are a combination of simple cubic EoS, such as Soave-Redlich-Kwong (SRK) or Peng-Robinson (PR), with the association term of the SAFT type models, derived from Werheim's first order perturbation theory [13-16]. However, such models are still mainly used for low molecular weight compounds and present less accurate predictions as the asymmetry of the system increases.

Better predictions can generally be expected with an equation such as the Statistical Associating Fluid Theory (SAFT) [17,18], derived from statistical mechanics. The SAFT EoS was initially developed by Chapman et al. [19], based on the perturbation theory of Wertheim [13-16]. Perturbation theories divide the interactions of molecules into a repulsive part and a contribution due to the attractive part of the potential. To calculate the repulsive contribution, a reference fluid is defined in which no attractions are present, and each perturbation is a correction, approaching the model to the behaviour of the actual mixture.

### 6.1.1. The SAFT equation of state

In SAFT, fluids are modelled as consisting of chains of tangential spherical segments. The reference fluid consists of the hard-core fluid with association sites, so that hydrogen bonding is explicitly calculated, whereas perturbation consists of weak dispersion interactions. In this way, the EoS is written as the sum of contributions due to hard sphere, chain formation, association and weak dispersion interactions. SAFT was developed with respect to the residual Helmholtz free energy and is expressed as:

$$\tilde{a} \equiv \frac{A}{NkT} = \tilde{a}^{seg} + \tilde{a}^{chain} + \tilde{a}^{assoc} \quad (6.1)$$

where  $\tilde{a}^{seg}$  is the part of the Helmholtz energy referent to segment-segment interactions,  $\tilde{a}^{chain}$  is the term relative to chain formation, and  $\tilde{a}^{assoc}$  accounts for the association between different molecules, as in the case of hydrogen bonding. Four important assumptions are made: only one bond can be formed at an associating site [15], only single bonds are formed between molecules, the property of the fluid is independent of the angles between association sites on the molecule [20], and finally, when solved by thermodynamic perturbation theory, the theory includes the effect of chain-like and tree-like associated clusters, but not ring clusters.

Due to the complementary character of this chapter, a detailed discussion of the mathematics behind the SAFT theory is not provided here, and can be found elsewhere [9,10], or more briefly in the work of Tihic [21].

Before the SAFT EoS can be applied to multi-compound mixtures, it is necessary to estimate parameters for the pure compounds. SAFT comprises five pure compound parameters. The first is the number of hard spheres,  $m$ , that form a molecule. The second parameter is the volume of a mole of these spheres when they are closely packed,  $v^{00}$  (expressed in  $\text{cm}^3 \cdot \text{mol}^{-1}$ ), and it accounts for their size. The third parameter is the segment energy,  $u^0$  (expressed in K), which determines segment-segment interactions. In addition to these three parameters for non-associating compounds, the equation has two associating parameters,  $\varepsilon^{AA}$  and  $\kappa^{AA}$ .  $\varepsilon^{AA}$  characterises the association energy, while  $\kappa^{AA}$  is related with the associating volume for the interaction between two sites of type  $A$ .

These parameters, which usually follow a simple relationship with molar mass within a given homologous series, facilitating the extrapolation to some other fluids, are normally determined by fitting experimental vapour pressure and liquid density data, leading to serious deviations in predictions around the critical point. In order to deal with this problem, two different solutions have been adopted. While some researchers developed an additional term to take into account density and composition fluctuations in the critical region [22-27], others tried a simpler approach, rescaling the pure compound parameters to the critical point of each pure fluid and then using them to predict the mixture behaviour [28-30]. This last approach leads to the existence of two different sets of molecular parameters, one for subcritical calculations and another for near-critical calculations.

The main utility of the equations of state is related to their application in phase equilibrium calculations involving mixtures, considering that the same EoS used for pure fluids can also be used for mixtures. In general, this is attained through the use of the so-called one-fluid approach, together with mixing rules and combining rules, which relate some of the characteristics of the pure compounds, such as the energy for intersegmental interactions or the number of molecular segments, to that of the mixtures. Mixing rules are commonly used in various mixture models ranging from cubic EoS to theoretically-based molecular models.

The mixing rule based on the van der Waals one-fluid theory, referred to as the vdW1 mixing rule, is applied in the SAFT EoS version presented by Chapman et al. [18]. Mixing rules are only required for the dispersion term in the SAFT EoS, for two parameters only,  $u/k$  and  $m$ . As before, the mathematical expressions regarding these rules can be found elsewhere [21].

Furthermore, an additional binary interaction parameter is used,  $k_{ij}$ , for the correction of the mean-field energy contribution of SAFT. This parameter is determined by fitting to experimental phase equilibrium data available for the mixture in question. It is in fact a way to remove the inaccuracy of the combining rule used in the mean-field energy contribution and/or to adapt the theory to the reality, so that the systems in question can be represented with higher accuracy. Thus, larger values of the binary interaction parameter are symptomatic that the applied model (or combining rule) may not be the best to represent the system and that different models or modifications could be used instead.

### 6.1.2. The PC-SAFT equation of state

An important variation of the SAFT equation of state is the PC-SAFT EoS [31]. The main difference between these two equations is the perturbation sequence. In PC-SAFT the mixture of hard-sphere chains is considered as being the reference system and then the dispersive attractions are introduced. The physical basis behind PC-SAFT is represented schematically in Figure 6.1, according to Tihic [21].

The PC-SAFT EoS was developed as an effort to model asymmetric systems, and systems presenting a high deviation from ideality. It has for instance, been applied to associating mixtures of alcohols in short-chain hydrocarbons [32], where both VLE and LLE were simultaneously described with a single binary interaction parameter.

In the framework of PC-SAFT, molecules are considered as chains of freely jointed spherical segments and can be expressed in terms of the reduced residual Helmholtz energy, according to the following expression:

$$\tilde{a} \equiv \frac{A}{NkT} = \tilde{a}^{id} + \tilde{a}^{hc} + \tilde{a}^{disp} + \tilde{a}^{assoc} \quad (6.2)$$

where  $\tilde{a}^{id}$  is the ideal gas contribution,  $\tilde{a}^{hc}$  is the contribution of the hard-sphere chain reference system,  $\tilde{a}^{disp}$  is the dispersion contribution arising from the square-well attractive potential, and  $\tilde{a}^{assoc}$  is the contribution due to association.

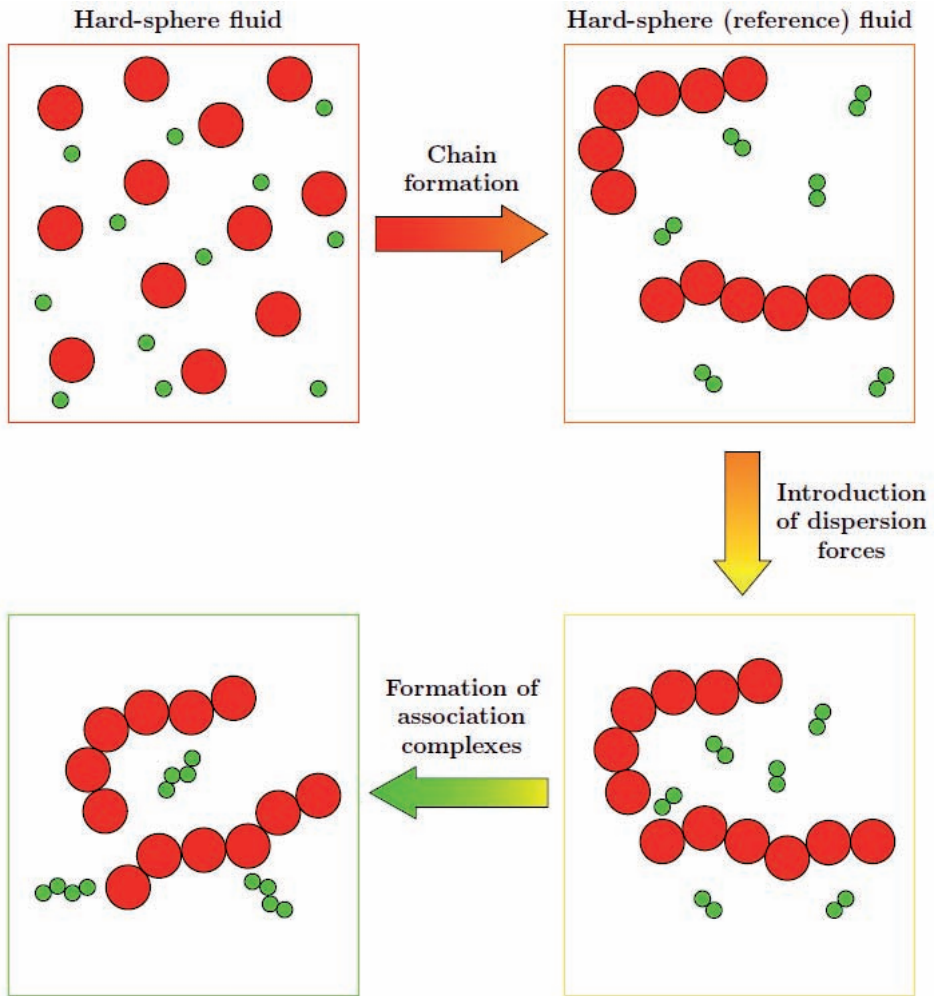


**Figure 6.1** – Schematic representation of the physical basis of PC-SAFT. Source: A. Tihic [21].

The hard-sphere chain contribution, which accounts for repulsion of the chain-like molecules, is given by the hard-sphere and the chain formation contributions:

$$\tilde{a}^{hc} = \bar{m} \tilde{a}^{hs} + \tilde{a}^{chain} = \bar{m} \tilde{a}^{hs} - \sum_i x_i (m_i - 1) \rho \frac{\partial \ln g_{ii}^{hs}}{\partial \rho} \quad (6.3)$$

where  $\bar{m}$  is the average number of segments per chain:

$$\bar{m} = \sum_{i=1}^{NC} x_i m_i \quad (6.4)$$

The hard-sphere term is given by the mixture version of the Carnahan-Starling [33] EoS for hard-spheres.

$$a^{hs} = \frac{1}{\zeta_0} \left[ \frac{3\zeta_1\zeta_2}{1-\zeta_3} + \frac{\zeta_2^3}{\zeta_3(1-\zeta_3)^2} + \left( \frac{\zeta_2^3}{\zeta_3^2 - \zeta_0} \right) \ln(1-\zeta_3) \right] \quad (6.5)$$

where  $\zeta_n$  are the partial volume fractions defined by:

$$\zeta_n = \frac{\pi\rho}{6} \sum_i x_i m_i d_i^n \quad n \in \{0, 1, 2, 3\} \quad (6.6)$$

and  $d_i$  is the Chen and Kreglewski [34] temperature-dependent segment diameter of the component  $i$ :

$$d_i = \sigma_i \left[ 1 - 0.12 \exp\left(-\frac{3\varepsilon_i}{kT}\right) \right] \quad (6.7)$$

The temperature-dependent segment diameter of component  $i$  is the outcome of the integration of the equation for the effective hard-collision diameter of the chain segments:

$$d_i = \int_0^\sigma \left[ 1 - 0.12 \exp\left(-\frac{3\varepsilon_i}{kT}\right) \right] \quad (6.8)$$

which is based on the modified square well potential for segment-segment interactions. The chain term in Equation 6.3, depends also on the radial distribution function at contact, which is given by:

$$g_{ij}^{hs}(d_{ij}) = \frac{1}{1-\zeta_3} + \left( \frac{d_i d_j}{d_i + d_j} \right) \frac{3\zeta_2}{(1-\zeta_3)^2} + \left( \frac{d_i d_j}{d_i + d_j} \right)^2 \frac{2\zeta_2^2}{(1-\zeta_3)^3} \quad (6.9)$$

The radial distribution function denotes the probability density for finding a hard-sphere belonging to a molecule  $j$ , at a distance  $d$  from a hard sphere belonging to a molecule  $i$ .

In most versions of the SAFT equation, the dispersion term contribution to the molecular Helmholtz energy is proportional to the number of segments. However, in PC-SAFT, the dispersion term is written for chains of segments based on second order perturbation theory, i.e. the attractive part of the chain interactions is calculated from a first and a second order perturbation, according to Barker and Henderson [35]. Basically, these are calculated by integrating the intermolecular interactions over the entire mixture volume, which leads to:

$$\tilde{a}^{disp} = -2\pi\rho I_1 m^2 \varepsilon \sigma^3 - \pi\rho\bar{m} \left( 1 + \tilde{a}^{hc} + \rho \frac{\partial \tilde{a}^{hc}}{\partial \rho} \right)^{-1} I_2 m^2 \varepsilon^2 \sigma^3 \quad (6.10)$$

The required integrals are approximated by power-series in density, where the coefficients of the power series are functions of the chain length:

$$I_1 = \sum_{i=0}^6 a_i(\bar{m}) \eta^i \quad (6.11)$$

$$I_2 = \sum_{i=0}^6 b_i(\bar{m}) \eta^i \quad (6.12)$$

The dependency of the coefficients  $a_i(\bar{m})$  and  $b_i(\bar{m})$  upon segment number is described by the equations:

$$a_i(\bar{m}) = a_{0i} + \frac{\bar{m}-1}{\bar{m}} a_{1i} + \frac{\bar{m}-1}{\bar{m}} \frac{\bar{m}-2}{\bar{m}} a_{2i} \quad (6.13)$$

$$b_i(\bar{m}) = b_{0i} + \frac{\bar{m}-1}{\bar{m}} b_{1i} + \frac{\bar{m}-1}{\bar{m}} \frac{\bar{m}-2}{\bar{m}} b_{2i} \quad (6.14)$$

and

$$m^2 \varepsilon^y \sigma^3 = \sum_{i=1}^{NC} \sum_{j=i}^{NC} x_i x_j m_i m_j \left( \frac{\varepsilon_{ij}}{kT} \right)^y \sigma_{ij}^3 \quad y \in \{1, 2\} \quad (6.15)$$

The cross-parameters are obtained from the combining rules:

$$\sigma_{ij} = \frac{\sigma_i + \sigma_j}{2} \quad (6.16)$$

$$\varepsilon_{ij} = \sqrt{\varepsilon_{ii}\varepsilon_{jj}}(1 - k_{ij}) \quad (6.17)$$

The constants in Equations 6.13 and 6.14 are considered to be universal, and are obtained by an indirect regression to experimental pure compound vapour pressures for a series of *n*-alkanes. The fitting procedure and the values of fitting constants can be found in the work of reference [31], based on results obtained by Chiew [36].

The association contribution is only included for systems containing components capable of self-associating and cross-associating (e.g. alcohols and acids). The association contribution is:

$$\tilde{a}^{assoc} = \sum_i x_i \sum_{A_i} \left( \ln X^{A_i} - \frac{1}{2} X^{A_i} + \frac{1}{2} \right) \quad (6.18)$$

where  $X^{A_i}$  is the fraction of sites *A* on a molecule *i* that do not form associating bonds with other active sites. This number is found through the solution of the non-linear system of equations:

$$X^{A_i} = \left( 1 + N_A \sum_j \rho_j \sum_{B_j} X^{B_j} \Delta^{A_i B_j} \right)^{-1} \quad (6.19)$$

where  $\rho_j$  is the molar density of component *j*, and  $\Delta^{A_i B_j}$  is a measure of the association strength between site A on molecule *i* and site B on molecule *j*. This parameter in turn is a function of the association volume  $k^{A_i B_j}$ , the association energy  $\varepsilon^{A_i B_j}$ , and the radial distribution function as follows:

$$\Delta^{A_i B_j} = \sigma_{ij}^3 g^{hs}(d^+) k^{A_i B_j} \left[ \exp\left(\frac{\varepsilon^{A_i B_j}}{kT}\right) - 1 \right] \quad (6.20)$$

where  $\Delta^{A_i B_j}$  is the so-called association strength. Note that the temperature independent diameter  $\sigma$  is used in Equation (6.20).

### 6.1.3. The simplified PC-SAFT equation of state

The simplified PC-SAFT (sPC-SAFT) [8] was developed in order to considerably reduce the computational time, with little or no compromise in the performance of the original model. In this model, the expressions for the contributions from the ideal gas,  $\tilde{a}^{id}$ , and dispersion,  $\tilde{a}^{disp}$ , are identical to those presented for PC-SAFT [31].

By assuming that all of the segments in the mixture have the same mean diameter,  $d$ , with the constraint that the mixture volume fraction calculated using this new diameter gives the same volume fraction as the actual mixture, the volume fraction is now based in a one-component mixture with a volume corresponding to:

$$\zeta_3 \equiv \eta = \frac{\pi \rho}{6} d^3 \sum_i x_i m_i \quad (6.21)$$

This average diameter is given by the following equation:

$$d = \left( \frac{\sum_i x_i m_i d_i^3}{\sum_i x_i m_i} \right)^{1/3} \quad (6.21)$$

Applying this to equations 6.5 and 6.9, the following expressions are obtained:

$$\tilde{a}^{hs} = \frac{4\eta - 3\eta^2}{(1-\eta)^2} \quad (6.22)$$

$$g^{hs} = \frac{1-\eta/2}{(1-\eta)^3} \quad (6.23)$$

The modifications implemented in the sPC-SAFT equation of state [8] relative to PC-SAFT EoS [31] are summarized in Table 6.1.

**Table 6.1** – Summary of the modifications implemented in the sPC-SAFT EoS relatively to the original PC-SAFT EoS.

PC-SAFT [31]	sPC-SAFT [8]
$\tilde{a}^{hs} = \frac{1}{\zeta_0} \left[ \frac{3\zeta_1\zeta_2}{1-\zeta_3} + \frac{\zeta_2^3}{\zeta_3(1-\zeta_3)^2} + \left( \frac{\zeta_2^3}{\zeta_3^2 - \zeta_0} \right) \ln(1-\zeta_3) \right]$	$\tilde{a}^{hs} = \frac{4\eta - 3\eta^2}{(1-\eta)^2}$
$g_{ij}^{hs}(d_j) = \frac{1}{1-\zeta_3} + \left( \frac{d_i d_j}{d_i + d_j} \right) \frac{3\zeta_2}{(1-\zeta_3)^2} + \left( \frac{d_i d_j}{d_i + d_j} \right)^2 \frac{2\zeta_2^2}{(1-\zeta_3)^3}$	$g^{hs} = \frac{1-\eta/2}{(1-\eta)^3}$

## 6.2. Results

The modelling results presented next, refer to representative binary systems, a binary mixture of two non-associating alkanes, consisting of methane and hexane, mixtures of an associating compound with a non-associating alkane, in this case *n*-hexane + water, *n*-octane + water and methanol + *n*-hexane, and finally a binary mixture of two associating compounds, water + methanol.

The Lorentz-Berthelot mixing rules were used for obtaining the parameters for unlike interactions between molecules, in accordance to the presented in equations 6.16 and 6.17, and the binary interaction parameter was introduced to correct the dispersion potentials for the mixtures.

The parameters relative to the alkanes used in the calculations were taken from the work presented by Gross et al. [31]. Different sets of parameters for water were taken from the work of Grenner et al. [37], although some of this sets had already been presented by von Solms et al. [38], and finally, for the methanol parameters, the work of Gross et al. [32] was considered. All the parameters are presented and summarised in table 6.2.

**Table 6.2** – Summary of the sets of PC-SAFT pure component parameters used in the present work.

Compound	Mol. weight	m	$\sigma$ (Å)	$\varepsilon/\kappa$ (K)	$\kappa^{AB}$	$\varepsilon^{AB}$	scheme <sup>a</sup>	Ref.
methane	16.043	1.000	3.7039	150.03	-	-	-	[31]
hexane	86.177	3.058	3.7983	236.77	-	-	-	[31]
octane	114.231	3.818	3.8373	242.78	-	-	-	[31]
methanol	32.042	1.526	3.2300	188.90	0.0352	2899.5	2B	[32]
water	18.015	2.000	2.3533	207.84	0.1550	1506.4	4C	[38]
		2.750	2.0794	183.61	0.3374	1354.1	4C	[38]
		3.500	1.9134	199.88	0.7901	839.0	4C	[38]
		1.500	2.6273	180.30	0.0942	1804.2	4C	[37]

<sup>a</sup> – associations schemes according to the notation proposed by Hwang and Radosz [17].

### 6.2.1. Binary System Methane + n-hexane

The binary system constituted by methane + *n*-hexane was modelled at six different temperatures, between 248 K and 411 K, by means of simplified PC-SAFT. Although being a simple mixture of two non-associating alkanes, the modelling included temperatures above the supercritical temperature of methane. A binary interaction parameter,  $k_{ij}$ , of 0.01 was used for all temperatures, in order to account for the interaction between the compounds. The results of the modelling are presented in the graph in Figure 6.2, together with experimental values found in the literature [39,40].

The plot in the figure evinces the ability of the model to provide a good description of the phase behaviour observed experimentally. As the mixture becomes richer in methane at these temperatures, it can be seen that the critical temperature is reached and that the mixture behaves as a retrograde condensing system. Also observable in the graph is the fact that the critical point of the mixture is overestimated. This fact is not surprising, as the pure component parameters used have not been modelled including the critical properties of the compounds and as mentioned earlier in this chapter, this may lead to serious deviations around the critical point. Figure 6.3 presents a close-up on the higher values of the molar fraction of methane. The model seems to be adequate to reproduce the phase behaviour of the binary system under consideration, including the change in the compositions at the point critical point of the mixture with temperature.

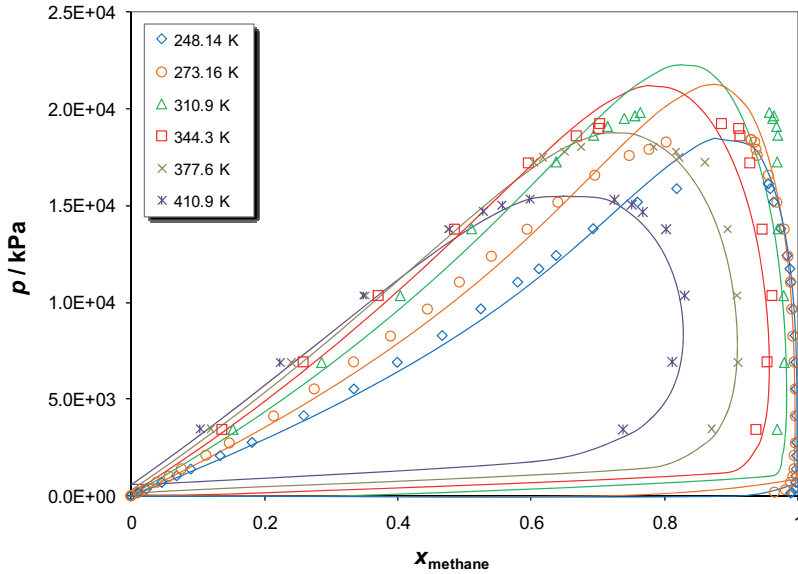


**Figure 6.2** – Results obtained in the modelling of the binary system methane + *n*-hexane, at isothermal conditions, between 248 K and 411 K, using simplified PC-SAFT correlations with  $k_{ij} = 0.01$ , and comparison with experimental data found in the literature [39,40].

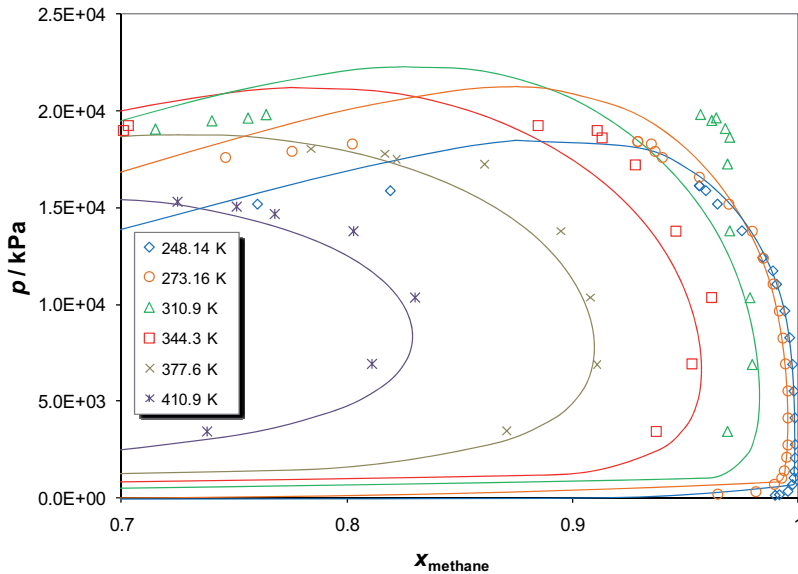


**Figure 6.3** – Results obtained in the modelling of the binary system methane + *n*-hexane, at isothermal conditions, between 248 K and 411 K, using simplified PC-SAFT correlations with  $k_{ij} = 0.01$ , and comparison with experimental data found in the literature [39,40]. Detail for higher values of the methane mole fraction.

## 6.2.2. Binary System *n*-hexane + Water

An analysis of the different sets of parameters presented for water by Grenner et al. [37], already presented in Table 6.1, was performed, through the modelling of the LLE of the binary system *n*-hexane + water. Figure 6.4, shows a comparison between the obtained results, using a value of  $k_{ij} = 0.00$ , and values found in the literature [41,42] for the system in question.

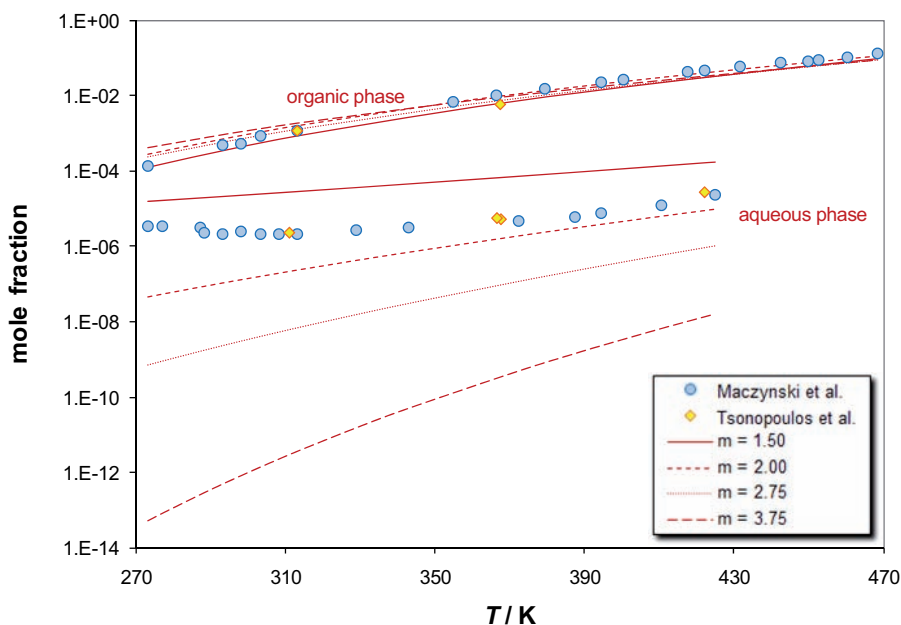


**Figure 6.4** – Results obtained in the modelling of the LLE for the binary system *n*-hexane + water with simplified PC-SAFT, using a  $k_{ij} = 0.00$  and different sets of parameters for water, and comparison with experimental data found in the literature [41,42].

The results show that the different sets of water parameters have little influence in the calculation of the molar fraction of water in the organic phase, something that was expected from the reduced amount of the compound in this phase. Relatively to the composition of the aqueous phase, the results obtained using  $m = 1.5$  and  $m = 2.0$  revealed a better performance. This last set of parameters allows the achievement of better results for the highest temperatures considered, but leads to greater deviations for the lower

temperatures. The set of parameters with  $m = 1.5$  arguably gives better results in the estimation of the composition of the organic phase, with the model closer to the experimental results at the lower end of the temperature scale.

This set of parameters ( $m = 1.5$ ) was then used in the modelling of the same system, this time using a binary interaction parameter different from zero. The results, presented in the graph of Figure 6.5, show the performance of the model using a  $k_{ij} = 0.0$ , and using a value of 0.055 for the binary interaction parameter, together with the literature data already exhibited in the previous graph.

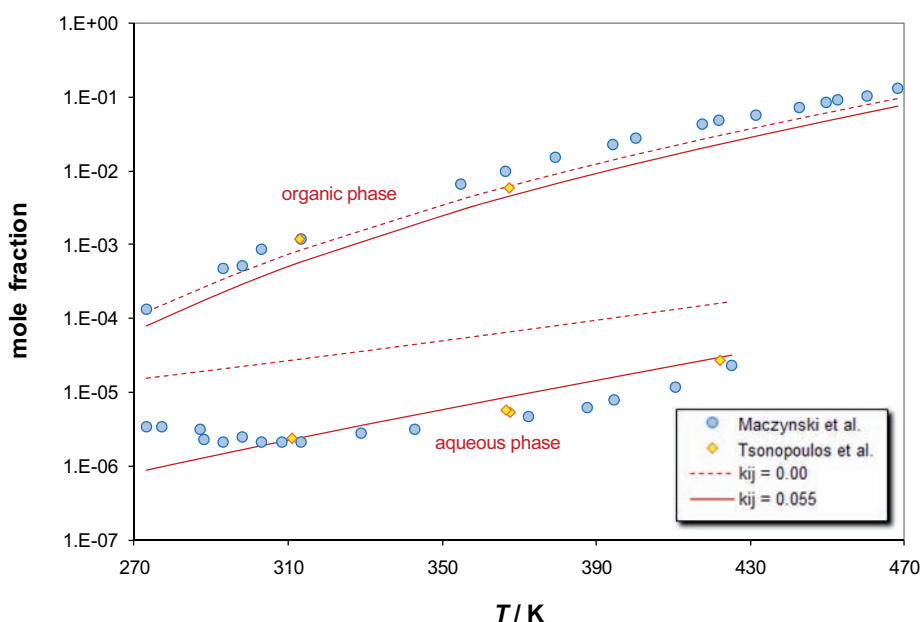


**Figure 6.5** – Results obtained in the modelling of the LLE for the binary system *n*-hexane + water with simplified PC-SAFT, using  $k_{ij} = 0.00$  and  $k_{ij} = 0.055$ , and comparison with experimental data found in the literature [41,42].

The value of  $k_{ij}$  used was adjusted by means of improving the performance of the model for the composition of the aqueous phase. It is noticeable that as a consequence, the predictions concerning the organic phase are less satisfactory, although in a relatively smaller extent. As verified before for the different sets of parameters, the influence of the value of  $k_{ij}$  is notoriously higher for the aqueous phase.

### 6.2.3. Binary System *n*-octane + Water

The simplified PC-SAFT equation of state was also used in the modelling of the vapour-liquid-liquid equilibrium (VLLE) for the binary system *n*-octane + water. Figure 6.6 shows the results of this study, obtained for a pressure of 8 MPa and a value for the binary interaction parameter,  $k_{ij}$  equal to 0.035. The plot also comprised data from the literature [41,43]. It should be pointed out however, that the experimental points relative to the work of Heidman and co-workers [43] correspond to the equilibrium pressure, which approaches a pressure of around 8 MPa for the higher temperatures considered, rather than referring to a constant pressure as used in the application of the model. It is expected that the influence of the pressure should be negligible in the composition of the liquid phases.

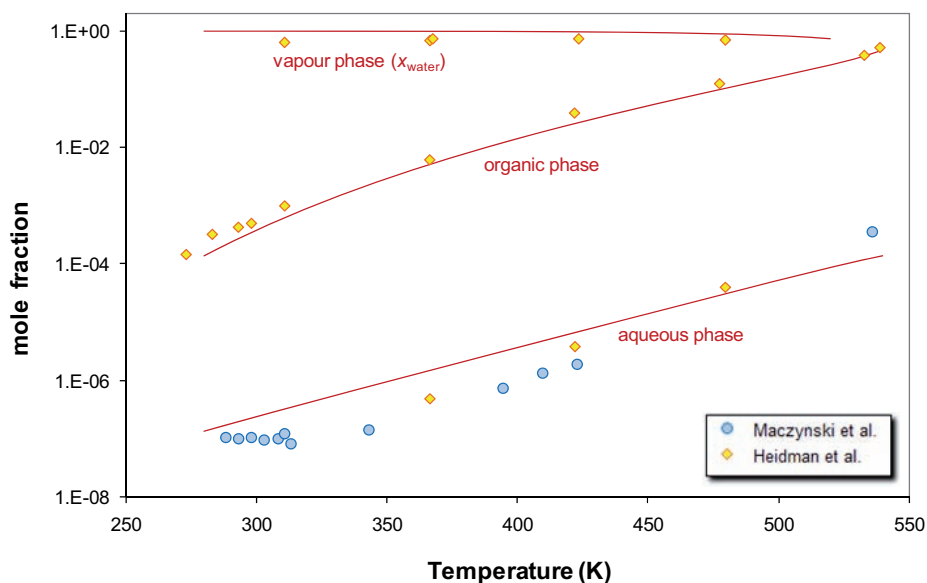


**Figure 6.6** – Results obtained in the modelling of the VLLE for the binary system *n*-octane + water with simplified PC-SAFT, using a  $k_{ij} = 0.035$ , and comparison with experimental data found in the literature [41,43].

The results evince once again the good performance of the model, even relatively to the composition of the gas phase in which some deviations from the behaviour observed experimentally could be expected, due to the difference in the pressure conditions. The

small value used for the  $k_{ij}$  was optimised taking into account the composition of the three phases simultaneously.

#### 6.2.4. Binary System *n*-hexane + Methanol

The modelling of the system *n*-hexane + methanol was performed considering a 2B associating scheme for methanol [32], according to the nomenclature proposed by Hwang and Radosz [17]. Figure 6.7 shows the results obtained in modelling of the vapour-liquid equilibrium for this system at 0.101 MPa, and the liquid-liquid equilibrium at 85 MPa, similar conditions to the experimental data presented by Blanco and Ortega [44], and by Hradetzky and Lempe [45], respectively. A value of  $k_{ij} = 0.03$  was considered for both correlations, a value obtained from the optimisation of the model to the LLE experimental data of Hradetzky and Lempe [45].

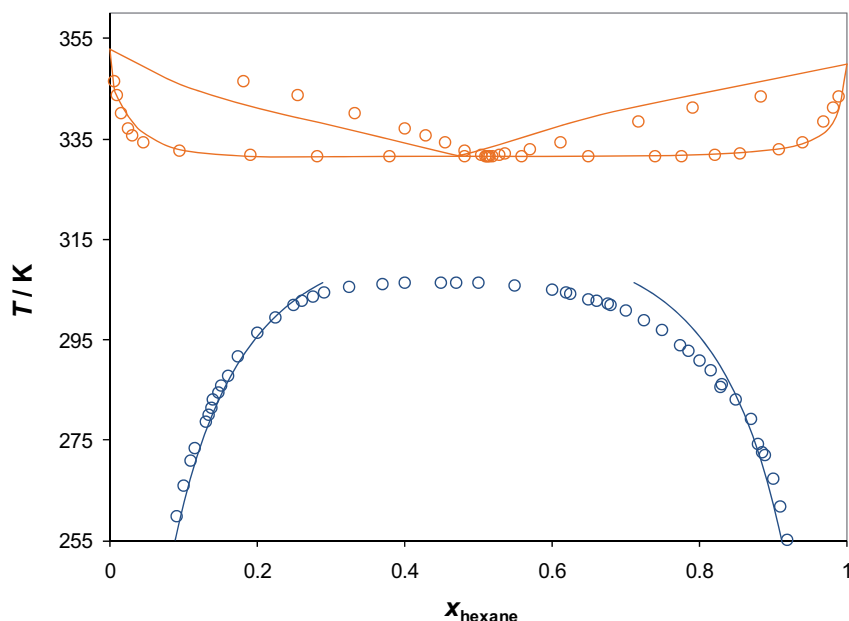


**Figure 6.7** – Results obtained in the modelling of the VLE at 0.101 MPa, and the LLE at 85 MPa for the binary system *n*-hexane + methanol, considering a  $k_{ij} = 0.03$ , and comparison with experimental values from literature [44,45].

It is noticeable that the attempt of using the same value of  $k_{ij}$  for both correlations, can lead to satisfactory results in the case of LLE, for which the  $k_{ij}$  was optimised, with a perfect representation of the azeotropic point and the bubble curve, but the same is not verified for the VLE, where the model fails in representing the dew curve.

### **6.2.5. Binary System Methanol + Water**

This binary system is considerably challenging since it is constituted by two associating compounds, in which hydrogen bonding interactions can occur not only between molecules of the same species (self-association), but also between molecules of different species (cross-association), leading to strong deviations from ideality in the behaviour of the mixture. The modelling of this binary system was performed considering an association scheme 4C for water, as presented by Grenner et al [37] and a 2B associating scheme for methanol [32], according to the nomenclature proposed by Hwang and Radosz [17]. Furthermore, the combining rules of Elliott for cross-association were taken into consideration.

Figure 6.8 presents the results obtained with the sPC-SAFT EoS in the correlation of vapour-liquid equilibrium data for the system under consideration, at a pressure equal to 0.101 MPa. In the same graph are also displayed the experimental values from ten different literature sources [46-55]. In order to obtain a satisfactory correlation of the experimental data used as reference, a value of  $k_{ij} = -0.04$  was used. As it shown in the plot, the model was able to successfully characterise this mixture in all the mole fraction range.

It is worth mentioning the fact that a negative  $k_{ij}$  has been used in the correlations performed for this system. Considering how this parameter has been defined, the use of a negative value translates the insufficiency of the calculation of the unlike interactions through the mixing rules between the two pure components, i.e., the existing of favourable interactions between the two components of the mixture, or cross-association, with a strength that is underestimated by Elliott's combining rule.

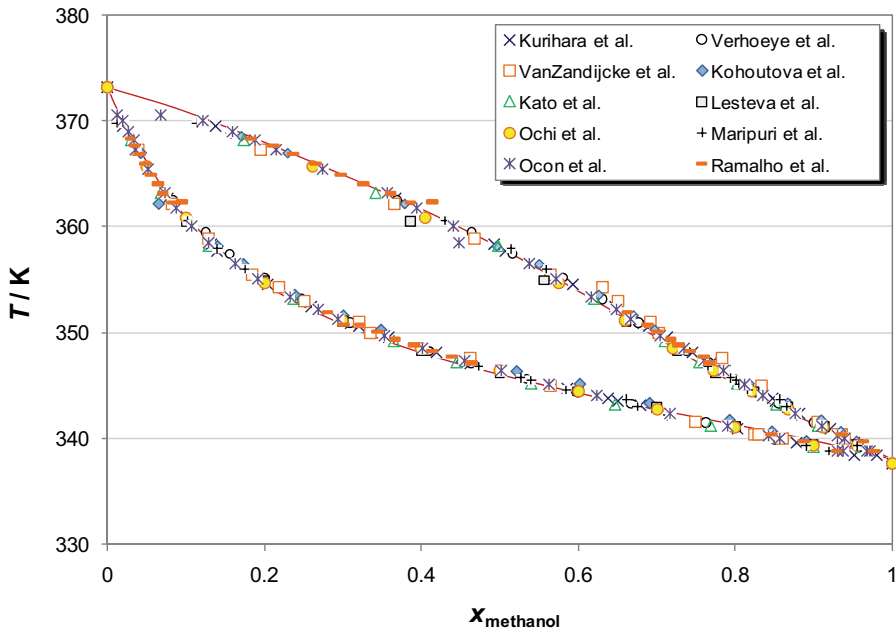


**Figure 6.8** – Results obtained in the correlation of isobaric VLE for the system methanol + water, at a pressure of 0.101 MPa, using simplified PC-SAFT and a  $k_{ij} = -0.04$ , and comparison with experimental literature data [46-55].

Figure 6.9 presents the results obtained in the correlation of the isothermal behaviour of same mixture at seven temperatures, in the interval between 298 K and 523 K. The same  $k_{ij}$  value determined previously for this system was used. The plot evinces a very good agreement between the results of the correlations and the experimental data found in the literature [56-58], especially in what the higher values of the considered temperature range is concerned. It is observable that for the lowest temperature, of 298.15 K, the pressures are slightly overestimated, leading to a somewhat considerable error in the prediction of the composition for a particular value of pressure. However it is important to notice the use of a same value of  $k_{ij}$ , independent of the temperature, and obtained from the correlation of the isobaric VLE experimental data.

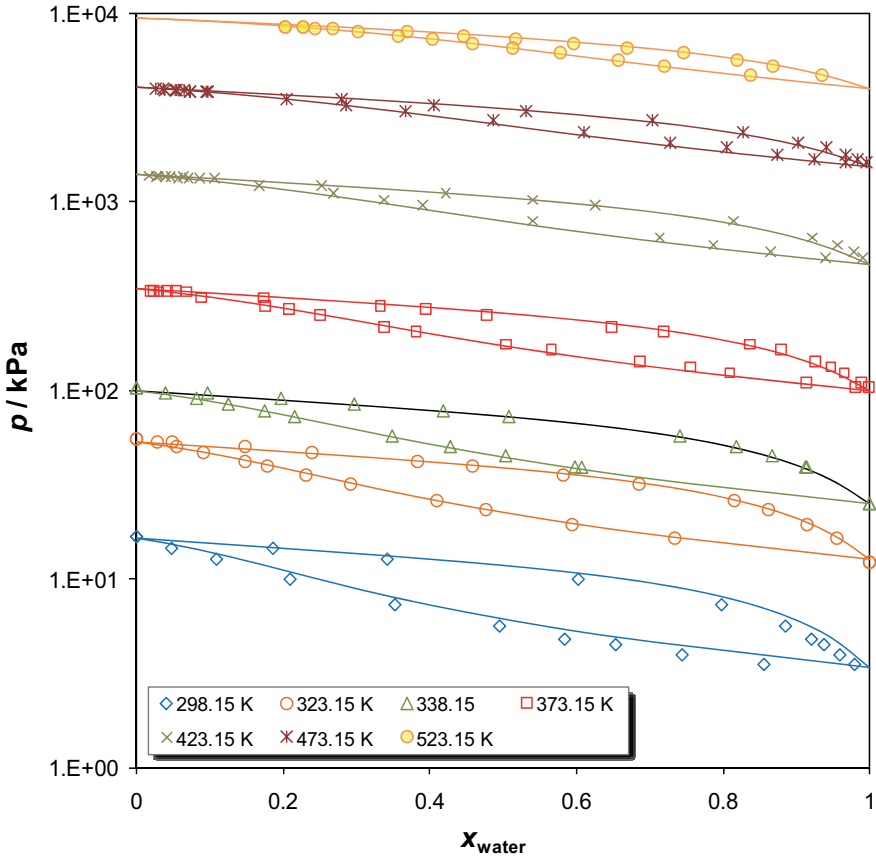


**Figure 6.9** – Simplified PC-SAFT correlation of the isothermal VLE behaviour of the system methanol + water, at 298.15 K, 323.15 K, 338.15 K, 373.15 K, 423.15 K, 473.15 K and 523.15 K, using  $k_{ij} = -0.04$ , and comparison with experimental data [56-58].

### 6.3. Conclusions

In this chapter, which has a complementary character in the present thesis in which the experimental work is assumed as the main focus, it was verified the applicability of the simplified version of the PC-SAFT EoS proposed by von Solms et al. [8] in the modelling of a number of binary mixtures containing water, hydrocarbons and methanol as a thermodynamic hydrate inhibitor. The model was successfully applied to different types of equilibrium, in a relatively wide range of both pressures and temperatures, with the need

for only small corrections, as indicated by the low values for the binary interaction parameter,  $k_{ij}$ , used most of the times.

An extension of this work should probably pass by an attempt to model the equilibrium in binary mixtures containing glycols, and to model the equilibrium in ternary mixtures containing simultaneously water, hydrocarbons and a hydrate inhibitor. In a further stage, the modelling of systems containing a hydrate phase would also be desirable.

## References

- [1] G. M. Kontogeorgis, M. L. Michelsen, G. K. Folas, S. Derawi, N. von Solms, E. H. Stenby, *Ind. Eng. Chem. Res.* 45 (2006) 4855-4868.
- [2] G. M. Kontogeorgis, M. L. Michelsen, G. K. Folas, S. Derawi, N. von Solms, E. H. Stenby, *Ind. Eng. Chem. Res.* 45 (2006) 4869-4878.
- [3] A. M. A. Dias, F. Llovel, J. A. P. Coutinho, I. M. Marrucho, L. F. Vega, *Fluid Phase Equilib.* 286 (2009) 134-143.
- [4] J. Gross, *J. Chem. Phys.* 131 (2009).
- [5] R. E. Martini, M. Cismondi, S. Barbosa, E. Brignole, *Sep. Sci. Technol.* 44 (2009) 2661-2680.
- [6] A. Tihic, N. von Solms, M. L. Michelsen, G. M. Kontogeorgis, L. Constantinou, *Fluid Phase Equilib.* 281 (2009) 60-69.
- [7] I. Tsivintzelis, A. Grenner, I. G. Economou, G. M. Kontogeorgis, *Ind. Eng. Chem. Res.* 48 (2009) 7860.
- [8] N. von Solms, M. L. Michelsen, G. M. Kontogeorgis, *Ind. Eng. Chem. Res.* 42 (2003) 1098-1105.
- [9] I. G. Economou, *Ind. Eng. Chem. Res.* 41 (2002) 953-962.
- [10] E. A. Muller, K. E. Gubbins, *Ind. Eng. Chem. Res.* 40 (2001) 2193-2211.

- [11] N. von Solms, J. Kristensen, *Int. J. Refrig.* 33 (2010) 19-25.
- [12] N. Muro-Sune, G. M. Kontogeorgis, N. von Solms, M. L. Michelsen, *Ind. Eng. Chem. Res.* 47 (2008) 5660-5668.
- [13] M. S. Wertheim, *J. Stat. Phys.* 35 (1984) 19-34.
- [14] M. S. Wertheim, *J. Stat. Phys.* 35 (1984) 35-47.
- [15] M. S. Wertheim, *J. Stat. Phys.* 42 (1986) 459-476.
- [16] M. S. Wertheim, *J. Stat. Phys.* 42 (1986) 477-492.
- [17] S. H. Huang, M. Radosz, *Ind. Eng. Chem. Res.* 29 (1990) 2284-2294.
- [18] W. G. Chapman, K. E. Gubbins, G. Jackson, M. Radosz, *Ind. Eng. Chem. Res.* 29 (1990) 1709-1721.
- [19] W. G. Chapman, G. Jackson, K. E. Gubbins, *Mol. Phys.* 65 (1988) 1057-1079.
- [20] D. Ghonasgi, W. G. Chapman, *Mol. Phys.* 80 (1993) 161-176.
- [21] A. Tihic, Ph.D. Thesis, Department of Chemical Engineering, Technical University of Denmark, Kgs. Lyngby, Denmark, 2008.
- [22] A. K. Wyczalkowska, J. V. Sengers, M. A. Anisimov, *Physica A* 334 (2004) 482-512.
- [23] S. B. Kiselev, *Fluid Phase Equilib.* 147 (1998) 7-23.
- [24] S. B. Kiselev, D. G. Friend, *Fluid Phase Equilib.* 162 (1999) 51-82.
- [25] J. Cai, J. M. Prausnitz, *Fluid Phase Equilib.* 219 (2004) 205-217.
- [26] L. Lue, J. M. Prausnitz, *J. Chem. Phys.* 108 (1998) 5529-5536.
- [27] J. W. Jiang, J. M. Prausnitz, *J. Chem. Phys.* 111 (1999) 5964-5974.
- [28] F. Llovel, J. C. Pamies, L. F. Vega, *J. Chem. Phys.* 121 (2004) 10715-10724.
- [29] F. J. Blas, L. F. Vega, *J. Chem. Phys.* 109 (1998) 7405-7413.

- [30] C. McCabe, A. Gil-Villegas, G. Jackson, *J. Phys. Chem. B* 102 (1998) 4183-4188.
- [31] J. Gross, G. Sadowski, *Ind. Eng. Chem. Res.* 40 (2001) 1244-1260.
- [32] J. Gross, G. Sadowski, *Ind. Eng. Chem. Res.* 41 (2002) 5510-5515.
- [33] N. F. Carnahan, K. E. Starling, *J. Chem. Phys.* 51 (1969) 635.
- [34] S. S. Chen, A. Kreglewski, *Ber. Bunsen Ges. Phys. Chem.* 81 (1977) 1048-1052.
- [35] J. A. Barker, D. Henderson, *J. Chem. Phys.* 47 (1967) 4714-4721.
- [36] Y. C. Chiew, *Mol. Phys.* 73 (1991) 359-373.
- [37] A. Grenner, J. Schmelzer, N. von Solms, G. M. Kontogeorgis, *Ind. Eng. Chem. Res.* 45 (2006) 8170-8179.
- [38] N. von Solms, M. L. Michelsen, C. P. Passos, S. O. Derawi, G. M. Kontogeorgis, *Ind. Eng. Chem. Res.* 45 (2006) 5368-5374.
- [39] Y. N. Lin, R. J. J. Chen, P. S. Chappellear, R. Kobayashi, *J. Chem. Eng. Data* 22 (1977) 402-408.
- [40] R. S. Poston, J. J. McKetta, *J. Chem. Eng. Data* 11 (1966) 362-363.
- [41] A. Maczynski, B. Wisniewska-Gocłowska, M. Goral, *J. Phys. Chem. Ref. Data* 33 (2004) 549-577.
- [42] C. Tsonopoulos, G. M. Wilson, *AIChE J.* 29 (1983) 990-999.
- [43] J. L. Heidman, C. Tsonopoulos, C. J. Brady, G. M. Wilson, *AIChE J.* 31 (1985) 376-384.
- [44] A. M. Blanco, J. Ortega, *Fluid Phase Equilib.* 122 (1996) 207-222.
- [45] G. Hradetzky, D. A. Lempe, *Fluid Phase Equilib.* 69 (1991) 285-301.
- [46] M. Kato, H. Konishi, M. Hirata, *J. Chem. Eng. Data* 15 (1970) 501-505.
- [47] J. Kohoutov, J. Suska, J. P. Novak, J. Pick, *Collect. Czech. Chem. Commun.* 35 (1970) 3210.

- [48] K. Kurihara, M. Nakamichi, K. Kojima, *J. Chem. Eng. Data* 38 (1993) 446-449.
- [49] T. M. Lesteva, S. K. Ogorodni, S. V. Kazakova, *Zh. Prikl. Khim.* 43 (1970) 1574.
- [50] V. O. Maripuri, G. A. Ratcliff, *J. Chem. Eng. Data* 17 (1972) 366-369.
- [51] K. Ochi, K. Kojima, *Kagaku Kogaku* 35 (1971) 583-586.
- [52] J. Ocon, C. Taboada, *An. R. Soc. Esp. Fis. Quim. Ser. B* 55 (1959) 255.
- [53] R. S. Ramalho, F. M. Tiller, W. J. James, D. W. Bunch, *Ind. Eng. Chem.* 53 (1961) 895-896.
- [54] F. Vanzandijcke, L. Verhoeye, *J. Appl. Chem. Biotech.* 24 (1974) 709-729.
- [55] L. Verhoeye, H. D. Schepper, *J. Appl. Chem. Biotech.* 23 (1973) 607-619.
- [56] J. A. V. Butler, D. W. Thomson, W. H. Maclennan, *J. Chem. Soc.* (1933) 674-686.
- [57] J. Griswold, S. Y. Wong, *Chem. Eng. Progr. Symp.* 48 (1952) 18-34.
- [58] M. L. Mcglashan, A. G. Williamson, *J. Chem. Eng. Data* 21 (1976) 196-199.

## **Chapter 7**

# ***Experimental Study and Modelling of the Quaternary System Methane + n-hexane + Methanol + Water***

---

After completing the testing of the analytical apparatus presented in Chapter 4, a quaternary system containing methane, *n*-hexane, methanol and water, for which no data was found in the literature, was studied at 298 K, under pressures between 7 MPa and 10 MPa. The version of the simplified PC-SAFT equation of state included in the commercial software package SPECS v5.10, developed within the research group, was also used in the prediction of the phase equilibrium for this system, at conditions similar to the experimental, using the binary interaction parameters obtained in correlations for the six binary systems formed with the constituents of this quaternary system. sPC-SAFT already found to be appropriate for the modelling of systems involving this type of compounds, as presented in Chapter 6.

### **7.1. Experimental Results**

In the preparation of these experiments, sPC-SAFT was used in a preliminary prediction of the equilibrium, in order to provide an idea for the feed of the mixture, if three-phase equilibrium is desired. If a high amount of methanol is used, relative to the quantities of water and *n*-hexane, only one liquid phase is found in equilibrium. The approximate global composition of the prepared mixture is given in Table 7.1.

**Table 7.1** – Approximate global composition of the quaternary mixture methane + *n*-hexane + methanol + water studied in this work, given in molar fraction of the components.

Compound	Molar fraction
methane	0.27
<i>n</i> -hexane	0.09
methanol	0.10
water	0.54

The quantification of methanol from the chromatograms was performed according to Equations 7.1 and 7.2, while for the determination of the amounts of *n*-hexane in the samples, Equations 7.3 and 7.4 were used. As for the quantification of water and methane, the same equations presented in Chapter 4 were used (Equations 4.12, 4.13 and 4.14).

$$Area_{TCD} = 2.3780 \times 10^8 \cdot n_{\text{methanol}} \quad (7.1)$$

$$Area_{FID} = 1.6646 \times 10^9 \cdot n_{\text{methanol}} \quad (7.2)$$

$$Area_{TCD} = 6.9965 \times 10^8 \cdot n_{\text{hexane}} \quad (7.3)$$

$$Area_{FID} = 1.5089 \times 10^{10} \cdot n_{\text{hexane}} \quad (7.4)$$

The mixture was first studied at a temperature of 298.42 K, and a pressure of 9.8 MPa. The results obtained in the analysis of the two liquid phases present at equilibrium are given in Table 7.2. The values are an average of at least 5 analyses for each phase. The individual data points are provided in Appendix 2.

No sampling was possible from the gas phase, since during the preparation of the mixture, the increase in the volume of the organic phase caused by the dissolution of the methane in this phase was not correctly taken into account. This led to the two upper samplers both being connected to the organic liquid phase. To solve this problem, the lower piston was manually activated, in order to decrease the level of the interfaces.

A new set of measurements was then performed at a temperature of 298.31 K, and a pressure of 7.3 MPa. The obtained results are given in Table 7.3. The amount of water in

the organic liquid phase and in the gas phase was below the detection limit of the chromatographic method used. As before, the individual data points are provided in Appendix 2.

**Table 7.2** – Results obtained in the study of the quaternary mixture methane + *n*-hexane + methanol + water, at 298.42 K and 9.8 MPa.

Compound	Molar fraction		
	aqueous phase	organic phase	gas phase
methane	$3.0 \times 10^{-3}$	0.160	--
<i>n</i> -hexane	$1.3 \times 10^{-5}$	0.818	--
methanol	0.167	$1.9 \times 10^{-2}$	--
water	0.830	$2.0 \times 10^{-3}$	--

**Table 7.3** – Results obtained in the study of the quaternary mixture methane + *n*-hexane + methanol + water, at 298.31 K and 7.3 MPa.

Compound	Molar fraction		
	aqueous phase	organic phase	gas phase
methane	$3.9 \times 10^{-2}$	0.425	0.975
<i>n</i> -hexane	$4.8 \times 10^{-2}$	0.529	$2.4 \times 10^{-2}$
methanol	0.149	$4.6 \times 10^{-2}$	$7.6 \times 10^{-4}$
water	0.764	$< 2 \times 10^{-4}$	$< 2 \times 10^{-4}$

A comparison between the two sets of data seems shows some noteworthy divergences, especially in the composition of the liquid organic phase, which appears to be richer in methane in the second set. Also for the aqueous phase, a tenfold increase in the amount of methane is observed, although the equilibrium pressure is lower than in the first set of data.

A possible explanation can be that during the first set of measurements a full equilibrium had not yet been achieved, although no significant change on the pressure values could be observed. This seems reasonable to explain the increase of the amount of methane in the liquid phases, especially in the aqueous phase. It is noticeable that the amount of *n*-hexane in the aqueous phase also had a considerable increase. However this is

hardly justified by a lack of equilibrium between the two liquid phases in the first set of experiments, since a good contact between the two phases exists.

Previous to the presented studies, a first set of measurements was performed at a pressure of 2.8 MPa, but the results were not satisfactory, due to the fact that the set of capillaries installed in the cell are those appropriate for higher pressure measurements. Thus, the sampling times required for the determination of the full composition of the phases at this pressure were too high, and had a negative effect on the shape of the chromatographic peaks. The substitution of the capillaries for the “low-pressure” set would have been possible before the experiments, but this would imply the time consuming disassembling of some of the parts in the apparatus, and these experiments were performed in a tight schedule.

The results presented in Tables 7.2 and 7.3, were also obtained with relatively long sampling times of 10 seconds, but without affecting the quality of the chromatographic peaks, as it can be seen in Figure 7.1, where an example of a chromatogram for a sample withdrawn from the organic phase during the study at 9.8 MPa is presented, showing the peaks corresponding to the four constituents of the system under study. Despite a slight tailing observed for the polar compounds, the chromatogram shows very well defined peaks.

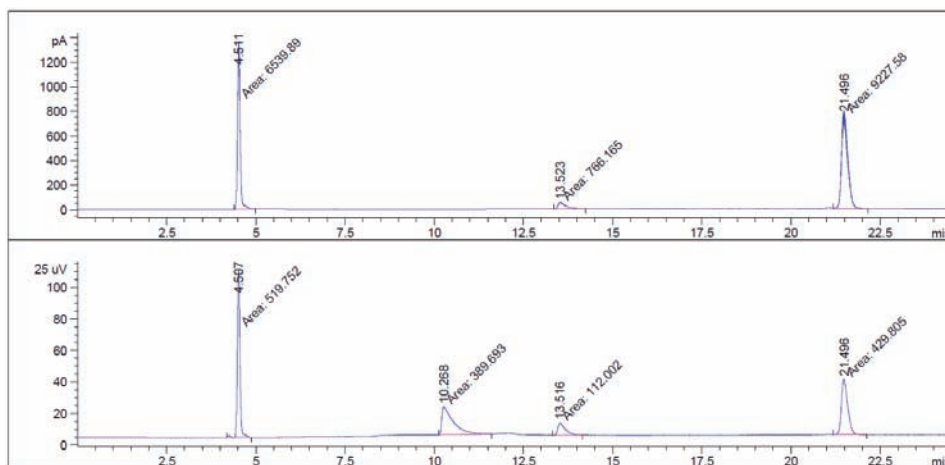


**Figure 7.1** – Example of a chromatogram relative to a sample withdrawn from the organic phase of the system methane + *n*-hexane + methanol + water, showing the peaks corresponding to the four constituents of the system.

## 7.2. Modelling

As mentioned, the sPC-SAFT EoS was used in the prediction of the phase equilibrium for the quaternary system under study, under the conditions similar to the experimental. The version used was the included in the commercial software package SPECS (v5.10, CERE, Denmark). A summary of the pure compound parameters used by this software, for the four components of the mixture studied, are given in Table 7.4.

For the modelling of this quaternary system, six binary interaction parameters are necessary, which can be determined by correlation of experimental data. In Chapter 6, the values of the  $k_{ij}$  for the binary mixtures methane + *n*-hexane, *n*-hexane + water, *n*-hexane + methanol and methanol + water were already determined. Further calculations were then necessary in order to establish the interaction parameters for the binary systems methane + water and methane + methanol. These calculations were also performed using the software SPECS.

**Table 7.4** – Summary of the sets of PC-SAFT pure component parameters used in the calculations presented in the current chapter, included in the SPECS software.

Compound	Mol. weight	m	$\sigma$ (Å)	$\varepsilon/\kappa$ (K)	$\kappa^{AB}$	$\varepsilon^{AB}$
methane	16.043	1.0000	3.7039	150.03	-	-
hexane	86.177	3.0576	3.7983	236.77	-	-
methanol	32.042	1.5250	3.2300	188.90	0.0352	2899.5
water	18.015	1.0656	3.0007	366.51	0.0349	2500.7

### 7.2.1. Binary System Methane + Water

The binary system methane + water was modelled at five different temperatures, between 283 K and 373 K. It was found that the value of the binary interaction parameter,  $k_{ij}$ , presents a strong dependence on temperature.

For a temperature of 283 K, a negative value of  $k_{ij} = -0.025$  was necessary in order to correctly correlate the experimental data. It was verified that the value of the  $k_{ij}$  has little or

no influence on the results produced by the model for the gas phase. Figure 7.2 presents the results of the modelling for the liquid phase, and a comparison with the values obtained in this work by the synthetic method, as well with values found in the literature [1-3]. As for the gas phase, the results are shown in Figure 7.3, together with experimental values found in the literature [4-7].

It should be underlined that although two separate graphs are presented, the modelling of the system was obviously performed considering simultaneously the data relative to both phases. The representation is made using different plots for different phases in order to allow a better observation of the performance of the model, due to the very low mutual solubilities of these compounds.

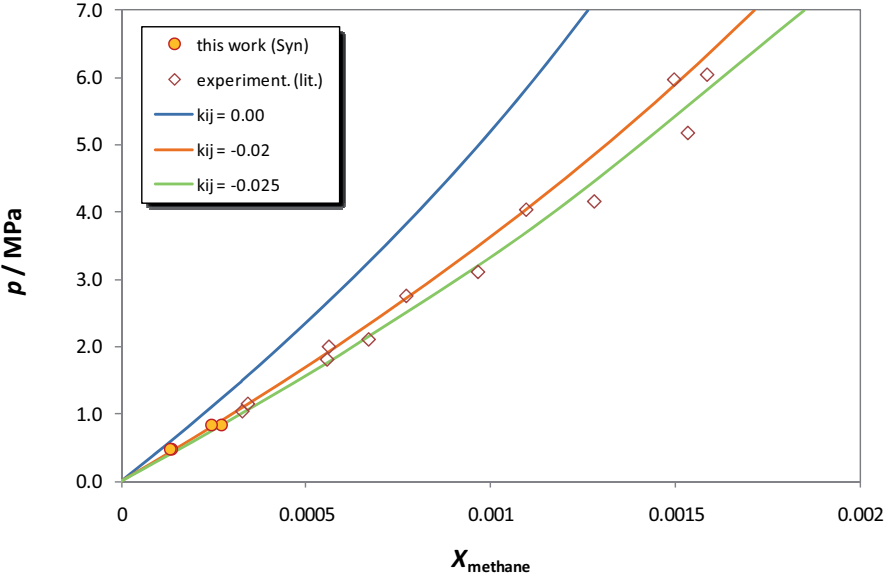


**Figure 7.2** – Modelling of the binary system methane + water, at 283 K, using sPC-SAFT correlations with different values of  $k_{ij}$ , and comparison with experimental data obtained in this work by the synthetic method and literature data for the liquid phase [1-3].

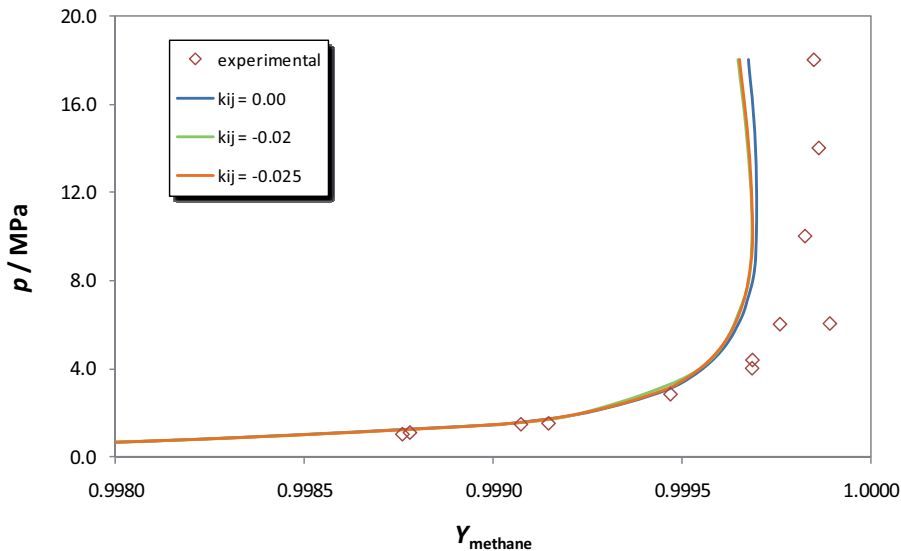


**Figure 7.3** – Modelling of the binary system methane + water, at 283 K, using sPC-SAFT correlations with different values of  $k_{ij}$ , and comparison with literature data for the gas phase [4-7].

For a temperature of 298 K, a value of  $k_{ij}$  equal to zero showed to be appropriate for the representation of the gathered experimental data. Such value accounts for a very good representation of the equilibrium in the liquid phase, as represented in Figure 7.4, where the experimental values obtained in the present work, both by the analytical and the synthetic method, as well as experimental data found in the literature [1,3,8-12] are also represented. Figure 7.5, shows the difficulty of the method to correctly describe the equilibrium in the gas phase regardless of the values of  $k_{ij}$  used in the calculations. In this plot, values obtained in the present work by the analytical method, and values found in the literature [4-6,12,13] are also represented for comparison.

Again, as in all other cases presented in this chapter, the modelling was performed considering simultaneously the data relative to both phases, despite the separate graphical representations.

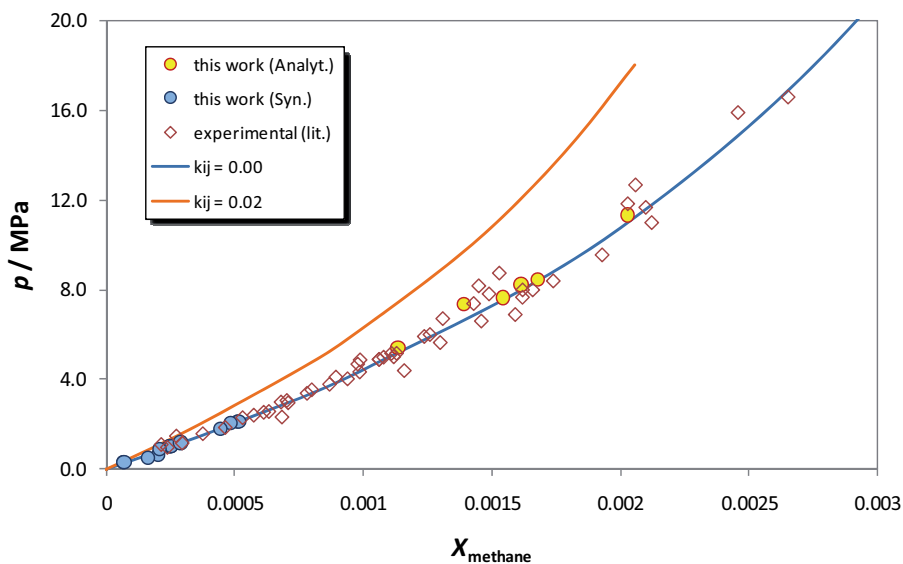


**Figure 7.4** – Modelling of the binary system methane + water, at 298 K, using sPC-SAFT correlations with different values of  $k_{ij}$ , and comparison with experimental data obtained in this work by the analytical and the synthetic method and data found in literature for the liquid phase [1,3,8-12].

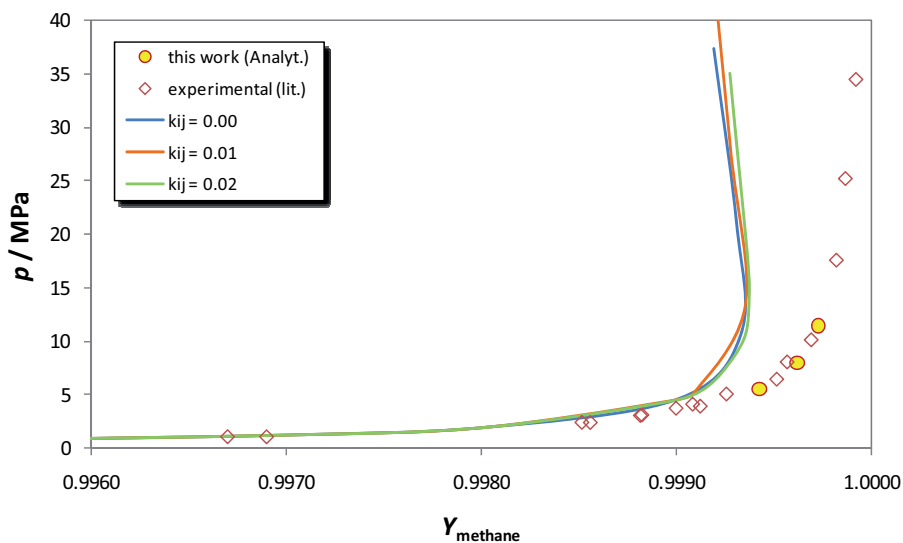


**Figure 7.5** – Modelling of the binary system methane + water, at 298 K, using sPC-SAFT correlations with different values of  $k_{ij}$ , and comparison with experimental data obtained in this work by the analytical method and data found in literature for the gas phase [4-6,12,13].

As for the calculations at 303 K, a value of  $k_{ij} = 0.007$  was found to be best for the representation of the experimental data. As in the calculations for 298 K, it was found that the model can give a very good representation of the equilibrium in the liquid phase, but fails to describe the gas phase. Figure 7.6 present the results of the modelling at this temperature for the liquid phase, together with the experimental data obtained in the present work, and with values found in the literature [2,8,14]. Figure 7.7 presents the results for the gas phase as well as experimental values obtained in this work by the analytical method and literature values [4,5].

For higher temperatures, the model started to reveal considerable difficulties in describing the equilibrium in the liquid phase. On the other hand, it seems more adequate for characterising the gas phase.

For a temperature of 323 K, a binary interaction parameter of 0.12 was found to be appropriate for the modelling of both phases, as presented in Figure 7.8 for the liquid phase, together with experimental values from the literature [15], and in Figure 7.9 for the gas phase, where values from the literature are also presented [12,13].

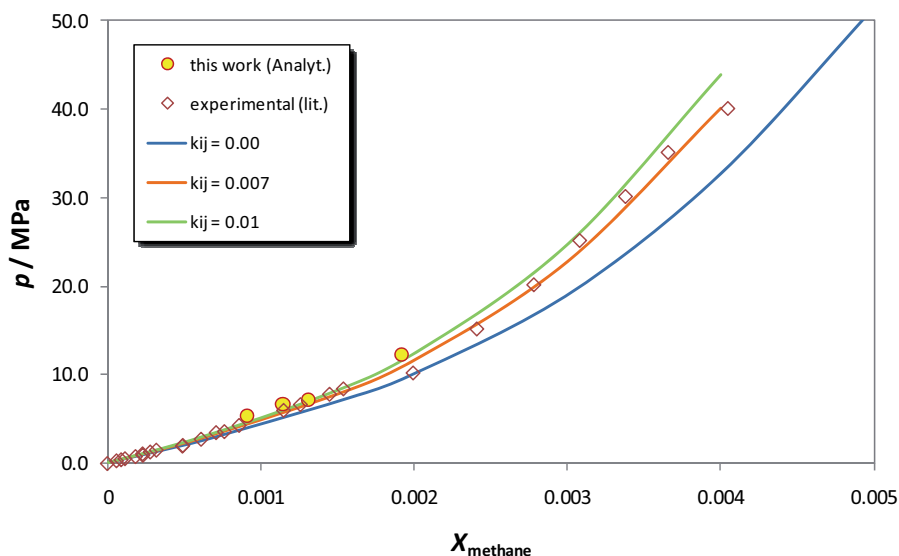


**Figure 7.6** – Modelling of the binary system methane + water, at 303 K, using sPC-SAFT correlations with different values of  $k_{ij}$ , and comparison with experimental data obtained in this work by the analytical method and data found in literature for the liquid phase [2,8,14].

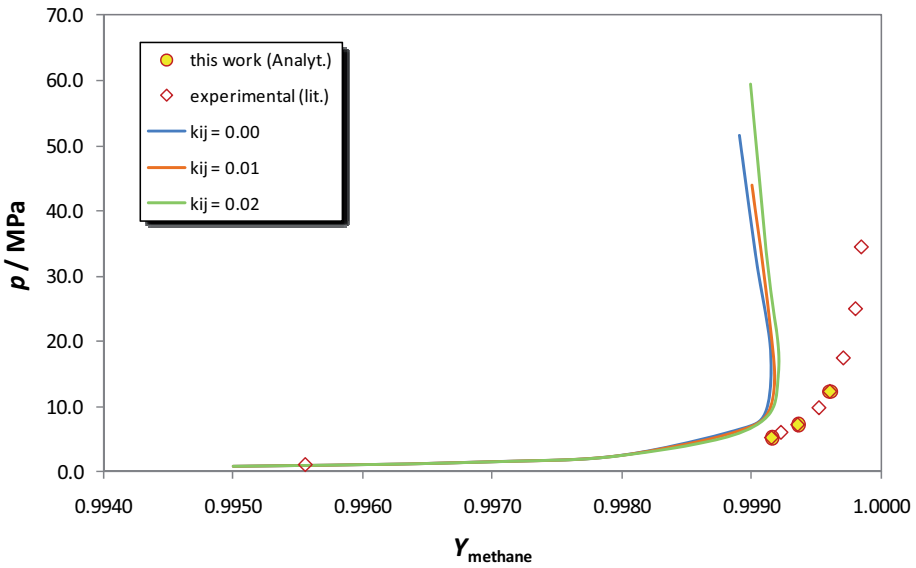


**Figure 7.7** – Modelling of the binary system methane + water, at 303 K, using sPC-SAFT correlations with different values of  $k_{ij}$ , and comparison with experimental data obtained in this work by the analytical method and data found in literature for the gas phase [4,5].

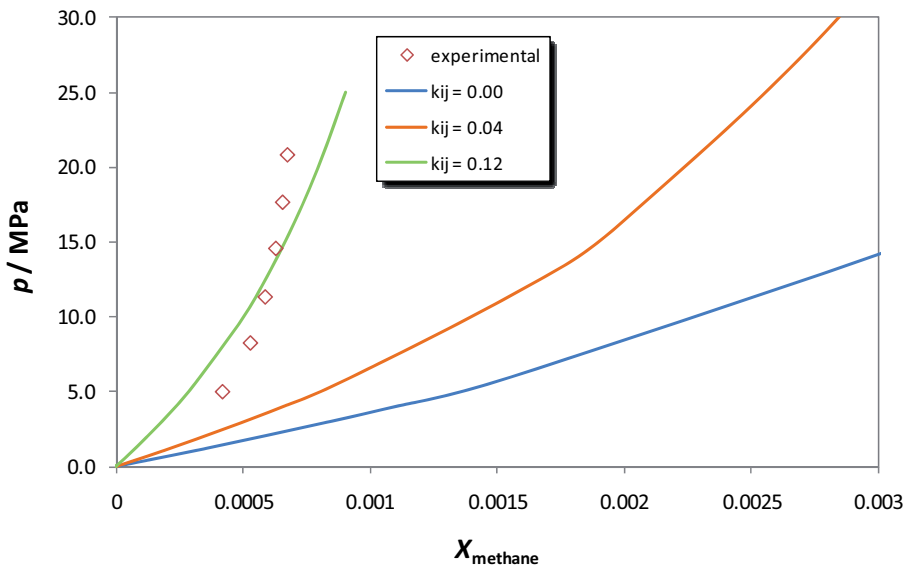


**Figure 7.8** – Modelling of the binary system methane + water, at 323 K, using sPC-SAFT correlations with different values of  $k_{ij}$ , and comparison with experimental data found in literature for the liquid phase [15].

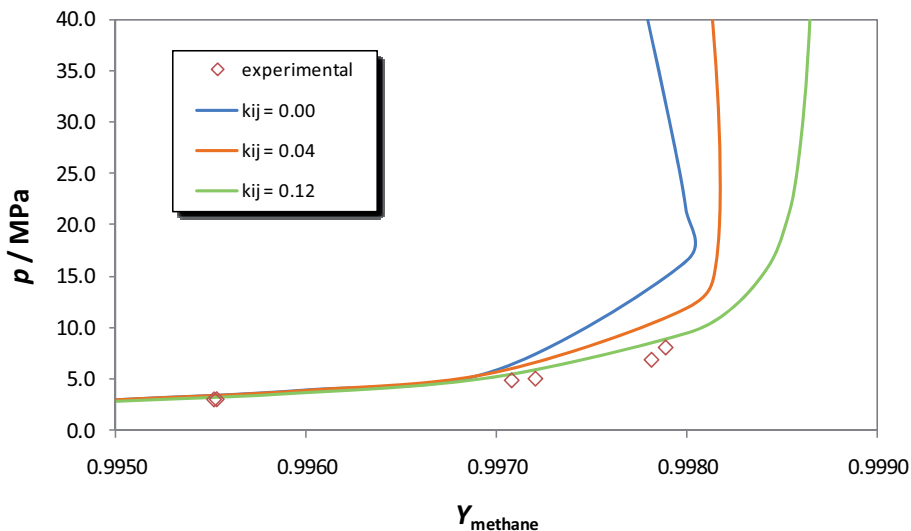


**Figure 7.9** – Modelling of the binary system methane + water, at 323 K, using sPC-SAFT correlations with different values of  $k_{ij}$ , and comparison with experimental data found in literature for the gas phase [12,13].

For a temperature of 373 K, an adequate modelling of this binary system can be achieved using a value of  $k_{ij}$  of 0.2, as shown in Figure 7.10 for liquid phase. Also observable in this graph is the discrepancy between the two sets of data found in the literature [14,15]. Since only these two sets of data were found in the literature for this range conditions, it is not possible to establish *a priori* which of the data sets is correct. However, judging by the tendencies observed for the other temperatures it can be assumed that the data of Kiepe et al. [14] may contain some errors. It is interesting to notice that the data of Michels et al. [15] was published in 1936, fact that shows that quality data maintains its relevance regardless of when it was measured.

The representation relative to the equilibrium for the gas phase at the temperature of 373 K is given in Figure 7.11, together with data found in literature [13].

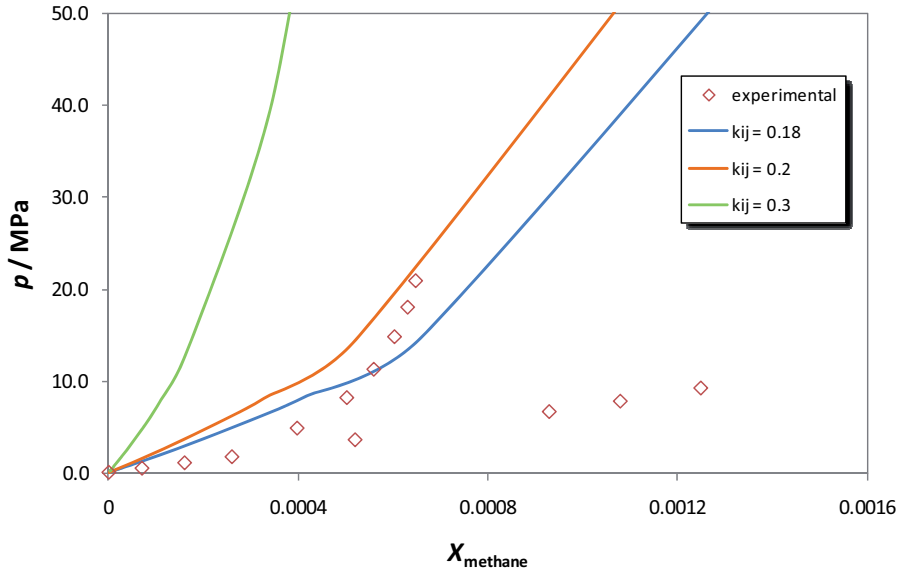


**Figure 7.10** – Modelling of the binary system methane + water, at 373 K, using simplified PC-SAFT correlations with different values of  $k_{ij}$ , and comparison with experimental data found in literature for the liquid phase [14,15].

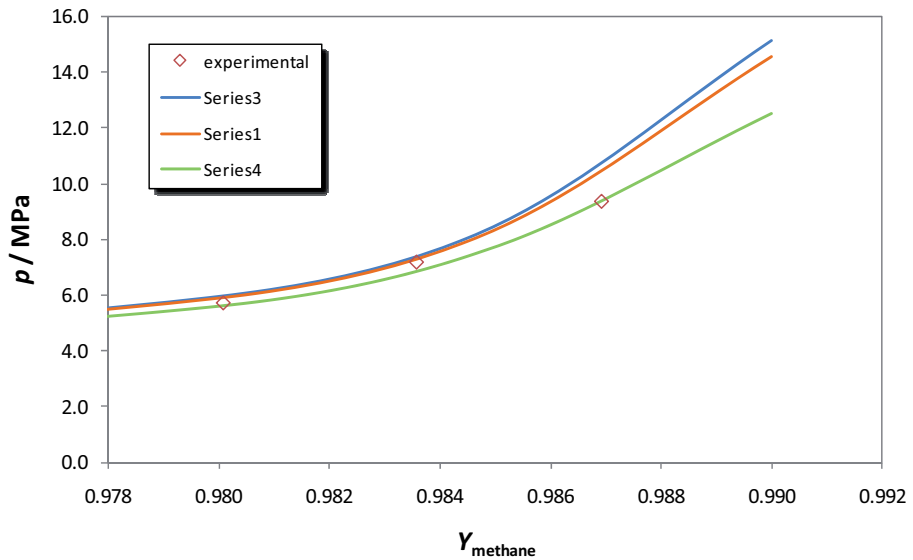


**Figure 7.11** – Modelling of the binary system methane + water, at 373 K, using simplified PC-SAFT correlations with different values of  $k_{ij}$ , and comparison with experimental data found in literature for the gas phase [13].

A summary of the  $k_{ij}$  values found in the modelling of this binary system for various temperatures is given in Table 7.5 and depicted in Figure 7.12, where it can be observed an almost linear dependence of the  $k_{ij}$  values with the temperature.

**Table 7.5** – Values of  $k_{ij}$  found in the modelling of the binary system methane + water, at five different temperatures between 283 K and 373 K.

$T / \text{K}$	$k_{ij}$
283	-0.025
298	0.000
303	0.007
323	0.120
373	0.200

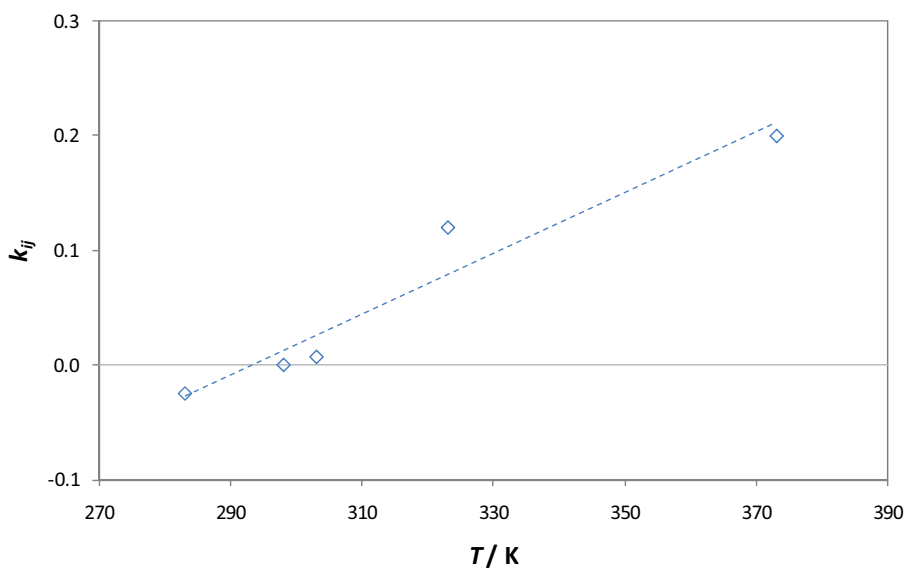


**Figure 7.12** – Values of  $k_{ij}$  found in the modelling of the binary system methane + water, at five different temperatures between 283 K and 373 K, showing the dependence of the  $k_{ij}$  values with temperature.

The modelling of this binary system was more challenging than initially expected. Although being a simple system, a temperature dependent  $k_{ij}$  has to be considered, and still, most often only one of the phases gets to be modelled correctly.

Also observed was the existence of discrepancies between different data sets. This was only presented for a temperature of 373 K since only two data sets are available for that temperature, but it was also verified for lower temperatures. However in those cases the existence of several data sets allow the identification of the anomalous data set, which was then not included in the calculations, nor in the graphical representations.

The complexity in the modelling, together with the discrepancy found between some sets of data, corroborates once again the importance of the new experimental quality measurements.

### 7.2.2. Binary System Methane + Methanol

The binary system methane + methanol was also modelled at 298 K. The correlation of the experimental data found in literature [16-18] is presented in Figure 7.13.

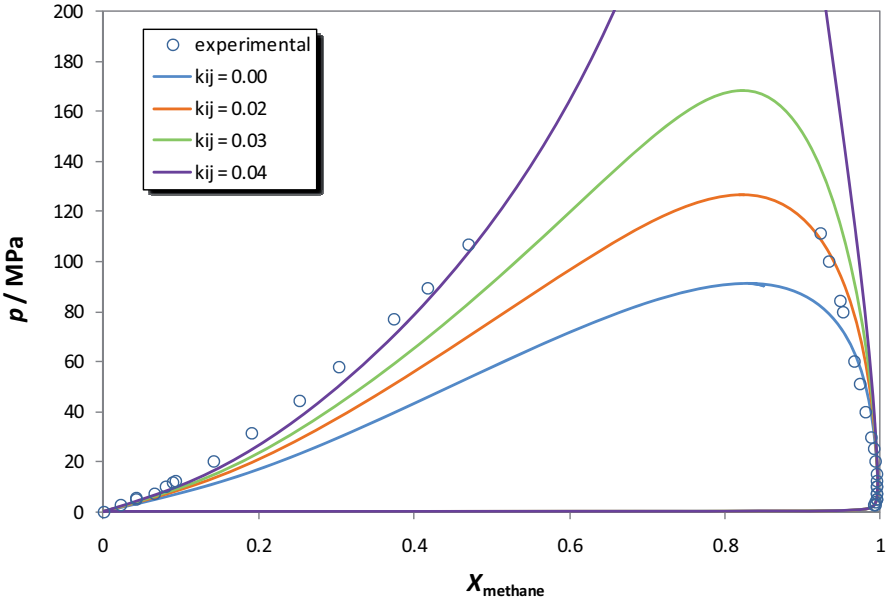


**Figure 7.13** – Results obtained in the modelling of the binary system methane + methanol, at 298 K, using sPC-SAFT correlations with different values of  $k_{ij}$ , and comparison with experimental data found in literature [16-18].

It is observable that a correct modelling of the liquid phase is achieved using a  $k_{ij}$  of 0.04. However, this value seems inadequate for the representation of the gas phase, for which a value of 0.02 for the  $k_{ij}$  would be preferable. For further calculations regarding the quaternary system studied in this chapter, the value of 0.04 will be used.

### 7.2.3. Quaternary System Methane + *n*-hexane + Methanol + Water

The quaternary system constituted by methane + *n*-hexane + methanol + water was modelled at conditions similar to the observed in the experimental measurements. The six binary interaction parameters used in this prediction are summarised in Table 7.6. As mentioned before, four of these parameters were already calculated and presented in Chapter 6.

**Table 7.6** – Values of  $k_{ij}$  found in the modelling of the six binary systems binary systems formed with the constituents of the quaternary system methane + *n*-hexane + methanol + water.

Compounds	$k_{ij}$
methane + <i>n</i> -hexane	0.01
methane + methanol	0.04
methane + water	0.00
<i>n</i> -hexane + methanol	0.03
<i>n</i> -hexane + water	0.055
Methanol + water	-0.04

These values of the binary interaction parameters were then used in a multiphase flash calculation for the temperature and pressure conditions studied experimentally. The results for 9.8 MPa are presented in Table 7.7, where a comparison with the experimental values obtained in this work is also given.

**Table 7.7** – Results obtained in a multiphase flash calculation using sPC-SAFT, for the mixture methane + *n*-hexane + methanol + water, at 298.42 K and 9.8 MPa, and comparison with experimental values.

Phase	Compound	Molar fraction		
		sPC-SAFT	experim. (this work)	deviation (%)
aqueous phase	methane	$5.18 \times 10^{-3}$	$3.01 \times 10^{-3}$	72
	<i>n</i> -hexane	$3.00 \times 10^{-5}$	$1.32 \times 10^{-5}$	127
	methanol	0.155	0.167	-7.2
	water	0.840	0.830	1.2
organic phase	methane	0.423	0.160	164
	<i>n</i> -hexane	0.566	0.818	-30
	methanol	$6.96 \times 10^{-3}$	$1.90 \times 10^{-2}$	-63
	water	$4.81 \times 10^{-3}$	$2.00 \times 10^{-3}$	140
gas phase	methane	0.982	--	--
	<i>n</i> -hexane	$1.64 \times 10^{-2}$	--	--
	methanol	$1.15 \times 10^{-3}$	--	--
	water	$6.74 \times 10^{-4}$	--	--

For the first set of results, at 9.8 MPa, the agreement of the calculations with the experimental values for the inorganic phase is remarkable, considering the predictive character of the calculation and the complexity of the system. The success of the model is evident even in the prediction of extremely small amounts, such as the mole fraction of *n*-hexane, in the order of  $10^{-5}$ . For the mole fraction of water and methanol, the prediction has accuracy better than 10%.

For the organic phase, the model seems to have overestimated the solubility of methane in this phase, and the results are less accurate than for the aqueous phase. Nevertheless, the calculated molar fraction of methanol and water do not differ greatly from the experimental values, again considering that these are very low values.

In an attempt to verify the influence of the value of  $k_{ij}$  relative to the binary system methane + *n*-hexane in the prediction of the composition of the organic phase, some calculations were performed. The results, presented in Table 7.8, show that the value of this binary interaction parameter influences greatly the composition of the organic phase, without altering significantly the compositions of the other two phases in equilibrium.

However, in order to achieve values in accordance to the experimental data obtained in this work, a  $k_{ij}$  of 0.15 is required, which would be too high for the modelling of the binary system under consideration.

**Table 7.8** – Influence of  $k_{ij}$  values for the binary system methane + *n*-hexane in the multiphase flash calculation for the mixture methane + *n*-hexane + methanol + water, at 298.42 K and 9.8 MPa.

$k_{ij}$	Compound	Molar fraction		
		aqueous phase	organic phase	gas phase
0.05	methane	$5.19 \times 10^{-3}$	0.342	0.983
	<i>n</i> -hexane	$3.40 \times 10^{-5}$	0.645	$1.52 \times 10^{-2}$
	methanol	0.155	$7.68 \times 10^{-3}$	$1.15 \times 10^{-3}$
	water	0.840	$5.33 \times 10^{-3}$	$6.73 \times 10^{-4}$
0.10	methane	$5.20 \times 10^{-3}$	0.252	0.985
	<i>n</i> -hexane	$3.80 \times 10^{-5}$	0.734	$1.34 \times 10^{-2}$
	methanol	0.155	$8.07 \times 10^{-3}$	$1.15 \times 10^{-3}$
	water	0.840	$5.72 \times 10^{-3}$	$6.71 \times 10^{-4}$
0.15	methane	$5.21 \times 10^{-3}$	0.181	0.987
	<i>n</i> -hexane	$4.10 \times 10^{-5}$	0.805	$1.14 \times 10^{-2}$
	methanol	0.155	$8.04 \times 10^{-3}$	$1.14 \times 10^{-3}$
	water	0.840	$5.86 \times 10^{-3}$	$6.69 \times 10^{-4}$

In fact, and recalling the analysis of the two experimental data sets, it is possible that the source of this divergence for the composition of the organic phase may be related to the quality of the first set of experimental data, and to the possible problem of non-equilibrium.

In order to better interpret the results of the predictive modelling, an analysis of the results obtained for a pressure of 7.3 MPa is helpful. The results for this pressure are presented in Table 7.9, where again, a comparison with the experimental values obtained in this work is also given.

In this case, the agreement with the results obtained for the inorganic phase is not as significant as before, but nevertheless a good agreement is observed, with exception for the amount of *n*-hexane, with is now 3 orders of magnitude lower than the experimental value.

**Table 7.9** – Results obtained in a multiphase flash calculation using sPC-SAFT, for the mixture methane + *n*-hexane + methanol + water, at 298.31 K and 7.3 MPa, and comparison with experimental values.

Phase	Compound	Molar fraction		
		sPC-SAFT	experim. (this work)	deviation (%)
aqueous phase	methane	$4.18 \times 10^{-3}$	$3.9 \times 10^{-2}$	-89
	<i>n</i> -hexane	$3.30 \times 10^{-5}$	$4.8 \times 10^{-2}$	-100
	methanol	0.155	0.149	4.0
	water	0.841	0.764	10
organic phase	methane	0.334	0.425	-21
	<i>n</i> -hexane	0.654	0.529	-24
	methanol	$7.24 \times 10^{-3}$	$4.6 \times 10^{-2}$	-84
	water	$5.13 \times 10^{-3}$	$< 2 \times 10^{-4}$	--
gas phase	methane	0.985	0.975	1.0
	<i>n</i> -hexane	$1.26 \times 10^{-2}$	$2.4 \times 10^{-2}$	-48
	methanol	$1.27 \times 10^{-3}$	$7.6 \times 10^{-4}$	67
	water	$7.22 \times 10^{-4}$	$< 2 \times 10^{-4}$	--

More important, is the improvement in the concordance observed for the organic liquid phase, caused by the significant changes in the experimental results, rather than by changes in the results of the model. This fact seems to support the idea that the first set of data was not the most accurate.

As for the composition of the gas phase, the agreement between the predictions of the model and the experimental values is again very good, demonstrating that the simplified PC-SAFT EoS shows a great potential for the prediction of equilibrium in these type of systems.

Relatively to the experimental results, it is necessary to take into account that this was the first actual measurements performed in a multiphase system, and unfortunately, within a very limited time frame. It is therefore natural that situations such as the verified in the measurement of the first set of data occur, as part of a natural process in which the real operating characteristics and sometimes limitations of the apparatus are acknowledged by the operator. This verifies not only for the case of a new apparatus, but for any situation in which a researcher begins working with previously existing equipment, following the popular proverb that practice leads to perfection.

This is one of the reasons why continuity is so important in experimental work, in order to make use of the experience acquired in the work with a particular set-up.

In the present work, further measurements and calculations would have been extremely useful in order to better identify the reasons of the divergences between the two sets of experimental data, and to continue the testing of the theoretical model applied. Unfortunately this was not possible due to the aforementioned time limitations.

## **References**

- [1] A. Chapoy, A. H. Mohammadi, D. Richon, B. Tohidi, *Fluid Phase Equilib.* 220 (2004) 113-121.
- [2] L. K. Wang, G. J. Chen, G. H. Han, X. Q. Guo, T. M. Guo, *Fluid Phase Equilib.* 207 (2003) 143-154.
- [3] Y. Wang, B. Han, H. Yan, R. Liu, *Thermochim. Acta* 253 (1995) 327-334.
- [4] A. Chapoy, C. Coquelet, D. Richon, *Fluid Phase Equilib.* 214 (2003) 101-117.
- [5] A. Chapoy, C. Coquelet, D. Richon, *Fluid Phase Equilib.* 230 (2005) 210-214.
- [6] A. Chapoy, A. H. Mohammadi, B. Tohidi, D. Richon, *J. Chem. Eng. Data* 50 (2005) 1157-1161.
- [7] G. K. Folas, E. W. Froyne, J. Lovland, G. M. Kontogeorgis, E. Solbraa, *Fluid Phase Equilib.* 252 (2007) 162-174.
- [8] J. R. Duffy, N. O. Smith, B. Nagy, *Geochim. Cosmochim. Acta* 24 (1961) 23-31.
- [9] Y. S. Kim, S. K. Ryu, S. O. Yang, C. S. Lee, *Ind. Eng. Chem. Res.* 42 (2003) 2409-2414.
- [10] R. K. Stoessel, P. A. Byrne, *Geochim. Cosmochim. Acta* 46 (1982) 1327-1332.
- [11] S. O. Yang, S. H. Cho, H. Lee, C. S. Lee, *Fluid Phase Equilib.* 185 (2001) 53-63.

- [12] C. Yokoyama, S. Wakana, G. Kaminishi, S. Takahashi, *J. Chem. Eng. Data* 33 (1988) 274-276.
- [13] M. Rigby, J. M. Prausnitz, *J. Phys. Chem* 72 (1968) 330-334.
- [14] J. Kiepe, S. Horstmann, K. Fischer, J. Gmehling, *Ind. Eng. Chem. Res.* 42 (2003) 5392-5398.
- [15] A. Michels, J. Gerver, A. Bijl, *Physica* 3 (1936) 797-808.
- [16] E. Brunner, W. Hultenschmidt, G. Schlichtharle, *J. Chem. Thermodyn.* 19 (1987) 273-291.
- [17] N. L. Yarymagaev, R. P. Sinyavskaya, I. I. Koliushko, L. Y. Levinton, *J. Appl. Chem. USSR* 58 (1985) 154-157.
- [18] N. L. Yarymagaev, R. P. Sinyavskaya, I. I. Koliushko, L. Y. Levinton, *Zh. Prikladnoi Khim.* 58 (1985) 165-168.

## **Chapter 8**

# ***Solubility of Carbon Dioxide in Aqueous Solutions of Amino-acid Salts***

---

As mentioned in the introduction, a part of the present work was dedicated to the topic of carbon dioxide capture, through the study of the sorption of this gas in amine and amino-acid salts solutions, as a contribution to a project currently on-going in the research group.

The solubility of carbon dioxide in aqueous solutions of amino-acid salts is currently under study by means of an analytical isobaric-isothermal method, more precisely through a semi-flow method, in which a synthetic gaseous mixture containing approximately 10% of carbon dioxide, simulating the composition of a typical flue gas, is continuously bubbled through the aqueous solution at pressures very close to atmospheric pressure, with the concentration of carbon dioxide being monitored in the effluent stream. Besides the determination of some kinetic parameters, this method also allows the calculation of the maximum load of carbon dioxide to be absorbed by the solution, through the integration over time of the concentration of carbon dioxide in the effluent stream.

Due to several characteristics of this recently developed apparatus, such as the fact that the equilibrium cell and other important parts are made entirely of glass, the impossibility for the inclusion in the system of a back-pressure regulator, or the type of sensor used for the quantification of the carbon dioxide concentration in the effluent stream, its applicability is limited to atmospheric pressure. However, it is of interest to

industry to have information on the sorption of carbon dioxide in these solutions at pressures around 0.2 MPa or 0.3 MPa [1]. Due to the relative simplicity of these systems, the solubility of carbon dioxide in a solution can easily be determined at different values of pressure using a synthetic method, as demonstrated in Chapter 5 with the measurement of the solubility of methane in water.

Furthermore, the conjugation of the two methods in the study of the same systems is also very interesting from an experimental perspective, since it allows inferring the consistency of the results produced by the two apparatus, both of them developed recently, and it allows the establishment of comparisons between the two methods, underlining the advantages and disadvantages of each one of them.

Previous to the study of the systems in question, with the aqueous solutions of amino-acid salts, preliminary measurements were performed using well known systems, in order to have a better understanding of the optimal conditions to be used in the experiments. This is an important step as it may allow the anticipation of experimental problems that may arise during the measurements. In this work, the solubility of carbon dioxide in pure water was firstly measured at temperatures close to 298 K. Subsequently, measurements of the solubility of carbon dioxide in an aqueous solution of 2-aminoethanol (monoethanolamine or MEA) were also performed at temperatures around 298 K, anticipating the measurements with amino-acid salts.

## ***8.1. Sorption of Carbon Dioxide in Amine-based Aqueous Solutions***

The separation and capture of carbon dioxide has been an important operation in different areas of industry for a long time, in cases such as natural gas production, in which CO<sub>2</sub> has to be removed since its presence in the final product is undesirable [2], but also in many other industries based in the various applications of carbon dioxide, such as enhanced oil recovery, supercritical processes, carbonation of brine, welding as an inert gas, food and beverage carbonation, dry ice, urea production and soda ash industry [3,4].

Nevertheless, the topic of carbon dioxide capture attained a whole new dimension with the recent environmental concerns related to the climate changes and the reducing of

the emissions of greenhouse gases. The contribution of carbon dioxide to enhancing the greenhouse effect is estimated to be around 60% [2], placing this gas in the centre of the majority of the current environmental policies, which in turn supports the substantial expansion in the research performed on this area.

From the different technologies available for separation and capture of carbon dioxide, such as absorption, adsorption, membrane separation, cryogenic separation or biological capture, all of them recently reviewed by different authors [3,5,6], absorption is presently the most commonly used technology, being regarded by some authors as the most viable solution for at least, the near-term future, when compared with the other methods [7]. Monoethanolamine (MEA) has been the most frequently used sorbent, presenting several advantages when compared with other amines, such as high reactivity, low cost, low molecular weight and consequently, a high absorbing capacity per mass unit, presenting also a reasonable thermal stability and degradation rate [2,8]. Among the disadvantages in the use of MEA, is a high enthalpy of reaction with CO<sub>2</sub>, leading to a higher energy consumption in the desorption process, the formation of a stable carbamate, the formation of degradation products under particular conditions, the inability to remove mercaptans and vaporisation losses caused by the relatively high vapour pressure of their aqueous solutions. Furthermore, MEA is also more corrosive than many other alkanolamines requiring sometimes the use of corrosion inhibitors [2,8].

Other amines have been considered as an alternative, among which (2-aminoethyl)ethanolamine (AEEA), a diamine offering a high absorption rate and a high absorption capacity, in addition to a much lower vapour pressure than MEA [2,9]. Methyl-diethanolamine (MDEA) and diethanolamine (DEA) have also been used for the CO<sub>2</sub> absorption in the gas industry [10,11]. Park and his co-workers conducted a series of studies during the last years, focusing on the sorption of carbon dioxide in a number of different sorbent materials, such as aqueous solutions of xanthan gum containing monoethanolamine [12], aqueous solutions of 1,8-diamino-*p*-menthane [13], aqueous solutions of 2-amino-2-methyl-1-propanol [14], among several other materials.

The process of amine absorption of carbon dioxide from the flue-gas of fossil-fuelled power plants usually consists in passing the flue-gas through an absorption column where an amine-based solvent is sprayed into the gas flow, with carbon dioxide being captured in the liquid phase, bonded through chemical reactions. The amine solution is then

regenerated in a different column, the desorber, where it is heated up to about 393 K (120 °C), resulting in a carbon dioxide stream with purity from 95% up to 99% which leaves the desorber, being the lean amine solution recycled to the absorber column. This process is represented in Figure 8.1.

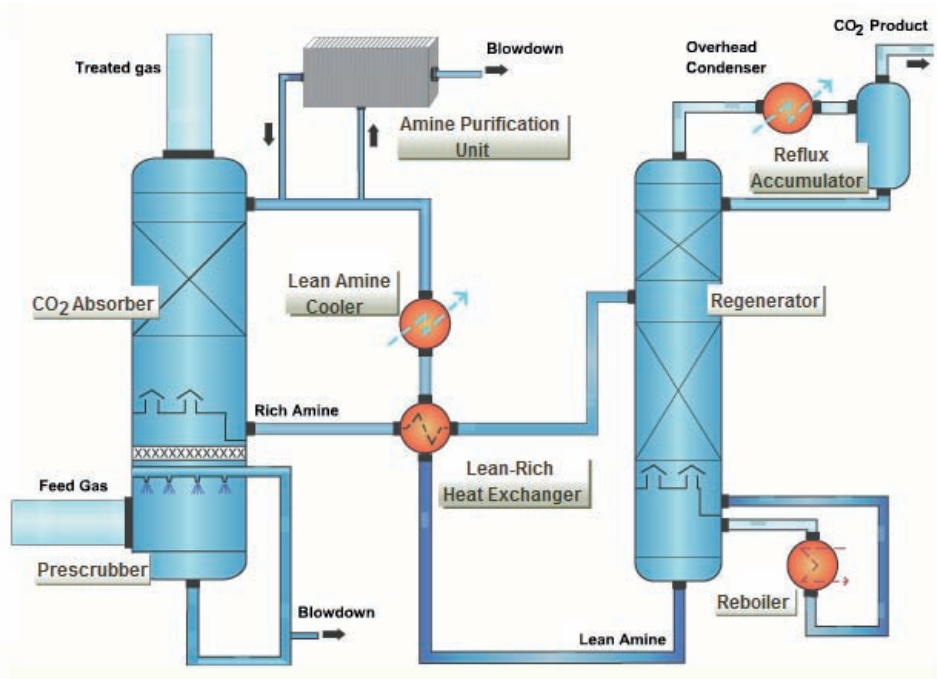


**Figure 8.1** – Flow-sheet of the amine absorption process of carbon dioxide, from the flue-gas of fossil-fuelled power plants. Source: Cansolv [15].

However the current absorption technologies for carbon dioxide capture are somewhat energy intensive, and consequently costly, having an adverse affect in the economics of many industrial processes. Improvements are therefore imperative, in order to overcome these aspects, either through innovative process design, or through the selection of new and better sorbents [9].

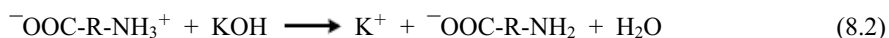
Recently, as part of the search for new sorbent materials, a significant number of works were published on the subject of the use of ionic liquids for the capture of carbon dioxide [16-27]. Another recent tendency is the use of amino-acid salt solutions [28-37]. Aqueous alkaline salts of amino-acids, usually potassium or lithium salts, but also sodium

salts in some cases, are an interesting alternative for the currently used alkanolamines. Generally these solutions are characterized by lower vapour pressures due to their ionic nature, and amino-acids have the same functional groups as alkanolamines, and thus expected to behave similarly towards carbon dioxide, although presenting a higher stability towards oxidative degradation [32,38]. In fact, the chemical reactivity with carbon dioxide is comparable or even higher than those of alkanolamines, presenting also further advantages such as a higher CO<sub>2</sub> loading and, most importantly, relative low energy requirements for regeneration. Another interesting characteristic is their ability to precipitate solids when absorbing carbon dioxide, which in some cases can contribute to a further increase in the loading capacity. The high surface tension of the aqueous solutions of amino-acid salts makes them an interesting alternative to be considered for gas-liquid membrane applications, without the requirements for expensive membranes as it happens in the case of MEA [35,36].

Considering an amino-acid with the generic formula HOOC-R-NH<sub>2</sub> dissolved in water, the following equilibrium is established, in which the neutral molecule assumes the form of a zwitterion:



The addition of potassium hydroxide removes a proton from the amino-acid, leaving the molecule with a -NH<sub>2</sub> group similar to the active group in the alkanolamines:



The reaction of the potassium salt of the amino-acid with carbon dioxide follows the typical path of the reaction of an alkanolamine, with the formation of carbamate and bicarbonate.

*Carbamate formation:*



*Carbamate hydrolysis:*



*Bicarbonate formation:*



The hydrolysis of the carbamate is usually not very important for primary amines, and most of the absorbed carbon dioxide will be in the form of carbamate, and thus, it can be considered that two moles of the original amine, or of the amino-acid salt, are required to absorb one mole of carbon dioxide.

Under certain conditions, with high amino-acid salt concentration and/or high  $\text{CO}_2$  loadings, precipitation may occur, which can either be constituted by the zwitterions, a product of reaction 8.3, or by a bicarbonate salt. In any case, this precipitation will shift the equilibrium 8.3 to the formation of more products, increasing the absorption capacity of the solution, and consequently also shifting the equilibrium pressure downwards. Figure 8.2 presents a plot of an equilibrium curve relative to a solution with a concentration of  $6 \text{ mol}\cdot\text{dm}^{-3}$  of an undisclosed amino-acid salt, at a temperature of 313 K (40 °C), according to the work presented by Brouwer et al. [37].

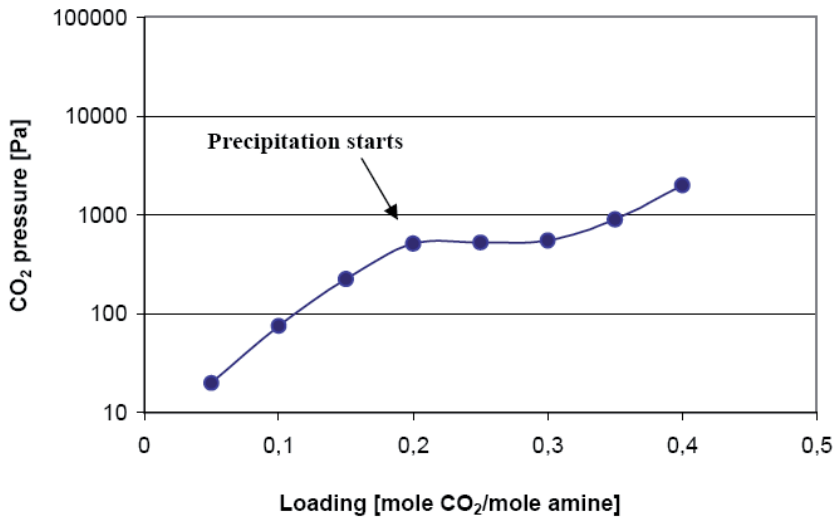


**Figure 8.2** – Equilibrium curve relative to a solution with a concentration of  $6 \text{ mol}\cdot\text{dm}^{-3}$  of an undisclosed amino-acid salt, at a temperature of 313 K (40 °C), according to the presented by Brouwer et al. [37].

A plateau in the carbon dioxide equilibrium pressure can be seen, caused by the occurrence of precipitation for a CO<sub>2</sub> loading of around 0.2. From this point on, the equilibrium pressure does not increase with the increase of the loading, until a loading value of about 0.3 is reached, where no further significant precipitation occurs. The overall consequence is a significant increase in the total solvent loading for a particular pressure, allowing a reduction in the costs associated to the CO<sub>2</sub> capture process. Nonetheless, it is necessary to take into account that, in order to make a good use of this precipitation phenomenon at industrial level, several modifications need to be implemented in terms of process design and in the equipment typically used with the amine solutions.

By increasing the temperature, the precipitate re-dissolves, allowing the regeneration of the solvent in process similar to that used with the alkanolamines. Furthermore, another advantage of the use of amino-acid salt solutions, is the fact that a lower temperature is required for the regeneration of the absorbent, which can be performed at temperatures around 353 K (80 °C), instead of the approximately 393 K (120 °C) commonly used for the regeneration of MEA. Alternatively, the regeneration can be performed at temperatures similar to those used for MEA, leading to a higher extent of regeneration, in any case allowing a further reduction in the costs of the process.

In their work, Brouwer and his co-workers [37] presented a study of the costs associated to the CO<sub>2</sub> capture using the amino-acid salt technology, concluding that it can result in a price per ton of removed CO<sub>2</sub> of about one half of the price inherent to the MEA-based process, emphasising the great potential of this new technology.

Recent news shows that this potential is being seriously taken into account by industry. In April 2008 the Royal Society of Chemistry announced in the online news the intention of the Netherlands to implement the use of amino-acid-based sorbents, in a project ran by TNO, The Netherlands Organisation for Applied Scientific Research, in which a pilot unit will be fitted to a 1040 MW coal-fired plant run by E.ON Benelux, for extraction of 90% of the carbon dioxide contained in 5% of the plant's flue gas waste stream, wich translates into around 6 tonnes of CO<sub>2</sub> per day [39]. In June 2009, a joint press release from Siemens AG and TNO announced a cooperation agreement aimed at the further development of the amino-acid salt-based carbon capture technology, using the experience acquired by Siemens AG who is using the amino-acid process for CO<sub>2</sub> capture in the industrial park in Frankfurt Höchst, Germany, and the knowledge and experience of

TNO in this area, with the aim of developing a full-scale demonstration plant by 2014 [40]. Also in 2009, E.ON announced the start-up of a pilot plant, due in the summer of that year and expected to operate until the end of 2010, putting the amino-acid salt concept to the test under real operating conditions at the Staudinger 5 hard-coal-fired plant in Grosskrotzenburg near Hanau, in Germany, ran by E.ON Kraftwerke GmbH [41]. In the same article, a joint project between Siemens AG and the Norwegian state-owned company Statkraft was also announced, in order to adapt the amino-acid salt technology for carbon capture to the use at combined cycle plants [41].

## **8.2. Experimental Results**

As previously mentioned, before proceeding with the experiments using aqueous solutions of amino-acid salts, preliminary measurements on the solubility of carbon dioxide in pure water and in an aqueous solution of 2-aminoethanol (MEA) were performed at temperatures around 298 K.

### **8.2.1. Solubility of Carbon Dioxide in Water**

The results of a literature survey performed for the binary system carbon dioxide and water is presented in Table 8.1, together with information on the temperature and pressure ranges for each of the cited references. In addition to these works, several reviews can also be found in the literature, such as the one by Diamong and Akinfiev [42] already mentioned in this work in a previous chapter, for a wide range of temperatures and pressures, from 272 K to 373 K and from 0.1 MPa to 100 MPa. Another review was presented by Spycher et al. [43] for an interval of temperatures between 285 K and 373 K, and pressures up to 60 MPa. Previous to these two works are the reviews presented by Carroll et al. [44] for the solubility of carbon dioxide in water at moderate pressures, up to 1 MPa, and by Crovetto [45], relative to the solubility of the gas in a range of temperatures going up to the critical temperature of water, at 647 K.

**Table 8.1** – List of references found in a literature search for the binary system carbon dioxide + water.

$T / \text{K}$	$p / \text{MPa}$	Ref.
298 - 373	1.7 - 5.1	[46]
273 - 348	2.5 - 30.4	[47]
285 - 323	2.5 - 82.9	[48]
323 - 373	0.1 - 70.9	[49]
273 - 373	0 - 3.7	[50]
373 - 473	0.3 - 8.1	[51]
285 - 373	2.5 - 70.9	[52]
323 - 323	10.1 - 30.1	[53]
288 - 313	5.2 - 20.3	[54]
323 - 348	10.1 - 15.2	[55]
323 - 323	6.8 - 17.7	[56]
298 - 298	3.6 - 11.0	[57]
323 - 353	10.1 - 25.3	[58]
373 - 473	0.5 - 6.7	[59]
383 - 623	10 - 300	[60]
323 - 623	20 - 350	[61]
473 - 603	20.3 - 60.8	[62]
244 - 296	1.5 - 6.1	[63]
323 - 343	3.1 - 8.8	[64]
344 - 344	10 - 100	[65]
374 - 393	2.3 - 70.3	[66]
498 - 548	114 - 311	[67]
273 - 273	2.5 - 2.5	[68]
348 - 421	10 - 20	[69]
353 - 471	2.0 - 10.2	[70]
278 - 338	0.1 - 0.1	[71]
298 - 298	0.1 - 0.1	[72]
273 - 353	0.1 - 0.1	[73]
448 - 523	1.5 - 9	[74]
373 - 423	5 - 5	[75]
348 - 348	5 - 5	[76]
283 - 303	0.1 - 2.03	[77]
293 - 293	0.5 - 1.9	[78]
278 - 318	0.47 - 8.0	[79]

The measurements of the solubility of carbon dioxide in water were performed in the cell presented in Chapter 5, according to the synthetic isothermal method, in a procedure similar to that described for the measurements of the solubility of methane in water. The experiments were carried out at temperatures around 298 K, and at pressures varying between 0.3 MPa and 0.9 MPa. Carbon dioxide with a purity of 99.995%, produced by Linde AG, Germany, and supplied by AGA A/S, Denmark, was used in the experiments, together with deionised water. The amount of carbon dioxide charged into the cylinder was determined gravimetrically, by means of an analytical balance Mettler-Toledo PR1203 with a precision of 0.001 g. The obtained results are presented in Table 8.2 and represented in Figure 8.3, where values from literature [44,50,79], used for comparison, are also shown.

**Table 8.2** – Results obtained in the in the measurements of the solubility of carbon dioxide in pure water, at temperatures around 298 K.

$T / \text{K}$	$p / \text{MPa}$	$x_{\text{CO}_2} \times 10^3$
299.64	0.342	1.712
299.76	0.551	3.193
299.61	0.752	4.125
298.10	0.558	3.011
298.23	0.305	1.645
298.11	0.311	1.715
298.10	0.861	5.036
298.09	0.435	2.454
298.09	0.435	2.476

It is noticeable that for the lower pressures studied, some of the results obtained in this work are slightly lower than literature. Nevertheless a very good agreement is observed, especially considering the low quantities in question.

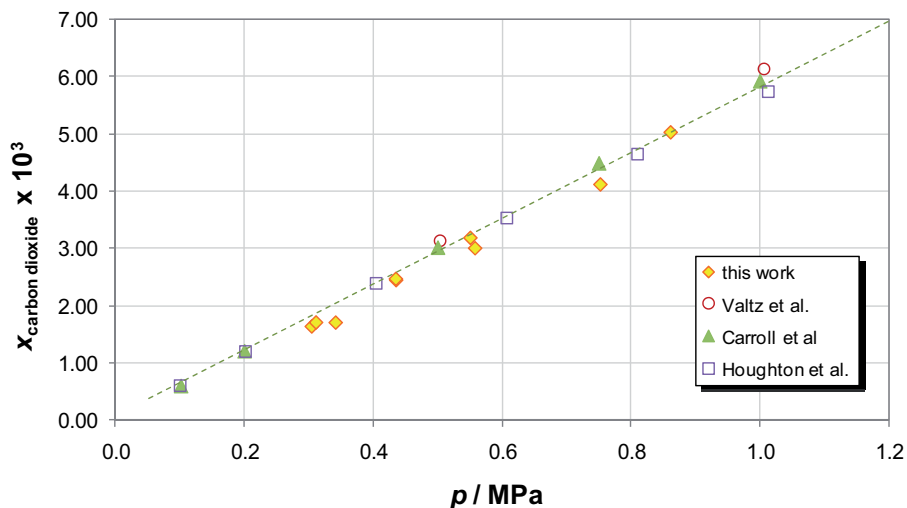


**Figure 8.3** – Results obtained in the measurements of the solubility of carbon dioxide in pure water, at temperatures around 298 K, and comparison with values from literature [44,50,79]. The dashed line in the graph is given merely for eye guidance, although based in the literature data.

### **8.2.2. Solubility of Carbon Dioxide in Aqueous Solutions of 2-aminoethanol**

The measurements of the solubility of carbon dioxide in an aqueous solution of MEA, (2-aminoethanol) were performed according to the same synthetic isothermal method already described. The gas used was carbon dioxide with a purity of 99.995%, produced by Linde AG, Germany, and supplied by AGA A/S, Denmark. The amount of gas used in each experiment was determined gravimetrically, by means of an analytical balance Mettler-Toledo PR1203 with a precision of 0.001 g. The same balance was used in the preparation of the MEA solution, for which deionised water was used, together with an adequate amount of 2-aminoethanol with a purity superior to 99%, from Sigma-Aldrich. The exact concentration of the solution used in the experiments, prepared simultaneously gravimetrically and volumetrically, was 29.6 wt%, equivalent to 4.84 mol.dm<sup>-3</sup>. The experiments were performed at temperatures around 298 K, and at pressures less than 0.6 MPa. The results are presented in Table 8.3 and in Figure 8.4, together with experimental values from literature [8,80] and with the extended UNIQUAC model [81].

**Table 8.3** – Results obtained in the in the measurements of the sorption of carbon dioxide in an aqueous solution of 2-ethanolamine 30 wt%, at temperatures around 298 K.

$T / \text{K}$	$p / \text{MPa}$	loading ( $\text{mol}_{\text{CO}_2} / \text{mol}_{\text{MEA}}$ )
298.15	0.006	0.269
298.07	0.432	0.730
300.13	0.523	0.736
298.17	0.510	0.742
298.17	0.049	0.582

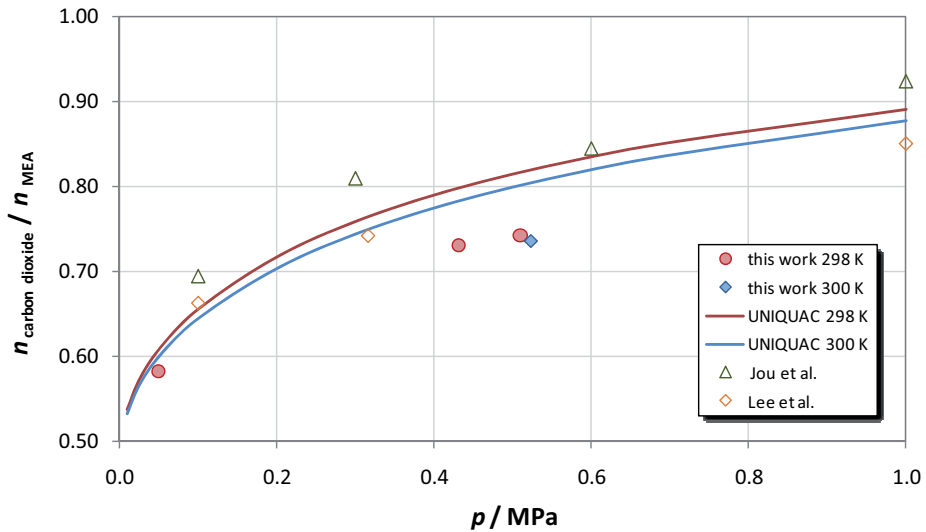


**Figure 8.4** – Results obtained in the measurements of the sorption of carbon dioxide in an aqueous solution of 2-ethanolamine 30 wt%, at temperatures around 298 K, and comparison with experimental values from literature [8,80] and with the extended UNIQUAC model [81].

As it can be seen in the graph, the results obtained in the present work are considerably lower than the values found in literature, both the experimental and the predicted by the extended UNIQUAC model. This fact is worrying since the fundament of these preliminary measurements was to attest the possibility of study of amino-acid solutions.

Despite the deviations to the literature, it is possible to observe in the results the influence of the temperature in the loading, a sign that the results are most certainly affected by a systematic error, rather than by scattering, or by uncertainty associated to the experimental method. In addition, the agreement between the results of different experiments performed under the same conditions is remarkable. With this in mind, an analysis of all the experimental conditions and possible sources of errors was performed, leading to the conclusion that the origin of the deviations in the results was possibly the degradation of MEA, since the solution used in the experiments was not freshly prepared, as it had been prepared for other experiments carried out in another experimental set-up.

To illustrate this possibility, Figure 8.5 shows the same experimental results corrected for a MEA degradation of 5%.

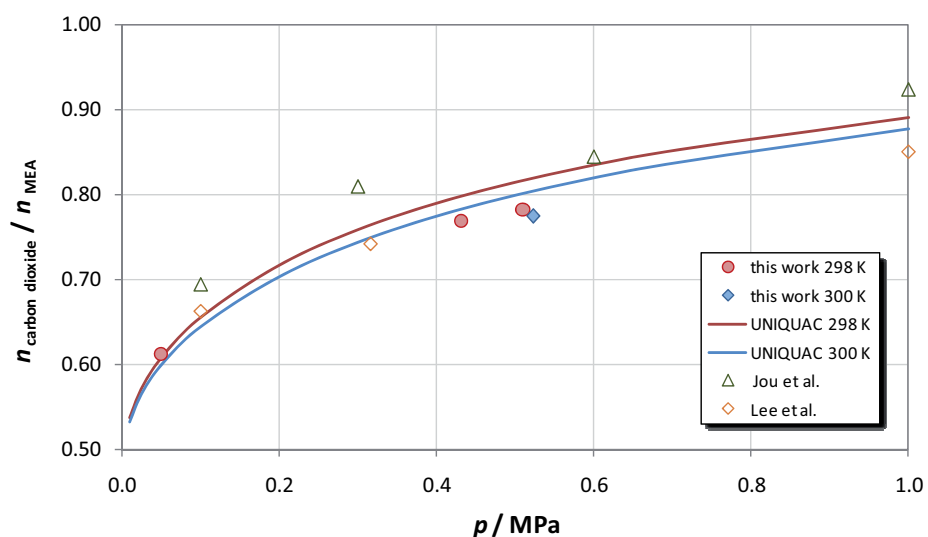


**Figure 8.5** – Results obtained in the measurements of the sorption of carbon dioxide in an aqueous solution of 2-ethanolamine 30 wt%, at temperatures around 298 K, corrected for a possible degradation of 5% of 2-ethanolamine, and comparison with experimental values from literature [8,80] and with the extended UNIQAC model [81].

Although still lower than the predictions of the extended UNIQAC model [81], or the values obtained by Jou et al. [8], the results are now in a good agreement with the values published by Lee et al. [80]. Assuming a degradation of 8% would lead to the results being in perfect agreement with the model presented.

Since the calculations of the results were performed *a posteriori*, it was not possible to verify the validity of this idea with the titration of the solution. However, the exchange of ideas with several colleagues seems to corroborate that the degradation of MEA should be the most probable cause for the results achieved.

### **8.2.3. Solubility of Carbon Dioxide in Aqueous Solutions of Amino-acid Salts**

As mentioned, this part of the work is a contribution to another project, for which other researchers within the research group previously performed a series of screening experiments using the aforementioned semi-flow apparatus. The results of these screening experiments pointed out the amino-acid L-proline as one of the more suitable sorbents, a result in agreement with the work of van Holst [36], who studied the behaviour of solutions of potassium salts of seven different amino-acids, having reached the conclusion that, for equal concentrations, L-proline and sarcosine were the most promising absorbents.

#### ***L-proline***

The experiments focused on the determination of the loading capacity of the solutions of this amino-acid at 300 K, and on desorption at 353 K (80 °C). Furthermore, longer experiments were performed, with temperature cycles between these two temperatures, in order to evaluate the possible influence of the cycles in the absorption capacity of the amino-acid at 300 K.

A first aqueous solution of the potassium salt of L-proline was prepared simultaneously volumetrically and gravimetrically, in an analytical balance Mettler-Toledo PR1203, with a precision of 0.001 g, using deionised water, L-proline with a purity of superior to 99%, according to the analysis performed by the supplier, Sigma-Aldrich, using thin layer chromatography, and potassium hydroxide with a purity of better than 85% acquired also from Sigma-Aldrich. The exact concentration of the solution used in the experiments was 7.00 molal, which is equivalent to 38.9 wt% and to 4.10 mol.dm<sup>-3</sup>. The viscosity of the solution was determined to be 8.3 mPa.s at 298 K, by using an Anton Paar

AMV 200 rolling ball microviscometer. During these measurements, a density of  $1.215 \text{ g.cm}^{-3}$  was determined at the same temperature. A second solution was also used, with a concentration of 6.99 molal, or  $4.04 \text{ mol.dm}^{-3}$ .

Carbon dioxide with a purity of 99.995%, produced by Linde AG, Germany, and supplied by AGA A/S, Denmark was used in the experiments. As before, the amount of gas used in each experiment was determined gravimetrically, using the aforementioned analytical balance. The experiments were performed according to the synthetic isothermal procedure described previously, at temperatures of 300 K and 353 K, and at pressures up to 0.7 MPa. The results obtained in these few experiments are presented in Table 8.4 and represented in Figure 8.6, together with the value found by Lerche at 0.1 MPa, using a semi-flow method [82].

**Table 8.4** – Results obtained in the in the measurements of the sorption of carbon dioxide in an aqueous solution of L-proline 7.0 molal, at temperatures of 300 K and 353 K.

$T / \text{K}$	$p / \text{MPa}$	loading ( $\text{mol}_{\text{CO}_2} / \text{mol}_{\text{salt}}$ )
299.85	0.289	0.821
300.14	0.282	0.782
352.95	0.640	0.462 <sup>a</sup>

*a* – Value obtained in the calculations not taking into account the amount of water in the gas phase.

The comparison of the values obtained at 0.3 MPa to the value found by Lerche [82] at 0.1 MPa, shows an increase of 12% in the loading, a value very similar to the increase verified by Lee et al. [80] for a solution of MEA with the same concentration (7 molal) in the same pressure range. For solutions of the same molality, L-proline presents a loading 8% superior to the verified for MEA under similar conditions.

The occurrence of precipitate was observed during the experiments at 300 K, both for in this work and in the work of Lerche [82]. From the pressure profiles recorded during the experiments, it was possible to determine that the formation of precipitate started when a loading of  $0.72 \text{ mol}_{\text{CO}_2} / \text{mol}_{\text{salt}}$  was achieved, at pressure close to 0.47 MPa.

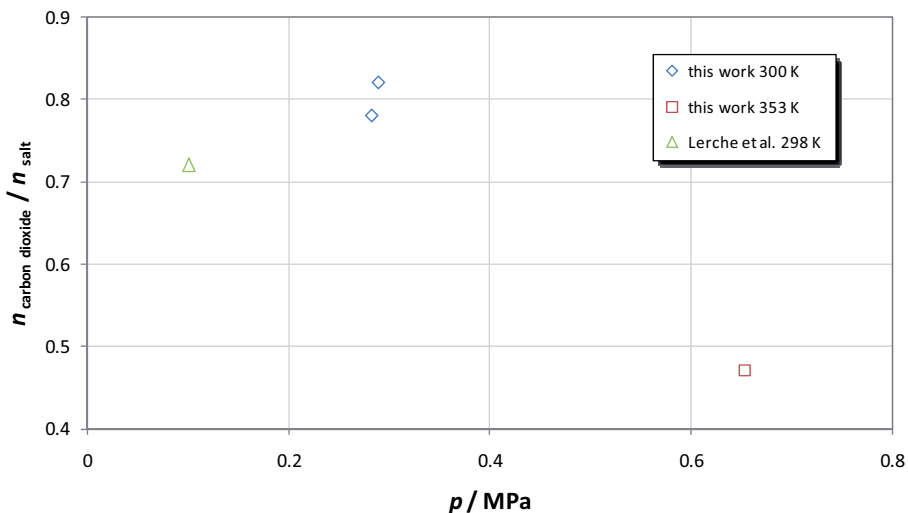


**Figure 8.6** – Results obtained in the in the measurements of the sorption of carbon dioxide in aqueous solutions of L-proline 7.0 molal, at 300 K and 353 K, and comparison with values from literature [82].

The experiments included up to 4 temperature cycles between 298 K and 353 K, which revealed no influence of the temperature cycling in the loading of CO<sub>2</sub> measured at 300 K.

It should be pointed out that the value obtained for 353 K was calculated not taking into account the amount of water present in the gas phase at this temperature, which should not be negligible. The value is presented to give a first idea of the absorption at that temperature. For a more accurate determination, the amount of water vapour should be taken into account, as well as its influence in the density of the gas phase, required in the calculations when using this synthetic method.

For both temperatures, further experiments are required, in order to better evaluate the influence of pressure in the loading values. Experiments at lower pressures can be used to better verify the concordance between the results produced through both experimental methods, although the results should not be exactly similar. In the current method, the calculated value of the loading is in fact a sum of the chemical absorbed CO<sub>2</sub> with the physically adsorbed gas, into a previously degassed solution, while in the semi-flow method a non-degassed solution is used. Furthermore, the use of a gas mixture of only 10% of CO<sub>2</sub> should influence the amount of this gas physically adsorbed into the solution.

## References

- [1] Erling Stenby, CERE, Center for Energy Resources Engineering, DTU, Technical University of Denmark, Kgs. Lyngby, Denmark, Personal Communication, 2009.
- [2] S. Ma'mun, H. F. Svendsen, K. A. Hoff, O. Juliussen, *Energy Convers. Manage.* 48 (2007) 251-258.
- [3] A. B. Rao, E. S. Rubin, *Environ. Sci. Technol.* 36 (2002) 4467-4475.
- [4] T. Suda, M. Iijima, H. Tanaka, S. Mitsuoka, T. Iwaki, *Environ. Prog.* 16 (1997) 200-207.
- [5] B. Freeman and R. Rhudy, *Assessment of Post-Combustion Capture Technology Developments*, EPRI, Electric Power Research Institute, Inc., 2007.
- [6] Jostein Gabrielsen, Ph.D. Thesis, Department of Chemical Engineering, Technical University of Denmark, Kgs. Lyngby, Denmark, 2007.
- [7] A. Meisen, X. S. Shuai, *Energy Convers. Manage.* 38 (1997) S37-S42.
- [8] F. Y. Jou, A. E. Mather, F. D. Otto, *Can. J. Chem. Eng.* 73 (1995) 140-147.
- [9] I. Kim, H. F. Svendsen, *Ind. Eng. Chem. Res.* 46 (2007) 5803-5809.
- [10] F. Y. Jou, A. E. Mather, F. D. Otto, J. J. Carroll, *Ind. Eng. Chem. Res.* 34 (1995) 2526-2529.
- [11] S. Ma'mun, R. Nilsen, H. F. Svendsen, O. Juliussen, *J. Chem. Eng. Data* 50 (2005) 630-634.
- [12] S. W. Park, B. S. Choi, K. W. Song, K. J. Oh, J. W. Lee, *Sep. Sci. Technol.* 42 (2007) 3537-3554.
- [13] K. S. Hwang, D. W. Kim, S. W. Park, D. W. Park, K. J. Oh, S. S. Kim, *Sep. Sci. Technol.* 44 (2009) 3888-3910.
- [14] S. W. Park, D. W. Park, K. J. Oh, S. S. Kim, *Sep. Sci. Technol.* 44 (2009) 543-568.

- [15] <http://www.cansolv.com/en/co2captureschema.ch2>, Cansolv, accessed 20 Jan. 2010.
- [16] J. B. Tang, Y. Q. Shen, M. Radosz, W. L. Sun, *Ind. Eng. Chem. Res.* 48 (2009) 9113-9118.
- [17] B. J. Hwang, S. W. Park, D. W. Park, K. J. Oh, S. S. Kim, *Sep. Sci. Technol.* 44 (2009) 1574-1589.
- [18] D. Almantariotis, T. Gefflaut, A. A. H. Padua, J. Y. Coxam, M. F. C. Gomes, *J. Phys. Chem. B* 114 (2010) 3608-3617.
- [19] B. E. Gurkan, J. C. de la Fuente, E. M. Mindrup, L. E. Ficke, B. F. Goodrich, E. A. Price, W. F. Schneider, J. F. Brennecke, *J. Am. Chem. Soc.* 132 (2010) 2116.
- [20] W. Ren, B. Sensenich, A. M. Scurto, *J. Chem. Thermodyn.* 42 (2010) 305-311.
- [21] H. N. Song, B. C. Lee, J. S. Lim, *J. Chem. Eng. Data* 55 (2010) 891-896.
- [22] P. J. Carvalho, V. H. Alvarez, I. M. Marrucho, M. Aznar, J. A. P. Coutinho, *J. Supercrit. Fluids* 50 (2009) 105-111.
- [23] S. O. Nwosu, J. C. Schleicher, A. M. Scurto, *J. Supercrit. Fluids* 51 (2009) 1-9.
- [24] J. E. Bara, D. E. Camper, D. L. Gin, R. D. Noble, *Acc. Chem. Res.* 43 (2010) 152-159.
- [25] J. Kumelan, D. Tuma, A. P. S. Kamps, G. Maurer, *J. Chem. Eng. Data* 55 (2010) 165-172.
- [26] Y. J. Heintz, L. Sehabiague, B. I. Morsi, K. L. Jones, D. R. Luebke, H. W. Pennline, *Energy Fuels* 23 (2009) 4822-4830.
- [27] M. Hasib-ur-Rahman, M. Siaj, F. Larachi, *Chem. Eng. Process.* In Press, Accepted Manuscript.
- [28] A. F. Portugal, J. M. Sousa, F. D. Magalhaes, A. Mendes, *Chem. Eng. Sci.* 64 (2009) 1993-2002.

- [29] S. W. Park, Y. S. Son, D. W. Park, K. J. Oh, *Sep. Sci. Technol.* 43 (2008) 3003-3019.
- [30] P. S. Kumar, J. A. Hogendoorn, P. H. M. Feron, G. F. Versteeg, *Ind. Eng. Chem. Res.* 42 (2003) 2832-2840.
- [31] P. S. Kumar, J. A. Hogendoorn, S. J. Timmer, P. H. M. Feron, G. F. Versteeg, *Ind. Eng. Chem. Res.* 42 (2003) 2841-2852.
- [32] P. S. Kumar, J. A. Hogendoorn, G. F. Versteeg, P. H. M. Feron, *AIChE J.* 49 (2003) 203-213.
- [33] D. M. Munoz, A. F. Portugal, A. E. Lozano, J. G. de la Campa, J. de Abajo, *Energy Environ. Sci.* 2 (2009) 883-891.
- [34] M. E. Majchrowicz, D. W. F. Brilman, M. J. Groeneveld, *Energy Procedia* 1 (2009) 979-984.
- [35] P.H.M. Feron, N. ten Asbroek, New solvents based on amino-acid salts for CO<sub>2</sub> capture from flue gases in: E.S.Rubin, D.W.Keith, C.F.Gilboy, M.Wilson, T.Morris, J.Gale, K.Thambimuthu (Eds.), *Greenhouse Gas Control Technologies 7*, pp. 1153-1158 Elsevier Science Ltd, 2005.
- [36] J. van Holst, G. F. Versteeg, D. W. F. Brilman, J. A. Hogendoorn, *Chem. Eng. Sci.* 64 (2009) 59-68.
- [37] J. P. Brouwer, P. H. M. Feron, and N. ten Asbroek, Amino-acid salts for CO<sub>2</sub> capture from flue gases, poster 147, Fourth Annual Conference on Carbon Dioxide Capture & Sequestration, Alexandria, Virginia, USA, 2005.
- [38] R. J. Hook, *Ind. Eng. Chem. Res.* 36 (1997) 1779-1790.
- [39] <http://www.rsc.org/chemistryworld/News/2008/April/04040802.asp>, Dutch power ahead with carbon capture, accessed 20 Jan. 2010.
- [40] J. J. de Mooij, Siemens and TNO agree strategic cooperation in the field of flue-gas carbon capture in fossil-fueled power plants - Press release 2009-37, TNO Science and Industry, Media Relations, 2009.

- [41] <http://www.allbusiness.com/energy-utilities/utilities-industry-electric-power/13576595-1.html>, Carbon dioxide capture - Siemens favours the amino acid salt solution., accessed 10 Feb. 2010.
- [42] L. W. Diamond, N. N. Akinfiev, *Fluid Phase Equilib.* 208 (2003) 265-290.
- [43] N. Spycher, K. Pruess, J. Ennis-King, *Geochim. Cosmochim. Acta* 67 (2003) 3015-3031.
- [44] J. J. Carroll, J. D. Slupsky, A. E. Mather, *J. Phys. Chem. Ref. Data* 20 (1991) 1201-1209.
- [45] R. Crovetto, *J. Phys. Chem. Ref. Data* 20 (1991) 575-589.
- [46] A. D. King, C. R. Coan, *J. Am. Chem. Soc.* 93 (1971) 1857-1862.
- [47] I. P. Sidorov, Y. S. Kazarnovsky, A. M. Goldman, *Tr. Gos. Nauchno-Issled. Inst. Proektn Inst. Azotn. Promsti. Org. Sint.* 1 (1953) 48.
- [48] R. Wiebe, V. L. Gaddy, *J. Am. Chem. Soc.* 62 (1940) 815-817.
- [49] R. Wiebe, V. L. Gaddy, *J. Am. Chem. Soc.* 61 (1939) 315-318.
- [50] G. Houghton, A. M. McLean, P. D. Ritchie, *Chem. Eng. Sci.* 6 (1957) 132-137.
- [51] G. Muller, E. Bender, G. Maurer, *Ber. Bunsen Ges. - Phys. Chem. Chem. Phys.* 92 (1988) 148-160.
- [52] R. Wiebe, *Chem. Rev.* 29 (1941) 475-481.
- [53] R. Dohrn, A. P. Bunz, F. Devlieghere, D. Thelen, *Fluid Phase Equilib.* 83 (1993) 149-158.
- [54] M. B. King, A. Mubarak, J. D. Kim, T. R. Bott, *J. Supercrit. Fluids* 5 (1992) 296-302.
- [55] R. Dsouza, J. R. Patrick, A. S. Teja, *Can. J. Chem. Eng.* 66 (1988) 319-323.
- [56] J. A. Briones, J. C. Mullins, M. C. Thies, B.-U. Kim, *Fluid Phase Equilib.* 36 (1987) 235-246.

- [57] T. Nakayama, H. Sagara, K. Arai, S. Saito, *Fluid Phase Equilib.* 38 (1987) 109-127.
- [58] J. Chrastil, *J. Phys. Chem.* 86 (1982) 3016-3021.
- [59] A. Zawisza, B. Malesinska, *J. Chem. Eng. Data* 26 (1981) 388-391.
- [60] S. Takenouchi, G. C. Kennedy, *Am. J. Sci.* 262 (1964) 1055-1074.
- [61] K. Todheide, E. U. Franck, *Ber. Bunsen Ges. Phys. Chem.* 67 (1963) 836.
- [62] S. D. Malinin, *Geochem. Int.* 3 (1959) 292-306.
- [63] H. W. Stone, *Ind. Eng. Chem.* 35 (1943) 1284-1286.
- [64] F. Pollitzer, E. Strebel, *Z. Phys. Chem. Stoechiom. Verwandtschafts.* 110 (1924) 768-785.
- [65] A. Dhima, J. C. de Hemptinne, J. Jose, *Ind. Eng. Chem. Res.* 38 (1999) 3144-3161.
- [66] C. F. Prutton, R. L. Savage, *J. Am. Chem. Soc.* 67 (1945) 1550-1554.
- [67] A. E. Mather, E. U. Franck, *J. Phys. Chem.* 96 (1992) 6-8.
- [68] D. Zelvinsky, *J. Phys. Ind. (U. S. S. R.)* 14 (1937) 1250.
- [69] T. Sako, T. Sugeta, N. Nakazawa, T. Okubo, M. Sato, T. Taguchi, T. Hiaki, *J. Chem. Eng. Jpn.* 24 (1991) 449-455.
- [70] J. A. Nighswander, N. Kalogerakis, A. K. Mehrotra, *J. Chem. Eng. Data* 34 (1989) 355-360.
- [71] D. Q. Zheng, T. M. Guo, H. Knapp, *Fluid Phase Equilib.* 129 (1997) 197-209.
- [72] T. J. Morrison, F. Billett, *J. Chem. Soc.* (1952) 3819-3822.
- [73] L. W. Winkler, *Ber. Dtsch. Chem. Ges.* 34 (1901) 1408-1422.
- [74] A. J. Ellis, R. M. Golding, *Am. J. Sci.* 261 (1963) 47-&.
- [75] S. D. Malinin, N. A. Kurovskaya, *Geochem. Int.* 12 (1975) 199.
- [76] S. D. Malinin, N. I. Savelyeva, *Geochem. Int.* 17 (2010) 9.

- [77] E. Bartholomé, H. Fritz, Chem. Ind. Tech. 28 (1956) 706-708.
- [78] I. R. Kritschewsky, N. M. Shaworonkoff, V. A. Aepelbaum, Z. Phys. Chem. Abt. A: 175 (1935) 232-238.
- [79] A. Valtz, A. Chapoy, C. Coquelet, P. Paricaud, D. Richon, Fluid Phase Equilib. 226 (2004) 333-344.
- [80] J. I. Lee, F. D. Otto, A. E. Mather, Journal of Applied Chemistry and Biotechnology 26 (1976) 541-549.
- [81] L. Faramarzi, G. M. Kontogeorgis, K. Thomsen, E. H. Stenby, Fluid Phase Equilib. 282 (2009) 121-132.
- [82] B. M. Lerche, Unpublished work.

# **Chapter 9**

## **Conclusions and Future Work**

---

### **9.1. Conclusions**

The amount of work initially expected for the length of this project was not entirely achieved, mainly due to the delays related with the production of the parts necessary for the equilibrium cell. Although the cell was built in the workshop of the department, and the CAD SolidWorks files relative to all the parts were supplied by the author, in a format also used by the workshop, it took over one year to have the main body of the cell finished, and an additional period of six more months to get it equipped with all the necessary connections.

This time was naturally used in other activities, such as performing several tests and attempts to re-commission the existing cell which had not been in use for several years, preparing extensive bibliographic surveys, reading, etc. However, there is an inevitable chronological sequence in the development of new experimental equipment, where some tasks are dependent on the completion of others, especially in the case of a complex apparatus such as the one under consideration here, in which several different parts have to be built and bought for further assembling, in a process that will invariably require additional adjustments. This implies that the delay of one of the earlier stages will have a negative influence on the timing of the subsequent steps, and consequently, in the whole project.

During the assembly and test of the apparatus, further difficulties were encountered, which led to additional delays. Although modern and well equipped, the laboratories of the research group do not have yet an established routine, possibly due to the more theoretical tradition of the group, meaning that what otherwise would be a simple and small task, became in this case more complex and time consuming. This was particularly evident in the development of the analytical method, in which the lack of chromatographic expertise in the group led to a substantial lengthening of this process, occasionally through some misled steps.

Nonetheless, the main purpose of this work was achieved, with the successful development of two new high-quality experimental set-ups, one of them of a considerable complexity, capable of producing reliable results, characterised by a superior precision and accuracy, as confirmed by the number of tests performed, and with a versatility that allows their use by means of different methods. Although it was not possible to achieve a significant amount of results in the time scale of the work, both apparatus should be regarded as an important and solid contribution to the future, constituting a basis that will simplify the implementation of future research projects with an experimental component. It should also be emphasised that the option for carefully carrying out an extensive range of tests, by means of assuring the correct functioning of the equipment, prevented the very early attainment of “publishable” results.

Another aspect worth mentioning is related with the costs of the equipment, in times where the economics have a significant role in the administration of any research group, and where the experimental work often involves nearly prohibitive costs. The first analytical apparatus presented was completely planned, designed and built for a current project, with an overall cost several times less than the commercial solutions available. Furthermore, this allowed a higher degree of customisation, avoiding the need for compromises, always inevitable where commercial equipment is concerned. The second apparatus presented, constitutes a good example of the reuse of decommissioned equipment, with substantial improvements in the quality of the set-up, at very low cost.

In this thesis, an effort was made to fully describe the developed apparatus, in a comprehensive manner, underlining the grounds for the design or the selection of all the parts used. Furthermore, all results and tests were presented, including the less successful ones, in an attempt to illustrate the type of problems that often occur in experimental work,

but that very seldom get published. The idea is that this thesis can also be used as a useful guide for future experimental work, to be developed in the described equipment or in a new one, in an effort to transmit some of the acquired know-how, rather than just presenting the results obtained.

Besides the developed set-ups, this thesis comprises also a review of the experimental methods available for the measurement of phase equilibria, with up-to-date examples of their applications, something that can also be found in published literature reviews, although in a more summarised form [1,2]. Simultaneously, a comparison of the various methods is presented, with an analysis of the advantages and disadvantages of each method, making of Chapter 3 a helpful guide for any researcher in need to implement a new experimental method for a particular type of measurements, something that happens frequently in an active laboratory as recently stated by Richon [3], in a work already several times mentioned in the present thesis.

A literature review on the existent data for the systems considered of interest to this work was also presented, with special attention on providing the original source of data, giving the reader the possibility for evaluation of the quality of the data, and avoiding its indiscriminate use, sometimes taken as experimental values when the numbers are in fact, already the product of smoothing processes and extrapolations. In order to simplify the search for data for particular systems, a database was created using common software.

In a complementary part of the work, modelling was also performed, firstly in the verification of the applicability of the simplified PC-SAFT equation of state, by the correlation a number of binary systems and in a second stage in the prediction of the equilibrium phase compositions in a quaternary system studied experimentally.

## **9.2. Future work**

Although focusing on the study of hydrate inhibitor systems and on the topic of carbon dioxide capture, the nature of the work developed was characterised by a rather broader perspective. Nevertheless, from an experimental point of view, it is possible to provide a set of advices for the future experimental work with these equilibrium cells in the laboratories of the group.

Rather than pointing a specific path, the commissioning of these two apparatus can be regarded as the opening of a new range of opportunities, for different projects, since the applicability of these experimental set-ups is not limited to the type of systems under consideration in the particular areas focused on this work. It is important to take into account however, that as versatile as the existing equipment may be, often there is the need for new customised set-ups, as recently pointed out by Richon [3]. As mentioned in Chapter 3, it is necessary to take into account the fact that there is not a single method that is suitable for all the different types of measurements in phase equilibrium, often being impossible to assert which method is the most appropriate for a specific determination.

Of extreme importance is the continuity in the use of the equipment, which tends to suffer a precocious ageing, leading to malfunctions, sometimes of an irreversible character, when not used, as demonstrated with the equilibrium cell recovered in the present work. A new experimental apparatus constitutes an investment whose profitability in terms of results is time limited, before it becomes obsolete, which in the current days might happen relatively fast due to the constant technological developments placed at the service of instrumentation.

Further improvements for the developed apparatus are dependent on future applications. For the analytical apparatus, the enhancement of the analytical methods represents a good possibility, with the application of analytical techniques which can contribute to an increase in the sensitivity of the phase analysis, as discussed previously in the thesis. Other possible modifications include the adaption to a re-circulation method, in order to promote a faster achievement of the equilibrium, as already mentioned before.

As for the second apparatus described, possible improvements might for instance include the adoption of an analytical method without sampling, through the use of spectroscopic techniques, for example.

The spare material available from the development of the two apparatus, consisting mainly in a sapphire tube, a high-precision temperature compensated pressure transmitter, a pair of high-precision platinum resistance thermometers and some valves, provide a substantial part of the material necessary to develop a new and simple equilibrium cell of small dimensions, according to the schematic representation in Figure 9.1.

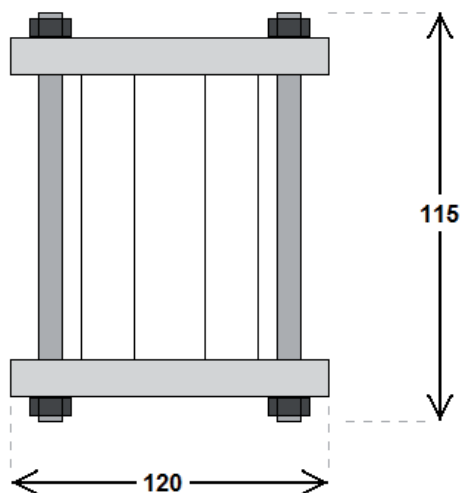


**Figure 9.1** – Schematic representation of a hypothetical equilibrium cell of small dimensions, to be built from the spare material available from this work. The displayed dimensions are given in millimetres.

The view cell represented in the figure, has an internal volume of  $22 \text{ cm}^3$  and it can be built simply by placing two metal discs, one on each side of the sapphire tube, hold together by four screws, in a design somewhat similar to the equilibrium cell developed in the present work, although excluding the parts of the cell containing the pistons. On account of this design, the cell allows the observation of the totality of its contents. The sapphire tube was dimensioned to withstand pressures up to 40 MPa, while the pressure sensor is characterised by a range of pressures going up to 50 MPa. Similar to the solution adopted in the cell presented in this work, the metal discs constitute an optimal location for the monitoring of the temperature of the cell, through the positioning of the platinum resistance thermometers in their interior.

The advantages of such a small cell are obvious in the study of phase equilibria of systems involving expensive compounds, such as the case of some amino-acids. Each of the experiments mentioned in the Chapter 8, using the synthetic method, required the use of at least around  $100 \text{ cm}^3$  of solution, which means that a set of experiments using a concentrated solution can be considerably expensive.

Another advantage of a cell with such a reduced volume is the possible application to the study of toxic compounds, such as mercaptans for example, compounds of interest in the gas industry. Reducing the used amounts of toxic compounds is obviously desirable,

from the safety point of view, reducing the risks of serious consequences in case of accident. A smaller cell can also be installed easily in more confined spaces equipped with better ventilation, such as laboratory fume hoods.

The reduced internal volume of the cell also facilitates the mixing of the different components in the system, allowing a faster attainment of the equilibrium. Other advantage is the portability of the cell, and its relatively low weight, making possible the application of a gravimetric method, for example.

Another inexpensive equilibrium cell, focusing on LLE at atmospheric pressure, can also be easily developed, based for example, in the design of the cell used by Folas et al. [4] in the Statoil Research Centre in Trondheim, Norway, and represented in Figure 9.2.

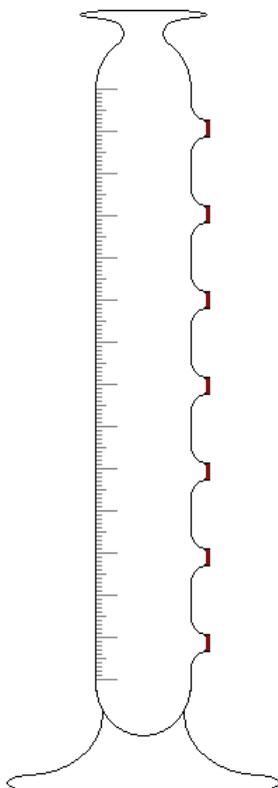


**Figure 9.2** – Schematic representation of a hypothetical inexpensive LLE cell, based in the design of the cell used by Folas et al. [4] in the Statoil Research Centre in Trondheim, Norway.

Such a cell can be constructed in glass, either for use within a temperature chamber, or built with a double wall for thermostatisation through recirculation on an appropriate fluid. Of an extremely simple concept, it allows the sample of different phases in equilibrium, regardless of its volumes. Using an analytical method, this cell could be used in the study of complex systems, at pressures close to atmospheric, complementing the range of pressures of the equipment developed in this work, focusing on high-pressures.

Furthermore, if used in with the same type of compounds, the operation of this cell can be planned in a way to share the same GC unit in use with the high pressure analytical equipment developed and presented in this work, contributing for an even lower cost of the whole set-up. In addition to the significant reduction in the costs, using the same GC unit could also allow the saving of the considerable amount of time usually required for calibrations.

## **References**

- [1] R. Dohrn, S. Peper, J. M. S. Fonseca, *Fluid Phase Equilib.* 288 (2010) 1-54.
- [2] J. M. S. Fonseca, S. Peper, R. Dohrn, *Fluid Phase Equilib.*, *In press*
- [3] D. Richon, *Pure Appl. Chem.* 81 (2009) 1769-1782.
- [4] G. K. Folas, G. M. Kontogeorgis, M. L. Michelsen, E. H. Stenby, E. Solbraa, J. *Chem. Eng. Data* 51 (2006) 977-983.



# ***Appendix 1***

## ***Tables and List of References for Experimental Data for Systems Related to Hydrate Inhibition***

---

As mentioned in Chapter 2, a database developed by the author was used in the generation of a series of tables, which contain information on the experimental data found in the literature for the systems under consideration in this work. The 22 tables are organised according to the types of systems they refer to. The first two tables present a series of references for systems containing mixtures of methane and ethane with other light *n*-alkanes. Following, Tables A.3 to A.13 refer to mixtures of hydrocarbons and water, while tables A.14 to A.16 deal with mixtures of hydrate inhibitors and hydrocarbons. Tables A.17 and A.18 refer to mixtures of inhibitors with water, and Tables A.19 and A.20 contain information regarding mixtures of hydrocarbons, water and hydrate inhibitors. Table A.21 presents a series of references to systems consisting of hydrocarbons, water and salts, and finally, Table A.22 comprises information on a small number of additional systems, not included in the previous tables.

For each of the systems presented, the composition of the system is given, or otherwise defined in the caption of the table, and the intervals of pressure and temperature to which the experimental works refer to are also presented, as well as the bibliographic information on the data sources.

**Table A1.1** – List of references for systems containing mixtures of methane and other hydrocarbons.

Components (methane + ...)	$T / K$	$p / \text{MPa}$	Ref.
ethane	278 - 361	0.6 - 10.2	[1]
ethane	130 - 200	0.2 - 0.5	[2]
propane	298 - 298	0 - 9	[3]
propane	290 - 293	5.4 - 8.6	[4]
propane	130 - 214	0 - 0.7	[5]
<i>n</i> -butane	298 - 298	0 - 10	[3]
<i>n</i> -pentane	298 - 298	0 - 11	[3]
<i>n</i> -pentane	311 - 411	0.1 - 16	[6]
<i>n</i> -pentane	173 - 273	0.1 - 15	[7]
<i>n</i> -pentane	186 - 282	4 - 15	[8]
<i>n</i> -pentane	378 - 378	7 - 14	[9]
<i>n</i> -pentane	311 - 377	3 - 21	[10]
<i>n</i> -hexane	295 - 333	0.1 - 0.1	[11]
<i>n</i> -hexane	298 - 298	0 - 9	[3]
<i>n</i> -hexane	182 - 185	0.1 - 0.1	[12]
<i>n</i> -hexane	348 - 383	2 - 20	[13]
<i>n</i> -hexane	311 - 423	10 - 10	[14]
<i>n</i> -hexane	138 - 164	0.6 - 2	[15]
<i>n</i> -hexane	190 - 273	0.1 - 18	[16]
<i>n</i> -hexane	190 - 273	0.1 - 18	[17]
<i>n</i> -hexane	311 - 444	2 - 20	[18]
<i>n</i> -hexane	311 - 444	2 - 34	[19]
<i>n</i> -hexane	163 - 423	0.2 - 16	[20]
<i>n</i> -hexane	311 - 378	6 - 41	[21]
<i>n</i> -hexane	311 - 377	3 - 21	[10]
<i>n</i> -heptane	169 - 182	0.1 - 0.1	[12]
<i>n</i> -heptane	295 - 313	0.1 - 0.1	[11]
<i>n</i> -heptane	273 - 313	0.1 - 23	[17]
<i>n</i> -heptane	278 - 511	1 - 68	[22]
<i>n</i> -octane	298 - 298	0 - 10	[3]
<i>n</i> -octane	163 - 423	0.1 - 7.1	[23]
<i>n</i> -octane	155 - 191	1 - 5	[24]
<i>n</i> -nonane	223 - 423	1 - 32	[25]
<i>n</i> -nonane	323 - 423	2 - 28	[26]

**Table A1.1 (Cont.)** – List of references for systems containing mixtures of methane and other hydrocarbons.

Components (methane + ...)	$T / K$	$p / MPa$	Ref.
<i>n</i> -decane	311 - 423	10 - 10	[14]
<i>n</i> -decane	248 - 423	1 - 10	[27]
<i>n</i> -decane	311 - 377	3 - 17	[28]
<i>n</i> -decane	294 - 394	2 - 31	[29]
<i>n</i> -decane	240 - 315	1 - 40	[30]
ethane <i>n</i> -hexane	194 - 204	60 - 60	[31]
ethane <i>n</i> -heptane	194 - 204	60 - 60	[31]
ethane <i>n</i> -heptane	200 - 255	11 - 11	[32]
ethane <i>n</i> -heptane	168 - 210	70 - 70	[31]
ethane <i>n</i> -octane	198 - 222	7 - 7	[33]
propane <i>n</i> -heptane	200 - 255	11 - 11	[32]
propane <i>n</i> -octane	198 - 213	6 - 6	[34]
propane <i>n</i> -decane	278 - 511	3 - 28	[35]
propane <i>n</i> -decane	278 - 511	69 - 69	[36]
<i>n</i> -butane <i>n</i> -octane	196 - 206	6 - 6	[37]
<i>n</i> -butane <i>n</i> -octane	253 - 473	3 - 83	[38]
<i>n</i> -butane <i>n</i> -decane	353 - 353	3 - 28	[35]
<i>n</i> -pentane <i>n</i> -octane	190 - 200	6 - 6	[39]
<i>n</i> -hexane <i>n</i> -octane	178 - 194	5 - 5	[39]
<i>n</i> -hexane <i>n</i> -decane	258 - 298	0.9 - 19	[40]

**Table A1.2** – List of references for systems containing mixtures of ethane and other hydrocarbons.

Components (ethane + ...)	$T / K$	$p / MPa$	Ref.
<i>n</i> -hexane	298 - 298	0.5 - 3.6	[41]
<i>n</i> -hexane	295.3 - 328	0.1 - 0.1	[11]
<i>n</i> -heptane	298 - 313	0.1 - 0.1	[11]
<i>n</i> -heptane	360 - 483	0.7 - 1.4	[42]

**Table A1.3** – List of references for binary systems containing methane and water.

Components	$T / K$	$p / \text{MPa}$	Ref.
	311 - 511	2.7 - 69	[43]
	283 - 313	0.5 - 2.8	[44]
	278 - 298	0.5 - 4.4	[45]
	298 - 373	2.4 - 9.4	[46]
	298 - 323	3.0 - 8.0	[47]
	243 - 283	1.0 - 6.1	[48]
	311 - 378	2.5 - 71	[49]
	298 - 338	2.5 - 12.5	[50,51]
	233 - 273	1.0 - 10.1	[52]
	344 - 344	7.2 - 1.3	[53]
	275 - 313	1.0 - 18	[54]
	283 - 318	1.0 - 34.6	[55]
	283 - 318	1.0 - 34.6	[56]
	253 - 293	1.5 - 18.0	[57]
	298 - 298	0.0 - 14.0	[3]
	298 - 298	3.0 - 18.0	[58]
	298 - 345	1.0 - 16.0	[59]
	298 - 444	2.0 - 68.0	[60]
	311 - 311	0.0 - 3.0	[61]
	298 - 303	0.3 - 5.2	[62]
	325 - 398	10.1 - 61.6	[63]
	311 - 313	0.5 - 21.0	[64]
	311 - 344	4.0 - 34.0	[65]
	423 - 523	20 - 250	[66]
	427 - 479	3.0 - 192	[67]
	298 - 298	2.4 - 5.2	[68]
	277 - 573	1.1 - 13.2	[69]
	283 - 298	1.1 - 5.2	[70]
	273 - 363	3.5 - 3.5	[71]
	298 - 298	2.3 - 12.7	[72]
	274 - 284	3.5 - 6.5	[73]
	298 - 298	2.3 - 16.6	[74]
	298 - 311	4.0 - 33	[75]
	344 - 344	2.5 - 100	[76]

**Table A1.3 (Cont.)** – List of references for binary systems containing methane and water.

Components	$T / K$	$p / \text{MPa}$	Ref.
	283 - 303	2.0 - 40	[77]
	283 - 303	0.1 - 0.1	[78]
	311 - 478	3.5 - 110	[79]
	313 - 373	0.0 - 9.3	[80]
	-	-	[81]
	632 - 647	22.1 - 50	[82]
	298 - 298	0.1 - 0.1	[83]
	298 - 298	0.1 - 0.1	[84]
	373 - 373	0.0 - 9.8	[85]
	473 - 523	9.0 - 98	[86]
	324 - 376	5.6 - 62	[87]
	298 - 298	0.1 - 0.1	[88]
	275 - 313	0.1 - 0.1	[89]
	273 - 353	0.1 - 0.1	[90]
	274 - 303	0.1 - 0.1	[91]
	278 - 318	0.1 - 0.1	[92]
	278 - 308	0.1 - 0.1	[93]
	278 - 298	0.1 - 0.1	[94]
	288 - 288	0.1 - 0.1	[95]
	278 - 298	0.1 - 0.1	[96]
	275 - 328	0.1 - 0.1	[97]
	293 - 323	0.1 - 0.1	[98]

**Table A1.4** – List of references for binary systems containing ethane and water.

Components	$T / K$	$p / \text{MPa}$	Ref.
	311 - 511	2.2 - 68	[99]
	298 - 373	2.3 - 3.6	[100]
	289 - 305	3.4 - 4.8	[101]
	283 - 293	0.5 - 3.0	[44]
	311 - 411	2.6 - 28.2	[102]
	311 - 378	3.4 - 34.7	[103]
	288 - 303	3.4 - 4.6	[104]
	311 - 444	0.4 - 8.4	[59]
	273 - 323	0.7 - 0.7	[71]
	283 - 303	0.5 - 4.0	[77]
	298 - 298	1.4 - 3.9	[74]
	311 - 444	0.4 - 68.5	[105]
	473 - 673	20.0 - 370	[106]
	344 - 344	20.0 - 100	[76]
	283 - 303	0.5 - 4.0	[77]
	283 - 303	0.1 - 0.1	[78]
	278 - 303	0.3 - 4.6	[107]
	315 - 467	3.5 - 110	[79]
	274 - 343	0.4 - 5.0	[108]
	621 - 647	22.1 - 49.8	[82]
	298 - 298	0.1 - 0.1	[83]
	298 - 298	0.1 - 0.1	[84]
	344 - 344	0.1 - 65	[109]
	273 - 273	0.1 - 0.5	[42]
	298 - 298	0.1 - 0.1	[88]
	275 - 313	0.1 - 0.1	[89]
	274 - 353	0.1 - 0.1	[90]
	278 - 318	0.1 - 0.1	[92]
	278 - 308	0.1 - 0.1	[93]
	278 - 298	0.1 - 0.1	[94]
	288 - 288	0.1 - 0.1	[95]
	275 - 323	0.1 - 0.1	[97]

**Table A1.5** – List of references for binary systems containing propane and water.

Components	$T / \text{K}$	$p / \text{MPa}$	Ref.
	285 - 422	0.7 - 19.3	[110]
	289 - 359	0.0 - 0.0	[111]
	282 - 300	0.6 - 0.9	[101]
	300 - 300	-	[112]
	311 - 311	1.4 - 1.4	[113]
	298 - 343	1.0 - 2.6	[104]
	-	-	[114]
	344 - 344	0.5 - 1.3	[115]
	278 - 368	0.4 - 3.9	[116]
	473 - 663	20 - 330	[117,118]
	289 - 411	0.1 - 3.5	[119]
	312 - 647	1.4 - 48.6	[82]
	298 - 298	0.1 - 0.1	[83]
	298 - 298	0.1 - 0.1	[84]
	370 - 370	4.3 - 4.3	[120]
	273 - 273	0.0 - 0.1	[121]
	298 - 298	0.1 - 0.1	[88]
	293 - 303	0.1 - 0.1	[89]
	585 - 660	15 - 200	[122]
	278 - 318	0.1 - 0.1	[92]
	278 - 308	0.1 - 0.1	[93]

**Table A1.6** – List of references for binary systems containing *n*-butane and water.

Components	$T / K$	$p / \text{MPa}$	Ref.
	311 - 425	0.4 - 4.4	[123]
	344 - 344	0.9 - 0.9	[102]
	311 - 411	0.4 - 3.4	[124]
	311 - 511	0.1 - 4.1	[125]
	311 - 378	7.3 - 69.4	[126]
	278 - 294	0.3 - 0.7	[127]
	293 - 353	0.2 - 1.1	[104]
	628 - 637	25.5 - 112.5	[106]
	311 - 411	0.1 - 6.0	[128]
	496 - 707	9.0 - 310	[129]
	298 - 423	0.1 - 4.1	[130]
	344 - 344	2.5 - 100	[76]
	600 - 700	19.3 - 276	[131]
	326 - 647	0.5 - 49.8	[82]
	298 - 298	0.1 - 0.1	[83]
	298 - 298	0.1 - 0.1	[84]
	423 - 423	4.2 - 4.2	[120]
	-	-	[132]
	298 - 298	0.1 - 0.1	[88]
	293 - 303	0.1 - 0.1	[89]
	278 - 318	0.1 - 0.1	[92]
	278 - 308	0.1 - 0.1	[93]
	278 - 298	0.1 - 0.1	[94]

**Table A1.7** – List of references for binary systems containing *n*-pentane and water.

Components	$T / K$	$p / \text{MPa}$	Ref.
	279 - 298	0.1 - 0.1	[127]
	273 - 298	0.1 - 0.1	[133]
	293 - 353	0.1 - 0.5	[104]
	298 - 428	-	[134]
	273 - 453	0.0 - 3.6	[135]
	288 - 308	0.1 - 0.1	[136]
	378 - 647	0.8 - 47.3	[82]
	298 - 298	0.1 - 0.1	[83]
	300 - 352	15.2 - 70.9	[137]
	298 - 298	0.1 - 0.1	[84]
	463 - 463	4.5 - 4.5	[120]

**Table A1.8** – List of references for binary systems containing *n*-hexane and water.

Components	$T / K$	$p / \text{MPa}$	Ref.
	273 - 273	0.1 - 0.1	[127]
	273 - 298	0.1 - 0.1	[133]
	298 - 353	0.5 - 0.5	[104]
	298 - 428	0.0 - 0.0	[134]
	288 - 308	0.1 - 0.1	[136]
	313 - 473	0.0 - 3.5	[138]
	555 - 699	19.8 - 247	[129]
	293 - 313	0.1 - 0.1	[139]
	396 - 495	0.7 - 5.3	[140]
	419 - 647	1.1 - 47.3	[82]
	298 - 298	0.1 - 0.1	[83]
	610 - 675	15 - 140	[141]
	298 - 298	0.1 - 0.1	[84]
	492 - 498	5.3 - 5.3	[120]
	298 - 298	0.1 - 0.1	[142]
	493 - 645	0.1 - 0.1	[143]
	304 - 443	0.1 - 0.1	[144]

**Table A1.9** – List of references for binary systems containing *n*-heptane and water.

Components	$T / K$	$p / \text{MPa}$	Ref.
	283 - 298	0.1 - 0.1	[127]
	276 - 298	0.1 - 0.1	[145]
	273 - 298	0.1 - 0.1	[133]
	298 - 298	-	[134]
	289 - 308	0.1 - 0.1	[136]
	273 - 323	0.1 - 0.1	[139]
	415 - 647	0.7 - 49.9	[82]
	298 - 298	0.1 - 0.1	[83]
	295 - 355	17.2 - 55.7	[137]
	298 - 298	0.1 - 0.1	[84]
	519 - 519	6.3 - 6.3	[120]
	295 - 295	0.1 - 0.1	[146]
	295 - 298	0.1 - 0.1	[147]
	690 - 690	0.0 - 300	[148]
	306 - 444	0.1 - 0.1	[144]
	298 - 313	0.1 - 0.1	[149]

**Table A1.10** – List of references for binary systems containing *n*-octane and water.

Components	$T / K$	$p / \text{MPa}$	Ref.
	293 - 293	0.1 - 0.1	[127]
	273 - 298	0.1 - 0.1	[133]
	298 - 298	-	[134]
	288 - 308	0.1 - 0.1	[136]
	311 - 553	0.1 - 8.9	[150]
	298 - 473	6.5 - 6.5	[151]
	418 - 647	0.6 - 45.6	[82]
	298 - 298	0.1 - 0.1	[83]
	298 - 298	0.1 - 0.1	[84]
	540 - 540	7.4 - 7.4	[120]
	483 - 533	0.1 - 0.1	[152]
	303 - 456	0.1 - 0.1	[144]

**Table A1.11** – List of references for binary systems containing *n*-nonane and water.

Components	$T / \text{K}$	$p / \text{MPa}$	Ref.
	298 - 298	-	[134]
	448 - 654	1.1 - 50.8	[82]
	555 - 555	8.6 - 8.6	[120]
	298 - 313	0.1 - 0.1	[149]

**Table A1.12** – List of references for binary systems containing *n*-decane and water.

Components	$T / \text{K}$	$p / \text{MPa}$	Ref.
	573 - 593	15 - 20	[153]
	466 - 649	1.5 - 42.1	[82]
	569 - 569	9.6 - 9.6	[120]
	298 - 313	0.1 - 0.1	[149]
	374 - 569	0.1 - 11.2	[154]

**Table A1.13** – List of references for multi-component systems of hydrocarbons and water.

Components (water + ...)		$T / \text{K}$	$p / \text{MPa}$	Ref.
methane	ethane	344.3 - 344.3	20 - 100	[76]
methane	ethane	275.2 - 283.2	1.0 - 4.0	[77]
methane	<i>n</i> -butane	311.0 - 411.0	1.3 - 24.3	[155]
methane	<i>n</i> -butane	344.3 - 344.3	2.5 - 100	[76]
methane	<i>n</i> -heptane	275.5 - 275.5	0.1 - 2.0	[145]
methane	ethane <i>n</i> -butane	303.0 - 361.4	0.5 - 4.9	[45]
methane	ethane <i>n</i> -butane	288.2 - 313.1	6.0 - 17.5	[156]
methane	ethane <i>n</i> -butane	277.8 - 292.9	0.5 - 3.0	[157]
methane	ethane <i>n</i> -butane	278.1 - 313.1	1.0 - 14.4	[54]
ethane	propane	279.3 - 297.6	4.1 - 4.1	[101]

**Table A1.14** – List of references for systems containing methanol and hydrocarbons.

Components (methanol + ...)	$T / K$	$p / MPa$	Ref.
methane	298 - 333	0.0 - 12.5	[50]
methane	303 - 498	12.3 - 145.5	[158]
methane	297 - 513	8.1 - 300	[159]
methane	298 - 373	3.0 - 106.6	[160]
methane	283 - 303	5.1 - 40.1	[77]
methane	200 - 330	1.4 - 41.4	[161]
methane	283 - 303	0.1 - 0.1	[78]
methane	298 - 298	0.1 - 0.1	[162]
methane	298 - 298	0.1 - 0.1	[163]
methane	273 - 348	2.5 - 70	[164]
methane	153 - 153	0.1 - 10	[165]
methane	213 - 248	0.1 - 4.0	[166]
methane	220 - 330	0.7 - 41.4	[167]
ethane	245 - 248	20.0 - 95	[168]
ethane	194 - 309	0.2 - 5.2	[169]
ethane	240 - 298	0.4 - 4.2	[170]
ethane	251 - 496	3.7 - 17.9	[171]
ethane	288 - 308	3.4 - 5.3	[172]
ethane	266 - 515	8.1 - 17.8	[173]
ethane	298 - 298	1.1 - 4.1	[41]
ethane	298 - 298	1.0 - 6.8	[174]
ethane	298 - 298	0.1 - 0.1	[175]
ethane	283 - 303	0.5 - 3.0	[77]
ethane	283 - 303	0.1 - 0.1	[78]
ethane	298 - 298	0.1 - 0.1	[162]
ethane	233 - 373	2.0 - 6.0	[176]
propane	370 - 497	4.2 - 8.7	[171]
propane	313 - 373	0.4 - 4.3	[177]
propane	311 - 474	0.1 - $p_{eq}$	[178]
<i>n</i> -butane	264 - 293	5 - 140	[179]
<i>n</i> -butane	470 - 470	0.1 - $p_{eq}$	[178]
<i>n</i> -butane	250 - 265	0.1 - 0.1	[180]
<i>n</i> -pentane	294 - 307	0.1 - 0.1	[181]
<i>n</i> -pentane	278 - 313	0.1 - 0.1	[182]

**Table A1.14 (Cont.)** – List of references for systems containing methanol and hydrocarbons.

Components (methanol + ...)	$T / K$	$p / \text{MPa}$	Ref.
<i>n</i> -pentane	270 - 289	0.1 - 0.1	[183]
<i>n</i> -pentane	272 - 316	5 - 140	[179]
<i>n</i> -pentane	278 - 283	0.1 - 0.1	[184]
<i>n</i> -pentane	373 - 423	0.3 - 2.5	[185]
<i>n</i> -pentane	303 - 333	0.1 - 0.1	[186]
<i>n</i> -hexane	294 - 315	0.10 - 0.10	[187]
<i>n</i> -hexane	280 - 340	1.0 - 150	[188]
<i>n</i> -hexane	317 - 347	0.14 - 0.14	[181]
<i>n</i> -hexane	278 - 307	0.10 - 0.10	[189]
<i>n</i> -hexane	278 - 313	0.10 - 0.10	[182]
<i>n</i> -hexane	278 - 308	0.10 - 0.10	[184]
<i>n</i> -hexane	322 - 337	0.10 - 0.10	[190]
<i>n</i> -hexane	303 - 303	0.02 - 0.05	[191]
<i>n</i> -hexane	293 - 293	0.01 - 0.03	[192]
<i>n</i> -hexane	298 - 298	0.02 - 0.02	[193]
<i>n</i> -hexane	245 - 307	0.10 - 0.10	[194]
<i>n</i> -hexane	403 - 513	0.51 - 8.06	[195]
<i>n</i> -hexane	245 - 307	0.10 - 0.10	[196]
<i>n</i> -hexane	256 - 299	0.10 - 0.10	[197]
<i>n</i> -hexane	283 - 316	0.10 - 0.10	[198]
<i>n</i> -hexane	298 - 298	0.02 - 0.04	[199]
<i>n</i> -hexane	298 - 307	0.10 - 0.10	[200]
<i>n</i> -heptane	278 - 324	0.1 - 0.1	[182]
<i>n</i> -heptane	317 - 357	1.0 - 150.9	[201]
<i>n</i> -heptane	315 - 329	0.1 - 0.1	[183]
<i>n</i> -heptane	278 - 313	0.1 - 0.1	[184]
<i>n</i> -heptane	313 - 313	0.027 - 0.004	[202]
<i>n</i> -heptane	313 - 313	0.012 - 0.046	[203]
<i>n</i> -heptane	298 - 323	0.1 - 0.1	[204]
<i>n</i> -heptane	298 - 298	0.004 - 0.017	[193]
<i>n</i> -heptane	313 - 313	0.012 - 0.046	[205]
<i>n</i> -heptane	718 - 540	0.5 - 7.1	[195]
<i>n</i> -heptane	303 - 318	0.1 - 0.1	[200]
<i>n</i> -octane	278 - 339	0.1 - 0.1	[182]

**Table A1.14 (Cont.)** – List of references for systems containing methanol and hydrocarbons.

Components (methanol + ...)	$T / K$	$p / MPa$	Ref.
<i>n</i> -octane	324 - 372	0.9 - 151	[201]
<i>n</i> -octane	278 - 313	0.1 - 0.1	[184]
<i>n</i> -octane	298 - 333	0.1 - 0.1	[204]
<i>n</i> -octane	419 - 541	1.2 - 7.5	[195]
<i>n</i> -nonane	349 - 387	1.0 - 150	[188]
<i>n</i> -nonane	278 - 313	0.1 - 0.1	[182]
<i>n</i> -nonane	330 - 356	0.1 - 0.1	[183]
<i>n</i> -nonane	298 - 333	0.1 - 0.1	[204]
<i>n</i> -nonane	415 - 537	1.2 - 7.5	[195]
<i>n</i> -decane	359 - 390	1.0 - 100	[188]
<i>n</i> -decane	278 - 313	0.1 - 0.1	[182]
<i>n</i> -decane	298 - 333	0.1 - 0.1	[204]
<i>n</i> -decane	422 - 540	1.3 - 7.7	[195]
methane            ethane	275 - 283	5 - 40	[77]

**Table A1.15** – List of references for systems containing MEG and hydrocarbons.

Components (MEG + ...)	$T / K$	$p / MPa$	Ref.
methane	298 - 298	-	[206]
methane	283 - 303	5.0 - 40.1	[77]
methane	298 - 398	0.1 - 19.7	[207]
methane	278 - 323	5.0 - 20.0	[208]
methane	323 - 398	0.2 - 39.6	[209]
ethane	298 - 398	0.1 - 20.3	[210]
ethane	298 - 308	0.1 - 0.1	[175]
ethane	283 - 303	0.5 - 4.0	[77]
ethane	298 - 298		[206]
propane	298 - 298		[206]
propane	298 - 398	0.1 - 20.3	[211]
<i>n</i> -butane	298 - 298	-	[206]
<i>n</i> -hexane	308 - 330	0.1 - 0.1	[212]
<i>n</i> -heptane	316 - 352	0.1 - 0.1	[212]
<i>n</i> -heptane	316 - 341	0.1 - 0.1	[213]
methane            ethane	275 - 283	5 - 40	[77]

**Table A1.16** – List of references for systems containing DEG, TEG or TeEG and hydrocarbons.

Components		$T / K$	$p / \text{MPa}$	Ref.
ethane	DEG	298 - 398	0.0 - 20.5	[214]
methane	DEG	298 - 398	0.0 - 20.5	[207]
<i>n</i> -heptane	DEG	313 - 353	0.1 - 0.1	[212]
<i>n</i> -heptane	DEG	278 - 450	0.1 - 0.1	[215]
methane	TEG	298 - 317	0.0 - 9.0	[216]
methane	TEG	298 - 398	0.1 - 20.2	[217]
ethane	TEG	298 - 398	0.1 - 20.5	[217]
propane	TEG	298 - 398	0.0 - 6.5	[217]
propane	TEG	373 - 373	4.0 - 45	[218]
<i>n</i> -heptane	TEG	309 - 351	0.1 - 0.1	[212]
<i>n</i> -heptane	TEG	321 - 410	0.1 - 0.1	[219]
<i>n</i> -heptane	TEG	298 - 325	0.1 - 0.1	[220]
<i>n</i> -heptane	TEG	323 - 393	0.1 - 0.1	[221]
<i>n</i> -octane	TEG	323 - 393	0.1 - 0.1	[221]
<i>n</i> -nonane	TEG	323 - 393	0.1 - 0.1	[221]
<i>n</i> -decane	TEG	323 - 393	0.1 - 0.1	[221]
propane	TeEG	373 - 373	4.0 - 45	[218]
<i>n</i> -heptane	TeEG	306 - 354	0.1 - 0.1	[212]
<i>n</i> -heptane	TeEG	311 - 403	0.1 - 0.1	[219]
<i>n</i> -heptane	TeEG	293 - 322	0.1 - 0.1	[222]
<i>n</i> -heptane	TeEG	323 - 393	0.1 - 0.1	[221]
<i>n</i> -octane	TeEG	323 - 393	0.1 - 0.1	[221]
<i>n</i> -nonane	TeEG	323 - 393	0.1 - 0.1	[221]
<i>n</i> -decane	TeEG	323 - 393	0.1 - 0.1	[221]

**Table A1.17** – List of references for systems containing methanol and water.

Components	$T / K$	$p / \text{MPa}$	Ref.
	298 - 298	0.1 - 0.1	[223]
	323 - 333	0.0 - 0.1	[224]
	373 - 373	0.1 - 0.3	[225]
	171 - 253	0.1 - 0.1	[226]
	144 - 173	0.1 - 0.1	[227]
	158 - 273	0.1 - 0.1	[228]
	189 - 273	0.1 - 0.1	[229]
	320 - 420	0.0 - 1.3	[230]
	308 - 338	0.0 - 0.1	[231]
	333 - 333	0.1 - 0.1	[232]
	323 - 323	0.1 - 0.1	[233]
	190 - 273	0.1 - 0.1	[234]
	320 - 420	0.0 - 1.3	[235]
	373 - 373	0.1 - 0.4	[236]
	515 - 647	-	[237]

**Table A1.18** – List of references for systems containing MEG, DEG, TEG or TeEG and water.

Components (water + ...)	$T / K$	$p / MPa$	Ref.
MEG	343 - 363	0.006 - 0.1	[238]
MEG	371 - 395	0.004 - 0.2	[239]
MEG	217 - 273	0.1 - 0.1	[240]
MEG	210 - 273	0.1 - 0.1	[241]
MEG	213 - 273	0.1 - 0.1	[229]
MEG	238 - 270	0.1 - 0.1	[242]
MEG	239 - 270	0.1 - 0.1	[243]
MEG	237 - 269	0.1 - 0.1	[244]
MEG	239 - 269	0.1 - 0.1	[245]
DEG	321 - 389	0.013 - 0.1	[246]
DEG	393 - 393	0.004 - 0.1	[247]
TeEG	298 - 298	0.001 - 0.003	[248]
TeEG	373 - 405	0.1 - 0.1	[249]
TeEG	298 - 298	0.0 - 0.0	[250]

**Table A1.19** – List of references for systems containing water, methanol and hydrocarbons.

Components (methanol + water + ...)	$T / K$	$p / MPa$	Ref.
methane	298 - 313	2.5 - 12.5	[251]
methane	252 - 273	2.5 - 12.5	[252]
methane	283 - 303	5.1 - 40.1	[77]
ethane	283 - 303	0.5 - 3.0	[77]
propane	273 - 293	0.1 - 0.1	[180]
<i>n</i> -butane	273 - 293	0.1 - 0.1	[180]
<i>n</i> -hexane	278 - 328	0.1 - 0.1	[253]
<i>n</i> -hexane	298 - 318	0.1 - 0.1	[254]
<i>n</i> -heptane	298 - 298	0.1 - 0.1	[255]
methane            ethane	275 - 283	1.3 - 40	[77]

**Table A1.20** – List of references for systems containing water, MEG, DEG, TEG or TeEG as hydrate inhibitor and hydrocarbons.

Components (water + ...)		$T / \text{K}$	$p / \text{MPa}$	Ref.
DEG	methane	298.2 - 323.2	3.0 - 8.0	[47]
MEG	methane	283.2 - 303.2	5.0 - 40.1	[77]
MEG	methane	278.2 - 298.2	5.0 - 20	[208]
MEG	ethane	283.2 - 303.2	0.5 - 4.0	[77]
MEG	<i>n</i> -hexane	283.1 - 313.1	0.1 - 0.1	[256]
DEG	<i>n</i> -heptane	298.0 - 435.0	0.1 - 0.1	[215]
MEG	<i>n</i> -heptane	293.1 - 293.1	0.1 - 0.1	[256]
MEG	<i>n</i> -octane	293.1 - 293.1	0.1 - 0.1	[256]
MEG	<i>n</i> -nonane	293.1 - 293.1	0.1 - 0.1	[256]
MEG	<i>n</i> -decane	293.1 - 293.1	0.1 - 0.1	[256]
TEG	nat. gas	289.0 - 311.0	3.5 - 13.8	[257]
MEG	methane      ethane	275.2 - 283.2	0.5 - 40	[77]

**Table A1.21** – List of references for systems containing methane, water and salts.

Components (water + ...)		$T / K$	$p / \text{MPa}$	Ref.
methane	NaCl	303.0 - 303.0	1.5 - 5.3	[62]
methane	NaCl	324.7 - 398.2	20.3 - 20.7	[63]
methane	NaCl	298.0 - 298.0	2.4 - 5.2	[68]
methane	CaCl <sub>2</sub>	298.0 - 303.0	1.1 - 7.5	[62]
methane	CaCl <sub>2</sub>	298.0 - 298.0	2.4 - 5.2	[68]
methane	CaCl <sub>2</sub>	298.2 - 344.2	10 - 60	[258]
methane	KCl	298.0 - 298.0	2.4 - 5.2	[68]
methane	KCl	298.0 - 298.0	2.4 - 5.2	[68]
methane	KCl	313.2 - 373.2	0.01 - 9.8	[80]
methane	LiCl	313.1 - 353.3	0.003 - 9.5	[80]
methane	Na <sub>2</sub> CO <sub>3</sub>	298.0 - 298.0	2.4 - 5.2	[68]
methane	NaHCO <sub>3</sub>	298.0 - 298.0	2.4 - 5.2	[68]
methane	NaHCO <sub>3</sub>	324.2 - 403.2	5.1 - 58	[87]
methane	K <sub>2</sub> CO <sub>3</sub>	298.0 - 298.0	2.4 - 5.2	[68]
methane	KHCO <sub>3</sub>	298.0 - 298.0	2.4 - 5.2	[68]
methane	Na <sub>2</sub> SO <sub>4</sub>	298.0 - 298.0	2.4 - 5.2	[68]
methane	K <sub>2</sub> SO <sub>4</sub>	298.0 - 298.0	2.4 - 5.2	[68]
methane	MgSO <sub>4</sub>	298.0 - 298.0	2.4 - 5.2	[68]
methane	KBr	313.2 - 353.2	0.01 - 8.4	[80]
methane	LiBr	313.2 - 353.2	0.01 - 10.2	[80]
methane	NaCl    CaCl <sub>2</sub>	303.0 - 303.0	2.5 - 5.2	[62]
methane	brine	277.2 - 573.2	1.9 - 12.7	[69]
methane	sea water	298.0 - 298.0	2.4 - 5.2	[68]

**Table A1.22** – List of references for other relevant systems.

Components			$T / K$	$p / \text{MPa}$	Ref.
natural gas	water	NaHCO <sub>3</sub>	323 - 403	5.2 - 57.7	[87]
methane	heavy water		278 - 298	0.1 - 0.1	[94]
ethane	heavy water		278 - 298	0.1 - 0.1	[94]
<i>n</i> -butane	heavy water		278 - 298	0.1 - 0.1	[94]
water	CaCl <sub>2</sub>	MEG	253 - 380	0.1 - 0.1	[259]

## References

- [1] H. H. Reamer, B. H. Sage, W. N. Lacey, *Ind. Eng. Chem.* 42 (1950) 534-539.
- [2] I. Wichterle, R. Kobayashi, *J. Chem. Eng. Data* 17 (1972) 9-12.
- [3] P. K. Frolich, E. J. Tauch, J. J. Hogan, A. A. Peer, *Ind. Eng. Chem.* 23 (1931) 548-550.
- [4] E. F. May, T. J. Edwards, A. G. Mann, C. Edwards, *Int. J. Thermophys.* 24 (2003) 1509-1525.
- [5] I. Wichterle, R. Kobayashi, *J. Chem. Eng. Data* 17 (1972) 4-9.
- [6] W.-E. Reiff, P. Peters-Gerth, K. Lucas, *J. Chem. Thermodyn.* 19 (1987) 467-477.
- [7] T. C. Chu, R. J. J. Chen, P. S. Chappellear, R. Kobayashi, *J. Chem. Eng. Data* 21 (1976) 41-44.
- [8] V. P. Voronov, M. Y. Belyakov, E. E. Gorodetskii, V. D. Kulikov, A. R. Muratov, V. B. Nagaev, *Transp. Porous Media* 52 (2003) 123-140.
- [9] N. W. Prodany, B. Williams, *J. Chem. Eng. Data* 16 (1971) 1-6.
- [10] B. H. Sage, D. C. Webster, W. N. Lacey, *Ind. Eng. Chem.* 28 (1936) 1045-1047.
- [11] A. S. McDaniel, *J. Phys. Chem.* 15 (1911) 587-610.
- [12] A. J. Davenport, J. S. Rowlinson, *Trans. Faraday Soc.* 59 (1963) 78-84.
- [13] M. J. Cebola, G. Saville, W. A. Wakeham, *J. Chem. Thermodyn.* 32 (2000) 1265-1284.
- [14] S. Srivastan, N. A. Darwish, K. A. M. Gasem, R. L. Robinson, *J. Chem. Eng. Data* 37 (1992) 516-520.
- [15] K. D. Luks, J. D. Hottovy, J. P. Kohn, *J. Chem. Eng. Data* 26 (1981) 402-403.
- [16] Y. N. Lin, R. J. J. Chen, P. S. Chappellear, R. Kobayashi, *J. Chem. Eng. Data* 22 (1977) 402-408.

- [17] R. J. J. Chen, P. S. Chappellear, R. Kobayashi, *J. Chem. Eng. Data* 21 (1976) 213-219.
- [18] R. S. Poston, J. J. McKetta, *J. Chem. Eng. Data* 11 (1966) 362-363.
- [19] R. S. Poston, J. J. McKetta, *J. Chem. Eng. Data* 11 (1966) 364-365.
- [20] J. Shim, J. P. Kohn, *J. Chem. Eng. Data* 7 (1962) 3-8.
- [21] E. P. Schoch, A. E. Hoffmann, F. D. Mayfield, *Ind. Eng. Chem.* 33 (1941) 688-691.
- [22] H. H. Reamer, B. H. Sage, W. N. Lacey, *Ind. Eng. Chem. Chem. Eng. Data Series* 1 (1956) 29-42.
- [23] J. P. Kohn, W. F. Bradish, *J. Chem. Eng. Data* 9 (1964) 5-8.
- [24] J. P. Kohn, K. D. Luks, P. H. Liu, D. L. Tiffin, *J. Chem. Eng. Data* 22 (1977) 419-421.
- [25] L. M. Shipman, J. P. Kohn, *J. Chem. Eng. Data* 11 (1966) 176-180.
- [26] P. Rousseaux, D. Richon, H. Renon, *Fluid Phase Equilib.* 11 (1983) 153-168.
- [27] J. M. Beaudoin, J. P. Kohn, *J. Chem. Eng. Data* 12 (1967) 189-191.
- [28] H. H. Reamer, R. H. Olds, B. H. Sage, W. N. Lacey, *Ind. Eng. Chem.* 34 (1942) 1526-1531.
- [29] B. H. Sage, H. M. Lavender, W. N. Lacey, *Ind. Eng. Chem.* 32 (1940) 743-747.
- [30] M. P. W. M. Rijkers, M. Malais, C. J. Peters, J. D. Arons, *Fluid Phase Equilib.* 71 (1992) 143-168.
- [31] F. M. Llave, K. D. Luks, J. P. Kohn, *J. Chem. Eng. Data* 31 (1986) 418-421.
- [32] L. D. Van Horn, R. Kobayashi, *J. Chem. Eng. Data* 12 (1967) 294-303.
- [33] J. D. Hottovy, J. P. Kohn, K. D. Luks, *J. Chem. Eng. Data* 26 (1981) 135-137.
- [34] J. D. Hottovy, J. P. Kohn, K. D. Luks, *J. Chem. Eng. Data* 27 (1982) 298-302.

- [35] H. C. Wiese, H. H. Reamer, B. H. Sage, *J. Chem. Eng. Data* 15 (1970) 75-82.
- [36] H. H. Reamer, V. M. Berry, B. H. Sage, *J. Chem. Eng. Data* 14 (1969) 447-454.
- [37] F. M. Llave, T. H. Chung, *J. Chem. Eng. Data* 33 (1988) 123-128.
- [38] T. Yang, W. D. Chen, T. M. Guo, *Chem. Eng. Sci.* 52 (1997) 259-267.
- [39] R. C. Merrill, K. D. Luks, J. P. Kohn, *J. Chem. Eng. Data* 28 (1983) 210-215.
- [40] V. Uribe-Vargas, A. Trejo, *Fluid Phase Equilib.* 238 (2005) 95-105.
- [41] K. Ohgaki, F. Sano, T. Katayama, *J. Chem. Eng. Data* 21 (1976) 55-58.
- [42] L. Czerski, A. Czaplinski, *Ann. Soc. Chim. Polonorum* 36 (1962) 1827-1834.
- [43] R. H. Olds, B. H. Sage, W. N. Lacey, *Ind. Eng. Chem* 34 (1942) 1223-1227.
- [44] A. H. Mohammadi, A. Chapoy, D. Richon, B. Tohidi, *Ind. Eng. Chem. Res.* 43 (2004) 7148-7162.
- [45] A. Chapoy, A. H. Mohammadi, B. Tohidi, D. Richon, *J. Chem. Eng. Data* 50 (2005) 1157-1161.
- [46] M. Rigby, J. M. Prausnitz, *J. Phys. Chem* 72 (1968) 330-334.
- [47] C. Yokoyama, S. Wakana, G. Kaminishi, S. Takahashi, *J. Chem. Eng. Data* 33 (1988) 274-276.
- [48] N. E. Kosyakov, B. I. Ivchenko, P. P. Krishtopa, *Vopr. Khim. Tekhnol.* 47 (1982) 33-36.
- [49] V. V. Ugrozov, *Zh. Fiz. Khim.* 70 (1996) 1328-1329.
- [50] N. L. Yarymagaev, R. P. Sinyavskaya, I. I. Koliushko, L. Y. Levinton, *Zh. Prikladnoi Khim.* 58 (1985) 165-168.
- [51] N. L. Yarymagaev, R. P. Sinyavskaya, I. I. Koliushko, L. Y. Levinton, *J. Appl. Chem. USSR* 58 (1985) 154-157.

- [52] N. E. Kosyakov, B. I. Ivchenko, P. P. Krishtopa, *Zh. Prikladnoi Khim.* 52 (1979) 922-923.
- [53] J. Lukacs, D. B. Robinson, *Soc Petrol Eng J* 3 (1963) 293-297.
- [54] A. Chapoy, A. H. Mohammadi, D. Richon, B. Tohidi, *Fluid Phase Equilib.* 220 (2004) 113-121.
- [55] A. Chapoy, C. Coquelet, D. Richon, *Fluid Phase Equilib.* 214 (2003) 101-117.
- [56] A. Chapoy, C. Coquelet, D. Richon, *Fluid Phase Equilib.* 230 (2005) 210-214.
- [57] G. K. Folas, E. W. Froyna, J. Lovland, G. M. Kontogeorgis, E. Solbraa, *Fluid Phase Equilib.* 252 (2007) 162-174.
- [58] A. Michels, J. Gerver, A. Bijl, *Physica* 3 (1936) 797-808.
- [59] O. L. Culberson, A. B. Horn, J. J. McKetta, *Trans. Soc. Min. Eng. AIME* 189 (1950) 1-6.
- [60] O. L. Culberson, J. J. McKetta, *Trans. Soc. Min. Eng. AIME* 192 (1951) 223-226.
- [61] J. E. Davis, J. J. McKetta, *Petrol. Refiner.* 39 (1960) 205-206.
- [62] J. R. Duffy, N. O. Smith, B. Nagy, *Geochim. Cosmochim. Acta* 24 (1961) 23-31.
- [63] T. D. O'sullivan, N. O. Smith, *J. Phys. Chem.* 74 (1970) 1460-1466.
- [64] R. G. Sultanov, V. G. Skripka, A. Y. Namiot, *Gazov. Prom.* 17 (1972) 6-7.
- [65] B. Amirijaf, J. M. Campbell, *Soc Petrol Eng J* 12 (1972) 21-27.
- [66] M. Sanchez, F. Demeer, *An. Quim.* 74 (1978) 1325-1328.
- [67] L. C. Price, *AAPG Bull.* 63 (1979) 1527-1533.
- [68] R. K. Stoessell, P. A. Byrne, *Geochim. Cosmochim. Acta* 46 (1982) 1327-1332.
- [69] S. D. Cramer, *Ind. Eng. Chem. Process Des. Dev.* 23 (1984) 533-538.
- [70] Y. Wang, B. Han, H. Yan, R. Liu, *Thermochim. Acta* 253 (1995) 327-334.

- [71] K. Y. Song, G. Feneyrou, F. Fleyfel, R. Martin, J. Lievois, R. Kobayashi, *Fluid Phase Equilib.* 128 (1997) 249-259.
- [72] S. O. Yang, S. H. Cho, H. Lee, C. S. Lee, *Fluid Phase Equilib.* 185 (2001) 53-63.
- [73] P. Servio, P. Englezos, *J. Chem. Eng. Data* 47 (2002) 87-90.
- [74] Y. S. Kim, S. K. Ryu, S. O. Yang, C. S. Lee, *Ind. Eng. Chem. Res.* 42 (2003) 2409-2414.
- [75] O. L. Culberson, J. J. McKetta, *Trans. Soc. Min. Eng. AIME* 192 (1951) 297-300.
- [76] A. Dhima, J. C. de Hemptinne, G. Moracchini, *Fluid Phase Equilib.* 145 (1998) 129-150.
- [77] L. K. Wang, G. J. Chen, G. H. Han, X. Q. Guo, T. M. Guo, *Fluid Phase Equilib.* 207 (2003) 143-154.
- [78] M. Yaacobi, A. Bennaim, *J. Phys. Chem.* 78 (1974) 175-178.
- [79] M. Yarrison, K. R. Cox, W. G. Chapman, *Ind. Eng. Chem. Res.* 45 (2006) 6770-6777.
- [80] J. Kiepe, S. Horstmann, K. Fischer, J. Gmehling, *Ind. Eng. Chem. Res.* 42 (2003) 5392-5398.
- [81] R. G. Sultanov, V. G. Skripka, A. Y. Namiot, *Gazov. Prom.* 4 (1971) 6-13.
- [82] E. Brunner, *J. Chem. Thermodyn.* 22 (1990) 335-353.
- [83] C. McAuliffe, *J. Phys. Chem.* 70 (1966) 1267-1275.
- [84] C. McAuliffe, *Nature* 200 (1963) 1092.
- [85] J. J. Carroll, F. Y. You, A. E. Mather, F. D. Otto, *Can. J. Chem. Eng.* 76 (1998) 945-951.
- [86] R. G. Sultanov, V. G. Skripka, A. Y. Namiot, *Viniti* 4387 (1972) 72.
- [87] J. Gao, D. Q. Zheng, T. M. Guo, *J. Chem. Eng. Data* 42 (1997) 69-73.

- [88] T. J. Morrison, F. Billett, *J. Chem. Soc.* (1952) 3819-3822.
- [89] W. F. Claussen, M. F. Polglase, *J. Am. Chem. Soc.* 74 (1952) 4817-4819.
- [90] L. W. Winkler, *Ber. Dtsch. Chem. Ges.* 34 (1901) 1408-1422.
- [91] S. Yamamoto, J. B. Alcauskas, T. E. Crozier, *J. Chem. Eng. Data* 21 (1976) 78-80.
- [92] D. B. Watlauffer, S. K. Malik, L. Stoller, R. L. Coffin, *J. Am. Chem. Soc.* 86 (1964) 508-514.
- [93] W. Y. Wen, J. H. Hung, *J. Phys. Chem.* 74 (1970) 170-180.
- [94] A. Ben-Naim, J. Wilf, M. Yaacobi, *J. Phys. Chem.* 77 (1973) 95-102.
- [95] A. Ben-Naim, M. Yaacobi, *J. Phys. Chem.* 78 (1974) 170-175.
- [96] J. A. Muccitelli, W. Y. Wen, *J. Solution Chem.* 9 (1980) 141-161.
- [97] T. R. Rettich, Y. P. Handa, R. Battino, E. Wilhelm, *J. Phys. Chem.* 85 (1981) 3230-3237.
- [98] M. C. Serra, F. L. P. Pessoa, A. M. F. Palavra, *J. Chem. Thermodyn.* 38 (2006) 1629-1633.
- [99] H. H. Reamer, R. H. Olds, B. H. Sage, W. N. Lacey, *Ind. Eng. Chem.* 35 (1943) 790-793.
- [100] A. D. King, C. R. Coan, *J. Am. Chem. Soc.* 93 (1971) 1857-1862.
- [101] K. Y. Song, R. Kobayashi, *Fluid Phase Equilib.* 95 (1994) 281-298.
- [102] R. G. Anthony, J. J. McKetta, *J. Chem. Eng. Data* 12 (1967) 17-20.
- [103] R. G. Anthony, J. J. McKetta, *J. Chem. Eng. Data* 12 (1967) 21-28.
- [104] S. Mokraoui, C. Coquelet, A. Valtz, P. E. Hegel, D. Richon, *Ind. Eng. Chem. Res* 46 (2007) 9257-9262.
- [105] O. L. Culberson, J. J. McKetta, *Trans. Soc. Min. Eng. AIME* 189 (1950) 319-322.

- [106] A. Danneil, K. Todheide, E. U. Franck, *Chem. Ing. Tech.* 39 (1967) 816-822.
- [107] A. Chapoy, C. Coquelet, D. Richon, *J. Chem. Eng. Data* 48 (2003) 957-966.
- [108] A. H. Mohammadi, A. Chapoy, B. Tohidi, D. Richon, *Ind. Eng. Chem. Res.* 43 (2004) 5418-5424.
- [109] D. R. Burris, W. G. Macintyre, *Environ. Toxicol. Chem.* 4 (1985) 371-377.
- [110] R. Kobayashi, D. Katz, *Ind. Eng. Chem.* 45 (1953) 446-451.
- [111] F. H. Poettman, M. R. Dean, *Petrol. Refiner.* 25 (1946) 125-128.
- [112] C. W. Perry, *Ind. Eng. Chem. Anal. Ed.* 10 (1938) 513-514.
- [113] K. H. Hachmuth, *Western Gas* 8 (1931) 55.
- [114] A. Harmens, E. D. Sloan, *Can. J. Chem. Eng.* 68 (1990) 151-158.
- [115] A. H. Wehe, J. J. McKetta, *Anal. Chem.* 33 (1961) 291-293.
- [116] A. Chapoy, S. Mokraoui, A. Valtz, D. Richon, A. H. Mohammadi, B. Tohidi, *Fluid Phase Equilib.* 226 (2004) 213-220.
- [117] M. Sanchez, *R. Coll, An. Quim.* 74 (1978) 1329-1335.
- [118] M. Sanchez, *R. Coll, An. Quim.* 74 (1978) 1336-1339.
- [119] A. Azarnoosh, J. J. McKetta, *Petrol. Refiner.* 37 (1958) 275-278.
- [120] J. G. Roof, *J. Chem. Eng. Data* 15 (1970) 301-303.
- [121] S. Umamo, Y. Nakano, *Kogyo Kagaku Zasshi* 61 (1958) 536.
- [122] T. De Loos, A. J. M. Wijen, G. A. M. Diepen, *J. Chem. Thermodyn.* 12 (1980) 193-204.
- [123] H. H. Reamer, R. H. Olds, B. H. Sage, W. N. Lacey, *Ind. Eng. Chem.* 36 (1944) 381-383.
- [124] A. H. Wehe, J. J. McKetta, *J. Chem. Eng. Data* 6 (1961) 167-172.

- [125] H. H. Reamer, B. H. Sage, W. N. Lacey, *Ind. Eng. Chem.* 44 (1952) 609-615.
- [126] W. B. Brooks, G. B. Gibbs, J. J. McKetta, *Petrol. Refiner.* 30 (1951) 118-120.
- [127] C. Black, G. G. Joris, H. S. Taylor, *J. Chem. Phys.* 16 (1948) 537-543.
- [128] J. G. Le Breton, J. J. McKetta, *Hydrocarb. Proc Petrol. Ref.* 43 (1964) 136-138.
- [129] T. Yiling, T. Michelberger, E. U. Franck, *J. Chem. Thermodyn.* 23 (1991) 105-112.
- [130] J. J. Carroll, F. Y. Jou, A. E. Mather, *Fluid Phase Equilib.* 140 (1997) 157-169.
- [131] Y. Tian, X. Zhao, L. Chen, H. Zhu, H. Fu, *J. Supercrit. Fluids* 30 (2004) 145-153.
- [132] D. S. Tsiklis, V. Y. Maslenni, *Dokl. Akad. Nauk USSR* 157 (1964) 426.
- [133] J. Polak, B. C. Y. Lu, *Can. J. Chem.* 51 (1973) 4018-4023.
- [134] L. C. Price, *AAPG Bull.* 60 (1976) 213-244.
- [135] F. Y. Jou, A. E. Mather, *J. Chem. Eng. Data* 45 (2000) 728-729.
- [136] J. Å. Jönsson, J. Vejrosta, J. Novák, *Fluid Phase Equilib.* 9 (1982) 279-286.
- [137] J. F. Connolly, *J. Chem. Eng. Data* 11 (1966) 13-16.
- [138] C. Tsonopoulos, G. M. Wilson, *AIChE Journal* 29 (1983) 990-999.
- [139] B. A. Énglin, A. F. Platé, V. M. Tugolukov, M. A. Pryanishnikova, *Chem. Technol. Fuels Oils* 1 (1965) 722-726.
- [140] I. K. Kamilov, G. V. Stepanov, I. M. Abdulagatov, A. R. Rasulov, E. I. Milikhina, *J. Chem. Eng. Data* 46 (2001) 1556-1567.
- [141] T. De Loos, W. G. Penders, R. N. Lichtenthaler, *J. Chem. Thermodyn.* 14 (1982) 83-91.
- [142] J. W. Roddy, C. F. Coleman, *Talanta* 15 (1968) 1281-1286.
- [143] C. J. Rebert, K. E. Hayworth, *AIChE Journal* 13 (1967) 118-121.
- [144] C. Marche, C. Ferronato, J. Jose, *J. Chem. Eng. Data* 48 (2003) 967-971.

- [145] R. Susilo, J. D. Lee, P. Englezos, *Fluid Phase Equilib.* 231 (2005) 20-26.
- [146] R. G. Sultanov, V. G. Skripka, *Russ. J. Phys. Chem.* 46 (1972) 1245.
- [147] H. J. Bittrich, H. Gedan, G. Feix, *Z. Phys. Chem. - Leipzig* 260 (1979) 1009-1013.
- [148] K. Brollos, K. Peter, G. M. Schneider, *Ber. Bunsen Ges. Phys. Chem.* 74 (1970) 682.
- [149] P. Schatzberg, *J. Phys. Chem.* 67 (1963) 776-779.
- [150] J. L. Heidman, C. Tsonopoulos, C. J. Brady, G. M. Wilson, *AIChE Journal* 31 (1985) 376-384.
- [151] D. J. Miller, S. B. Hawthorne, *J. Chem. Eng. Data* 45 (1999) 78-81.
- [152] L. S. Budantseva, T. M. Lesteva, N. M. Nemtsov, *Russ. J. Phys. Chem.* 50 (1976) 814.
- [153] Y. Shimoyama, Y. Iwai, M. Yamakita, I. Shinkai, Y. Arai, *J. Chem. Eng. Data* 49 (2004) 301-305.
- [154] I. G. Economou, J. L. Heidman, C. Tsonopoulos, G. M. Wilson, *AIChE Journal* 43 (1997) 535-546.
- [155] J. J. Mcketta, D. L. Katz, *Ind. Eng. Chem.* 40 (1948) 853-863.
- [156] A. H. Mohammadi, A. Chapoy, B. Tohidi, D. Richon, *Ind. Eng. Chem. Res.* 43 (2004) 7137-7147.
- [157] A. H. Mohammadi, A. Chapoy, B. Tohidi, D. Richon, *Ind. Eng. Chem. Res.* 45 (2006) 4825-4829.
- [158] E. Brunner, *J. Chem. Thermodyn.* 17 (1985) 671-679.
- [159] A. Z. Francesconi, H. Lentz, E. U. Franck, *J. Phys. Chem.* 85 (1981) 3303-3307.
- [160] E. Brunner, W. Hultenschmidt, G. Schlichtharle, *J. Chem. Thermodyn.* 19 (1987) 273-291.

- [161] J. H. Hong, P. V. Malone, M. D. Jett, R. Kobayashi, *Fluid Phase Equilib.* 38 (1987) 83-96.
- [162] F. L. Boyer, L. J. Bircher, *J. Phys. Chem.* 64 (1960) 1330-1331.
- [163] A. Lannung, J. C. Gjaldbaek, *Acta Chem. Scand.* 14 (1960) 1124-1128.
- [164] I. R. Kritschewsky, M. Koroleva, *Acta Physiochim. USSR* 15 (1941) 327.
- [165] R. L. Horton, G. C. Dysinger, *Adv. Cryo. Eng.* 25 (1979) 629.
- [166] E. R. Shenderyev, Y. D. Zelvensky, F. P. Ivanovsky, *Gazov. Prom.* 6 (1962) 42.
- [167] W. L. Weng, M. J. Lee, *J. Chem. Eng. Data* 37 (1992) 213-215.
- [168] Z. Alwani, G. M. Schneider, *Ber. Bunsen Ges. - Phys. Chem. Chem. Phys.* 80 (1976) 1310-1315.
- [169] L. Ruffine, A. Barreau, I. Brunella, P. Mougin, J. Jose, *Ind. Eng. Chem. Res* 44 (2005) 8387-8392.
- [170] S. Zeck, H. Knapp, *Fluid Phase Equilib.* 25 (1986) 303-322.
- [171] E. Brunner, *J. Chem. Thermodyn.* 17 (1985) 871-885.
- [172] J. P. Kuenen, *Philos. Mag.* 48 (1899) 180-203.
- [173] J. P. Kuenen, *Philos. Mag.* 6 (1903) 637-653.
- [174] K. Ishihara, H. Tanaka, M. Kato, *Fluid Phase Equilib.* 144 (1998) 131-136.
- [175] J. C. Gjaldbæk, H. Niemann, *Acta Chem. Scand.* 12 (1958) 1015-1023.
- [176] Y. H. Ma, J. P. Kohn, *J. Chem. Eng. Data* 9 (1964) 3-5.
- [177] F. Galivel-Solastiouk, S. Laugier, D. Richon, *Fluid Phase Equilib.* 28 (1986) 73-85.
- [178] A. D. Leu, D. B. Robinson, S. Y. K. Chung, C. J. Chen, *Can. J. Chem. Eng.* 70 (1992) 330-334.
- [179] U. Haarhaus, G. M. Schneider, *J. Chem. Thermodyn.* 20 (1988) 1121-1129.

- [180] K. Noda, K. Sato, K. Nagatsuka, K. Ishida, *J. Chem. Eng. Jpn.* 8 (1975) 492-493.
- [181] A. M. Blanco, J. Ortega, *Fluid Phase Equilib.* 122 (1996) 207-222.
- [182] R. W. Kiser, G. D. Johnson, M. D. Shetlar, *J. Chem. Eng. Data* 6 (1961) 338-341.
- [183] D. Bernabe, A. Romero martinez, A. Trejo, *Fluid Phase Equilib.* 40 (1988) 279-288.
- [184] B. Orge, M. Iglesias, A. Rodriguez, J. M. Canosa, J. Tojo, *Fluid Phase Equilib.* 133 (1997) 213-227.
- [185] R. A. Wilsak, S. W. Campbell, G. Thodos, *Fluid Phase Equilib.* 33 (1987) 157-171.
- [186] F. C. Tenn, R. W. Missen, *Can. J. Chem. Eng.* 41 (1963) 12.
- [187] A. Trejo, P. Yanez, R. Eustaquio-Rincon, *J. Chem. Eng. Data* 51 (2006) 1070-1075.
- [188] I. F. Hölscher, G. M. Schneider, J. B. Ott, *Fluid Phase Equilib.* 27 (1986) 153-169.
- [189] P. Alessi, M. Fermiglia, I. Kikic, *J. Chem. Eng. Data* 34 (1989) 236-240.
- [190] J. D. Raal, R. K. Code, D. A. Best, *J. Chem. Eng. Data* 17 (1972) 211-216.
- [191] M. Goral, P. Oracz, S. Warycha, *Fluid Phase Equilib.* 152 (1998) 109-120.
- [192] M. Goral, P. Oracz, S. Warycha, *Fluid Phase Equilib.* 169 (2000) 85-99.
- [193] M. Hongo, T. Tsuji, K. Fukuchi, Y. Arai, *J. Chem. Eng. Data* 39 (1994) 688-691.
- [194] G. Hradetzky, D. A. Lempe, *Fluid Phase Equilib.* 69 (1991) 285-301.
- [195] T. W. de Loos, W. Poot, J. de Swaan Arons, *Fluid Phase Equilib.* 42 (1988) 209-227.
- [196] G. Hradetzky, H. J. Bittrich, *Int. Data Ser.* 3 (1986) 216.
- [197] F. C. Radice, H. N. Knickle, *J. Chem. Eng. Data* 20 (1975) 371-372.
- [198] V. Rothmund, *Z. Phys. Chem. - Leipzig* 26 (1908) 433.

- [199] S. C. Hwang, R. L. Robinson, *J. Chem. Eng. Data* 22 (1977) 319-325.
- [200] C. G. Savini, D. R. Winterhalter, H. C. Van Ness, *J. Chem. Eng. Data* 10 (1965) 171-172.
- [201] J. B. Ott, I. F. Holscher, G. M. Schneider, *J. Chem. Thermodyn.* 18 (1986) 815-826.
- [202] J. H. Oh, S. J. Park, *J. Chem. Eng. Data* 50 (2005) 1564-1569.
- [203] J. J. Segovia, M. C. Martin, C. R. Chamorro, M. A. Villamanan, *J. Chem. Thermodyn.* 31 (1999) 1231-1246.
- [204] H. Higashiuchi, Y. Sakuragi, Y. Iwai, Y. Arai, M. Nagatani, *Fluid Phase Equilib.* 36 (1987) 35-47.
- [205] K. Kammerer, G. Oswald, E. Rezanova, D. Silkenbäumer, R. N. Lichtenthaler, *Fluid Phase Equilib.* 167 (2000) 223-241.
- [206] J. Y. Lenoir, P. Renault, H. Renon, *J. Chem. Eng. Data* 16 (1971) 340-342.
- [207] F. Y. Jou, F. D. Otto, A. E. Mather, *Can. J. Chem. Eng.* 72 (1994) 130-133.
- [208] G. K. Folas, O. J. Berg, E. Solbraa, A. O. Fredheim, G. M. Kontogeorgis, M. L. Michelsen, E. H. Stenby, *Fluid Phase Equilib.* 251 (2007) 52-58.
- [209] D. Q. Zheng, W. D. Ma, R. Wei, T. M. Guo, *Fluid Phase Equilib.* 155 (1999) 277-286.
- [210] F. Y. Jou, K. A. G. Schmidt, A. E. Mather, *Fluid Phase Equilib.* 240 (2006) 220-223.
- [211] F. Y. Jou, F. D. Otto, A. E. Mather, *J. Chem. Thermodyn.* 25 (1993) 37-40.
- [212] S. O. Derawi, G. M. Kontogeorgis, E. H. Stenby, T. Haugum, A. O. Fredheim, *J. Chem. Eng. Data* 47 (2002) 169-173.
- [213] L. A. K. Staveley, G. L. Milward, *J. Chem. Soc.* (1957) 4369-4375.

- [214] F. Y. Jou, K. A. G. Schmidt, A. E. Mather, *J. Chem. Eng. Data* 50 (2005) 1983-1985.
- [215] G. C. Johnson, A. W. Francis, *Ind. Eng. Chem* 46 (1954) 1662-1668.
- [216] D. Jerinic, J. Schmidt, K. Fischer, L. Friedel, *Fluid Phase Equilib.* 264 (2008) 253-258.
- [217] F. Y. Jou, R. D. Deshmukh, F. D. Otto, A. E. Mather, *Fluid Phase Equilib.* 36 (1987) 121-140.
- [218] A. N. Sabirzyanov, P. Marteau, F. M. Gumerov, B. Le Neindre, *Theor. Found. Chem. Eng.* 35 (2001) 573-578.
- [219] B. S. Rawat, G. Prasad, *J. Chem. Eng. Data* 25 (1980) 227-230.
- [220] M. A. Hughes, Y. Haoran, *J. Chem. Eng. Data* 35 (1990) 467-471.
- [221] P. P. Sun, G. H. Gao, H. Gao, *J. Chem. Eng. Data* 48 (2003) 1109-1112.
- [222] M. A. Al Qattan, T. A. Al-Sahhaf, M. A. Fahim, *J. Chem. Eng. Data* 39 (1994) 111-113.
- [223] J. A. V. Butler, D. W. Thomson, W. H. MacLennan, *J. Chem. Soc.* (1933) 674-686.
- [224] K. Kurihara, T. Minoura, K. Takeda, K. Kojima, *J. Chem. Eng. Data* 40 (1995) 679-684.
- [225] J. Griswold, S. Y. Wong, *Chem. Eng. Prog. Symp. Ser.* 48 (1952) 18-34.
- [226] G. A. Miller, D. K. Carpenter, *J. Chem. Eng. Data* 9 (1964) 371-373.
- [227] G. Vuillard, M. Sanchez, *Bulletin de la Societe Chimique de France* (1961) 1877-1880.
- [228] J. B. Ott, J. R. Goates, B. A. Waite, *J. Chem. Thermodyn.* 11 (1979) 739-746.
- [229] H. K. Ross, *Ind. Eng. Chem.* 46 (1954) 601-610.
- [230] H. Yokoyama, M. Uematsu, *J. Chem. Thermodyn.* 35 (2003) 813-823.

- [231] M. L. McGlashan, A. G. Williamson, *J. Chem. Eng. Data* 21 (1976) 196-199.
- [232] M. Broul, K. Hlavaty, J. Linek, *Collect. Czech. Chem. Commun.* 34 (1969) 3428.
- [233] K. A. Dulitskaya, *J. Gen. Chem. USSR (Engl. Transl. )* 15 (1945) 9-21.
- [234] N. A. Pushin, A. A. Glagoleva, *J. Chem. Soc.* 121 (1922) 2813-2822.
- [235] O. Osada, M. Sato, M. Uematsu, *J. Chem. Thermodyn.* 31 (1999) 451-463.
- [236] Z. Bao, M. Liu, J. Yang, N. Wang, *J. Chem. Ind. Eng. (China)* 46 (1995) 230-233.
- [237] W. L. Marshall, E. V. Jones, *J. Inorg. Nucl. Chem.* 36 (1974) 2319-2323.
- [238] O. Chiavone-Filho, P. Proust, P. Rasmussen, *J. Chem. Eng. Data* 38 (1993) 128-131.
- [239] A. Lancia, D. Musmarra, F. Pepe, *J. Chem. Eng. Jpn.* 29 (1996) 449-455.
- [240] D. R. Cordray, L. R. Kaplan, P. M. Woyciesjes, T. F. Kozak, *Fluid Phase Equilib.* 117 (1996) 146-152.
- [241] J. B. Ott, J. R. Goates, J. D. Lamb, *J. Chem. Thermodyn.* 4 (1972) 123-126.
- [242] J. C. Olsen, A. S. Brunjes, J. W. Olsen, *Ind. Eng. Chem.* 22 (1930) 1315-1317.
- [243] F. H. Conrad, E. F. Hill, E. A. Ballman, *Ind. Eng. Chem.* 32 (1940) 542-543.
- [244] J. Spangler, E. Davies, *Ind. Eng. Chem. Anal. Ed.* 15 (1943) 96-99.
- [245] G. O. Curme, C. O. Young, *Ind. Eng. Chem.* 17 (1925) 1117-1120.
- [246] K. Jelinek, F. Lesek, M. Sivokova, *Collect. Czech. Chem. Commun.* 41 (1976) 2650-2656.
- [247] E. S. Klyucheva, N. L. Yarymagaev, *J. Appl. Chem. USSR* 53 (1980) 794-796.
- [248] M. Herskowitz, M. Gottlieb, *J. Chem. Eng. Data* 29 (1984) 450-452.
- [249] Y. X. Yu, J. G. Liu, G. H. Gao, *J. Chem. Eng. Data* 45 (2000) 570-574.
- [250] T. Tsuji, T. Hiaki, M. Hongo, *Ind. Eng. Chem. Res* 37 (1998) 1685-1691.

- [251] R. P. Sinyavskaya, N. L. Yarymagaev, I. I. Koliushko, *Gazov. Prom.* 7 (1984) 39-40.
- [252] R. P. Sinyavskaya, N. L. Yarymagaev, I. I. Koliushko, *Gazov. Prom.* 2 (1985) 26-27.
- [253] M. Iglesias, R. Gonzalez-Olmos, D. Salvatierra, J. M. Resa, *J. Mol. Liq.* 130 (2007) 52-58.
- [254] J. Liu, Z. Qin, J. Wang, *J. Chem. Eng. Data* 47 (2002) 1243-1245.
- [255] T. M. Letcher, S. Wootton, B. Shuttleworth, C. Heyward, *J. Chem. Thermodyn.* 18 (1986) 1037-1042.
- [256] P. Sentenac, C. Berro, E. Rauzy, I. Mokbel, J. Jose, *J. Chem. Eng. Data* 49 (2004) 1577-1580.
- [257] J. A. Porter, L. S. Reid, *Trans. Soc. Min. Eng. AIME* 189 (1950) 235-240.
- [258] C. Blanco, N. O. Smith, *J. Phys. Chem.* 82 (1978) 186-191.
- [259] R. Masoudi, B. Tohidi, A. Danesh, A. C. Todd, R. Anderson, R. W. Burgass, J. Yang, *Chem. Eng. Sci.* 60 (2005) 4213-4224.

## Appendix 2

### List of Individual Experimental Data Points Obtained in the Analytical Measurements

**Table A2.1** – List of individual data points obtained for the water mole fraction in the gas phase, in the analytical study of the system methane + water.

$T / \text{K}$	$p / \text{MPa}$	$y_{\text{water}} \times 10^3$ (FID)	$y_{\text{water}} \times 10^3$ (TCD)	$y_{\text{water}} \times 10^3$ (av.)
298.289	5.509	0.5640	0.5756	0.5698
298.290	5.504	0.5720	0.5838	0.5779
298.290	5.500	0.5851	0.5966	0.5909
297.789	5.592	0.5689	0.5798	0.5744
298.289	5.583	0.5663	0.5772	0.5717
298.288	5.473	0.5647	0.5757	0.5702
298.288	7.964	0.3848	0.3931	0.3890
298.289	7.950	0.3688	0.3768	0.3728
298.293	7.937	0.3898	0.3976	0.3937
298.295	7.923	0.3875	0.3948	0.3911
298.299	7.897	0.3578	0.3648	0.3613
298.297	11.506	0.2744	0.2828	0.2786
298.298	11.484	0.2713	0.2826	0.2769
298.302	11.462	0.2626	0.2703	0.2665
298.302	11.441	0.2566	0.2639	0.2603
298.303	11.419	0.2787	0.2866	0.2826

**Table A2.1 (Cont.)** List of individual data points obtained for the water mole fraction in the gas phase, in the analytical study of the system methane + water.

$T / \text{K}$	$p / \text{MPa}$	$y_{\text{water}} \times 10^3$ (FID)	$y_{\text{water}} \times 10^3$ (TCD)	$y_{\text{water}} \times 10^3$ (av.)
298.301	11.397	0.2788	0.2866	0.2827
303.286	5.249	0.8344	0.8487	0.8416
303.275	5.240	0.8245	0.8373	0.8309
303.275	5.232	0.8405	0.8534	0.8469
303.276	5.223	0.8437	0.8565	0.8501
303.276	5.214	0.8340	0.8465	0.8403
303.277	5.319	0.8494	0.8593	0.8543
303.283	7.276	0.6270	0.6405	0.6337
303.283	7.262	0.6048	0.6178	0.6113
303.282	7.247	0.6359	0.6495	0.6427
303.283	7.233	0.6141	0.6264	0.6202
303.283	7.219	0.6580	0.6708	0.6644
303.282	7.206	0.6721	0.6842	0.6782
303.276	12.411	0.3953	0.4051	0.4002
303.276	12.384	0.3875	0.3973	0.3924
303.280	12.358	0.3952	0.4048	0.4000
303.280	12.332	0.3935	0.4030	0.3982
303.280	12.305	0.3861	0.3955	0.3908
303.281	12.279	0.3746	0.3837	0.3792

**Table A2.2** – List of individual data points obtained for the methane mole fraction in the aqueous phase, in the analytical study of the system methane + water.

$T / \text{K}$	$p / \text{MPa}$	$x_{\text{methane}} \times 10^3$
298.287	5.450	1.1346
298.284	5.434	1.1459
298.284	5.424	1.0371
298.284	5.409	1.2208
298.301	7.650	1.5619
298.301	7.634	1.4433
298.301	7.627	1.5106
298.305	7.362	1.3864
298.312	7.341	1.3924
298.304	7.327	1.3964
298.286	8.452	1.6345
298.285	8.443	1.7177
298.289	8.230	1.5759
298.289	8.225	1.6193
298.290	8.215	1.5117
298.291	8.210	1.5752
298.291	8.205	1.7797
298.300	11.374	2.0099
298.300	11.361	2.0385
298.300	11.333	2.0860
298.301	11.321	1.9956
298.300	11.307	2.0010
303.277	5.359	0.8033
303.277	5.349	0.8686
303.272	5.344	1.0198
303.272	5.334	0.9594
303.272	5.329	0.8456
303.272	5.324	0.9487
303.270	6.726	1.1780
303.271	6.706	1.1181
303.270	6.698	1.1128
303.270	6.687	1.1175
303.270	6.678	1.1049

**Table A2.2 (Cont.)** – List of individual data points obtained for the methane mole fraction in the aqueous phase, in the analytical study of the system methane + water.

$T / \text{K}$	$p / \text{MPa}$	$x_{\text{methane}} \times 10^3$
303.269	6.654	1.2154
303.280	7.184	1.2909
303.279	7.177	1.3391
303.275	7.163	1.2891
303.282	12.236	1.9255
303.282	12.219	1.9316
303.283	12.202	1.8650
303.281	12.267	1.9555

**Table A2.3** – List of individual data points obtained in the analytical study of the system methane + *n*-hexane + methanol + water, at 298 K and 9.8 MPa.

Phase	<i>T</i> / K	<i>p</i> / MPa	Compound			
			methane	<i>n</i> -hexane	methanol	water
aqueous phase	298.502	9.837	$3.01 \times 10^{-3}$	$1.66 \times 10^{-5}$	0.165	0.832
	298.488	9.827	$2.94 \times 10^{-3}$	$1.43 \times 10^{-5}$	0.167	0.830
	298.475	9.819	$3.13 \times 10^{-3}$	$1.14 \times 10^{-5}$	0.166	0.831
	298.456	9.809	$3.05 \times 10^{-3}$	$1.16 \times 10^{-5}$	0.175	0.822
	298.419	9.792	$3.01 \times 10^{-3}$	$1.24 \times 10^{-5}$	0.165	0.832
organic phase	298.298	9.649	0.131	0.847	0.0052	$4.61 \times 10^{-3}$
	298.304	9.642	0.130	0.861	0.0095	$1.54 \times 10^{-3}$
	298.311	9.634	0.140	0.847	0.0137	$9.82 \times 10^{-3}$
	298.318	9.627	0.154	0.828	0.0174	$2.35 \times 10^{-3}$
	298.309	9.618	0.186	0.770	0.0442	$1.83 \times 10^{-3}$
	298.315	9.611	0.189	0.792	0.0187	$1.00 \times 10^{-3}$
	298.318	9.603	0.193	0.783	0.0243	$2.35 \times 10^{-3}$

**Table A2.4** – List of individual data points obtained in the analytical study of the system methane + *n*-hexane + methanol + water, at 298 K and 7.3 MPa.

Phase	<i>T</i> / K	<i>p</i> / MPa	Compound			
			methane	<i>n</i> -hexane	methanol	water
aqueous phase	298.299	7.452	0.0470	0.0576	0.149	0.747
	298.302	7.448	0.0418	0.0494	0.149	0.760
	298.301	7.442	0.0296	0.0360	0.148	0.786
organic phase	298.342	7.423	0.394	0.572	0.0232	--
	298.349	7.419	0.414	0.545	0.0405	--
	298.354	7.413	0.438	0.515	0.0570	--
	298.318	7.364	0.446	0.485	0.0649	--
gas phase	298.295	7.213	0.976	0.0237	$5.5 \times 10^{-4}$	--
	298.295	7.201	0.969	0.0304	$6.3 \times 10^{-4}$	--
	298.299	7.183	0.976	0.0236	$3.7 \times 10^{-4}$	--
	298.299	7.171	0.978	0.0214	$8.0 \times 10^{-4}$	--
	298.300	7.164	0.978	0.0206	$1.47 \times 10^{-3}$	--



Center for Energy Resources Engineering  
Department of Chemical and  
Biochemical Engineering  
Technical University of Denmark  
Søltofts Plads, Building 229  
DK-2800 Kgs. Lyngby  
Denmark

Phone: +45 4525 2800  
Fax: +45 4525 4588  
Web: [www.kt.dtu.dk](http://www.kt.dtu.dk)

ISBN: 978-87-92481-27-6